Technical University of Eindhoven
Faculty of Mechanical Engineering

Technical University of München
Forschungsstelle Zahnrad und Getriebebau

Tooth Root Strength of Bevel and Hypoid Gears

Development of a Practical Design Method for Rear Axle Gears in Commercial Vehicles

PROEFSCHRIFT

ter verkrijging van de graad van doctor aan de Technische Universiteit Eindhoven, op gezag van de Rector Magnificus, prof.dr. M. Rem, voor een commissie aangewezen door het College voor Promoties in het openbaar te verdedigen op vrijdag 26 januari 2001 om 16.00 uur

door

Mathias Johannes Maria Cuijpers

geboren te Eindhoven

Dit proefschrift is goedgekeurd door de promotoren:

prof.dr.ir. M.J.W. Schouten
en
Prof.Dr.-Ing. B.-R. Höhn

It does not matter if you try and fail and then try and fail again
But it does matter if you try and fail and then fail to try again

Charles F. Kettering

To my Father and Mother

ISBN 90-386-2692-4

Ontwerp omslag: Mitsy Selhorst

Acknowledgements

This dissertation is mainly the summarising result of several years of investigations at the Development Department for rear axles of DAF Trucks at Eindhoven, Netherlands.
During the period of 1988 to 1994, several types of rear axles have been developed for a relatively wide range of vehicles. The range covered rear axles for heavy vans of about 4 tonne to rear axles for long distance trucks with 40 tonne payload. During the course of these developments, several driveline endurance testrig tests have been performed on the gears, as well as an evaluation of the failures.
Lateron, I took it on me to analyse and to evaluate all the test results of these endurance tests. The goal for this was to create a practical calculation method for bevel and hypoid rear axle gears, that would be especially suitable for commercial vehicles. Practical here means that the calculation method has been verified by the results of actual testrig measurements. In the field of rear axle gear applications, the designer is forced to use special and dedicated calculations, that mostly are to be developed and verified on actual test results. The results of these relatively large scale tests form the basis of this dissertation.

I would like to express my thanks to the Development Department of DAF Trucks Eindhoven NL for their kind permission of publishing several of these results.
My former colleagues of the design group Rear Axles for their support with experience and knowledge, especially Wim Geurink, Piet van Deursen, Toon de Boer and Peter Venhuizen.
Thanks to the people of the Testing Driveline and Central laboratory who made it possible to peform the driveline tests, to evaluate the test results and to investigate metallurgical aspects.
Special thanks to Jos Van Heck for his mathematical generosity by deriving difficult recurrent expressions for the equivalent torque, Neil Lawrence for screening the text and Herman Lut for editing many of the equations in the text.

To those who have heard for several years that this work was to be finished: It took more effort and time than I anticipated. I had to write this dissertation next to my normal work.

I would like to express my special gratitude to both Prof.Dr.Ir. M.J.W. Schouten of the Faculty of Mechanical Engineering of the Technical University Eindhoven and Prof.Dr.Ing. B.R. Höhn of the Forschungsstelle Zahnrad und Getriebebau at the Technical University of München for their support in this work.

Langenargen, october 2000

SUMMARY

These investigations are focussed on the tooth root strength of rear axle gears for trucks.
Four different standards for calculating the tooth root stress of bevel gears have been compared and analysed. Although the expressions that are used in these standards appear to be quite different, they have been rewritten in such a way that the individual load, geometry and material factors can be directly compared. This shows that in fact these standards are all built up in a comparable way.
A calculation example has been performed on two hypothetical gear sets, representative for truck applications. The largest differences are attained on the Allowable Stress, the Tooth Form Factor and the Face Load Distribution Factor. Smaller differences may be observed on the Load Sharing, the Helical and the Size Factor. The calculated stresses and the allowable material stresses are to be closely linked to each other within one and the same calculation standard. The Face Load Distribution Factor was calculated to be 1.30 instead of the normally recommended value of 1.50 according to DIN, by considering a reviewed stress distribution over the gear facewidth.

Three normally applied methods for calulating tooth root stress of hypoid gears have been compared. The differences between these methods are mainly determined by the geometry of the virtual bevel gears. The influence of hypoid offset on tooth root stress, calculated according to these three methods showed very large differences. The tendencies of these calculations have been compared with results of other investigations. This has shown that the influence of hypoid, calculated according to Winter, showed the best correlation with results of external investigations.

Several endurance driveline tests have been performed on four different types of rear axle hypoid gears, assembled in a driving head. The tests were run at a constant amplitude load and speed, until fatigue breakage of the pinion teeth occurred.
The testresults were statistically evaluated and have been described by a lognormal and a two parameter Weibull failure distribution. A damage analysis on several of the failed pinions showed consistent failure types that partly correspond to assumptions in stress calculations.
The DIN 3991 method was used for calculating the tooth root stress, by using the Winter method for determining the geometry of the virtual bevel gears. These were then fitted with the test results, by which a synthetic SN curve was established.
The established fatigue limit is in line with standard values. The slope of the SN curve and the ratio of static to endurance strength were however different from the values, used for helical gears of the same material. This is believed to be caused by the non linearity of the stress-torque relationship, being a consequence of the growth of the contact pattern with increasing torque. In all standards however, the stress is calculated as being linear with torque. Therefore, a Load Factor is introduced to account for the influence of the contact pattern. This assures a non linear relation between torque and tooth root stress for bevel and hypoid gears. When this factor is applied, comparable slope values for the SN curve of helical gears in identical materials may be used. With this mathematical adaptation, the difference between calculated and registered endurance lifes for three of four axle types became far less than plus-minus 10% for a failure probability of 10%.

Vehicle Driveline Loading Spectra have been measured and calculated. A comparison shows good agreement. On this basis, several loading spectra have been simulated for typical vehicle routes. Two basic types of loading spectra have been determined here, for which

analytical expressions have been developed as well as equations for the equivalent torque.
A limited number of endurance tests at variable amplitude loading have been performed on one axle type. It was found that the fatigue damage accumulation theory according to Corten-Dolan was the best suitable for variable amplitude loading when the non linear stress-torque relation was used, although still a reduction in endurance strength may be noticed. At variable amplitude loading mostly a mix of failures may be expected, where the early occurence of surface damage may influence the endurance limit for tooth root fatigue.

A simple relation has been derived for the gear outer diameter of bevel and hypoid gears, based on the maximum output torque. For preliminary dimensioning, this torque can be considered to be mainly based on the vehicle weight. With this expression, it is possible to give a practical first order estimate on the gear outer diameter for a given vehicle weight.

ZUSAMMENFASSUNG

Diese Untersuchungen beziehen sich auf die Zahnfußfestigkeit von Verzahnungen für LKW Hinterachsen. Vier Berechnungsmethoden für Zahnfußspannung an Kegelrädern sind verglichen und analysiert worden. Obwohl die Ausdrückungen dieser Berechnungen sehr verschieden aussehen, sind sie in einer Weise geschrieben worden, daß die individuelle Faktoren für Last, Geometrie und Werkstoff direkt mit einander verglichen werden können. Einige Berechnungen sind ausgeführt worden an zwei hypothetischen Getriebesätzen, die representativ sind für LKW Anwendungen. Die größten Unterschiede treten auf bei den Faktoren für Zahnform und Breitenlastverteilung. Kleinere Unterschiede treten auf bei den Faktoren für Spannungskonzentration, Lastaufteilung, Zahnschrägung und Größeneinfluß. Die berechneten und die zulässigen Spannungen einer Berechnungsmethode sollten aber immer zueinander gehören. Der Breitenlastverteilungsfaktor nach DIN ist berechnet worden auf einem Wert von 1.30 anstatt den normalerweise gebräuchlichen Wert von 1.50, durch die Annahme eine geänderte Spannungsverteilung über die Zahnbreite.

Drei normal angewendete Methoden zur berechnung der Zahnfußspannung von Hypoidräder sind verglichen. Die Unterschiede zwischen diese Methoden werden hauptsächlich bestimmt von der Geometrie der virtuelle Kegelräder. Der Einfluß von Hypoid Achsversatz auf die Zahnfußspannung, berechnet nach diese drei Methoden ergab große Unterschiede. Die Tendenzen dieser Berechnungen sind verglichen mit Ergebnisse anderer Untersuchungen. Hieraus hat sich erstellt daß der Einfluß von Hypoid Achsversatz, errechnet nach Winter, die beste Übereinstimmung hat mit die Erbegnisse von andere Untersuchungen.

Es sind verschiedene Lebensdauererprobungen ausgeführt worden an Hypoid Verzahnungen die in Hinterachsgehäusen eingebaut sind. Die Erprobung hat unter einer Last mit konstanter Amplitude und Drehzahl stattgefunden, bis zum Ermüdungsbruch der Ritzelzähne.
Die Ergebnisse der Lebensdauererprobungen sind statistisch evaluiert worden; sie konnten beschrieben worden von einer Lognormaler und einer zwei parameter Weibull Verteilung. Eine Schadensanalyse an einigen Ritzel hat ein konsistentes Versagen nachgewiesen, das jedoch nur zum Teil übereinstimmt mit Annahmen der Spannungsberechnung. Die DIN 3991 ist benutzt worden zur Berechnung der Zahnfußspannung, wobei die Berechnung der Geometrie für die virtuelle Kegelräder auf Winter basiert. Zusammen mit den realisierten Lebensdauern wurde dann eine synthetische Wöhlerlinie zusammengestellt.
Die Ermüdungsfestigkeit stimmte überein mit normalen Werten. Die Steigung der Wöhlerlinie

und das Verhältnis von statischer Festigkeit zur Ermüdungsfestigkeit zeigten aber andere Werte als die für Schrägstirnräder aus dem gleichen Werkstoff. Es wird angenommen, dass dieses verursacht wird durch das nicht lineare Verhältnis zwischen Drehmoment und Zahnfußspannung, welche eine Konsequenz der Tragbildausbreitung bei zunehmendem Drehmoment ist. In allen Berechnungsmethoden wird jedoch mit einem linearen Verhältnis gerechnet. Deshalb ist ein Lastfaktor für den Einfluß des Tragbildes eingeführt worden. Dieser sichert ein nichtlineares Verhalten zwischen Drehmoment und Zahnfußspannung für Kegel- und Hypoidräder. Mit diesem Faktor können die Steigungswerte der Wöhlerlinie für Schrägzahnräder auch für Hypoidräder benutzt werden, unter Voraussetzung von gleichem Werkstoff. Der Unterschied zwischen berechneter und gemessener Ermüdungsfestigkeit war für drei der vier Achstypen deutlich weniger als plus/minus 10% für eine Ausfallwahrscheinlichkeit von 10%.

Antriebslastkollektive sind ermittelt und berechnet worden. Ein Vergleich zeigte gute Übereinstimmung zwischen beiden. Dabei sind verschiedene Lastkollektive für einige typische Einsatzfälle simuliert worden. Zwei Haupttypen von Lastkollektiven sind zu erkennen, für die analytische Ausdrücke entwickelt worden sind sowie Gleichungen für das äquivalente Drehmoment.

Eine beschränkte Anzahl Lebensdauer Erprobungen mit variabler Lastamplitude sind ausgeführt worden. Es hat sich gezeigt, dass die Schadensakkumulationshypothese nach Corten-Dolan die Ergebnisse am Besten beschreibt. Dennoch ist zu erwarten, daß unter einer Last mit variabler Amplitude eine Reduzierung der Ermüdungsfestigkeit auftritt, wobei frühzeitige Oberflächenschäden die Ermüdung für Zahnbruch reduzieren.
Ein einfacher Ausdruck ist abgeleitet worden zwischen Tellerrad Aussendurchmesser und maximalem Ausgangsdrehmoment, womit eine gute Ersteinschätzung gemacht werden kann vom Tellerrad Aussendurchmesser wenn nur das Fahrzeuggewicht bekannt ist.

SAMENVATTING

De uitgevoerde onderzoekingen hebben betrekking op de tandvoetsterkte van vertandingen voor achterassen van trucks. Vier verschillende normen voor het berekenen van tandvoetspanning aan kegel- en hypoidwielen zijn vergeleken en geanalyseerd. Ondanks dat de uitdrukkingen van deze normen de indruk geven onderling geheel verschillend te zijn, zijn deze herschreven op een dusdanige wijze dat de individuele belastings-, geometrie- en materiaalfactoren direct vergeleken kunnen worden. Dit toont aan dat deze berekeningen alle op een en dezelfde wijze zijn opgebouwd.
Een rekenvoorbeeld is uitgevoerd aan twee hypothetische tandwielsets, welke representatief zijn voor truck toepassingen. De grootste verschillen treden op bij de tandvormfactor en de factor voor de belastingverdeling. Kleinere verschillen treden op bij de factoren voor de belastingopdeling, de tandschuinte en de grootte. Berekende- en toelaatbare spanningen dienen nauw met elkaar verbonden te zijn binnen een en dezelfde berekeningsmethode.
Er is afgeleid dat de factor voor de belastingverdeling 1.30 dient te bedragen in plaats van de gangbaar aanbevolen waarde van 1.50 volgens DIN, door een andere belastingverdeling over de tandbreedte aan te nemen.

Voor het berekenen van de tandvoetspanning aan hypoidwielen zijn drie gangbare methoden met elkaar vergeleken. De verschillen tussen deze methoden worden voor een groot deel bepaald door de geometrie van de vervangende virtuele kegelwielsets. De invloed van de

hypoid offset op de tandvoetspanning, berekend volgens deze drie methoden gaf onderling zeer grote verschillen te zien. De tendensen van deze berekeningen zijn vergeleken met resultaten van andere onderzoekingen. Hieruit is gebleken dat de invloed van de hypoid offset, berekend volgens Winter, het beste overeenkomt met de resultaten van de externe onderzoekingen.

Er zijn verscheidene levensduurbeproevingen uitgevoerd aan de hypoidwielen van vier verschillende typen achterassen, welke compleet geassembleerd waren in een achteras. De beproevingen vonden plaats bij een constante amplitude van koppel en toerental, totdat er vermoeiingsbreuk van de rondselvertanding optrad.
De beproevingsresultaten zijn statistisch beoordeeld; ze zijn beschreven met een lognormale- en een twee parameter Weibull verdeling. Een schadeanalyse aan enkele van de gefaalde rondsels gaf een consistent schadebeeld te zien, welke ten dele overeenkomt met de aannamen in de spanningsberekeningen. De DIN 3991 methode is gebruikt voor het berekenen van de tandvoetspanning, waarbij de methode volgens Winter voor het bepalen van de vertandingsgeometrie van de virtuele kegelwielen is gebruikt.
De uit de beproevingen afgeleide waarde voor de vermoeiingsgrens komt overeen met normaal gehanteerde waarden. De helling van de SN-curve en de verhouding van de statische- tot de vermoeiingssterkte bleken echter te verschillen van de waarden die gebruikt worden voor cilindrische tandwielen uit hetzelfde materiaal. Dit verschil wordt veroorzaakt door de niet lineariteit in de relatie tussen tandvoetspanning en aandrijfkoppel, welke op zijn beurt een gevolg is van de draagbeeldgroei bij toenemend aandrijfkoppel. In alle berekeningsnormen wordt de spanning echter gerekend als zijnde lineair met het aandrijfkoppel. Om aan het effect van de draagbeeldgroei tegemoet te komen, wordt er een belastingsfactor geintroduceerd voor de invloed van het draagbeeld. Hierdoor wordt er rekenkundig een niet linear gedrag zeker gesteld tussen aandrijfkoppel en tandvoetspanning bij kegel- en hypoidwielen. Indien deze factor wordt gebruikt, kunnen ook dezelfde waarden gehanteerd worden voor de helling van de SN-curve bij cilindrische tandwielen. Het verschil tussen berekende- en gerealiseerde levensduur voor drie van de vier astypen werd hierdoor minder dan plus/minus 10% voor een uitvalwaarschijnlijkheid van 10%.

Er zijn enkele belastingsspectra aan de voertuigdrijflijn gemeten en berekend. Een vergelijking tusen beide geeft een goede overeenkomst aan. Op basis hiervan zijn er diverse belastingsspectra gesimuleerd voor enkele specifieke voertuigroutes. Er kunnen hier twee zogeheten basistypen van belastingsspectra worden onderkend, waarvoor analytische uitdrukkingen zijn ontwikkeld, alswel vergelijkingen voor het bepalen van het equivalente aandrijfkoppel.
Een beperkt aantal levensduurproeven bij variabele amplitude is uitgevoerd. Hierbij is gebleken dat de theorie voor de schade-accumulatie volgens Corten-Dolan de kleinste verschillen gaf tussen berekening en realisatie, alhoewel er nog steeds een reductie benodigd is voor de waarde van de vermoeiingsgrens, welke bij constante amplitude is bepaald. Bij variabele amplitude kunnen er in het algemeen verschillende schades tegelijkertijd optreden, waarbij vroegtijdige oppervlakteschade de vermoeiingsgrens voor tandvoetbreuk in negatieve zin beinvloedt.

Er is een eenvoudige uitdrukking afgeleid tussen de buitendiameter van het kroonwiel en het maximale uitgaande koppel. Hiermee kan de afmeting van een kroonwiel worden bepaald voor een allereerste dimensionering, indien enkel het voertuiggewicht bekend is.

Contents

1 INTRODUCTION

1.1 General Description

Since the beginning of automotive history, rear axles have been used in rear wheel driven vehicles, both in passenger cars as well as in commercial vehicles.
Typical commercial vehicle applications range from international long distance transport (long distance haulage) via inter regional transport to inter or inner-urban distribution. In general, tractor-trailer combinations or truck-trailers are used for this type of transport of goods.

The total vehicle or combination weights nowadays are maximum 40 or 44 tonne; mostly this is limited by general legislation rules of different countries. For inter-regional or national transport, vehicles in the range of 25 to 35 tonne are used. In the medium range, such as inter-urban transportation, vehicle weights mostly range from 7 to 20 tonne. These types of vehicles may also include vehicles for transport of goods such as sand, stones, rock, wood, concrete as well as off-the-road vehicles for militairy applications. For transportation of people, long distance coaches or touring cars as well as intercity or city busses are being used. Small commercial vehicles, the so called vans, are in use for vehicle weights from 2 to 6 tonne. Here, both front and rear wheel drives are utilised. At the lower side of vehicle weights such as passenger cars and motorbikes, rear axle drives are applied, although on a more limited scale due to the increasing application of front wheel drive.
Almost all commercial vehicles over 6 tonne are equipped with rear wheel drive, where the power is transmitted from the engine through a gearbox and drive shaft system to the rear axle of the vehicle.
Generally, two types of rear axles are applied in rear wheel driven vehicles; the single reduction and the hub reduction rear axle (figure 1.1 and 1.2). The single reduction rear axle consists of a spiral bevel or a hypoid gear. It is mostly used for typical long distance transport applications and it is most widely spread. The hub reduction axle is a two stage reduction axle, mostly consisting of a first stage spiral bevel gear reduction coupled with a planetary stage in each wheel hub. This axle configuration leads to a relatively small crownwheel diameter. Therefore these axle types are mostly used for off-the-road vehicles, where ground clearance is a very important item. The rear axle ratio's mostly cover a range of 2.5 to 7, depending on the axle and vehicle type. Long distance transport axles normally have a ratio of 3 to 4, whereas city busses will have a ratio of 4 to 6. These are however indicative values.

1.2 Design and Development Process for Rear Axles.

Three groups of general data may be introduced here for the description of the rear axle, that play a dominant role in the process of design and development. These are (figure 1.3):

* Vehicle Application for the complete vehicle.
* Functional Requirements for different vehicle components.
* Design Features for component parts.

The Vehicle Application gives a description of the vehicle type, its driveline and the use of the vehicle. These determine the Functional Requirements for the different vehicle components, such as the engine, chassis, cabine and rear axle. These are the minimal requirements to be achieved by every specific component, in order to assure a required reliability.

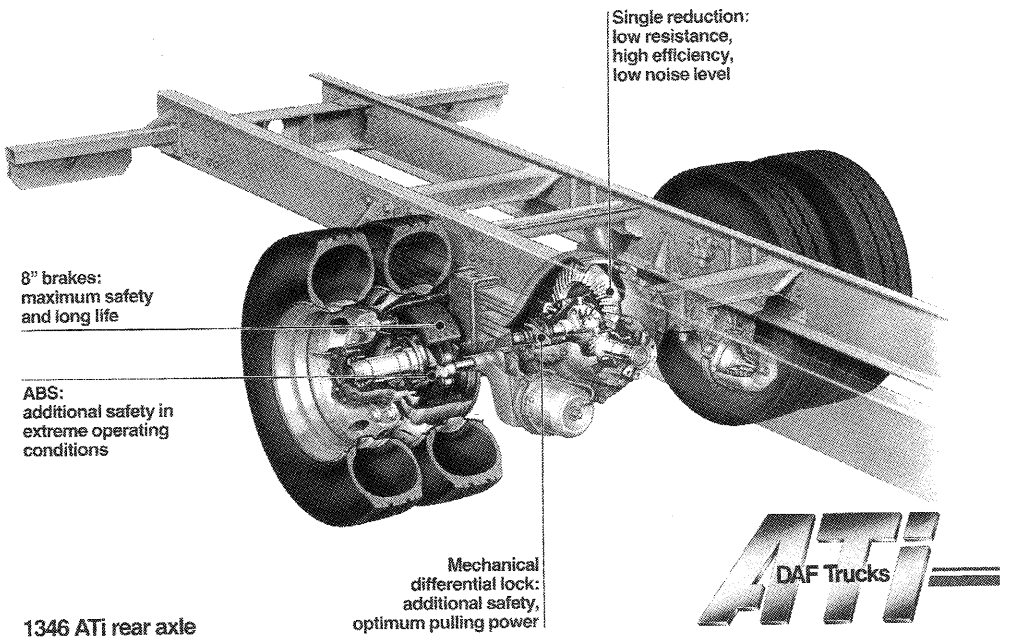

Fig. 1.1 Single Reduction Hypoid Rear Axle

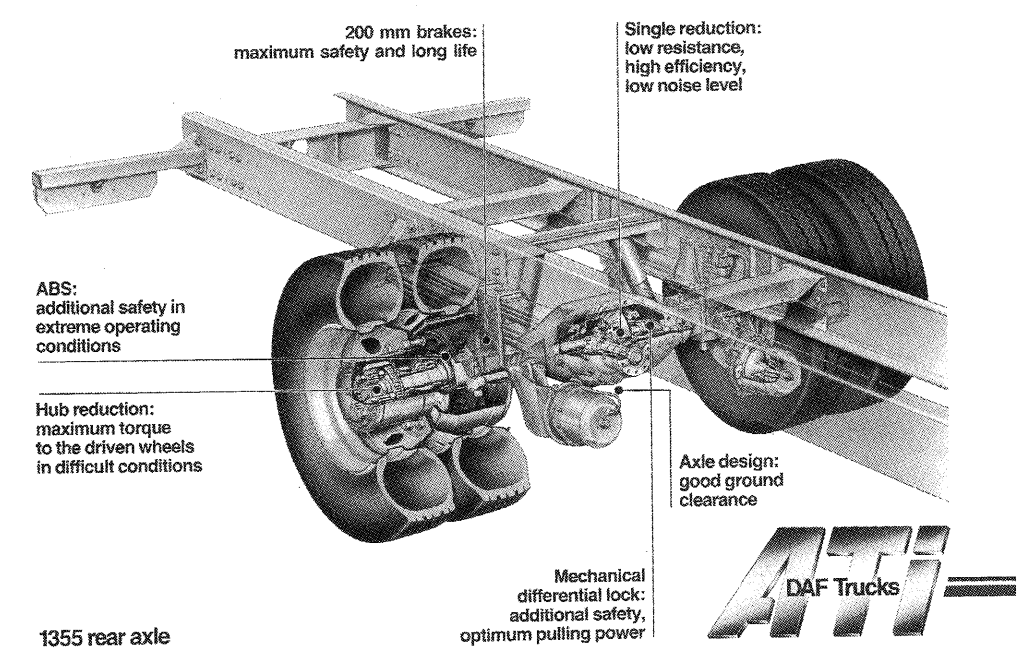

Fig. 1.2 Hub Reduction Spiral Bevel Rear Axle

For the design and development of different vehicle components, these Functional Requirements can be achieved by applying suitable Design Features. These Design Features can be considered as characteristic data for the design, by which Functional Requirements can be fullfilled. They are not only to be specified at the preliminary design, but also at the further development of each specific component.

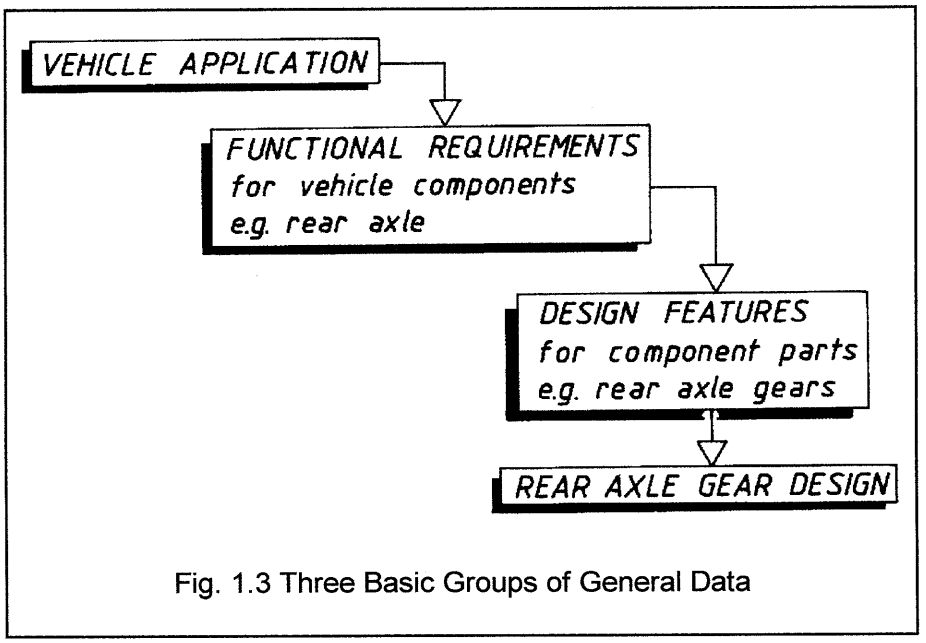

Fig. 1.3 Three Basic Groups of General Data

The Vehicle Application can best be described in terms of typical vehicle related items such as vehicle use, mass, type, configuration and general data on the driveline configuration, when the aim is focussed on driveline design (Table 1.1).
Generally a wide variation of Vehicle Applications can be expected. A vehicle for long distance transport will almost all the time travel on international highway with a cruising speed pattern, characterised by high speed/low torque and an average nominal vehicle loading of about 75%. On the other hand, an inter-urban distribution vehicle will travel a large amount through urban regions and on inter urban secondary roads, with a more or less stop-and-go speed pattern. These vehicles mostly will start fully laden and by distributing the goods, the vehicle load will gradually decrease until the vehicle curb weight. Therefore the average vehicle loading can be considered being about 50%. Each specific Vehicle Application will give different driveline loadings.

Departing from a Vehicle Application, several Functional Requirements can then be derived for different vehicle components, such as chassis, suspension, cabine, engine, gearbox and rear axle. These requirements are specific goals for each of the components that have to be met in the design and development process. The rear axle in general will have to fullfill two main functions. The first one is to carry part of the vehicle load, which is normally fullfilled by the rear axle housing. The second function is to transmit the engine power to the vehicle wheels. This function is realised by the rear axle rotating parts such as gears and bearings.

VEHICLE APPLICATION

***Vehicle Use**
- -Transportation type
- -Total and annual mileage
- -Route description:
  - Topografy flat / hilly / mountain
  - Road profile city / urban / secundary highway / off-road
  - Load pattern full / half laden / empty
  - Speed pattern cruising / stop-and-go

***Vehicle Mass**
- -Gross vehicle mass GVM
- -Gross combination mass GCM
- -Type of goods to transport
- -Overload Factor

***Vehicle Type**
- -Tractor / trailer; tractor / semi-trailer
- -Truck, Lorrey
- -Special transport vehicle
- -Van

***Vehicle Configuration**
- -Chassis and cabine type
- -Number of axles; single and tandem axle
- -Number of tyres; tyre type
- -Front area; Cw factor
- -Rolling resistance

***Driveline Configuration**
- -2x4 / 4x4 / 4x6
- -Engine data / exhaust brake / C-brake
- -Gearbox ratio's / ratio spread / DirectDrive or OverDrive
- -Secundary retarder / Intarder
- -Transfer gear box; ratio; front-rear ratio
- -Rear axle type / rear axle ratio

Table 1.1 Data on Vehicle Application

In the further course of this thesis, we will focus on the torque transmitting rear axle gears.

The specific Functional Requirements for the rear axle gears can best be described with the items as given in Table 1.2. Rear axle gears for off-the-road vehicles operating in rough terrain conditions will exhibit very often high peak torques caused by mis-use situations. Here, failures resulting from overload will play an important role. In contrast to these are the long distance transport vehicles, where the amount of peak loads is limited by the vehicle application and the relatively low wheel spin torque. Here the chance of fatigue failures will be more dominant than failures resulting from overload. The set of Functional Requirements also depends very much on the vehicle application.

FUNCTIONAL REQUIREMENTS
for Rear Axle Gears

***Strength**	-static overload / mis-use -dynamic loading / endurance
***Noise**	-exterior noise / objective measurement -interior noise / subjective indications
***Efficiency**	-fuel consumption -maximum temperature / extreme conditions
***Weight**	
***Manufacturing costs**	
***Serviceability**	
***Reliability**	
***Vehicle related Dimensional Constraints**	

Table 1.2 Most important Functional Requirements for Rear Axle Gears

In order to meet these Functional Requirements of the power transmitting parts of the rear axle, several Design Features can be defined or implemented in the specific development stages for the rear axle gears as indicated in Table 1.3 on the next page.
These Design Features in fact consist of all specific data that determine the final design of rear axle gears. The gear type, the gear geometry and the general manufacturing quality level of the gears themselves. The material that is used for the gears as well as it's heat treatment that is applied to obtain specific strength characteristics. Data on the lubricating oil and the specifics on the gear assembly in the driving head casing complete the set of typical Design Features for rear axle gears.

DESIGN FEATURES
for Rear Axle Gears

1. Gear Type and Gear Geometry
- Spiral Bevel or Hypoid Gears
- Macro and Micro geometry

2. Manufacturing Method
- Gleason / Oerlikon / Klingelnberg
- Conventional machining (incl. lapping)
- Hard finishing

3. General Quality Level
- Pitch and profile errors
- Tooth thickness and runout errors
- Surface roughness

4. Gear Material
- Case carburising steel; nitriding steel
- Total percentage alloying elements
- Alloying elements (Cr,Ni,Mo,Mn,V,Ti)
- Hardenability / Jominy curves
- Tensile strength / impact toughness

5. Heat Treatment
- Carburising and quenching process
- Surface hardness and casedepth (flank/root)
- Tensile strength in the core
- Retained austenite; decarburising
- Core structure; residual stresses

6. Final Surface Treatment
- Fosfating layers
- Grinding of gear surface
- Shot peening of gear surface
- PVD/CVD surface layers

7. Lubricating Oil
- Oiltype (mineral, semi/full synthetic)
- Viscosity range
- Multi or single grade oil
- Dope package (EP, FM, VI)
- Oil contamination

8. Gear Assembly
- Contact pattern (shape, size, position)
- Mounting distance; gear backlash
- Gear deflection under torque loading
- Stiffness drivinghead casing
- Bearing support and stiffness

Table 1.3 Some Typical Design Features for Rear Axle Gears

For the development of rear axles in general, and rear axle gears in specific, two separate stages in the design and development proces might be distinghuished. These are the Design Stage and the Testing Stage, where there is a feedback of testing results in order to adapt some design features on the basis of test results, if required. After validation of all functional requirements of the rear axle, by passing through the entire testing procedure, normally a Sign-Off will then be given. The definitive design will then obtain an official Production Release and the Production Stage can be entered then.

This basic scheme of the Development Proces (figure 1.4) is very schematically and it is only to be considered as a general indication. In practice some stages will progress in a sequential way, some others may progress in time parallel to each other. For different companies the sequences of design and development may differ, according to their development policy.
In this thesis we will focus on those elements of the Design Features, that mostly play a crucial role in the entire development proces of vehicle rear axle gears. The Design Stage for rear axle gears, consisting of the afore mentioned Vehicle Application, Functional Requirements and subsequent selection of Design Features, will cover the field of interest.

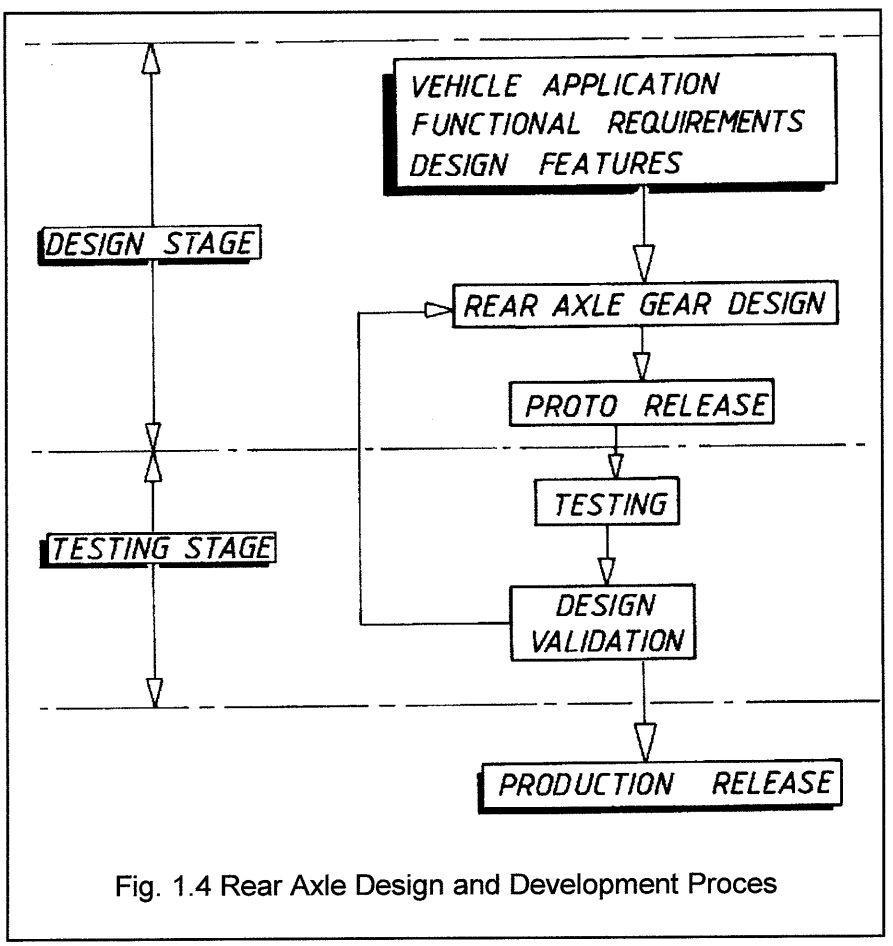

Fig. 1.4 Rear Axle Design and Development Proces

1.3 Basic Field of Interest

The group of Design Features for the rear axle gears has been subdivided into groups of distinctive parameters or variables, as indicated in table 1.3. Each of these groups consists of noumerous elements of which some of them are interrelated. In general the total number of all the Design Features mostly is relatively large. The designer of rear axle gears can, in principle, select the required design data out of this relatively large amount of variables in order to calculate and design a rear axle gear. With these variables, it is mostly possible to fulfill most or all functional requirements. If however for every new rear axle design, a selection would have to be made out of those variables, the work for a designer would be very time consuming and difficult!
In most of the cases however, many of the design variables are already established or may be considered as being fixed. In that situation, and this is mostly the case, the designer will be confronted with the following groups of design features that are already determined:

- Gear Quality Level
- Gear Material
- Heat Treatment
- Final Surface Treatment
- Lubricating Oil Type.

The Gear Quality Level, the Heat Treatment and the Final Surface Treatment, in terms of gear manufacturing method as well as heat treatment and final surface treatment installations, can be regarded as already determined, being mostly the installed and available production facilities. The Gear Material as well as it's supplier are mostly already given or known, as is the Oil Type for lubrication. A companies policy for using a specific gear type can be considered as fixed over a longer peroid, even from historical grounds. This situation refers to a relatively large company with at least several thousands of units per year as a production volume.
Purely for design purposes, the gear type and gear geometry as well as the gear assembly are the groups of Design Features in which a gear designer generally has a given freedom of selecting several variables in order to meet the Functional Requirements for rear axle gears. Therefore, the following groups will be the point of interest in this thesis:

- Gear Type and Gear Geometry
- Manufacturing Method
- Gear Assembly.

1.4 Aim of this Thesis

During the last years, most of the truck manufacturers have been confronted with ever more increasing demands on their products and on the development process. These demands are reflected in higher engine power, lower vehicle noise, higher fuel economy and shorter lead times in development.
Increasing engine power and higher power density, resulting in a higher loading of the driveline and more severe use of vehicles, set higher demands on the loadability and the endurance capability of the rear axle gears. The legislative stringent requirements for exterior vehicle noise especially in urban areas have increased, as well as a decreasing interior noise level which is considered as a quality item for commercial vehicles, also set high demands on the noise level of rear axle gears.

The need for fuel economy gives even more demand on the mechanical efficiency of the driveline in general and on the rear axle gears specifically. Rear axle efficiency under typical highway conditions, high speed and low torque, is required to be low for the vehicle overall fuel consumption. For a typical hillclimb condition, low speed and high torque, the rear axle efficiency requires a low value in order to limit the maximum temperature of the lubricating oil. The allowable leadtime for the development of rear axles has been reduced during the last ten years. The pace in which the market requirements change, requires a very flexible way of responding in the development of new products.
In most of the commercial vehicles, single stage hypoid gears are used in the rear axles. Not only does this give a better fuel consumption; the noise level mostly is lower. Also the number of rear axle parts is smaller and hence the weight of a single ratio hypoid axle will be lower than of a two stage hub reduction axle. For this reason, this thesis will be mainly focussed on single stage hypoid rear axle gears.

One of the most important aspects of rear axle gears is however the strength of the teeth, as it directly invokes the reliable functioning of the rear axle. Gear tooth breakage is in this aspect very important; this type of gear failure would immediately lead to a non acceptable standstill of the vehicle. Therefore the tooth root strength for rear axle gears will be further investigated in this thesis. The main focus will be the design of gears on basis of verified endurance tests.
Therefore, the **AIM** of this work will be:
a. To determine a practical design method for rear axle hypoid gears for commercial vehicles.
b. The calculation and design method should be focussed on tooth root strength.
c. The method should be practical applicable and therefore should be correlated with actual endurance life test results with constant amplitude loading.
d. In relation to Vehicle Applications, a link to variable amplitude loading is required.
e. A strategy should be given for the design of a vehicle rear axle gear.

Here the rear axle noise, weight, efficiency and manufacturing costs are not to be considered as boundaries or restrictions; the design should only be focussed on strength. As different calculation methods for bevel and hypoid gears already exist at the time, it is **NOT** the aim to give a quality indication on these calculation methods. Therefore, no judgement will be given on the applicability of these calculation methods. The only aim is to use a certain calculation method that will be made suitable to the design of rear axle gears, on a practical approach.

1.5 Procedure to be used

Starting point will be the already existing calculation standards for bevel gears, that are generally accepted and described in international standards.
The analytical expressions for calculating the tooth root stress for bevel gears will be analysed and compared. Not only the expressions for the individual factors will be compared; their numerical values also will be evaluated. Special attention will be paid on those parts of the calculations, that still leave a relatively large variation in their numerical value, which is a result of the specific application, such as vehicle rear axle gears.

Current theory on the dimensioning and strength of hypoid gears will be discussed. Hardly any international standard is available here; several manufacturers for gear production

installations give design directives for the dimensioning of hypoid gears. Mostly it is up to the individual designer or manufacturer of rear axle gears to apply specific hypoid calculation methods. Mostly he is forced to develop these methods by himself for the specific vehicle applications. During the last years however, many investigations have taken place by research institutes on the strength of hypoid gears. The latest findings of these recent investigations will be compared with already existing design directives for hypoid gears.

Endurance tests with Constant Amplitude Loading have been performed on rear axle hypoid gears of four different axle types, covering a range of dimensions. Statistical evaluation of the endurance results will be performed to determine the failure probability.
The results of theoretical calculations then will be compared with the experimental findings of the endurance tests. If necessary, several factors in the calculations will have to be adjusted in order to fit both results. The corrections in the calculations will have to be based on a physically acceptable basis. In this way, a rather practical correlation will be obtained between theoretically calculated and actually measured gear endurance life. These results will however then only take account for a constant amplitude loading.

As rear axle gears for vehicles are hardly submitted to constant loading, a link is required here to variable amplitude loading. Different types of driveline Loading Spectra for vehicle driveline components will be evaluated. On the basis of a unified loading spectrum, some tests with Variable Amplitude Loading will be performed on rear axle gears. The results of these tests will then give an indication on the required damage accumulation theory and possibly further corrections for life calculations.

Finally, a method will be introduced for designing rear axle gears in a preliminary way, with a relatively low amount of available data. Scale laws for rear axle gears will be derived in order to be able to design on a preliminary indication the most important dimensions.

1.6 General Remarks on Stress Calculations

Today, many international standards exist for gear calculations such as ISO, DIN, BS, and AGMA. All methods will give different calculated stress levels for a given gear geometry and known loading conditions. At this time, the ISO is working on an international standard which is based on the different existing standards. It should be advisable, of course, to have one and the same uniform and generally accepted method, all over the world. This will make the exchange and comparison of calculation results more accesible and thus profitable.
It is however very well understandable that at the time there are many different standards for gear strength calculations. This is not surprisingly, as each of these standards has been developed individually by verification of results with practical field experience over several years. As long as a calculation standard is verified on actual field experience, it will be a prefered method, despite the fact that it may hold several simplifications and assumptions.
It should always be remembered that strength calculations are a tool for designing gears. They are not a goal on their own; at least from the designers point of view.
Therefore simplifications on the actual gear loading and stress situation are well acceptable. The most important aspect is that stress calculations should always be linked to field experience or be compared to practical results. The fact that some parts of the calculations are simplifications on their exact physical phenomena, is in this view very well acceptable.

Loading conditions, such as variable torque and speed, vibrations and dynamic effects on gearload can hardly be determined accurately. They are very much dependent on the conditions of each specific application. Not only for new, but also for existing gear applications, it is very difficult to predict the actual loading conditions on the gears to a level of accuracy, that is comparable to which the geometry is described and designated.
On the material side, there will also be a variation in material characteristics such as for fatigue strength. These will always lead to a certain variation in endurance life, even by accurate and constant loading conditions. If the assumed values of loading conditions and material characteristics are not on the same level of accuracy as the geometry and stress calculations are, then it is not directly of interest to strive to one and the same uniform calculation method for gears. For the time being, it seems to be more important to bring the uncertainty in the loading conditions and the variation in material characteristics at the same level of accuracy as the stress and geometry calculations are.

In view of this, the statistical character of determining the loads will become more important in the future than the deterministic character of geometry and stress determination. Statistical prediction and simulation of loads and loadspectra will become the most challenging item for gear strength calculations in the years to come.
Therefore, more precise knowledge will be required on the actual loads that can be expected on the gears at their specific application, rather than further improving on the other parts of the calculation standards that are already accurate in their description. It appears to be not that necessary to improve the influence of several geometric effects on the calculated stress. A link between calculated stresses and actual loading conditions or vehicle applications here is much more required. Especially in the events of failure, a reference can be established as to what the goal should be to design gears.

If in the future gears will be loaded much more to their allowable stresses, then a uniform and clearly predictable calculation method will be necessary. For this, a generally accepted and uniform calculation method is advisable. But first, a correlation is required of this new method with a very large number of actual field experiences.

These considerations are applicable to gear strength calculations that are based on analytical expressions and equations. The last years, an increase in the use of numerical based calculation methods can be seen. For the time being, these applications are resticted to fundamental investigations and protoype comparison calculations. It has still not come to a scale of importance as on general industrial installations. Here also, the confirmation between calculated results and actual field experience is of vital importance. Furthermore, the required mathematical and computer experience of numerical calculation techniques is quite larger than it is for analytical techniques. In the end, the required accuracy for calculation methods need not to be higher than the highest accuracy of one of the endurance strength determining members such as material behaviour or loading conditions.
For design and development purposes however, in terms of relative improvements for different designs, numerical calculations generally will be superior to analytical calculations; especially when gears are loaded more and more to their limits. Not only will the experience of the user with the calculation software be of great importance; the model assumptions and the applied elements require a strict application when reliable results are expected.
In the end however, also these numerical calculation methods will require a comparison with and an evaluation on actual field experience or testing results. If this is not the case, then the accuracy of the calculation results will allways remain questionable, irrespective of the calculation method.

2 TOOTH ROOT STRESS CALCULATIONS OF BEVEL GEARS

2.1 Introduction

Gear tooth breakage can be considered as one of the major dimensions governing aspects of bevel and hypoid gears for automotive applications. It is a failure mode that will almost certainly lead to a standstill of the vehicle, which is an unacceptable situation for the user. In practical vehicle applications, this type of failure should therefore be prevented. A static tooth breakage may occur as a result of a mis-use situation of the vehicle driveline, leading to a sudden overloading of the gears. A fatigue breakage of the teeth may occur as a result of a vehicle use that goes beyond the specified application. As a result of it's importance, all standards on gear design calculations are still under development [2.1] [2.2].

In this chapter, first an overview will be given on the most current available analytical methods for calculating the tooth root stress for spiral bevel gears. The original expressions of the standards appear to have relatively large differences. When the individual terms of the stress equations are however rearranged, it will become clear that in fact they can be considered as all being built up in one and the same way. In this rearrangement of the several stress equations, the individual effects in different calculation methods can be compared directly. A comparison between the individual factors of the different methods will be given. Finally the difference in numerical values for the calculated tooth root stress will be discussed.
It will become clear that the differences in calculated tooth root stresses may be very large. The differences in calculated safety factors are, however relatively small. In view of this, most of the rear axle gears that have been designed all over the world with these different methods, resulting in very different stress values, have not led to large differences in gear dimensions for comparable vehicle applications. Therefore it is very important to realise that a given calculation method, resulting in specific stress values, should always be linked to the accompanying material values and safety factors. In that way it is possible to handle or compare different methods to calculate and to design automotive rear axle gears. If a particular method is verified with practical experience, then this will lead to a proven and reliable standard. If something here is changed, be it the material values or several calculation factors, then also the reference value needs to be altered likewise.

At this time several methods for bevel gear tooth root stress calculations are in existence. The two most important are the international standards for the gear industry, which are used for a very wide range of applications. Apart from these standards, the automotive industry has its own specific methods; mostly because in this field bevel gears have specific conditions and well known applications. In the course of the automotive history, specific standards have been developed by several automotive manufacturers, as well as by manufacturers of bevel gear machining systems such as Gleason, Oerlikon and Klingelnberg. These standards only consist of analytical calculations.

The calculation methods for bevel gears that will be studied and compared, are:
A. ANSI/AGMA 2003-A86; approved as National Standard in May 1986 [2.3].
B. DIN 3991, Part 1 and 3; Deutsche Norm, DK 621.833.2.001.24, September 1988 [2.4].
C. Gleason; Gleason Works publications [2.6] to [2.8].
D. Oerlikon Version VL; Oerlikon publications [2.18] to [2.20].

The Klingelnberg method [2.22, 2.23] is not included in this comparison. The reason for this is that this manufacturing system is not used on a comparative scale in the automotive industry as the other two systems are. In general industrial applications, however this gearing system is much more widely used.
Prior to stress calculations, the proper geometrical data have to be calculated, forming the first step in stress calculations. Therefore, first the different geometry calculations will be discussed.

2.2 Geometry calculations

2.2.1 Basic geometry expressions

All calculations on the geometry of bevel gears, required for stress calculations, come down to applying the so called virtual gears. First the virtual helical gears that are to substitute the bevel gears are determined. Finally these virtual helical gears are also substituted by spur gears of which the calculation basis is known. Extra factors are of course introduced for taking into account the difference between the real bevel gears and their virtual substitutes. This method is very well known and it is in use since a relatively long time. Generally the following scheme can be drawn:

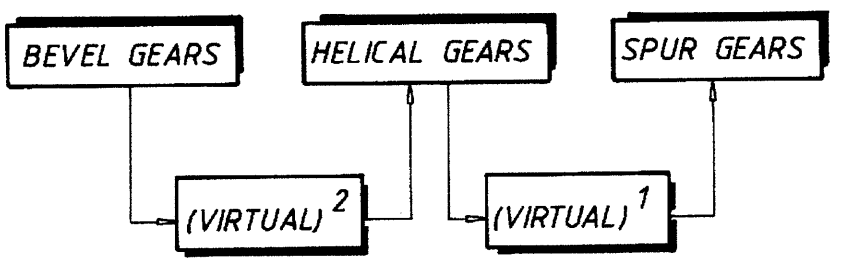

Fig. 2.1 Simplification of Geometry Calculations for Bevel Gears

Specific geometry data of spur gears are calculated in the normal section, where the geometry and the equations are well known. Helical gears are substituted by virtual spur gears, and these in their turn are calculated by the same methods, keeping in mind the difference between the actual helical and their virtual spur gears.
Bevel gears first are substituted by virtual helical gears. These in their turn are then represented by virtual spur gears. In fact these spur gears may then be considered as virtual^2 gears for the actual bevel gears to be calculated. In fact, for hypoid gears, the same procedure is applied for geometry calculations. This will be discussed in the following chapter.

The calculations of the gear geometry that are discussed here are all analytically, as the stress calculations are. During the last ten years however, several numerical calculation methods have been developed, that are mostly required for noise behaviour and contact pattern definition of bevel and hypoid gears. Representants of these calculation methods are [2.49], [2.50] and [3.13]. Whereas numerical calculations are suitable for parameter studies and prototype comparison, analytical methods are still widely in use for geometry and stress calculations.

2.2.2 Comparison of geometry calculations.

The DIN [2.4] and the Oerlikon standard [2.18] have explicite chapters on the geometry of the virtual gears. In the ANSI/AGMA standard [2.3] and the Gleason method [2.6], the calculation of these virtual gears is incorporated in the different expressions; they can be derived by explicitely rewriting several equations. The construction according to Tredgold [2.5] in which the virtual helical gears are determined to substitute bevel gears, is used by all the considered calculation methods. This means that the procedure of virtual gears is a generally accepted method of simplifying the calculation of geometry and stress on bevel gears. Also the middle of the gear facewidth is taken as the reference section for the basic geometry calculations on which later the stress calculation is based. The four calculation methods will now be compared on some aspects of geometry calculations of the virtual helical gears. Calculations of tooth proportions will first be compared, and secondly the profile and face contact ratio's will be discussed.

ANSI/AGMA

Most of the geometry data that are used as input for the calculations, are related to the outer diameter or the outer cone distance of the gear. Also data as module are refered to this section, mostly in the transverse section. Most of the gear data can then be recalculated to the mean face width by means of the ratio outer to mean cone distance. The tooth root stress is however calculated in the midface section. The profile contact ratio and the face contact ratio are calculated in the normal section. Several of the output data refer to the gear outer diameter. The active field of meshing is considered to be of an elliptic shape, resulting from the limited dimensions of the contact pattern. Therefore the overall contact ratio is called a modified contact ratio; it can be regarded as a vectorial addition of the profile and face contact ratio.

DIN 3991

This standard gives calculations of tooth proportions for gears with tapered and constant tooth height. Here the mean of the facewidth is the reference section for the virtual gears and the normal section is used. A limited contact pattern is taken into account by means of the effective face width, which generally is 85% of the geometrical face width. This effective facewidth is applied in the face contact ratio, the Helical Factor and the tooth root stress. The overall contact ratio is the same as for helical gears, being the sum of profile and face contact ratio.

Gleason

The calculations according this procedure are identical to the ANSI/AGMA standard. Most of the calculated geometry data are refered to the outside diameter and in transverse section. In comparison with ANSI/AGMA only some symbols have different designations. These calculations only refer to teeth of tapered tooth height.

Oerlikon

In this system, the P point on the gear face width is the reference for the stress calculations. Depending on several factors, but mainly on the ratio cutter diamater to mean cone distance, an Oerlikon gear may be of the so called P or N type of gearing. This reference point for stress calculations may differ from the mean face width of the teeth. These calculations are applicable to teeth of constant tooth height.

All four considered analytical geometry calculations hardly differ with regard to the calculation of:

* tooth proportions of the actual bevel gear geometry in the middle of the facewidth,
* virtual helical gears in the transverse and in the normal section.

2.2.2.1 Tooth proportions.

In general, there is a clear distinction in describing the tooth proportions between bevel gears with a tapered tooth height and those with a constant tooth height. Each type of tooth form has it's own geometrical parameters that describe the actual tooth proportions.
For a clear comparison of gears with similar dimensions, the comparison should be made in the middle of the facewidth, which is the reference point for all considered calculation standards.
Please note that in the text the words "crownwheel" and "gear" are both used to designate the driven member of the bevel or hypoid gearset, whereas "pinion" stands for the driving member.

Gears with tapered tooth height
For determining the tooth proportions of bevel gears with tapered tooth height at the **middle** of the gear facewidth, the following parameters are to be used [2.8]:

* gear addendum factor c_1
* depth factor k
* clearance factor c_c

Generally the values for these parameters depend on the gear type (hypoid or spiral bevel), the number of pinion teeth and the gear ratio. The guidelines [2.15, 2.16] distinguish automotive and non automotive applications, as well as different gear cutting methods.
The following tooth proportions are determined at the pinion and crownwheel **mean** diameter:

* whole depth h and working depth h_w
* addendum of pinion a_P and gear a_G
* dedendum of pinion b_P and gear b_G
* clearance c.

These are then calculated to the outer diameter of the gears by means of the ratio of mean to outer cone distance and the addendum and dedendum angles. Most of the calculation output of these standards contains information on tooth dimensions at the gear and pinion outer diameter. Some typical geometrical characteristics of these gears, such as module and gear diameter, almost always refer to the transverse plane at the gear outer diameter.
Corrections for machining characteristics and limitations are also given; these are not given here.

Gears with constant tooth height
The tooth proportions for bevel gears with constant tooth height are described by the following parameters, that refer to the **middle** of the gear facewidth [2.20]:

* addendum factor h_{fw}
* clearance factor k_s
* pinion profile shift factor x_{m1}

The following tooth proportions are determined at the pinion and crownwheel mean diameter:

* whole depth H_z and working depth H
* addendum of pinion H_{k1} and gear H_{k2}
* dedendum of pinion H_{f1} and gear H_{f2}
* clearance k_s.

When specific tooth proportion parameters are given, it may be possible to calculate the geometrical dimensions from a tapered tooth to a constant tooth and vice versa in the middle of the facewidth. The equations from table 2.1 can be used for this of which the dimensions are given in fig. 2.2.

Tooth Proportion Factor	Tapered Tooth Heigth	Constant Tooth Heigth
Working Depth	$h_w = ½ * k$	$H = 2 * (h_{fw} - k_s)$
Whole Depth	$h = ½ * k * (1+c_c)$	$H_z = (2 * h_{fw} - k_s)$
Clearance	$c = ½ * k * c_c$	k_s = given
Pinion Profile Shift	$- = ½ * k * (½ - c_1)$	x_{m1} = given
Gear Profile Shift	$- = ½ * k * (c_1 - ½)$	$x_{m2} = - x_{m1}$
Pinion Addendum	$a_P = ½ * k * (1 - c_1)$	$H_{k1} = (h_{fw} - k_s + x_{m1})$
Pinion Dedendum	$b_P = ½ * k * (c_1 + c_c)$	$H_{f1} = (h_{fw} - x_{m1})$
Gear Addendum	$a_G = ½ * k * c_1$	$H_{k2} = (h_{fw} - k_s - x_{m1})$
Gear Dedendum	$b_G = ½ * k * (1 - c_1 + c_c)$	$H_{f2} = (h_{fw} + x_{m1})$

Table 2.1
Geometrical Factors for Tooth Proportions in the Midddle of the Facewidth.

To obtain the absolute values for the different tooth proportions, the factors of Table 2.1 have to be multiplied by the mean normal module.

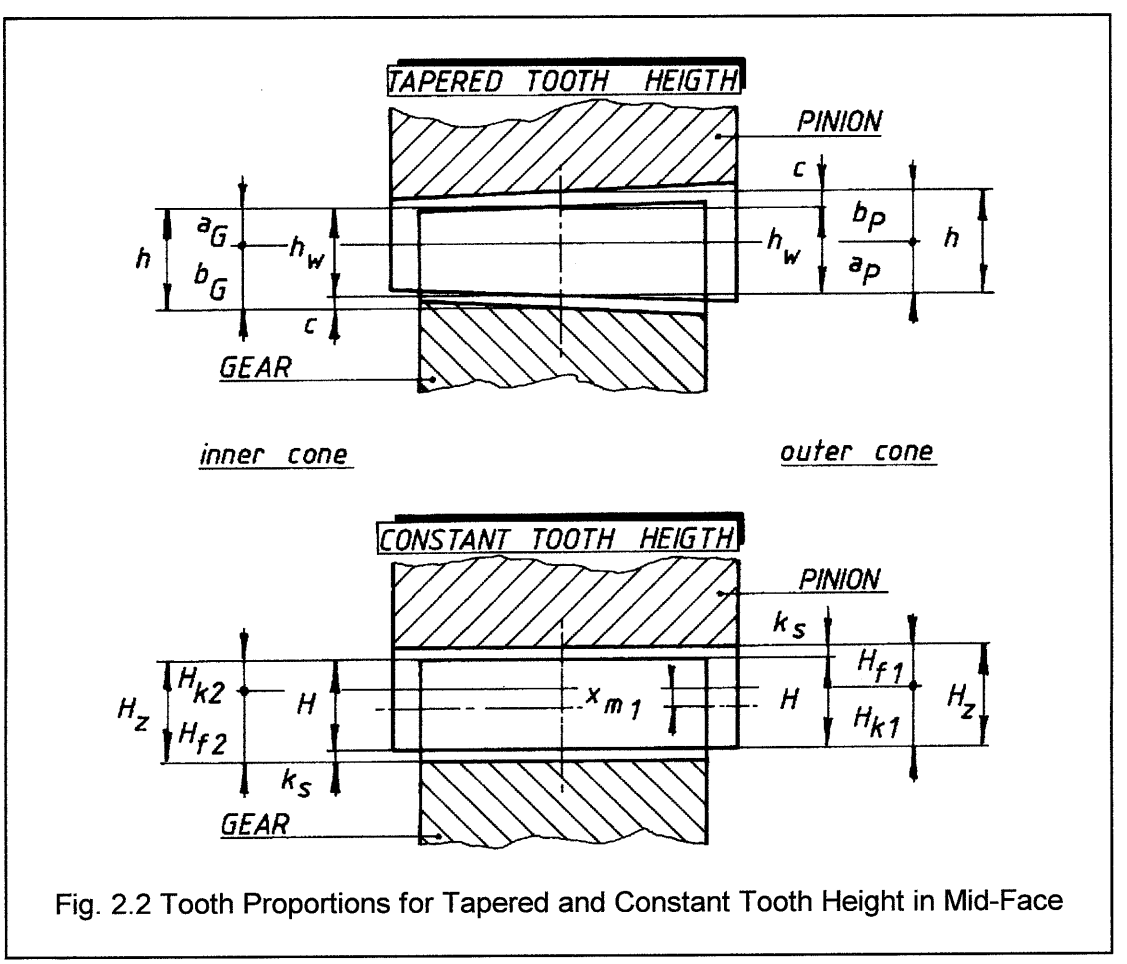

Fig. 2.2 Tooth Proportions for Tapered and Constant Tooth Height in Mid-Face

2.2.2.2 Profile and Face Contact Ratio

The expressions for the contact ratio's, based on the original equations for the different standards may be rewritten for reasons of comparison.
The **Oerlikon** expressions may be modified as:

$$\epsilon_{v\gamma} = \epsilon_{v\beta} * (1+\frac{\epsilon_{v\alpha}}{\epsilon_{v\beta}}) \qquad (2.1)$$

The **DIN** expression may be rewritten as:

$$\epsilon_{v\gamma} = 0.85 * \epsilon_{v\beta} * (1+\frac{1}{0.85}*\frac{\epsilon_{v\alpha}}{\epsilon_{v\beta}}) \qquad (2.2)$$

The **ANSI/AGMA** and **Gleason** equations as:

$$m_o = m_F * \sqrt{1+(\frac{m_p}{m_F})^2} \qquad (2.3)$$

Equation (2.2) includes the influende of the effective facewidth, which according to DIN is 85% of the geometric facewidth for general situations. The value of 0.85 is written here explicitely, whereas the expression for the face contact ratio ϵ_β is based on the full geometrical facewidth.

The individual values for the profile and the face contact ratio, calculated according to the four different methods for one and the same bevel gear geometry, do not differ substantially. The overall contact ratio's, however differ to some extent. The amount of the difference depends on the gear geometry. The ANSI/AGMA and Gleason methods determine a modified contact ratio; the limited contact dimensions are taken into account by assuming an elliptical shape for the contact pattern. The total contact ratio here is the vectorial sum of the profile and face contact ratio. In the DIN and the Oerlikon method, the total contact ratio is the numerical sum of profile and face contact ratio. The ratio of the total to the modified contact ratio may be expressed as:

$$\frac{\epsilon_{v\gamma}}{m_o} = \frac{1+\frac{\epsilon_{v\alpha}}{\epsilon_{v\beta}}}{\sqrt{1+(\frac{m_p}{m_F})^2}} \qquad (2.4)$$

A graphical representation of this last relationship is given in figure 2.3, as a function of the ratio of profile/face contact ratio. For most automotive applications, the ratio of the profile to the face contact ratio mostly lies between 0.5 - 1.0. It shows that for automotive bevel gears, the value for the total contact ratio according to Oerlikon generally is about 15 - 30% larger than the modified contact ratio calculated according to ANSI/AGMA and Gleason, when the efffective facewidth of 85% is assumed. When the effective facewidth of the gears is not taken into account (it then is equal to the geometrical facewidth), the difference will become 30-40%.

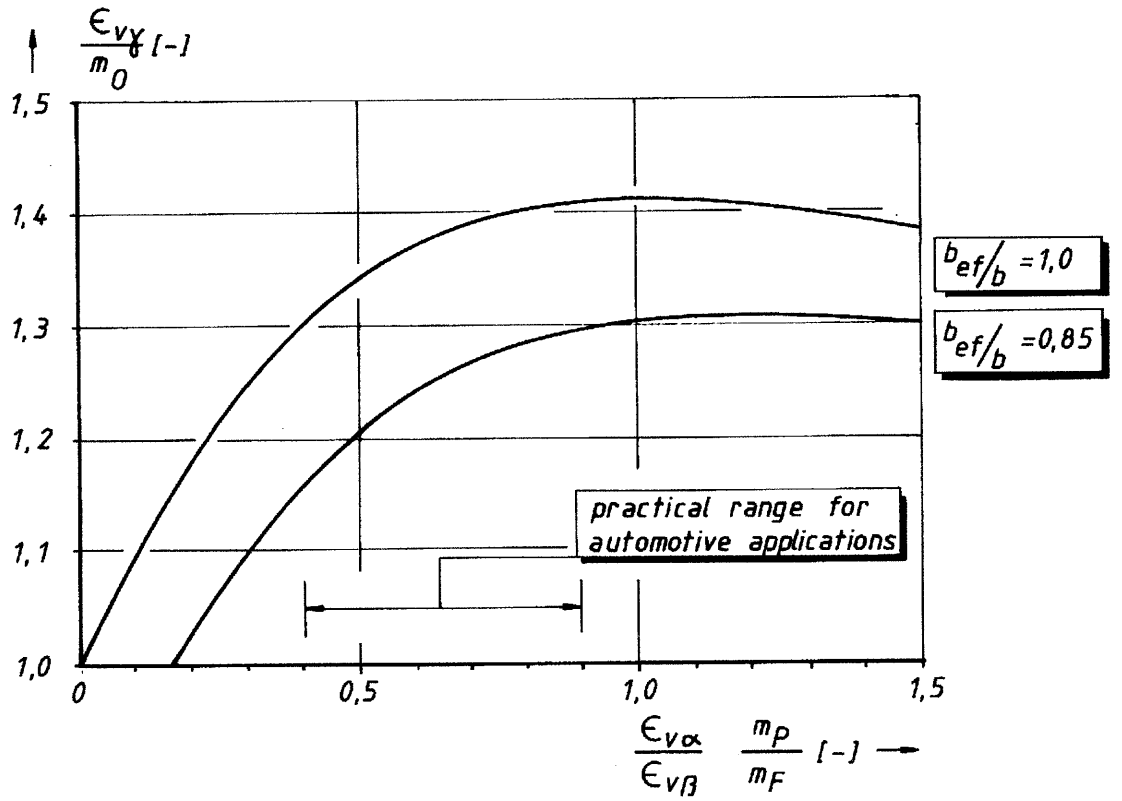

Fig. 2.3 Ratio of Total Contact to Modified Contact Ratio

* *All considered calculation standards use virtual helical gears for describing the tooth proportions of bevel gear teeth.*
* *The geometry in the normal section at the middle of the gear facewidth is used as the reference point for geometry calculations in all standards, some with minor modifications for the position of contact pattern.*
* *The individual values for the profile and face contact ratio are next to identical for one and the same gear geometry, when calculated by different standards.*
* *For the total and the modified contact ratio's, however, differences in the numerical values arise betweeen the different standards. This is a result of the different definitions for the total and the modified contact ratio.*
* *The total contact ratio of DIN and Oerlikon will be about 15-30% larger than the modified contact ratio of AGMA and Gleason and will be 30-40% larger when the effective facewidth according to DIN is not taken into account.*
* *This is valid for general automotive applications.*

2.3 Tooth Root Stress Calculations

2.3.1 Basic Stress Expressions

Since the beginning of analytical stress calculations on gear teeth, the model of a one side clamped cantilever beam with a specific section and loaded with a unit load, has been used. In [2.1] and [2.30] the history of gears and their calculations is given, as well as the important equations that have been used. In view of this it not surprisingly that the basis of almost all tooth root stress calculations is very close to this type of modelling. The calculation standards that are considered here, all are built up in a similar way. Therefore, this setup is taken over here. Nowadays, numerical calculation methods such as Finite Element Methods (FEM) or Boundary Element Methods (BEM) may be used, but these calculations are not considered here.
The basic set up of the analytical stress calculations for tooth root stress of gears in general and bevel gears in specific, can be seen as the product of three groups of independent factors, where each group on it's own is also a product of individual factors. These three groups of factors are the Load, the Geometry and the Material Factors. Generally the basic lay-out for root stress calculations is:

Actual Tooth Root Stress =
Load Factors * Generalised Stress * Geometry Factors

$$\sigma_{1,2} = \Pi K_{load} * \frac{F_{mt}}{b * m_{m_n}} * \Pi Y_{geometry} \qquad (2.5)$$

Actual Tooth Root Stress <
Allowable Tooth Root Stress * Material Factors

$$\sigma_{1,2} \leq \sigma_{all} * \Pi M_{material} \qquad (2.6)$$

2.3.2 Comparison of Stress Calculations

Recently, several comparisons have been made between the different standards of bevel gears. These comparisons have up to now only been performed on a more or less integral way. This means that the numerical values of the final calculation results are compared, together with a comparison of the basic set-up [2.36] to [2.39].
The individual load, geometry and material factors ought to be comparable, qualitatively and also quantatively, in order to perform a comparison of the individual standards. At a first glance, the expressions for tooth root stress appear to differ in a relatively large extent. However it is possible to rearrange all the used factors in these equations in one unified way, thereby giving the possibility of directly comparing all the different factors separately. The stress equations will be rearranged, keeping the sequence of the individual factors as much as possible the same, although in some way it may be slightly arbitrary. However, the idea is to make at least one kind of uniformity in these expressions. The original expressions of the several standards will be given in the original symbols.

The basis for this is the generalised tooth root stress. This generalised tooth root stress is defined as the tooth tangential load in the middle of the facewidth, divided by the geometrical facewidth and the mean normal module. It has the dimension of a stress. In this expression, a uniform and equally distributed tooth load along the facewidth is assumed.
This generalised tooth root stress is:

$$\frac{F_{mt}}{b*m_{m_n}} \qquad (2.7)$$

2.3.2.1 ANSI/AGMA

This standard is built up of fundamental rating formulas for bending strength and applies to tapered depth and uniform depth teeth. Only the major factors which are known to affect gear tooth fracture at the root are considered. It's use is intended to compare several different gear designs. It is based on the cantilever projection method that is modified in order to consider:

* the bending and the compressive tooth root stress
* inclined contact lines on the teeth
* stress concentration at the root fillet
* load sharing between adjecent teeth

Some of the most important conditions on which the ratings can be determined, are:

* proper lubrication
* normal misalignment and load deflection
* case carburised steels
* optimal or developed contact patterns

The original equations are:

$$S_t = \frac{2000*T_p*K_a}{K_v} * \frac{1}{F*d*m} * \frac{K_s*K_m}{K_x*J} \qquad (2.8)$$

$$J_{p,g} = \frac{Y_{k_{p,g}}}{m_N*K_i} * \frac{r_t}{r} * \frac{F_{ep}}{F_p} * \frac{m_m}{m} \qquad (2.9)$$

$$S_{wt} = \frac{S_{at}*K_L}{K_T*K_R} \qquad (2.10)$$

$$S_t \leq S_{wt} \qquad (2.11)$$

In the ANSI/AGMA standard, the Size factor is included in equations of the calculated stress for practical reasons, as indicated in Chapter 9 of that standard. This is also the case for the Gleason standard. When rewriting however the stress expressions of the standards in the unified way of equation (2.5), the Size Factor Ks of both the ANSI/AGMA and the Gleason standard will be designated here to the Material Factors.

Therefore, the calculated tooth root stress of the unified expression principally differs from the one of the original standard. For this reason the actual stress here will be designated by the sign ". Expressions (2.8) to (2.11) are rewritten in the same way as expressions (2.5) and (2.7), leading to the following unified expressions (Attachment 2.3.1):

$$S''_t = K_a * \frac{1}{K_v} * K_m * \frac{F_{mt}}{F * m_{m_n}} * \frac{1}{Y} \left(= \frac{m_{m_n}}{Y_K} * \frac{P_d}{K_f}\right) * K_f * m_N * K_i * \frac{1}{K_x} * \frac{r}{r_t} * \frac{F}{F_e}$$

$$S_t \leq S_{a_t} * \frac{1}{K_R} * K_L * \frac{1}{K_S} * \frac{1}{K_T} \qquad (2.13)$$

2.3.2.2 DIN

Principally this standard is based on the work of Winter and Niemann [2.5]. In later years the equations have been further developed, finally leading to the DIN 3990 standard for helical gears [2.4]. On basis of this the definitive DIN 3991 standard for bevel gears has been issued in 1988. The equations in this standard are valid for so-called Null or V-Null gears, this means that the value of the profile modification factors or its sum is zero. Furthermore it is limited to bevel gears of which the virtual helical gears have a contact ratio less than 2. The material values have a failure probability of 1%. The variation of geometric values as well as the estimate on real loadings, manufacture and mounting errors and lubrication give rise to some variation in results. The factors on the gear geometry have to be calculated according to the expressions of the standard. The load factors can be determined in four different ways, namely Method A, B, C and D. In the expressions, the method that has been used, will have to be indicated by an index. The accuracy and the amount of calculations differ between all four methods. The expressions of Method B have been used here.
The four basic expressions are:

$$\sigma_F = \sigma_{Fo} * K_A * K_V * K_{F_\beta} * K_{F_\alpha} \qquad (2.14)$$

$$\sigma_{F_o} = \frac{F_{mt}}{b_{ef} * m_{m_n}} * Y_{fa} * Y_{sa} * Y_\epsilon * Y_\beta * Y_K \qquad (2.15)$$

$$\sigma_{Fp} = \frac{\sigma_{FE}}{S_{F\min}} * Y_{\delta_{relT}} * Y_{R_{relT}} * Y_x = \frac{\sigma_{FG}}{S_{f\min}} \qquad (2.16)$$

$$S_f = \frac{\sigma_{FG}}{\sigma_F} \leq S_{f\min} \qquad (2.17)$$

Rewriting equations (2.14) to (2.17) to the same uniform way (Attachment 2.3) yields:

$$\sigma_F = K_A * K_v * K_{F_\beta} * K_{F_\alpha} * \frac{F_{mt}}{b * m_{m_n}} * Y_{fa} * Y_{sa} * Y_\varepsilon * Y_\beta * Y_K * \frac{b}{b_{ef}} \quad (2.18)$$

$$\sigma_F \leq \frac{\sigma_{FE}}{S_{F\min}} * Y_x * Y_{\delta_{relT}} * Y_{R_{relT}} \quad (2.19)$$

2.3.2.3 Gleason

This company has a very long experience on bevel and hypoid gear design and manufacture, mostly for automotive applications. The literature in which the stress calculations are given, [2.9] to [2.16], shows the development of their calculation method throughout the years. In fact the ANSI/AGMA standard and the Gleason method are very much interrelated to each other. The Gleason method is mostly applicable to automotive applications. The four most important expressions from this standard are next to identical to the ANSI/AGMA standard with the exception that the Gleason method uses American units.

$$S_t = \frac{W_t * K_o}{K_v} * \frac{P_d}{F} * \frac{K_s * K_m}{J * K_x} * 0.061 \quad (2.20)$$

$$J = \frac{Y_K}{m_N * K_i} * \frac{R_t}{R} * \frac{F_e}{F} * \frac{P_d}{P_m} \quad (2.21)$$

$$s_w = \frac{s_{at} * K_L}{K_T * K_R} \quad (2.22)$$

$$s_t \leq s_w \quad (2.23)$$

In Attachment 2.3 these equations are rewritten to the unified equation:

$$S''_t = K_o * \frac{1}{K_v} * K_m * \frac{F_{mt}}{F * m_{m_n}} * \frac{1}{Y} \left(= \frac{m_{m_n}}{Y_K} * \frac{P_d}{K_f} \right) * K_f * m_N * K_i * \frac{1}{K_x} * \frac{R}{R_t} * \frac{F}{F_e}$$

$$S_t \leq S_{at} * \frac{1}{K_R} * K_L * \frac{1}{K_S} * \frac{1}{K_T} \quad (2.25)$$

2.3.2.4 Oerlikon

The strength calculations are based on Niemann [2.17], and given in [2.18] to [2.20].

$$\sigma_b = B_w * q_w * z_e \tag{2.26}$$

$$B_w = C_s * C_D * C_T * C_\beta * B_e \tag{2.27}$$

$$B_e = \frac{10^3 * M_d}{d_{p1} * b * r_e} \tag{2.28}$$

$$\sigma_b \leq \frac{\sigma_D}{S_b} \tag{2.29}$$

Attachment 2.3 gives the unified expression of the Oerlikon equations, which is:

$$\sigma_b = C_S * C_D * C_T * \frac{F_{mt}}{b * m_{m_n}} * q_w * C_\beta * \cos\beta_m * \frac{d_m}{d_p} \tag{2.30}$$

$$\sigma_b \leq \sigma_D * \frac{1}{S_B} \tag{2.31}$$

Figure 2.4 gives all expressions for the four calculation methods, expressed in one and the same uniform way where the individual factors (i.e. Load Factors, Geometry Factors and Material Factors) now can directly be compared. The positioning of several factors into one of the three groups of Load, Geometry or Material Factors may be arbitrary at a first glance; the specific influences however described by these factors correspond physically very well to each other.
It can be seen that these methods are all built up in an identical way, although they originated and have been developed more or less independently of each other. The original expressions give the impression of relatively large differences in the basic set up, but after rewriting them it appears that the layout is basically very much comparable. Some calculation methods have aspects that others do not have. The AGMA and Gleason standards, for instance, do not have an explicit Helical Factor, but the influence of inclined contact lines is taken into account by the modelling of the Effective Facewidth and the Load Sharing Factor. The DIN and Oerlikon standards do not have an explicit Point of Load Application and Gear Cutter Factor.

* *The expressions for the tooth root stress according to the four standards can* *
* *and have been rewritten by separating Load, Geometry and Material Factors.* *
* *All expressions of the individual factors are now written similar and thus can* *
* *be compared directly in this way.* *

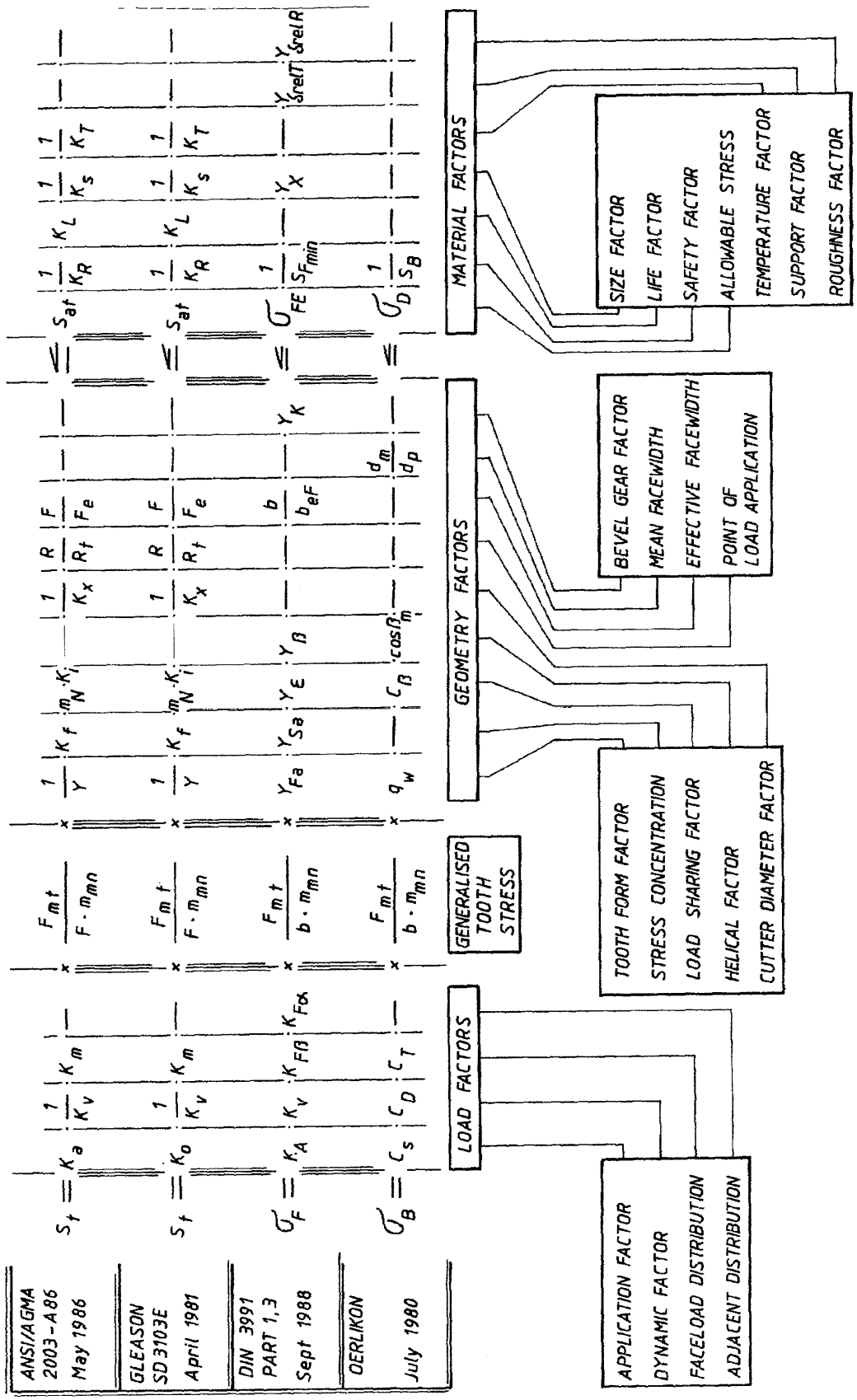

Fig. 2.4 Summary of Tooth Root Stress Calculation Methods with Individual Factors arranged

Several other specific influences on the calculated tooth root stress of bevel gears are not taken into account in these methods. These influences may be:

- The conical shaped form of the pinion body as well as the flat body of the gear.
- The possible small rim thickness of the crownwheel body beneath the teeth.
- The helicoidal form of the teeth over the pinion cone.
- The varying value of the spiral angle over the facewidth.
- The varying angle of the contactline over the facewidth.
- The sensibility of the contact pattern due to deflection and loading.
- The growth of the contact pattern due to deflection and loading.
- Concave/convex or convex/concave contact of both flanks.
- Non-symetrical tooth form because of different pressure angles at Coast and Drive.
- Mounting and assembly deviations of pinion and crownwheel.

Some of these mentioned factors may be of a relatively large influence, others may be of smaller interest. Some of these factors may possibly emerge in new standards, such as the ISO/DIS 6336. These go beyond the scope of this thesis; therefore these aspects are not dealt with here.

In the following part, the individual Load, Geometry and Material Factors will be compared and discussed. The summarising conclusions of the comparisons will be given in the text. Some individual formulations and their numerical values will be analysed in Appendix 2.2.

2.4 Load Factors in Stress Calculations

The four Load Factors account for the influence of:

* Varying loads due to changing load conditions in time: Application Factor.
* Dynamic loads of gear meshing during operation: Dynamic Load Factor.
* Load distribution along the face width: Faceload Distrubution Factor.
* Load distibution on adjacent teeth: Adjecent Load Distribution Factor.

In this part these load factors will be considered and compared for the four calculation methods.

2.4.1 Application Factor

In general, this Application Factor takes into account the loading on the gears, caused by external sources. The influence of the amount of vibrations and variable loading conditions is contained in this factor.
The Application Factor is directly related to the driveline loading spectrum which is determined by the actual loading conditions during operation. The values for the Application Factors can vary from 1.00 to 2.50 or even higher, depending on the application and the calculation standard. There are no mathematical expressions given in the different standards. Only indications are given as to what appropriate values may be used. The numerical value for the Application Factor is to be left to the specific application and the field experience the designer has with gears of similar applications. The range of applicabilty of the two international standards is relatively wide because of the intended use. The Gleason and Oerlikon standards refer mostly to automotive applications; some limited industrial use is however foreseen.
It becomes very obvious that the indicated values for the Application Factor are guidelines. Most of the other factors that are used in the strength calculations have a relatively high accuracy. In comparison to this, most other Factors are calculated with an accuracy of about 1-5%, whereas

the accuracy of the values for the Application Factor are about 50%. In view of this, it is very important to realise that it is necessary to try to estimate the exact value of this application factor. In fact it is much more important to designate the actual value of the application factor, than to try to improve on the accuracy of further geometry factors.

2.4.2 Dynamic Load Factor

This factor takes into account the additional dynamic gear loading, mostly as a result of gear meshing. In general the circumferencial speed at the pitch diameter and the gear quality are the two most important influences on the value of the dynamic factor.

In general the methods of ANSI/AGMA and Gleason give a non linear relation between the Dynamic Factor and circumferential speed. The DIN standard gives a linear dependency of the Dynamic Factor with speed; the Oerlikon method gives a next to linear relation with speed. If all gear qualities are comparable, then there is only a small difference in the numerical value for all four methods. This is only valid for a speed of about 10 m/s. For automotive applications the maximum pitch line velocity will be about 10-13 m/s; the load increase resulting from dynamic loads will therefore generally be very low. Incidental load increase that is caused by the gear shifting of the gearboxes is not incorporated in this factor; these loads are considered to be part of the loading spectrum and therefore belong to the Application Factor. Compared with specific literature [2.34], one might expect that the Gleason or ANSI/AGMA method gives a good description of load increase as a function of speed, being more or less non lineair with speed. Table 2.5 gives the different parameters that are covered by the dynamic factor for each method.

	Pitch Speed	Gear Quality	Gear Load	Gear Material	Contact Ratio
AGMA	X	X	--	X	--
DIN	X	X	X	--	--
Gleason	X	X	--	X	--
Oerlikon	X	X	X	X	X

Table 2.2 Parameters in the Dynamic Load Factor.

2.4.3 Face Load Distribution Factor

For spiral bevel gears this accomodates for the non uniform load distribution along the facewidth of the teeth. The load distribution factor generally is a function of:

- Gear facewidth and spiral angle.
- Gear quality and longitudinal correction or crowning.
- Gear deflections in different directions at a given gear load.

The ANSI/AGMA-standard gives a very clearly load-dependency of the Face Load Distribution Factor. The three other methods give a Face Load Distribution Factor, that has a constant value or is hardly independent of the gear unit load. A comparison of the parameters that are used in the different standards is given by Table 2.3.

	Bearing Support	Gear Quality	Gear Load	Gear Deflection	Face Width
AGMA	X	--	X	--	X
DIN	X	--	--	--	--
Gleason	--	--	--	X	X
Oerlikon	X	X	X	--	X

Table 2.3 Parameters in Face Load Distribution Factor.

In literature [2.40] to [2.47], a large number of parameters plays a role in the distribution of the gear load over the facewidth. As a result a relatively large variation in the value of the calculated Face Load Distribution Factor may be expected between different standards.
Generally, the accuracy by which the Face Load Distribution Factor is determined in the standards, is in contrast to the accuracy by which almost all other factors are determined. As the amount of the gear-to-pinion deflection will have a major influence on it, specific deflection measurements will be required to accurately determine the value for the Face Load Distribution Factor.

2.4.4 Adjacent Load Distribution Factor.

This implies a load distribution between adjacent teeth that may give rise to extra loading because of pitch errors. This phenomenon differs from the load sharing by ideal gears without pitch errors and a contact ratio larger than unity. In that situation the actual load on the tooth is lower than if only one tooth would take the entire load.
The only standard using this factor is the DIN. The other calculation standards do not give an explicit indication on this effect.
The ANSI/AGMA and Gleason standards have a so called inertia factor K_i. According to the text in these standards, this factor would allow for the same effect as the DIN used factor. However, this factor K_i is only described as a function of geometrical gear data and does not depend on pitch errors, gear quality and tooth stiffness. Therefore this K_i factor has been submitted here to the geometry factors, as can be seen in figure 2.4.

* *The Application Factor and the Face Load Distribution Factor are the two most* *
* *important stress determining values. Both values are however not determined* *
* *with the same accuracy as the other Load Factors are. For automotive rear axle* *
* *gears, both their numerical values are larger than the Dynamic Load factor and* *
* *the Adjecent Load Factor.* *
* *In some calulation standards the values of the Application Factor and the Face* *
* *Load Distribution Factor are however only given as relatively rough indications.* *
* *More acurately determining the value of both Load Factors will very well* *
* *improve the applicability of the calculation methods.* *

2.5 Geometry Factors in Stress Calculations

The Geometry Factors all take account of the influence of the gear teeth geometry on the value of the tooth root stress. Generally the following factors are used:

* Tooth Form Factor
* Stress Concentration Factor
* Load Sharing Factor
* Helical Factor
* Cutter Diameter Factor
* Effective Facewidth Factor
* Mean Facewidth Factor
* Point of Load Application
* Bevel Gear Factor

These factors originate from the beginning of the stress calculations. A distinct separation of the different Geometry Factors for all calculation standards and their individual influences has been made here. In this chapter, only the most important factors will be discussed where a comparison will be made between the different calculation standards.

2.5.1 Tooth Form Factor

The Tooth Form Factor describes the influence of the form of the tooth in terms of lever bending arm of the gear unit load and the relevant tooth root section. The principal stresses that are taken into account for the resultant root stress are also incorporated in the tooth form factor.
Therefore it incorporates:

* The position of the gear unit load
* The accompanying bending lever arm
* The critical section of the tooth root
* The principal stresses to account for in the critical section of the tooth root.

2.5.1.1 Tooth Loading Model for Tooth Root Stress

The loading on a tooth is relatively complex. Therefore a simplification of the actual stress condition has always been used in analytical calculations in order to be able to describe mathematically the stress situation at the tooth root as given in [2.25] to [2.31]. The following considerations are always used for a given and arbitrary tooth section with a loading:

* The normal tooth section is considered
* The tooth is considered as a cantilever beam
* The tooth load is distributed uniform along the facewidth
* Gear load is parallel to the root line of the tooth
* Gear unit load is Fn/b
* Tooth root thickness at the critical section is calculated
* Bending lever arm of the load h is calculated

The standards that are considered here, all use a comparable tooth model for calculating the tooth root stress. In the past, several different models have been proposed, such as the wedge shape [2.5.6], but these will not be considered here. The different calculation methods differ in the assumption that several principal stresses may participate in determining the effective stress.

This will further be analysed and discussed.
All calculations for the tooth form factor use a similar approach to the resulting stress value, where several idealised and principal stresses are active at the same time. The following principal stresses may be observed on the root tension side, exclusive the influence of stress concentration (see fig. 2.5):

* Bending stress:

$$\sigma_b = \frac{F_n}{b} * \frac{6h}{s^2} * \cos\varphi \qquad (2.32)$$

* Compressive stress:

$$\sigma_d = \frac{F_n}{b} * \frac{1}{s} * \sin\varphi \qquad (2.33)$$

* Shear stress:

$$\tau = \frac{F_n}{b} * \frac{1}{s} * \cos\varphi \qquad (2.34)$$

All calculation standards neglect the stresses, resulting from a non equal distributed compressive stress along the root section and the influence of a frictional component. Generally, the influence of both mentioned effects on the resulting stress level is less than 1 - 5%. The influences of residual stresses of final surface treatment and resulting from shrinkage fits, are also neglected.
For a more dimensional stress situation, the effective stress according to the theory of maximum energy [2.27] is:

$$\sigma_{id} = \sqrt{(\sigma_b - \sigma_d)^2 + (\alpha_0 * \tau)^2} \qquad (2.35)$$

The tooth root stress for one tooth and exclusive the stress concentration can be written as the generalised tooth root stress of equation (2.7), multiplied by the Tooth Form Factor.
The general expression for the Tooth Form Factor now can be expressed in terms of the geometric values of the tooth when the three principal stresses, bending, compressive and shear are taken into consideration and introduced in expression (2.35):

$$\sigma_{id} = \frac{F_{mt}}{b * m_{mn}} * \frac{m_{mn}}{s} * \frac{\cos\varphi}{\cos\alpha_n} * \sqrt{[6(\frac{h}{s}) - \tan\varphi]^2 + \alpha_o^{\,2}} \qquad (2.36)$$

As will be seen in the following part, the general expressions for the Tooth Form Factor in the investigated standards all use different combinations of principal stresses.
It will be shown that it is possible to rewrite all tooth form factors in a one and the same way in order to compare them, in a similar way as has been done with the stress equations.
One has to bear in mind that for the pinion and the gear, the tooth form factor has to be determined separately. For bevel gears with non equal pressure angles on both flanks, the tooth form factor will also differ for loading on different tooth sides.

2.5.1.2 Comparison of Tooth Form Factors

The expressions for the Tooth Form Factor according to the different standards are rewritten. The results of rearranging these expressions into a uniform way are summarised here.

ANSI/AGMA

In this standard the bending stress resulting from the tangential component of the gear normal load and the compressive stress resulting from the radial component, are both taken into account. The weakest section of the root is determined by the Lewis parabola. The point of load application is not at the tooth tip, but is determined on basis of theoretical contact lines; generally the load is tangent to the basecircle diameter.
The equation of the original Tooth Form Factor is:

$$Y_{P,G} = \frac{2}{3} * \frac{P_d}{K_f \left(\frac{1}{X_N} - \frac{\tan\phi_N}{3t_N}\right)} \qquad (2.37)$$

Rewriting this into a unified expression gives:

$$\frac{1}{Y} = \left(\frac{m_{mn}}{2t_N}\right) * \left[6\left(\frac{h_N}{2t_N}\right) - \tan\phi_N\right] \qquad (2.38)$$

In the original standard, the stress concentration factor is incorporated in the tooth form factor. The expression here 1/Y is written without the Stress Concentration Factor K_f and the diametral pitch P_d.

DIN

Here only the bending stress is considered. The weakest root section is determined by means of the 30°-tangent; the gear load is applied at the tooth tip.
The original expression is:

$$Y_{Fa} = \frac{6 * \frac{h_{Fa}}{m_{mn}} * \cos\alpha_{Fan}}{\left(\frac{s_{Fn}}{m_{mn}}\right)^2 * \cos\alpha_n} \qquad (2.39)$$

and it can be rewritten into:

$$Y_{Fa} = \left(\frac{m_{mn}}{s_{Fn}}\right) * \left(\frac{\cos\alpha_{Fan}}{\cos\alpha_n}\right) * \left[6\left(\frac{h_{Fa}}{s_{Fn}}\right)\right] \qquad (2.40)$$

Gleason

Here the expression is identical to the ANSI/AGMA formulation; there is only a slight difference in some symbols.

Oerlikon

In the equation for the tooth form factor, all three principal stresses, bending, compressive and shear stress are incorporated. For the shear stress, a factor of 2.5 was proposed [2.17]. The weakest root section is determined by the Lewis parabola; the point of load application is not at the tooth tip but is comparable with ANSI/AGMA and Gleason:

$$q_w = \frac{\cos\alpha}{\cos\alpha_i} * \frac{m_p}{s_f} * \sqrt{(6(\frac{l_i}{s_f}) - \tan\alpha)^2 + 6.25} \qquad (2.41)$$

is rearranged into:

$$q_w = \frac{m_{mn}}{s_{fn}} * \frac{\cos\alpha}{\cos\alpha_n} * \sqrt{(6(\frac{l_i}{s_f}) - \tan\alpha)^2 + (2.5)^2} \qquad (2.42)$$

Table 2.4 gives schematically the involved assumptions for determining the Tooth Form Factor of the calculation standards (see also fig. 2.5).

Calculation Standard	Principal Stresses involved	Point of Load Application	Critical Tooth Root Section
DIN	Bending Stress	Tooth Tip	30^0-Tangent
AGMA / Gleason	Bending Stress Compressive Stress	Upper Point of Single Mesh	Lewis Parabola
Oerlikon	Bending stress Compressive Stress Shear Stress	Upper Point of Single Mesh	Lewis Parabola

Table 2.4 Different Assumptions in Tooth Form Factors.

It will become clear that generally the numerical values of the Tooth Form Factors may be different when calculating one and the same gear geometry according to different standards. A comparison of equations (2.38), (2.40) and (2.42) already shows this. For one part there may be a difference in the bending lever arm and tooth root section; on the other hand the summation of several principal stresses will also influence the value of the tooth form factor. In general, the values of the Tooth Form Factor according to the standards will be quite different, when calculated for one and the same gear geometry. The reasons for this are:

* The bending lever arm of the gear unit load according to the DIN-standard is about two times the one according to ANSI/AGMA and Oerlikon.
* The root sections do not differ to a large extent; the Lewis parabola gives values that are about 10% larger than the root thickness according to the 30^0 -tangent of DIN.

* Different stress components are taken into account for the final Tooth Form Factor. The compressive stress will decrease the resultant calculated stress in comparison to a purely bending stress.

For normal automotive rear axle gear geometry, the calculated values for the Tooth Form Factors according to the different standards relate to each other in the following way.
Bending stress for ANSI/AGMA and Oerlikon is about 50% of the value according to DIN, mainly because of the difference in lever arm. Compressive stress for ANSI/AGMA and Oerlikon is about 10% of the bending stress in DIN. Shear stress according to Oerlikon is about 30% of the bending stress in DIN.
Therefore, the Tooth Form Factor according to Oerlikon is about 1.40-1.50 larger than the one according to ANSI/AGMA and Gleason. The tooth form factor according to DIN is about 2.0-2.5 larger than ANSI/AGMA and Gleason. These values are generally applicable and relate only to state of the art automotive rear axle gears. Larger differences may of course occur, a difference of a factor 4 can be considered as being possible [2.35] to [2.39], but these are considered as exceptions.

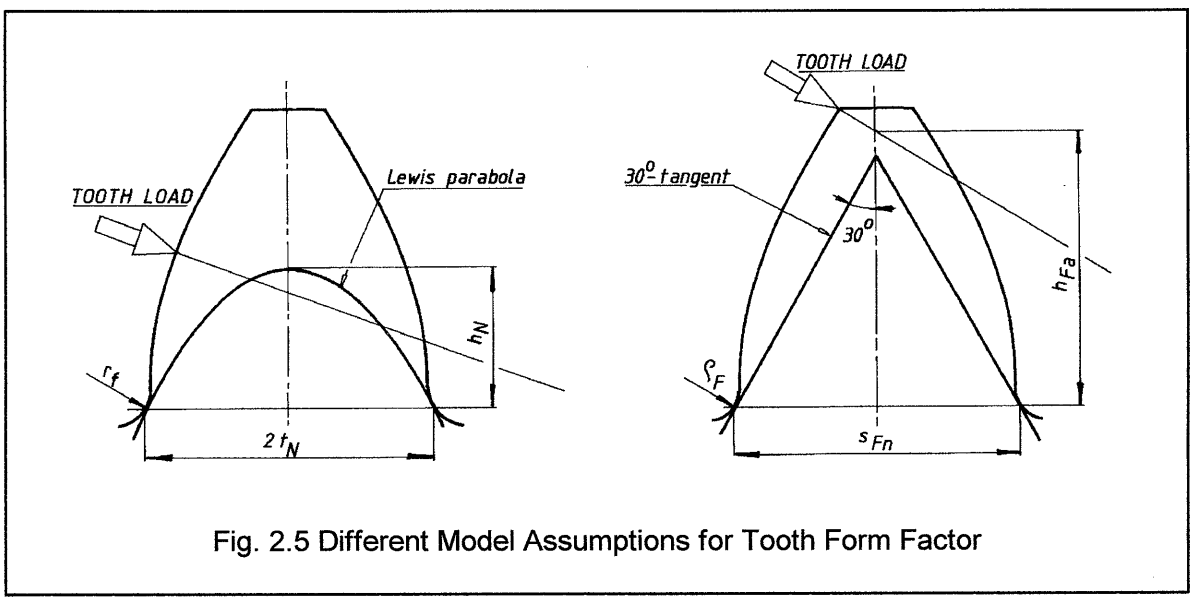

Fig. 2.5 Different Model Assumptions for Tooth Form Factor

2.5.2 Stress Concentration Factor

The loading of the tooth gives a local stress concentration that is normally located in the area of fillet radius which has a trochoidal form. The influence of this stress concentration on the tooth root bending stress is accounted for by the Stress Concentration Factor.

ANSI/AGMA
The effective stress concentration and the point of load application are considerd by this factor. It is determined by the work of Dolan/Broghammer [2.6] which is based on model tests on two dimensional gear templates under isochromatic light.

DIN
These equations are based on the work of Hirth [2.48] and have been generated by a comparison of measured and calculated stress values on actual helical gears. Here only the root radius, bending lever arm and tooth thickness are used as variables.

Gleason
These are the same as for the ANSI/AGMA standard.

Oerlikon
Because Niemann suggested a factor of 2.5 in the expression of the Tooth Form Factor [2.17], no further stress concentration effects have to be taken into account. This means that here the Stress Concentration Factor holds a value of unity.

Comparison of Stress Concentration Factors
A comparison of the calculated Stress Concentration Factors according to the four standards is given in fig. 2.6. Here they are plotted as a function of the ratio of root radius to tooth thickness at the point of maximum assumed stress. The parameter is the ratio of load bending arm to tooth thickness at the point of maximum stress. There are two differences in the sensitivity. The sensitivity of the stress concentration factor to the ratio of rootradius to toothhickness is roughly a factor 2 higher for DIN than as it is for ANSI/AGMA. The sensitivity of the stress concentration factor for the parameter of the ratio bending arm to tooth thickness is however by far larger for ANSI/AGMA than as it is for DIN. As the normal practical range of relative blade edge radii lies between 0.15 and 0.25 times the tooth thickness, the difference in calculated stress concentration factor between ANSI/AGMA and DIN will be relatively small. One has to bear in mind however that for one and the same gear geometry, the bending arm according to AGMA/Gleason/Oerlikon is smaller than the bending arm according to DIN.

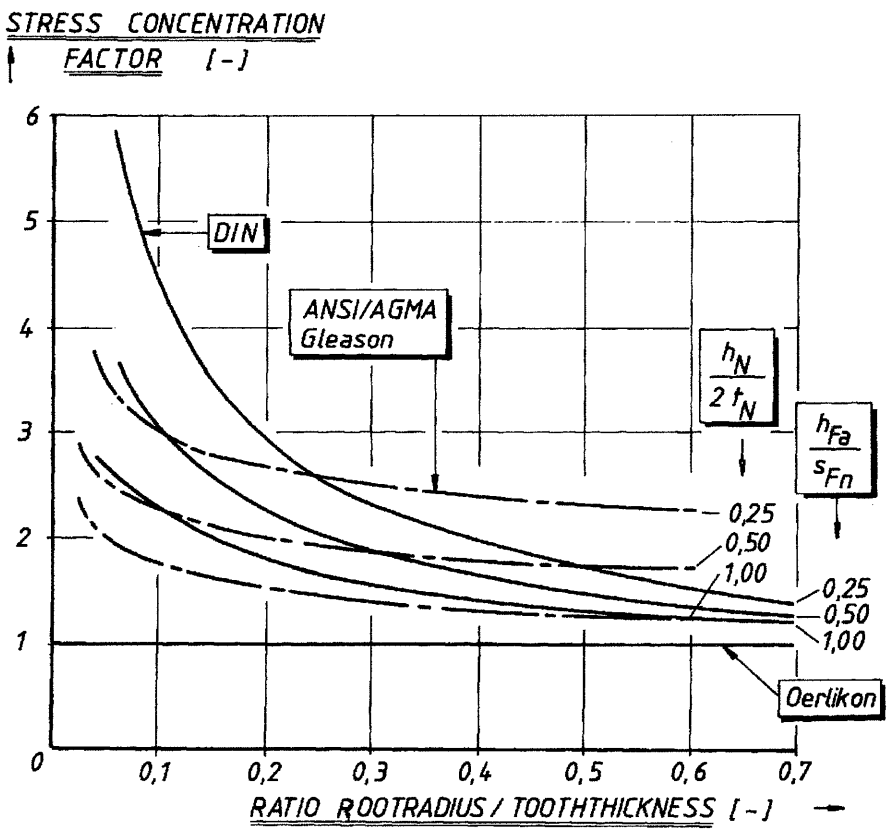

Fig. 2.6 Comparison of Stress Concentration Factors

Generally it can be seen that for gears with a relatively small blade edge radius of about 0.15 of the tooth thickness, the Stress Concentration Factor for DIN is about 10-15% larger than the one for AGMA and Gleason. For gears with a relatively large blade edge radius of about 0.25 times the tooth thickness, the Stress Concentration Factor according to DIN can be about 30-40% larger than the one calculated according to AGMA and Gleason. This means that the differences between the Stress Concentration Factors dependsamong others on actual blade edge radius.

2.5.3 Load Sharing Factor

The tooth root bending stress as calculated up to now can be considered as the result of one tooth taking the entire load. In most cases where the contact ratio is sufficient large, more teeth share the entire gear load. This is accounted for by means of this factor, which is generally called the Load Sharing Factor. In the standards, the profile contact ratio of the gears is the only parameter that influences the calculated value for the Load Sharing Factor.

ANSI/AGMA and Gleason

Here the product of the Load Sharing Factor m_N with the Inertia Factor $_iK_{,N}m_i$*K now is considered as the factor taking into account the sharing of the entire tangential load by several teeth. This Inertia Factor K_i is part of the Geometry Factor J. It accounts for the lack of smoothness of tooth meshing action at gears with a modified contact ratio less than two.
For modified contact ratio larger than 2, Gleason standard gives an expression that is used here. In some way it may seem to be arbitrary to combine the Inertia Factor with the Load Sharing Factor, but both factors are only dependent on the gear geometry. Therefore it is appropriate to range it under the geometry factors. The product of both m_N and K_i gives a continuous function when varying the modified contact ratio, as drawn in fig.2.7.

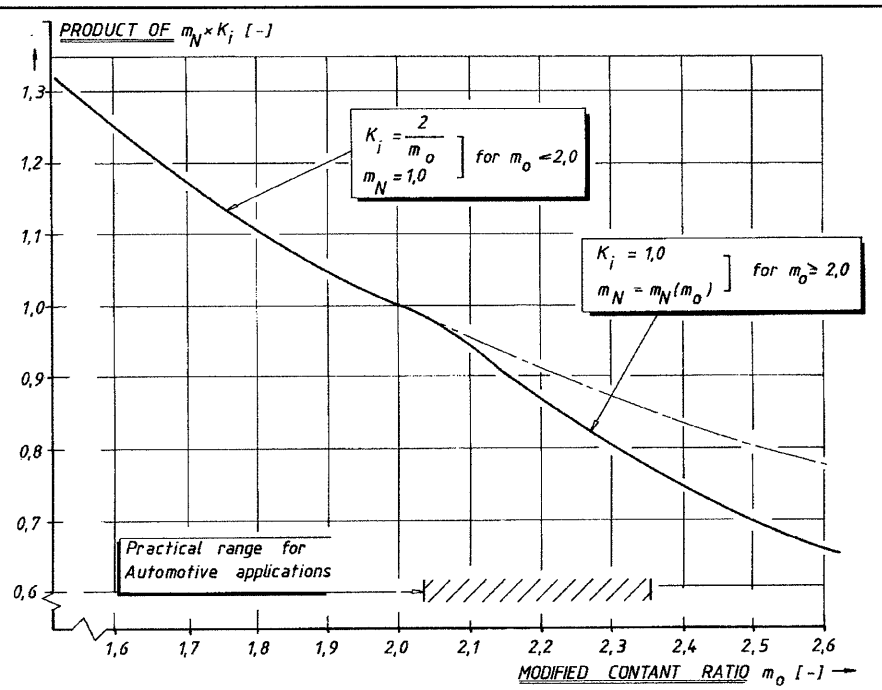

Fig. 2.7 Product of Load Sharing and Inertia Factor for ANSI/AGMA and Gleason

DIN
In this standard, the tooth root stress for the load at the tooth tip, is recalculated for the situation of the load at the point of outer single mesh.

Oerlikon
This expression is given in [2.17].

2.5.4 Helical Factor

In spiral bevel gears the contact lines are not parallel to the root line of the teeth. As a result of this, the tooth root is loaded differently. The Helical Factor takes account for this difference. In all standards the contact lines on the gear teeth are assumed to be straight lines that are positioned under an angle, determined by the base helical angle. For bevel gears, the base spiral angle gradually changes over the face width; normally it increase from the inner to the outer cone. This depends mostly on the ratio of gear cutter radius to outer cone distance or gear outer pitch diameter. Theoretically, the contact lines for bevel gears will therefore be curved and no straight lines, as is assumed in the calculation standards. Fig. 2.8 shows the contact lines of a hypoid gear that has been loaded during standstill. The contact lines are distinctively visible on the teeth, showing that the assumption of a straight contact line may very well be close to reality. For spiral angles from 30° - 40° and a face contact ratio larger than unity, the difference in calculated helical factors between DIN, ANSI/AGMA and Gleason values will be relatively small. The values according to Oerlikon may deviate more.

Fig. 2.8 Contact Lines on a Hypoid Pinion

The DIN Standard gives explicitely a Helical factor, whereas the others do not give this. In the AGMA/Gleason method, the influence of the inclined contact lines is incorporated in the Load Sharing and the Effective Facewidth. This is an important aspect that needs special attention, when comparing the different Factors with each other.

2.5.5 Cutter Diameter Factor

The American calculation methods indicate that there is an influence of the cutter radius on tooth root stress. The European standards do not give this influence. These differences will be analysed and discussed however in Chapter 2.8.3.

2.5.6 Point of Load Application

As the radius of the Point of Load Application does not coincide with the pitch radius of the virtual gears, the value of the gear unit load will have to be corrected for. For the ANSI/AGMA and Gleason standards, the ratio of the pitch diameter of the virtual gears to the radius of the point of load application determines the value of the required correction. The DIN and Oerlikon standard do not contain this factor.

2.5.7 Mean Facewidth Factor.

Only the Oerlikon method contains this factor, where the dseign point of the bevel gears, N-point, is recalculated to the mean facewidth.

2.5.8 Effective Facewidth Factor.

Because of the limited contact pattern on the tooth facewidth, the effective facewidth will differ from the geometrical.

2.5.9 Bevel Gear Factor.

Here only the DIN standard has given a possibility for the influence of the non involute profile of the bevel gear teeth. The last proposal brings the value of this factor to unity, which means that for the time being, no standard allows for any modification for typical bevel gear effects.

* *The Tooth Form Factor, the Stress Concentration and the Load Sharing Factor* *
* *have the largest differences of all the Geometry Factors.* *
* *The differences in the Tooth Form Factor are the result of the different tooth* *
* *loading models and the principal stresses that are taken into account.* *
* *The differences in the Load Sharing Factor result from the assumptions in* *
* *the distribution of the gear load over the meshing teeth.* *

2.6 Material Factors in Stress Calculations

In this part the material related aspects will be treated.
These material characteristics are given in the following factors:

* Allowable Material Stress
* Life Factor
* Size Factor
* Temperature, Roughness and Support Factor.
* Safety Factor

In practice, most automotive rear axle drive gears are made from case carburised gear steel. Therefore only this type of material will be considered here. The material data only refer to unidirectional loading, which means that only one side of the gear flanks is loaded. As the loading conditions of automotive gears are bidirectional, sometimes a correction may be necessary on the endurance values.

2.6.1 Allowable Material Stress

The Allowable Material Stress is determined by the material that is used, as well as by several metallurgical and heat treatment variables. The failure probability of the allowable endurance stress also determines the value.
The most important aspect however, is that the Allowable Material Stress is mainly determined by the calculation standard. Both should always be linked to each other. A change in one will lead to a different value of the Safety Factor. A change in the layout of the stress calculation or even a change on a part of it, requires a corresponding adaption of the Allowable Material Stress.

Features	ANSI/AGMA	DIN 3991	Gleason	Oerlikon
Failure Probability (%)	1	1	5	--
Endurance Limit (N/mm2)	380-480	640-1080	210	410-460
Endurance Cycles (-)	$1 * 10^7$	$3 * 10^6$	$6 * 10^6$	$2 * 10^6$
Slope SN curve: k (-)	7.65	--	5.68	5.00
Constant C (-)	8.22	--	15.39	--
Slope k_o (-)	30.96	--	infinite	infinite
Value C_o (-)	1.68	--	--	--
Static Limit (N/mm2)	700	--	700	--
Static Cycles (-)	$1 * 10^3$	--	$1 * 10^3$	--
Minimum Life Factor (-)	1.00	--	1.00	1.00
Max. Life Factor (-)	3.33	2.50	3.38	--

Table 2.5
Characteristic Material related Values for Bevel Gears for Hardened Case Carburised Steel, that have been established from data and graphical representations of the different standards.

Therefore the allowable material stess is not only purely material related, but very much dependent on the calculation method. This very important aspect is forgotten many times. It is the main reason for relatively large differences between the absolute values of the endurance limits for the different standards when identical materials are applied. The calculated stress and the allowable endurance stress should therefore always be linked to the calculation standard for which it is established. It cay never be that the value of a certain stress, calculated with a specific standard is compared with the allowable stress of a different standard!
In Table 2.5 the values for the allowable material stress in terms of endurance limits and failure probability according to the different standards are summarised.
Gleason gives a specific value with an accompanying failure probability; this is valid for automotive applications. Both international standards give for a specific failure probability a range for the allowable stress values, which is a result of the general applicability of these standards. Here each specific application will have it's own appropriate Allowable Material Stress.
Remarkable are the large differences between several allowable endurance stresses. The difference between the allowable value for Gleason and the maximum value for DIN is about a factor 5. In view of this, the difference between the endurance values for AGMA and Oerlikon is relatively small with about 4-8%. Compared with this, the difference between the endurance values of AGMA and Gleason is relatively large with about 80-130%. This means these allowable stress values are strictly to be used in the standard for which they have been determined.

2.6.2 Life Factor

When the designed gears are to operate on a number of loading cycles that differs from the number for infinitive life, the Life Factor accounts for the change in allowable maximum stress that may be allowed. This factor is based on the SN curves of the gear material or on the SN curves of the gears themselves. These curves are mostly generated by laboratory tests on specimen or on actual test gears with given dimensions.
From the four different standards, specific data have been derived on basis of the given endurance data; they are given in Table 2.5. Some of the values have been determined by analysing graphical representations of the different calculation standards. This means that not all values from Table 2.5 can directly be found within the standards.
The most important features that are related to the life factors are:

* Value for the Failure Probability
* Value for the Endurance and Static Limit
* Number of Cycles for Endurance and Static Limit
* Slope of the SN curve for the “limited life” and "infinite life” region.

The difference in the endurance limit is minimal a factor 2; it may even amount to a 5 fold difference between the DIN and Gleason recommended values. In this way, it is very evident that the calculated tooth root stress values and the accompanying allowable stress values should always be linked to each other within one and the same calculation standard.
The slope of the SN curves also shows very distinctive differences between the individual standards, as is the ratio of maximum allowable stress to endurance limit. In fig. 2.9 the Life Factors for bevel gears are drawn as a function of the number of cycles. In some way, this life factor may be considered as the basic form of the SN curve of the gear material according to the specific standard. In that graph, also the life factors for helical gears according to the AGMA, DIN and ISO/DIS standards for case carburised gears are given for reasons of comparison. It shows quite clearly that the slope of the line representing the life factor for bevel gears differs from the line of the Life Factor for helical gears.

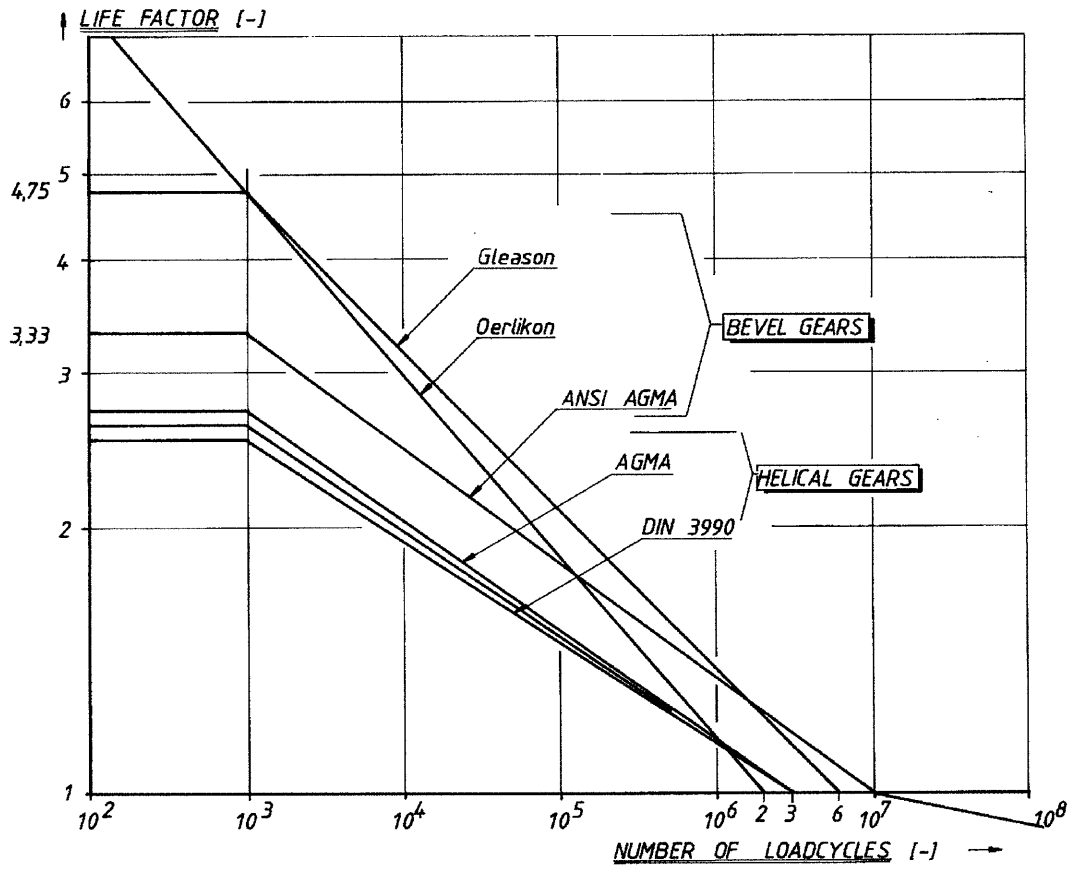

Fig. 2.9 Comparison of Life Factors that have been derived from Standards

2.6.3 Size Factor

This factor takes account for the influence of the gear dimensions. In both European standards this Size Factor is incorporated in the material related stress values. In the American standards this factor is included in the equations for the calculated stress. The reason for this is, as indicated in (2.3), that SN diagrams can be designed for a wide range of different gear sizes. For a direct comparison on calculated stresses of the four standards, this Size Factor has been designated to the group of Material Factors. The reason to do so is the fact that the size will likely influence the allowable material strength, than that it will influence the calculated stress.

ANSI/AGMA

It is recommended to use a value of unity for mean normal module less or equal than 5 mm. For larger moduli, a size factor larger than unity may be required, but hardly any information is available here. The corresponding appendix E, of which the text indicates that it is not to be considered as an official part of the standard, indicates that an ISO proposed Size Factor may be used. This should however be done with caution.

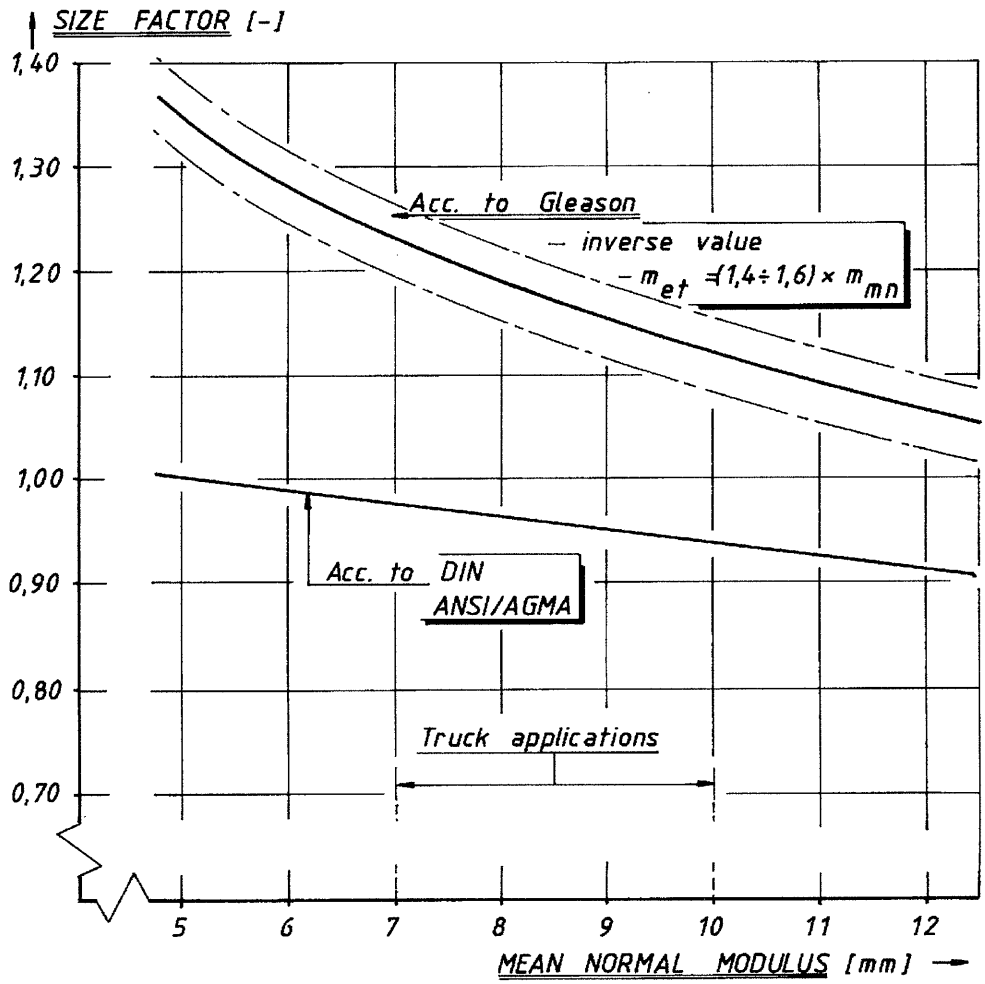

Fig. 2.10 Comparison of Size Factors

DIN
This Size Factor is identical as in the standard for helical gears.

Gleason
The Size Factor here is based on the diametral pitch at the outer end of the tooth.

For **Oerlikon** there is no Size Factor incorporated in the calculations.

A comparison of the Size Factors according to the different standards is given in fig. 2.10.
For a correct comparison of the Size Factors according to the scheme of figure 2.4, the inverse value of the Size Factors according to ANSI/AGMA and Gleason has to be taken.
The size factor is given as a function of the mean normal module. The independent variable of the Gleason expression has to be translated to the mean normal modulus. For many automotive rear axle gears the mean cone distance is about 85% of the outer cone distance; the mean spiral angle ranges between 30° to 40°. Therefore, the outer transverse modulus is about (1.4 - 1.6) x the mean normal modulus. This value has been used in fig. 2.10.

2.6.4 Temperature Factor

The ANSI/AGMA standard gives an indication on the decrease of the maximum stress value, when the peak operating blank temperature is higher than 120° C.

2.6.5 Roughness Factor

The DIN indicates the influence of surface roughness in the tooth root on the maximum stress. Two methods may be used, for which the simplified one will give sufficient accuracy. the maximum influence is a decrease of 10% for surface roughnesses in the root higher than R_z of 16 micron.

2.6.6 Support Factor

This influences the material characteristic for crack growth resistance. Only the DIN standard gives a relation. For case hardened steels, the support factor lies between 0.95 and 1.05. Assuming a value of unity will lead to a small error.

2.6.7 Safety Factor

The Safety Factor is a value that is called for in the DIN- and Oerlikon standards. The value of this factor should of course be determined by the application and the foregoing experience of succesfull and non successfull operations. In the ANSI/AGMA and Gleason standard the Power Ratings are indications on a potential succesfull design.

* *The Endurance Strength and the Size Factor give the largest difference in the* *
* *Material Factors for the different calculation standards.* *
* *The difference in the allowable endurance strength is the direct consequence* *
* *of the large differences in calculated stress levels between the standards.* *
* *It becomes clear, that the allowable strength and the calculated stress should* *
* *always be directly linked to each other within one calculation standard, rather* *
* *than being directly related to the material itself.* *
* *The Life Factors show distinct differences, mostly in reference to those of* *
* *helical gears. Apparently the slope of SN curves for bevel gears would differ* *
* *from the one for helical gears, when one and the same material is used.* *

2.7 Calculation Example

In the following part some results of the different calculation methods will be compared, based on the scheme of figure 2.3. The values for the Load, Geometry and Material Factors, as determined in the last chapter, will be compared as well as the final influence on the calculated tooth root stress. For this purpose, two fictional rear axle gear sets for a truck with a GVM of 32 tonne vehicle are used. The gear outer diameter is about 16.5", or 420-425 mm. The "Maximum Output Torque" for this axle type is 32.000 Nm, according to the definition of chapter 6.2.1.
Axle ratio's are 43/13=3.31 and 43/7=6.14, hereby covering the normal range of ratio's for this kind of application. Gear geometry data for these two fictional gear sets are given in Table 2.6. For each gear ratio, three different spiral angles are chosen, so that in fact the calculation results of six different gear geometries can be compared.

Rear Axle Ratio	(---)	3.31	6.14
Teeth Numbers	(---)	13 / 43	7 / 43
Mean Normal Modulus	(mm)	6.78	6.56
Gear Outer Diameter	(mm)	421	424
Gear Facewidth	(mm)	65	65
Mean Spiral Angle	(°)	30 / 36 / 42	32 / 38.5 / 45

Table 2.6 General Bevel Gear Geometry Data of Calculation Example

The results of this comparison are of course only valid for the gear geometry used here. For gears with a different gear geometry the results may vary, but the conclusions from this exercise may be considered as being representative for general automotive applications. Large differences are not very likely to be expected and the tendencies will remain the same. The stress values are given according to the expressions used in chapter 2.3. The values for the ANSI/AGMA and Gleason calculations will therefore differ from the official Gleason output on the Dimension Sheets, because of the shifted position of several factors, as for instance the Size Factor. From these calculation examples, the following conclusions may be drawn on the geometry calculations and the different Factors.

Geometry Calculations: Profile and Face Contact Ratio

The results of the calculations on the profile and face contact ratio's are given in Appendix 2.7, which are summarised in figure 2.11
The transverse profile contact ratio, calculated according to the different methods only lead to very small differences. The same can be concluded for the face contact ratio, when the full geometric facewidth is assumed. The face contact ratio according to DIN, when a 85% effective facewidth is taken into account, leads to 15% lower value in the calculated face contact ratio than the other methods. The value for the total contact ratio according to Oerlikon is about 30 - 40% higher than the modified contact ratio according to ANSI/AGMA and Gleason. The latter is about 15 - 30% lower than the total contact ratio calculated according to DIN, when a 85% effective facewidth is assumed.

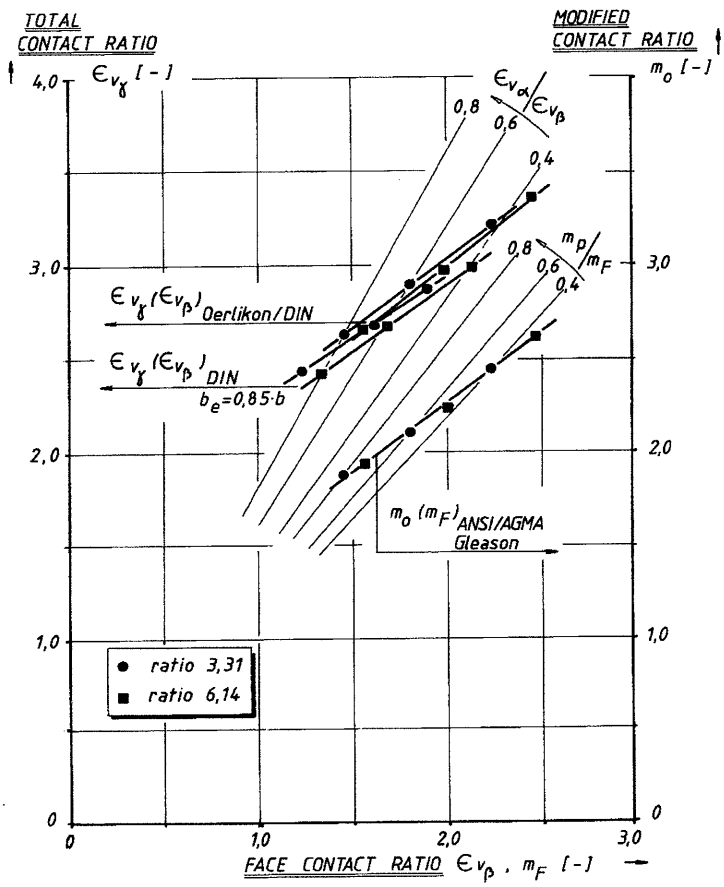

Fig. 2.11 Contact Ratio's acc. to Different Standards

Tooth Root Stress

In general the stresses calculated according to DIN give the highest values. The values according to Oerlikon give the lowest values. Here only the calculated nominal tooth root stresses are compared, meaning that all load factors are set to unity. Then generally a factor of 1.25 to 1.40 of difference exists between the Gleason and the Oerlikon calculated stresses. A factor of 1.35 to 1.80 between DIN and Oerlikon and a factor of 1.20 to 1.35 between DIN and Gleason may be expected with regard to the calculated pinion stresses. These differences between calculated stresses are generally to be expected for automotive rear axle gears with comparable gear geometry and when all load factors are set to unity. In this comparison, the size factor is incorporated in the material factors, which is different than the computer output of the official calculations. There the size factor is incorporated in the calculated stress value of the ANSI/AGMA and Gleason method, whereas it is not in the DIN and Oerlikon methods.

Load Factors

The Face Load Distribution Factors show a relatively large difference. There may be a difference of minimum 15% to maximum 60% between the values according to several standards, depending on the value of the torque. Not only the value but also the character of the Face Load Distribution Factor according to ANSI/AGMA is very different from those of other standards, as can be seen in figure 2.12.

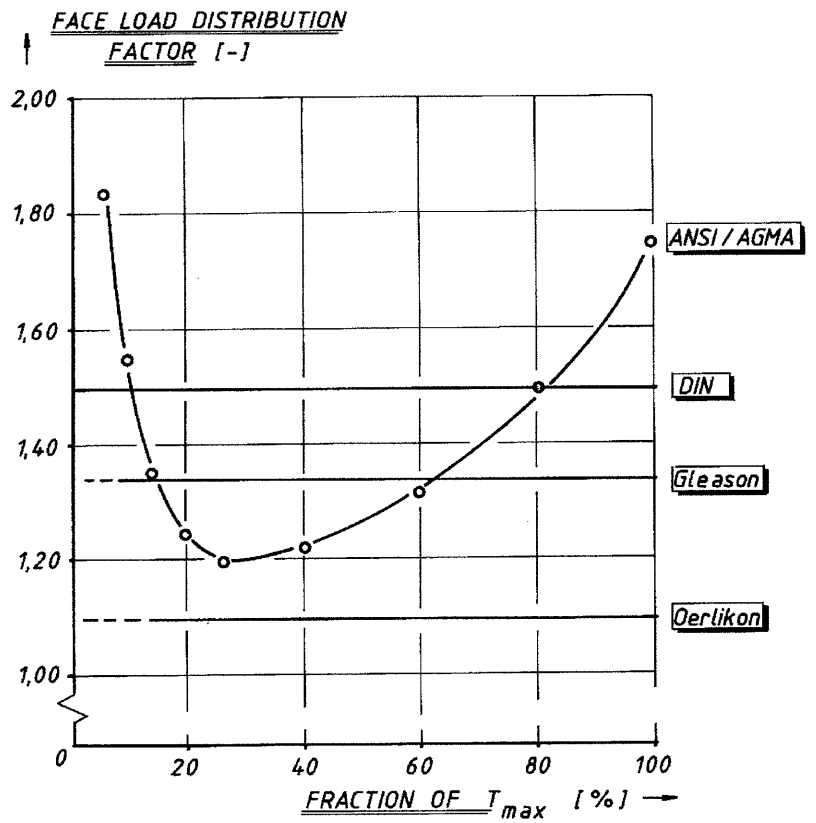

Fig. 2.12 Different Face Load Distribution Factors for the Calculation Examples

The Dynamic Factors have a very small difference. The circumferential speed and general gear quality of automotive rear axle gears normally lead to values for the Dynamic Load Factor that comes close to unity with differences between the individual values generally less than 10%.

Geometry Factors

The Tooth Form Factors differ to a very large extent; a difference of 150% may be attained. The Stress Concentration Factors may differ to 40% maximum. The Load Sharing Factors may differ to 20-35%, the Helical Factors to 10-25% and the Effective Facewidth gives 15% difference.

Material Factors

The Allowable Stress values differ to a very large extent. In fact, here it can be seen that the combination of calculated and allowable stress should be unique; values for allowable strength and calculated stress are not interchangeable. The Size Factor is incorporated in the stress values of ANSI/AGMA and Gleason. It is not in DIN and Oerlikon. This factor alone may already give differences from 15 to 30%. The Life Factors give differences to maximum 25%.

Safety Factors

Despite the relatively large differences in calculated root stress, the difference in Safety Factors between the different calculation standards is relatively small. Low calculated root stress and low allowable stress lead to comparable safety factors for high root stress and high allowable stress.

This comparison of the calculated tooth root stresses is based on the unified way of rewriting the original stress equations, as has been done in chapter 2.3.
The indicated differences are of course dependent on the gear geometry. When for instance a large tooth thickness correction and a small blade edge radius are used, several factors will change to a different extent than when a small tooth thickness correction and a large blade edge radius are used. Also when a small teeth number with a large spiral angle or a high teeth number with a small spiral angle are used, the differences between the several factors may change. The tendencies of the relative difference between the calculated stresses in general and between the individual factors in particular, will not change to a large extent however.
The indicated differences should therefore only be seen as general tendencies; they are however representative for normal automotive rear axle gears.
The ratio of calculated root stress between DIN and AGMA was about 1.15 - 1.50 for the pinion and 1.20 - 2.0 for the gear. For pinions with a large teethnumber (20 or more) the ratio of calculated stresses was about 2.50. This was exclusive the Application and the Face Load Distribution Factor, that were kept equal. The ratio of Safety Factors was about 1.0 - 1.5, which is smaller than the ratio of the calculated root stresses.
The most striking differences between several parts of the calculations are given in fig. 2.13. Here can be seen that the largest differences appear for the Face Load Distribution Factor, the Tooth Form Factor, the Load Sharing Factor and the Allowable Material Stress. In this figure, it is not indicated which calculation standard gives the lowest and which gives the highest value; only the relative difference between several methods is indicated.

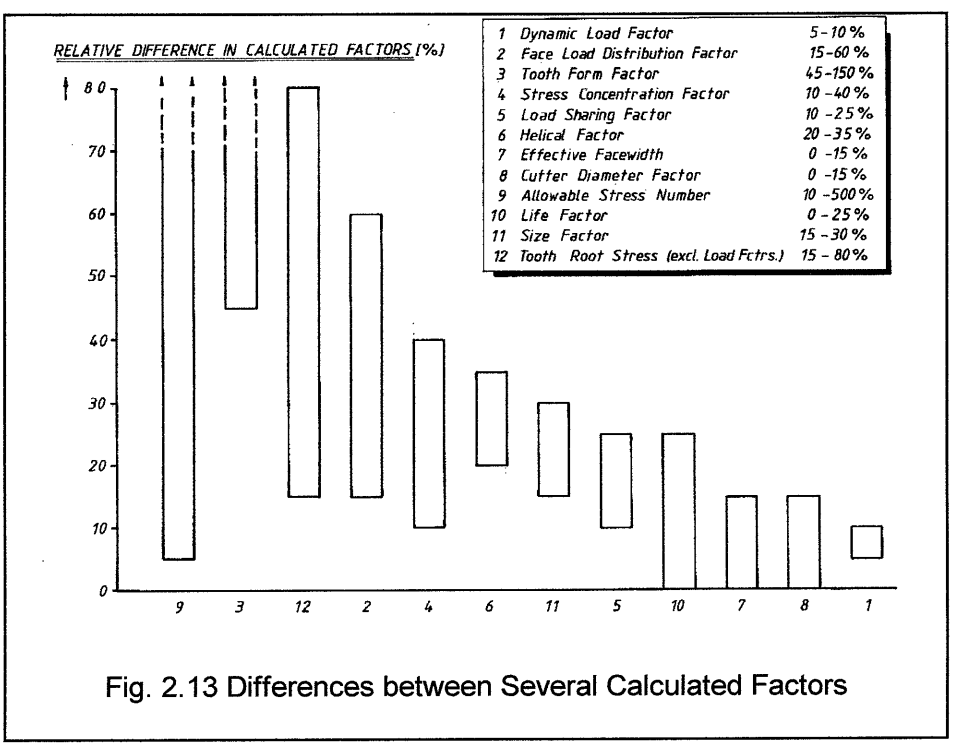

Fig. 2.13 Differences between Several Calculated Factors

A comparison on the calculated stress for bevel gears [2.35], in which 10 different gear geometries were compared, showed the calculated DIN stresses to be larger than the root stresses according to ANSI/AGMA. This is given in fig. 2.14. One may here observe the trend that in general the safety factors according to AGMA are lower than DIN for identical geometries. Differences between US and European market requirements, different Product Liability laws and differences in the requirements for vehicle weight are reflected here for a part.

Other studies on the comparison of calculated tooth root stresses for helical gears [2.10]-[2.13] indicate that the calculated tooth root stresses according to DIN are larger than those of AGMA. There appears to be no constant and uniform difference between both standards, which means that no simple conversion factor can be applied between both calculation methods. The ratio of tooth root stress for pinions according to DIN and AGMA lies in the range of 1,2 -2,0 with an average of 1.5; exclusive the influence of the Load Factors. It comes down to about the same ratio as has been found in the calculation example. Also the sensitivity of the calculated tooth root stress to a change in pressure angle, helical angle, profile shift factor and cutter edge radius, is different for the ANSI/AGMA, DIN, Gleason and Oerlikon method.
Literature very clearly indicates that although there are very large differences between the calculated stresses, the differences between the safety factors are remarkably smaller. This is caused by the values for the allowable material stress, as most of these methods have been verified with actual field experience to some extent.
The sensitivity of stress to changes on the geometry is different, so that optimum designs or relative geometry changes in order to obtain a required improvement will differ, depending on the applied calculation standard. Above all, the conclusions from the calculation example coincide very well with other findings on bevel gears and even on helical gears. Therefore the findings of both calculation examples may be considered to be representative for automotive applications.

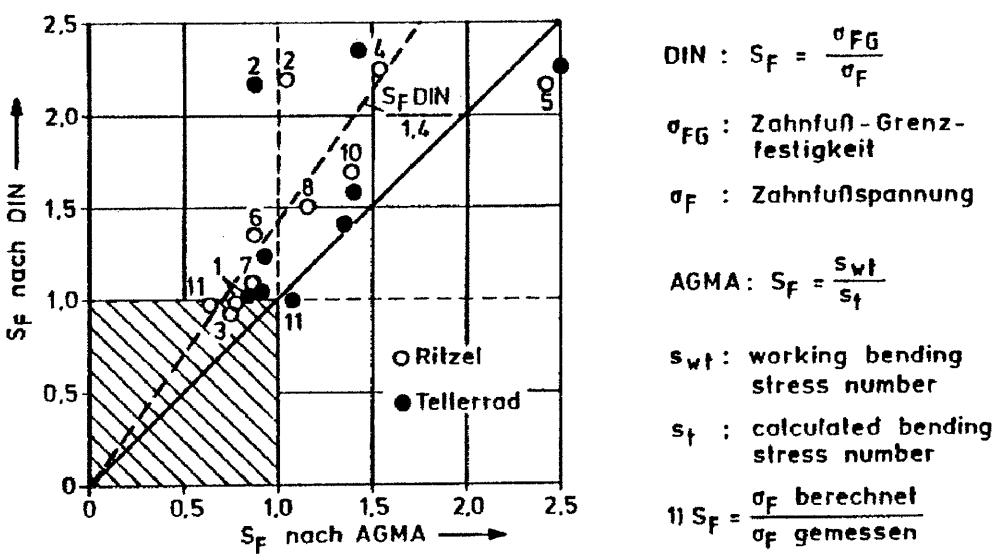

Fig. 2.14 Comparison of AGMA and DIN Calculations [2.35]

* *When calculating tooth root stress for gears that are representative for general automotive applications, the following differences may be observed: Difference in root stress may be 20-100% and even higher, but the difference in safety factors will be lower to a maximum of 50%. The calculated stress and the allowable stress are always linked within a calculation standard. Differences of individual Factors may amount to 40%, but the Tooth Form Factor and the Face Load Distribution Factor may show larger differences. The largest difference in the Face Load Distribution Factors attains about 60%; for the Tooth Form Factor the maximum difference may be 150%.* *

2.8 Comments on the Most Important Differences

When the numerical results of the individual factors for the different calculation methods are compared, then a striking difference can be seen. The Factors with the largest differences are:

* Face Load Distribution Factor
* Tooth Form Factor
* Gear Curvature Factor
* Size Factor.

2.8.1 Face Load Distribution Factor

From the calculation examples it has become clear that the Face Load Distribution Factor gives very large differences between the calculated tooth root stress. A review of this factor may lead to a more specified expression and hence a more accurate value. The value for the Face Load Distribution Factor and it's dependence on the crownwheel output torque needs to be designated therefore. For this reason, the deflection behaviour of the tested axles has been measured.

2.8.1.1 Deflection Measurements of Driving Head

In general, the gear deflection depends on the value of the applied torque, the gear geometry, the stiffness of the driving head, as well as the fixation of the driving head to the axle casing. On all the investigated axle types, deflection measurements have been performed with the driving head assembly mounted in the axle housing, so as to assure a similar deflection behaviour as

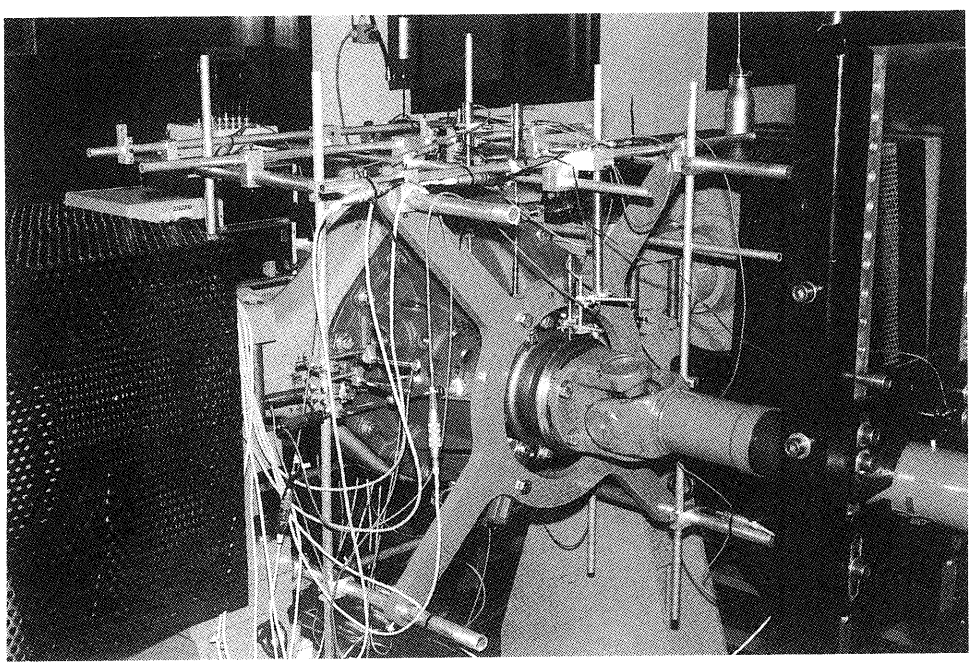

Fig. 2.15 Test Rig Lay-Out for Deflection Measurements

during the endurance tests. The deflection measurements have been performed on rear axles, with input torques increasing from zero to nominal value, both on Drive and Coast condition. Both input and output shafts rotated at low speed in order to minimise setting effects on bearing rings. These are standard procedures for rear axles, of which a description and the results are given in [4.17]. Gear deflections on only two axle ratio's have been measured, namely 4.10 and 2.93. All axles have a straddle mounted pinion and ring gear. Fig.2.15 shows the test rig lay-out.

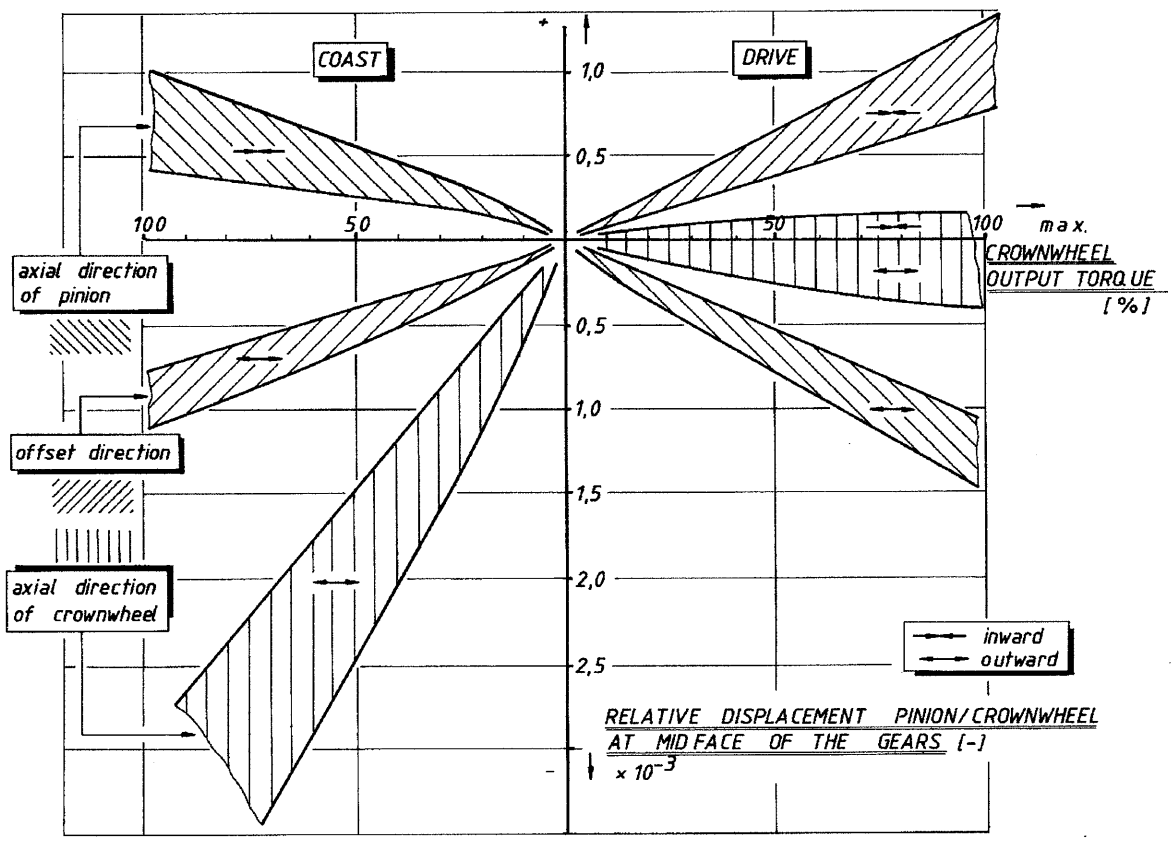

Fig. 2.16 Summarising Results of Deflection Measurements
Relative displacements between Pinion and Crownwheel at Midface

During the deflection measurements, the displacements of the pinion and the crownwheel are measured in the horizontal and vertical plane; both in axial and radial direction. From these values, the deflections between pinion and crownwheel have been calculated at the gear middle facewidth as a function of input torque for Drive and Coast condition. The results of these measured deflections for the tested rear axle gears are summarised in fig. 2.16. The deflections are related to the crownwheel outerdiameter, therefore they are called relative deflections.

From this, the following characteristics have been derived:

* All deflections can be considered as being proportional to the applied input torque; a linear relationship may be assumed here, with the exception for low torques.
* The displacement of the pinion is mainly influenced by the gear geometry of the pinion and the stiffness of the pinion bearings. Of the latter, the axial bearing preload and the roller geometry play a dominant role. A second order influence is the bending stiffness of the pinion shank; a small diameter may give rise to an additional shank deflection.

* The displacement of the crownwheel is mainly determined by the stiffness of the driving head casing and the gear geometry. The crownwheel itself as well as the satellitehousing on which it is bolted on, can be considered as a rigid and almost undeformable body which deflects under the influence of the gear loads. Bearing preload plays a minor role.
* The movement of pinion and crownwheel at Drive condition in the horizontal plane may be directed outward or even inward, mainly depending on the axle ratio.
* The axial load on the pinion diameter causes a bending moment which counteracts on the bending moment of the radial load. Depending on the amount of both bending moments, it may cause the pinion and crownwheel to move out or inward to each other. On axle ratio's of about 3, the relatively large pinion diameter originates a large bending moment causing both members to decrease their distance. On ratio's of 6 or 7 the influence of the separating load is dominant, forcing both members to move outward.

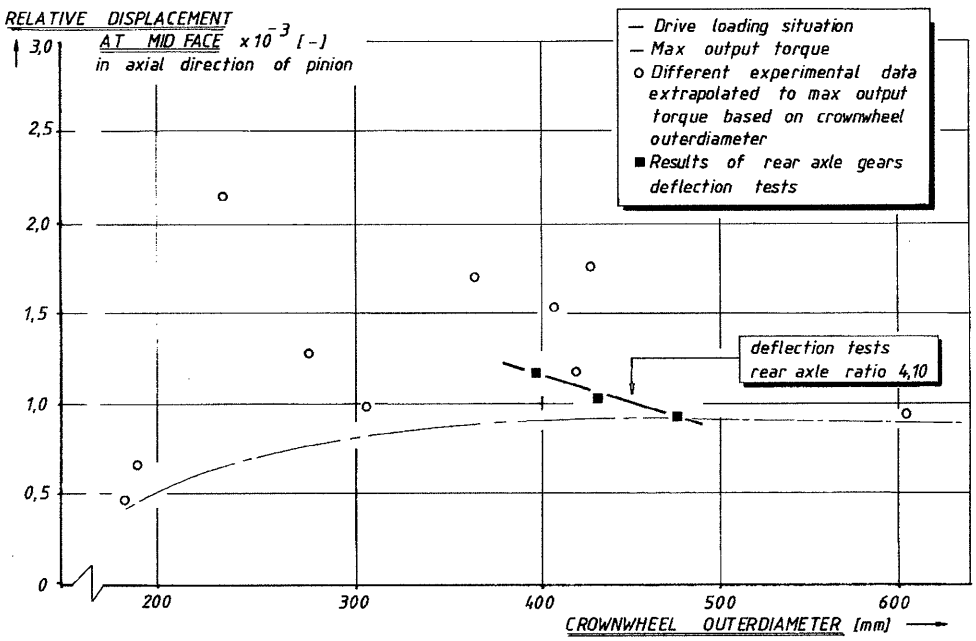

Fig. 2.17 Relative Displacements in Axial Direction

According to [2.41] there are only two important deflections that largely influence the face load distribution. These are the axial pinion displacement and the radial crownwheel displacement. These deflection values, at the nominal output torque, can be related to the crownwheel outer diameter. These measured values are given in fig. 2.17 and fig. 2.18. Added are some external values, [2.41] and [3.10]. These values have been corrected for the maximum torque according to the definition of Chapter 6. Here a typical relation between maximum output torque and crownwheel outer diameter has been established. The measured deflections from both sources have been corrected for an assumed maximum torque, that is based on the apparent crownwheel diameter. In all situations, a linear relation between torque and deflection was assumed. This means that the external derived deflection values of figures 2.17 and 2.18 actually differ from the measured values; they are however scaled so they can directly be compared with the registered deflections from the tested rear axle gears. It should be noted that the external added values are for rear axle drives with an overhung pinion mounting. Therefore they are larger, apart from the two small axles. The tested axles have straddle mounted pinions.

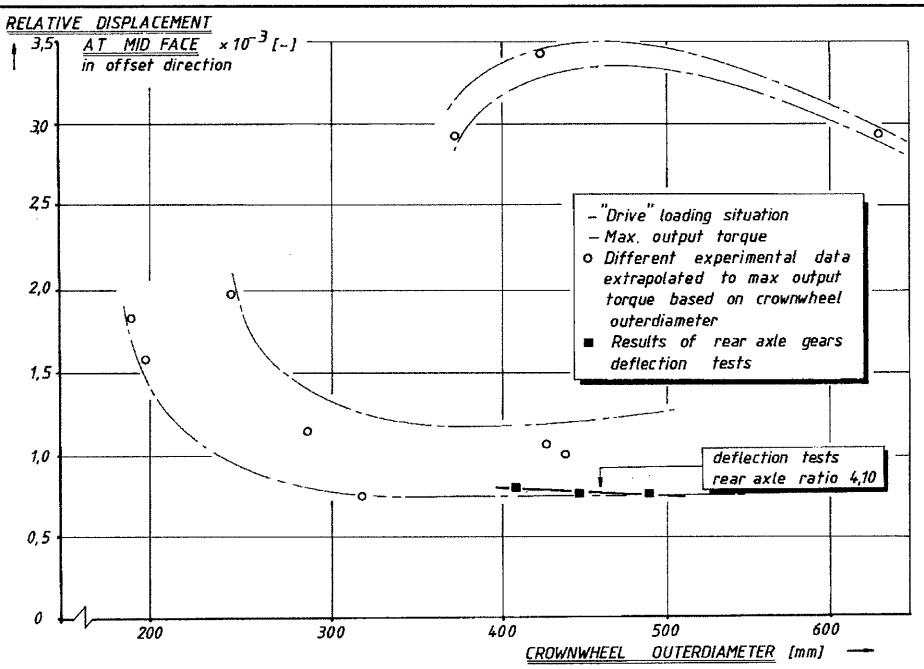

Fig. 2.18 Relative Displacements in Vertical Direction

From the graphical representations, it may be concluded that both f_a* and f_v* range between 1.00 and 2.00. The ratio f_a/f_v is about 1.5 to 2.0. It may be concluded that generally the deflections of the tested rear axle gears are well within the range of or even smaller than for comparable rear axles with overhung pinions. The deflections are directly proportional to the applied output torque, as has been shown in figure 2.16. Only for the low torque range there may not be a clear relation between deflection and torque, as here the gear backlash, bearing preload and other non linearities from housing geometry may distort a pure linear relation.

2.8.1.2 Proposal for Face Load Distribution Factor

The difference in the values of the Face Load Distribution Factors according to the different standards is very pronounced. Not only does the absolute value differ, the dependency of this value with the torque varies to a large extent for the different standards. The Face Load Distribution Factor is mainly influenced by the:

* type of bearing support for pinion and crownwheel
* deflection behaviour of both gears
* amount of lengthwise crowning.

According to the DIN standard, the stress on gears with lengthwise crowning is considered to be increased by 50% in comparison to non crowned gears, as indicated by the multiplication factor of 1.50. Here the equal distribution of the faceload which has a rectangular form over the facewidth, would change into an elliptic form at crowned gears, even when no gear deflection or misalignment occurs. No indication can be found on the reason for this value of 1.50. It is expected that the purely elliptical distribution of the gearload over the face width might be the reason for this value of 1.50. By considering a different, more practical function for the load distribution, the multiplication factor may correspondingly attain a different value.

Now the integral of a given load distribution over a certain length, is equal to the actual load itself. Therefore the general equation for the total tooth load, based on a given faceload distribution function f(x) is expressed as:

$$F_{tot} = f_m * b' = \int f(x)dx \qquad (2.43)$$

Here the integration boundaries are determined by the arc length of the total gear facewidth b'. The equally over the total facewidth distributed faceload is $f_m = F/b'$.
In DIN, the rectangular distribution of the faceload for line contact is replaced by an elliptic form. This assumption is valid when both ends of the crowned teeth are not loaded at full torque. Now the following expression for an elliptic faceload distribution function may be introduced:

$$f(x) = f_m * [1-(\frac{2x}{b'})^2] \qquad (2.44)$$

When this expression is integrated conform equation (2.43) over the full arc of the facewidth b', then the maximum value of the faceload, in the middle of the facewidth, appears to be 1.50 times larger than the equally distributed load F/b' (Attachment 2.8.1). It does not mean that this value of 1.50 for the face load multiplication factor is the same as the factor that is used in the DIN standard, but the correlation is striking. This may be the reason for the value of 1.50.

The assumption of a pure elliptical load distribution over the contact lines may however not correspond to the actual situation. It may be more realistic to assume a faceload distribution in which the region of maximum load is more stretched out on a greater length than when a purely elliptic load distribution is assumed. When a third order term is introduced, by which 90% of the maximum load is stretched out over 50% of the facewidth, the following face load distribution function can be applied:

$$f(x) = f_m * [1+(\frac{2x}{b'})^2 - 10(\frac{x}{b'})^3] \qquad (2.45)$$

Now when this function is integrated, the maximum value for the faceload is 1.30 times the value for the equally distributed faceload. As this last faceload distribution is assumed to be more realistic, a value of 1.30 for the faceload distribution factor should be used for a straddle mounted pinion. Likewise, the multiplication factor in the expressions for the faceload distribution factor according to DIN may also be changed into 1.30 instead of using the current value of 1.50.

Paul [2.41] has derived on basis of his strain measurements several expressions for the face load distribution value. For normal deflections and standard crowning values in automotive rear axle gears, his expressions yield figures for the face load distribution factor that are considerably lower than 1.50. Fresen [3.8] has stated that in any case the minimum value of the face load distribution factor is more than 1.00, being a result of the different values for the tooth stiffness at toe and at heel. It may well be that a minimum value of 1.10-1.15 can therefore be assumed, which would resemble an actual minimal value of face load factors to be encountered in automotive rear axle gears. In this view, the value of 1.30 for the multiplication value of the Face Load Distribution Factor appears to be realistic for automotive rear axle gears that have a normal facewidth with regard to the crownwheel outer diameter and that have standard crowning values. This is irrespective of the type of bearing, straddle mounted or overhung.

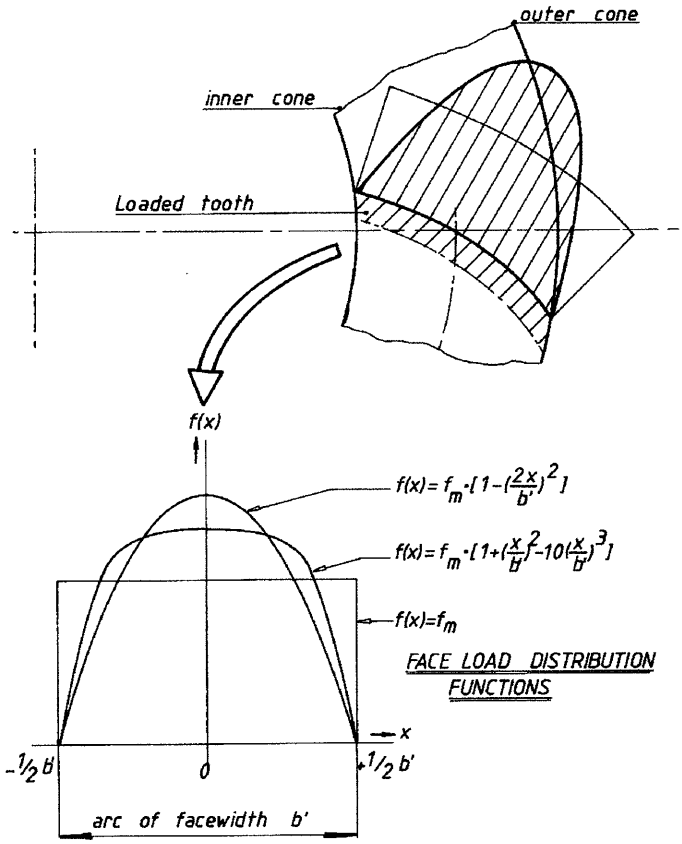

Fig. 2.19 Different Functions for the Face Load Distribution

Therefore it is suggested to use for bevel gears with normal deflections, a value of 1.30 for the multiplication factor of the Faceload Distribution Factor, instead of the 1.50 value of the DIN Standard. When a linear relation between misalignment and torque loading is present, then the value for the Faceload Distribution Factor is constant and independent of the torque.

2.8.2 Tooth Form Factor

The difference in the values of the Tooth Form Factor, calculated according to the four standards, is purely a result of the different stress models for the tooth root. First the principal stresses that contribute to the final tooth root stress and second the length of the bending arm. For DIN, only the bending stress is assumed, where the tooth load is applied at the tooth tip hereby giving a maximum bending lever arm. ANSI/AGMA and Gleason take next to the bending stress also the compressive stress. Oerlikon also adds the shear stress. The bending arm for the tooth form factor according to ANSI/AGMA, Gleason and Oerlikon is about half the value of the bending arm according to DIN. As a result of these assumptions, the difference between the several tooth form factors may amount to a value of about 2 - 2.5. The largest difference is between DIN and ANSI/AGMA, whereas the Oerlikon calculated value mostly lies in between. As these differences in the respective tooth form factors are a direct result of the different stress models in the standards, the differences will have to be accepted as they are inherently related to the specific standards.

2.8.3 Gear Curvature Factor

Only the ANSI/AGMA and Gleason standards take account for this influence. Here, literature gives some contradictory comments on this issue which requires some further examination.
Fresen [3.8] has performed strain measurements on models of gear and pinion teeth that were loaded with a point load that was positioned at one point of the facewidth. Hardly any influence of curvature on tooth root stress was found here. Coleman [2.20] performed strain measurements on Aluminum models of gear teeth with uniform depth. Apart from the lengthwise tooth curvature, the pressure angle was also changed. The conclusions are not very clear, but one might expect an influence of curvature since later on this was introduced in the standard.
Coleman [2.11] reported the results of life tests on actual gears that were built in driving heads. There was a distinct difference in endurance results between a 7.5" and a 12" cutter for a crownwheel outer diameter of 12.5". These life results, of which it is to be expected that all other aspects such as driving head and gear geometry were kept unchanged, show a clear difference in endurance life between both cutter radii, as indicated in figure 2.20.
According to the SN curves that were established out of these test results, the relative difference in gear life when changing the cutter diameter, depends on the stress level. At a high stress level the difference in life is about two to threefold, whereas for lower stress levels the difference increases. Both SN curves have different slopes, and thus different values of the k-faktor in the expression for the endurance life. This is an indication to different stress situations.

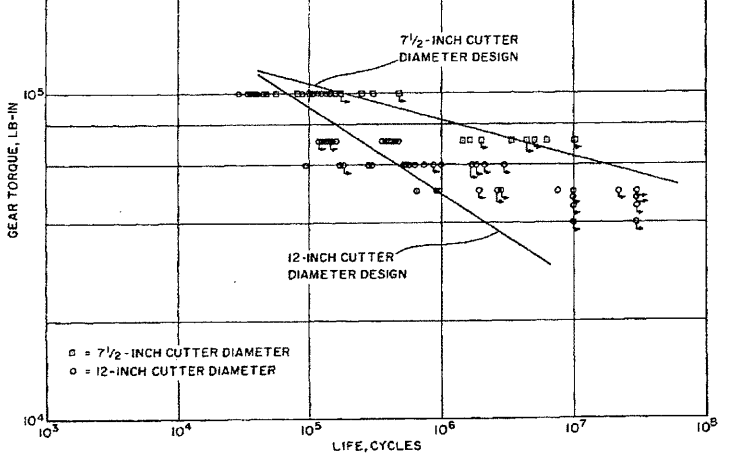

Fig. 2.20 Measured Endurance Cycles [2.11]

Stadtfeld [3.13] did theoretical FEM-calculations on constant tooth height gears. He also found hardly any influence on the calculated root stress when the cutter/diameter-ratio was reduced from 0.52 to 0.34. For smaller cutterdiameters, the calculated pinion tooth root stress decreased by about 20% at high torque values. In these situations, no deflections between crownwheel and pinion were assumed. When deformations are incorporated, however, he found that the calculated pinion tooth root stress increased at an increasing cutterdiameter.

This was beleived to be the result of the higher sensibility of the contact pattern to deformations, when a larger tooth curvature was applied. Gears with small curvatures tend to be more stable than gears with a large curvature, with regard to contact pattern sensitivity at given deflections.

The model stress measurements had a load position on the tooth model that remained unchanged, irrespective of the value of the load or the cutter radius. The endurance tests were performed on complete driving head assemblies. Here the load on the teeth will have a different position by the contact pattern shift due to deflections. This may well explain why the stress on a gear model without deformations will not or hardly change when the gear curvature is altered, whereas it will change on an assembled gearset with deformations. This means that the curvature of the gear teeth themselves would have hardly any influence on the stress for a fixed load position.

When the cutter/gear-ratio is changed, is does not only changes the tooth curvature; the sensitivity of the contact pattern due to deflections will also be changed. This means that the contact pattern of the gears under an increasing load will shift when mounted in a driving head and are exerted to deflections. This contact pattern sensitivity is mostly determined by the cutter/gear-ratio. Mostly the shift of the contact pattern is to the toe side. For taper tooth height gears, this will lead to an increase in root stress because of the smaller normal tooth thickness. This effect is smaller at constant tooth height gears, where the normal tooth thickness only slightly changes over the facewidth. At these gear types mostly the cutter/gear ratio is relatively low. It is possible that this effect is more pronounced at taper height gears than at constant height gears, simply because of the different ratio's of cutter-to-crownwheeldiameter. This effect may be the reason for not finding any influence on measured strain at models where the point of load application remains the same, irrespective of the load. However, on a built-in gearset the centre of the contact pattern and thus the point of load application may shift under load, depending on the cutter/gear ratio, hereby increasing the root stress. This means that the influence of gear curvature on tooth root stress will only be noticeable on gears that are assembled in the driving head casing and not on gear models with a fixed load position.

It may well be that the change in tooth root stress will not or hardly be influenced by the curvature of the gear teeth themselves, but will mainly be changed by the shift of the contact pattern under load as a result of a changing contact pattern sensitivity. The influence on tooth root stress will be small when the contact pattern does not shift to a large amount. However, when the contact pattern shifts remarkably under the influence of load, the tooth root stress will change as a result of a different tooth section at a different position on the face width. For calculations at variing loads, this aspect then needs to be incorporated, because this will influence the cumulative fatigue damage. The influence of the cutter diameter on stress will probably be more pronounced on bevel gears with a tapered tooth height than on bevel gears with a constant tooth height, altough this mainly depends on the ratio of cutter-to-crownwheeldiameter.

The influence of gear curvature on tooth root stress may be taken into account by the following parameters:
* ratio of gear curvature to crownwheel diameter
* change of tooth profile over the face width
* sensitivity of contact pattern under load
* amount of load variation during operation.

The first two aspects are purely geometrical, whereas the last two are related to load and deflections. The sensitivity of the contact pattern to load will be directly related to the ratio of cutter diameter to crownwheel diameter, in which case only three items remain to be described.

Further investigations may be necessary however, where the gear curvature factor of ANSI/AGMA and Gleason may serve as a starting point. As this issue is not a basic subject of this thesis, therefore no actual proposal will be given here. At the end of chapter 4 however, an indication will be given in what way the influence of the gear curvature may be incorporated in future calculations.

2.8.4 Size Factor

Although there is little difference in the values of the Size Factors, there is one important remark to be made. In the DIN standard, the Size Factor appears at the Material dependent Factors. The US standards apply this Size Factor in the expressions for the calculated tooth root stress. The reason for doing so is more of a practical kind, by which SN-diagrams may be prepared for a wide range of tooth sizes, as is indicated in chapter 9 of the ANSI/AGMA standard.
Comparing a calculated stress according to ANSI/AGMA or Gleason with the DIN output, will always imply a difference of 15 to 30%, apart from the other numerical differences. It is simply a result of the different positions of the Size Factor.
When the position of the size factor is always kept at the Material Factors, the differences in tooth root according to the different standards will become smaller. It will have, however, no influence on the comparison of the safety factors.

* *Two representative rear axle gears have been calculated according to the* *
* *different standards. The values for the individual factors have been compared.* *
* *It shows that there are relatively large differences between the Face Load* *
* *Distribution Factor, the Tooth Form Factor, the Gear Curvature Factor and the* *
* *Size Factor.* *
* *The differences in the Tooth Form Factors are a direct result of the assumptions* *
* *in the principal stress and the length of the bending arm.* *
* *The Size Factor may be moved to the Material Factors.* *
* *The reason for the influence of the Gear Curvature Factor has been explained.* *
* *At a fixed tooth loading position, there is hardly any influence of gear curvature.* *
* *The sensitivity of contact pattern change is directly influenced by gear curvature,* *
* *therefore it will have an influence on stress at assembled gearsets.* *
* *Here an expression is required for the change in contact pattern sensitivity in* *
* *function of the ratio cutter radius / crownwheel radius.* *
* *For the Face Load Distribution, the assumed elliptical load distribution over the* *
* *facewidth may be the cause for the multiplication factor of 1.50.* *
* *For straddle mounted pinions, the Face Load Distribution Factor may become* *
* *1.30 and this value is independent of the load.* *

2.9 Resumee

Four standards for tooth root stress calculations have been compared.
All calculation standards apply virtual helical gears to substitute the actual bevel gears for geometry and stress calculations. All standards use virtual helical gears, although in some standards the use of virtual geometry is not explicitely indicated.

The ANSI/AGMA and Gleason standards have different ways of designating tooth proportions of the basic gear geometry than the DIN and Oerlikon methods. Special expressions have been developed to calculate tooh proportions in the middle of the facewidth from gears with constant teeth height to gears with tapered teeth height.
There are hardly any differences in the tooth proportions at the mean face width of all four standards, for comparable gear geometries. In the direction of the outer or the inner cone distance however, the differences between the tooth proportions increase, being the result of a tapered or a constant height tooth depth.

The individual profile and face contact ratio, calculated according to the different standards, hardly have any differences in numerical values for a given gear geometry. Between the total and the modified contact ratio, however, there are relatively large differences. At an effective face width of 85% of the geometrical face width, as recomended in the DIN standard, the difference between the modified and total contact ratio is 15 to 30%. Generally the modified contact ratio gives smaller values than the total contact ratio. This is mainly a result of the different definitions.

The tooth root stress calculations for all considered standards are based on the normal section in the middle of the face width. The basic set-up of tooth root stress calculations in the different standards is principally the same, although the originally equations do not give that expression. They all can and have been rewritten into one and the same uniform equation, by which all individual Load, Geometry and Material Factors are grouped in a uniform way. Then it becomes clear that the expressions for tooth root stress in fact are all comparable. The number of features, taken into account by the standards, differ however.
A calculation example on two hypothetical and for automotive use representative gear sets, has been performed in order to identify the specific and individual differences between the standards.

The Face Load Distribution Factor gives differences that may amount to 60%, depending on the value of the output torque and the considered standards.
Of the Geometry factors, the Tooth Form Factor differs the most. The ratio of the highest and the lowest Tooth Form Factor may attain a value of 2.0 to 2.5.
These differences are caused by the length of the bending lever arm and the different principal stresses that are taken into consideration for the calculated bending stress at the root.
The Load Sharing Factor also leads to significantly differences between the standards.
The Gear Curvature Factor also causes a difference in calculated stress values, as it is used in both US standards, whereas it is not applied in both European standards.

The tooth root stress, solely based on the geometry factors, gives for DIN values that are a factor 1.25 to 1.85 larger than the stress according to ANSI/AGMA and Gleason. The stress according to Oerlikon lies in between. When the load factors are taken into consideration, the differences will decrease, but this is very much dependent on the torque level, as the face load distribution factor of ANSI/AGMA is strongly dependent on torque. The material factors differ almost only in the value of the allowable stress. These allowable material values have differences up to a factor of 2, when comparable failure probabilities are considered.

The Safety Factors, as calculated by the different standards, give a smaller difference than the root stresses, although a ratio of 1.0 to 1.5 between the most extreme values may occur. Generally, the tooth root stress of automotive rear axle gears, calculated according to DIN is larger than the one calculated according to ANSI/AGMA.
It is very clear that the allowable stress values and the calculated root stress should always be linked to one another within the same calculation standard. In this way one is likely to obtain safety values that can be considered as being reliable.

There is hardly any difference in quality between the considered calculation standards. The US based standards have the largest number of influences taken into account in different factors. In general the same global gear dimensions can be expected for a given application, when using the different standards. The different preferences on specific gear geometries for the designer will be more dominant on the final gear geometry than the influence of the calculation method. Different optimal geometry data can be expected however for one and the same gear, when calculated according to different standards. This is mainly the result of different sensitivities of tooth root stress for gear geometry variables.

It is proposed to use a Face Load Distribution Factor of 1.30 for automotive rear axle gears that are straddle mounted and have normal deflection values. This Face Load Distribution Factor is considered to be independent on the gear load and therefore it's value is constant.
The load distribution over the gear facewidth here is assumed to be flattened than a pure elliptical load distribution is.

The gear curvature will play a role in the tooth root stress. As measurements on gear teeth models with fixed load positions have shown hardly any influence on measured root stress, the curvature of the gear teeth will hardly influence the root stress. The gear curvature does however have quite a large influence on the sensitivity of the contact pattern shift under load, when built in a rear axle casing. The effect of cutter radius on endurance life has been shown by tests.
The ratio of the cutter-to-geardiameter here is the determining element. The effect of gear curvature on root stress should therefore be included in the stress calculations. It will be proposed lateron to incorporate the gear curvature in the Contact Pattern Factor.

3 TOOTH ROOT STRESS CALCULATIONS OF HYPOID GEARS

3.1 Introduction

For hypoid gears no official standards are available when calculating gear geometry and strength. Here only specific calculation methods exist that have been introduced by companies that apply these gears on a large scale or by the companies that produce the manufacturing machines for hypoids. Primarely the three world manufacturing systems for bevel and hypoid gears, Gleason, Oerlikon and Klingelnberg have developed standards for hypoid gear calculations [3.3] to [3.6].

Since the beginning of the application of hypoid gears, the emphasis of the gear manufacturers has been on understanding the geometry and aspects of the gear strength; the latter in comparison to bevel gears. In automotive applications hypoid gears are used during a relatively long time and on a large scale. The first hypoid gear equipped car was introduced in the mid twenties of last century [3.1]. It took about ten years before machinery and manufacturing methods as well as basic understanding of hypoid gears were at a level that succesfully application of hypoid gears was possible [3.2]. Apart from that, there are also specific industrial applications where hypoid gears are employed.

The most dominant aspect of hypoid gear geometry is the hypoid offset. The amount of this offset determines to a large extent most of the hypoid gears characteristics in general. It appears that the geometry and stress calculations for hypoid gears can be systemised on a similar way as for bevel gears. First, the actual hypoid gears are substituted by virtual bevel gears. Secondly, these virtual bevel gears are then substituted by virtual helical gears and these are replaced by spur gears (fig. 3.1). In fact this is an extension of the procedure that is described in chapter 2.

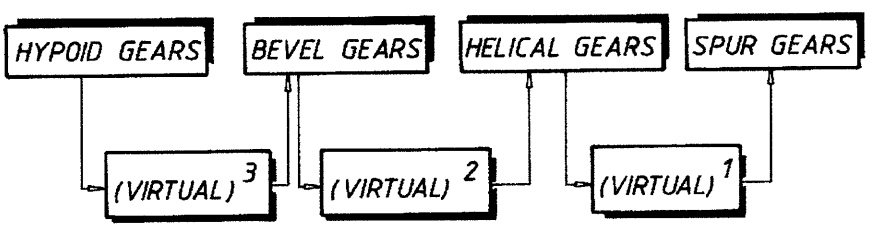

Fig. 3.1 Simplification of Hypoid Gear Geometry by Virtual Gears

First, some consequences of hypoid offset will be discussed. Then the different geometry and the strength calculations will be analysed and compared in the following parts of this chapter.

3.2 Hypoid Offset and it's Consequences

The most important aspect of hypoid gears is the hypoid offset as it determines the hypoid gear characteristics. The following general consequences of hypoid offset can be given, where the geometrical, the kinematical and the axle lay-out characteristics are considered.
Principally there are four different possibilities for a hypoid offset; they may result in an increase or even a decrease of the pinion dimensions. Important in this aspect are the direction of the crownwheel spiral angle and the direction of the offset. Here, only the hypoid offset that leads to an increase of the pinion diameter will be regarded, as this option is mostly used.

Geometrical consequences.

* The pinion spiral angle increases (when the gear spiral angle remains constant).
* The pinion outer diameter increases.
* The pinion face width increases.
* The face and cone angles of pinion/crownwheel change.
* The tooth profile becomes asymetric, leading to different pressure angles on both flanks.

As a result of this, the pinion shaft and the pinion top may increase to a larger dimension and hereby strengthening and stiffening the pinion shank as well as giving the possibility for mounting relatively large pinion bearings. Also the mounting of a pinion top bearing is possible so as to admit a straddle mounted pinion. The increase of the pinion diameter results from the increase of the pinion mean spiral angle that increases the tangential modulus, as in the case of increasing helix angle at helical gears. The mean normal modulus remains unchanged.

Kinematical consequences.

* Both profile contact ratio and face contact ratio increase.
* Relative sliding in lengthwise direction occurs.

The latter is positive in terms of strength, noise production and lapping characteristics. It is well accepted that hypoid gears have a higher loadability and that they are more silent than bevel gears with comparable gear geometry. As a result of the additional sliding, hypoid gears do not have the risk of destroying the contact pattern when the lapping operation takes too long.
A negative aspect is the higher risk of scoring as a result of large relative sliding. This sets higher requirements for the lubricating oil; generally for hypoid gears a GL5 oil is required whereas for bevel gears a GL4 quality is sufficient. Also the stationary oiltemperature may be higher than for bevel gears with comparable geometry, loading and casing.

Axle Lay-out consequences.

* The position of the pinion lowers in vertical direction.
* The axial mounting distance of the pinion decreases.
* The axial loads on bearings increase.
* Larger pinion deflections; axially and horizontally.
* Sensitivity for built-in deviations decreases.

As the amount of hypoid offset has a large influence on the general axle lay-out, it's value always needs to be checked for several limitations and restrictions.

In order to characterise hypoid gears, the relative offset is mostly used. This is the ratio of the vertical hypoid offset, relative to the crownwheel outer diameter. Fig. 3.2 gives in a graphical way the relative hypoid offset plotted against the crownwheel outer diameter for some rear axles. In this graph, normally available data of several axle manufacturers [6.2] are represented.

One may roughly distinguish two different area's for the relative hypoid offset:

$$\frac{a_k}{d_{e2}} = 0.12 \div 0.20 \quad for \quad d_{e2} \leq 230mm \qquad (3.1)$$

$$\frac{a_k}{d_{e2}} = 0.05 \div 0.12 \quad for \quad d_{e2} \geq 230mm \qquad (3.2)$$

In the range of 180 - 500 mm crownwheel diameter, the absolute value of the pinion offset lies between 25 and 40 mm. The large variation in the amount of relative offset, ranging from 5% to almost 20%, is an indication for the variaty of reasons for choosing a relative hypoid offset. Requirements for noise production, lay-out or manufacturing reasons, even historical experience of a manufacturer may be the reason for applying a certain relative hypoid offset.

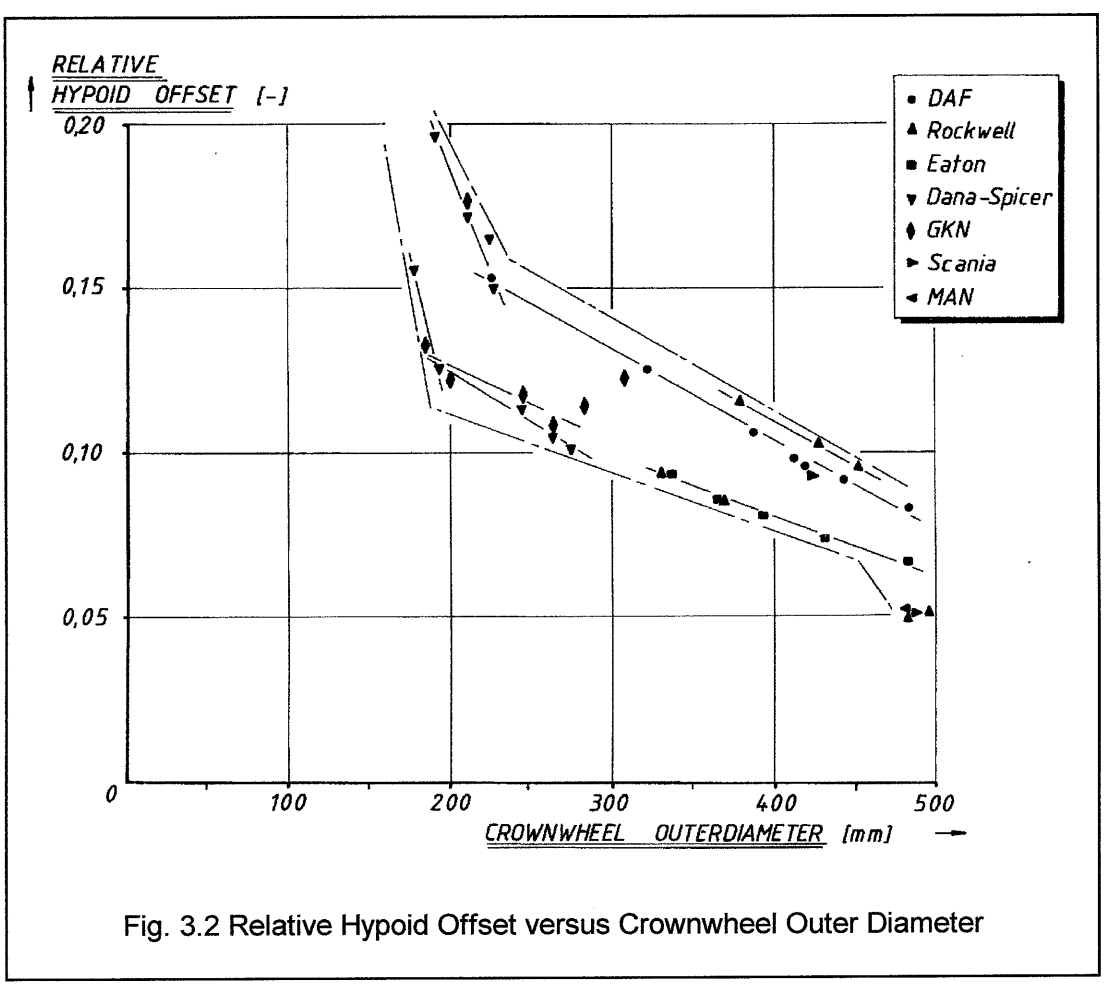

Fig. 3.2 Relative Hypoid Offset versus Crownwheel Outer Diameter

3.3 Geometry Calculations

For the calculation of hypoid gear geometry, there are no official standards like ANSI/AGMA or DIN. Here the only analytical calculation methods have been developed by the three manufacturers of bevel and hypoid gear generators, Klingelnberg, Oerlikon and Gleason. Apart from these, Winter has published some design directives [2.5]. In correspondence to chapter 2, the calculation methods according to Gleason, Oerlikon and Winter will be briefly analysed. The major criterium of the geometry calculations is the selection of the virtual bevel gears that are to substitute the actual hypoid gears. All methods use this construction of virtual bevel gears. There is however a large difference between the individual methods, in which the geometry of the actual hypoid gears is substituted into the geometry of the virtual bevel gears. This is mainly determined by the spiral angle and the facewidth that is used for the virtual bevel gears.

Oerlikon
The virtual bevel gears here obtain both the spiral angle and facewidth of the hypoid pinion. The geometry of the virtual bevel gears is determined by the hypoid pinion.

Gleason
The mean spiral angle of the virtual bevel gears is the mathematical mean value of both spiral angles of the hypoid pinion and gear. The facewidth is the same as for the hypoid crownwheel.

Winter
Here, the facewidth and spiral angle of the gear here determine the virtual bevel gears.

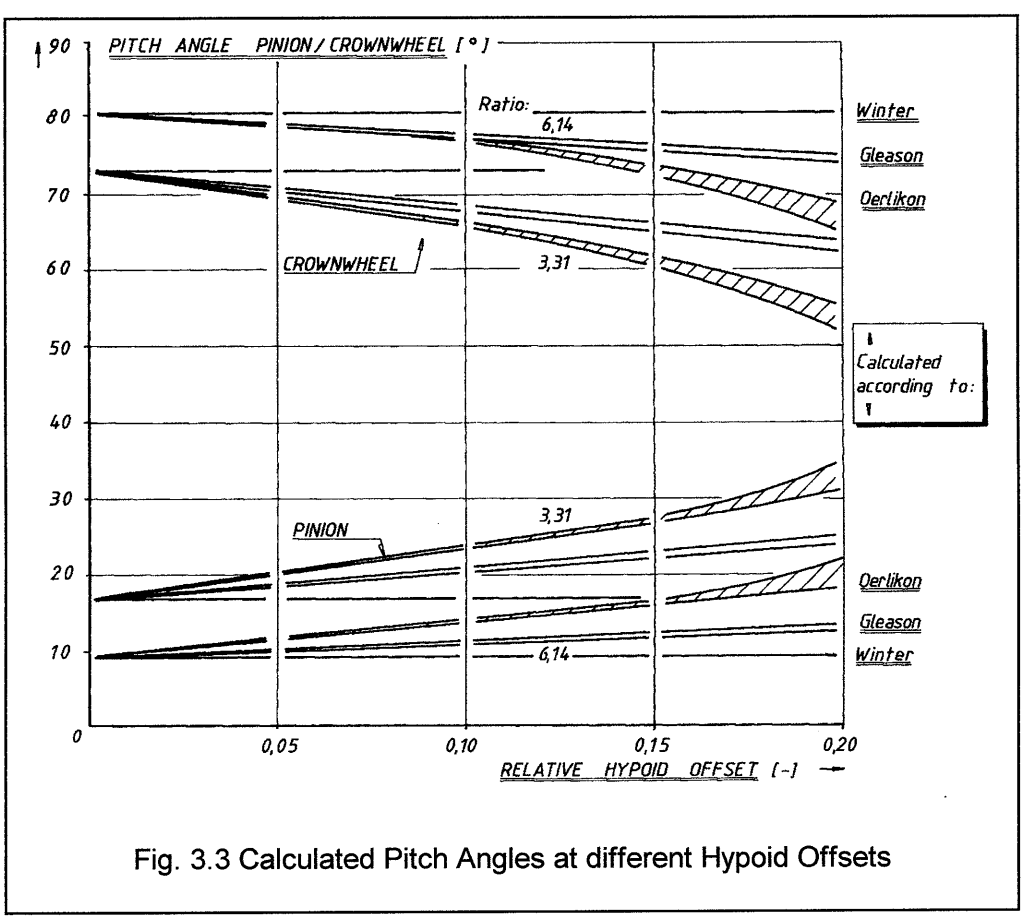

Fig. 3.3 Calculated Pitch Angles at different Hypoid Offsets

Although in all methods a virtual bevel gear geometry is choosen, based on the actual hypoid gears, there are substantial differences between the several standards in the geometry of the virtual bevel gears that substitute the actual hypoid gears.
The most important factors of the virtual bevel gear geometry, namely the representative spiral angle and face width, have their influence on the calculated face contact ratio and the strength. The influence of hypoid offset on gear geometry is the strongest taken into account by the Oerlikon method, where both the larger facewidth and the larger mean spiral angle of the pinion lead to relatively strong virtual bevel gears with a larger face contact ratio. The method according to Winter selects the smaller facewidth and the smaller spiral angle of the gear. This implies the smallest influence of hypoid offset for geometry and strength. The method of Gleason can be considered as ranging in between both (figure 3.3).

Both calculation examples of chapter 2 are used here. Starting from the bevel gear at zero offset, the pitch angles are calculated at increasing relative hypoid offsets of 5, 10, 15 and 20%. As can be seen, the pinion pitch angles calculated according to Gleason are smaller than when calculated according to Oerlikon. This implies that the diameter and the teeth number of the virtual helical pinion for the Gleason method will be smaller than the one calculated according to Oerlikon. For the method according to Winter, there is only minor influence of hypoid offset on the pitch angles.

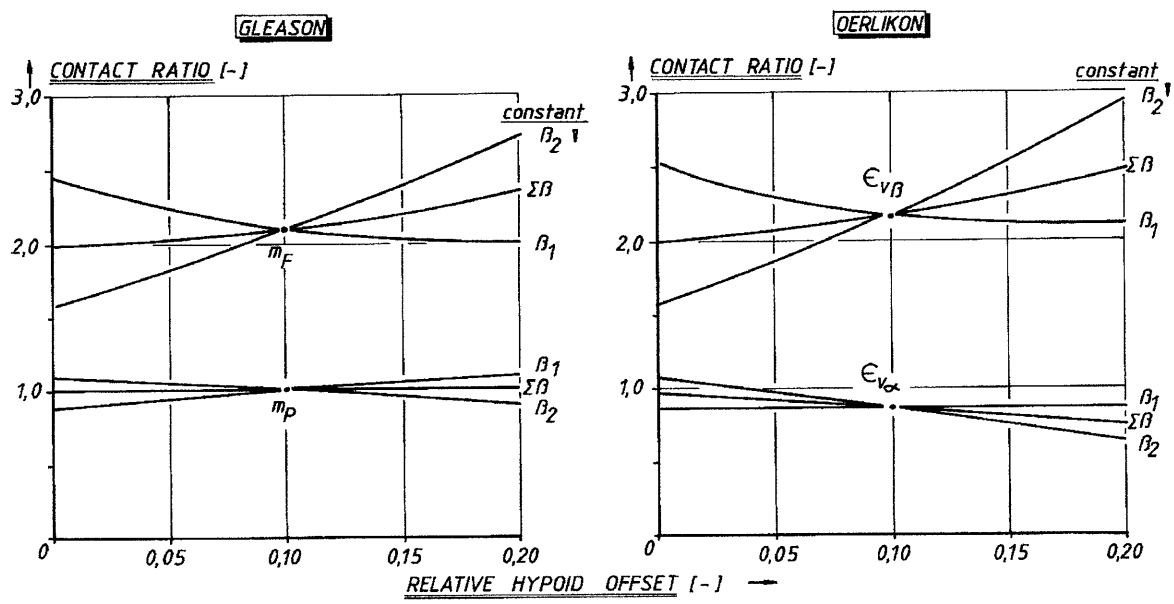

Fig. 3.4 Profile and Face Contact Ratio at different Hypoid Offset for Ratio i=6.14

The influence of hypoid offset on the profile and face contact ratio, according to the calculations of Oerlikon and Gleason has been determined for the ratio 6.14. The results are given in fig. 3.4 for three different design strategies:

* Constant pinion spiral angle.
* Constant crownwheel spiral angle.
* Constant sum of pinion and crownwheel spiral angle.

Here also, discrete points have been calculated at 5, 10, 15 and 20% relative hypoid offset. The lines between the points have been drawn continuously for reasons of clarity.

For bevel gears, at zero hypoid offset, the profile and the face contact ratio calculated according to the different standards are all identical, as has been shown in chapter 3.
At an increasing hypoid offset, the profile contact ratio, calculated according to Oerlikon, remains constant for a constant pinion spiral angle. This is the same for the Gleason calculations, when the sum of spiral angles remains constant. The face contact ratio according to both standards increases at increasing hypoid offset, mainly due to increasing facewidth. Calculated according to Gleason, gives a more constant effect (fig. 3.4). These effects reflect the basis of the choice for the virtual bevel gears substituting the hypoid gears.

3.4 Tooth Root Stress Calculations

In this part several calculation methods on tooth root stress of hypoid gears will be compared, with special emphasis on the influence of hypoid offset.
First the calculation methods according to Gleason, Oerlikon and Winter will be compared. Secondly, the results that can be derived from different investigations on hypoid gears will be analysed and compared. The calculation method of Klingelnberg is not included here, because the author had no possibilities available to perform stress calculations with this method.

3.4.1 Analytical Stress Calculations

In general there are three different strategies that can be used when applying a hypoid offset:

* Constant pinion spiral angle.
* Constant crownwheel spiral angle.
* Constant sum of pinion and gear spiral angle.

These three strategies have been applied for the calculation methods of Gleason, Oerlikon and Winter. For the last method, the stress calculations according to DIN have been used to determine the tooth root stress of the virtual bevel gears, that have been determined by the method of Winter. Both axle ratio's of the calculation examples of chapter 2 have been calculated, each with the above mentioned design strategies regarding the spiral angle. The results of these calculations are summarised in fig.3.5 and 3.6.
It can be seen that the influence of hypoid offset on calculated tooth root stress is different for the three calculation methods; even separate regions can be distinguished.

Calculations according to Winter show a relatively small influence of hypoid offset on tooth root stress, whereas Oerlikon gives the largest influence. The Gleason results lie in between both methods. This is comparable to the influence of the virtual bevel gear geometry.

It may be concluded that the three calculation methods differ to a large extent, as the influence of hypoid offset on the stress decrease is concerned. The calculated influence of hypoid offset on the stress decrease according to the Oerlikon method, where in fact the mean spiral angle and the facewidth of the **pinion** determine the geometry of the virtual bevel gears, is significantly more than calculated according to Gleason and Winter. In the latter, the spiral angle and facewidth of the **crownwheel** determine the geometry of the virtual bevel gears. In the method according to Gleason, the geometry of the virtual bevel gears is determined by an average value of the mean spiral angle of **pinion and crownwheel**. As a consequence, the difference in the individual methods may therefore be considered to be very large.

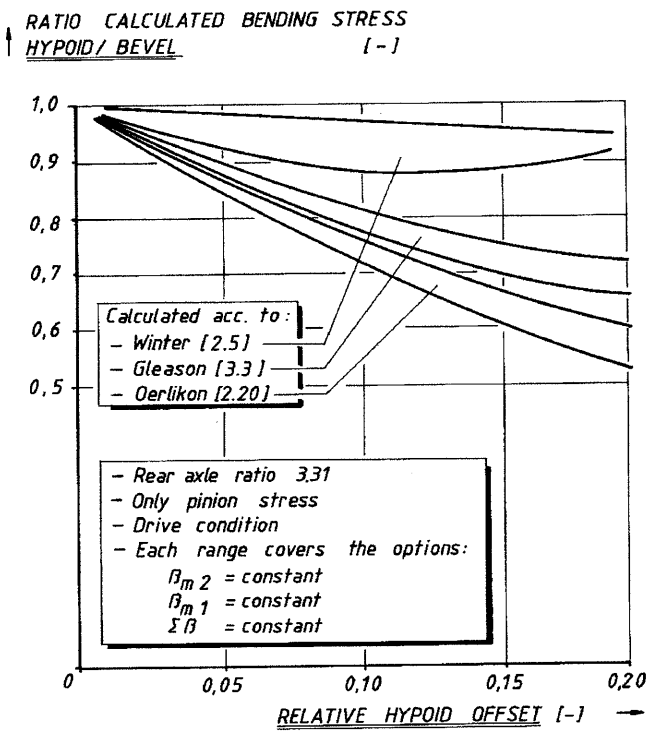

Fig. 3.5 Calculated Decrease of Tooth Root Stress at Hypoid Offset

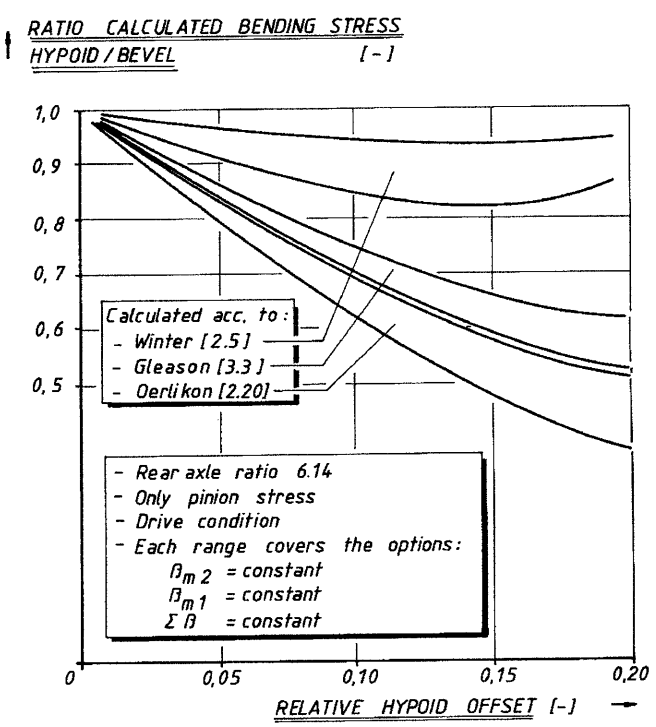

Fig. 3.6 Calculated Decrease of Tooth Root Stress at Hypoid Offset

3.4.2 Other Investigations on Hypoid Offset

Several other investigations have been performed recently, in order to determine the influence of hypoid offset on gear strength. Here only the results regarding the effect on tooth root stress will be summarised and discussed.

Fresen [3.8] has performed endurance tests and damage investigations on hypoid gears. The results made it difficult to clearly indicate what the influence of purely offset was on strength. A very clearly fatigue breakage of the pinion teeth did hardly occur; there was a mix of failures on both pinion and gear as well as some cases of pitting. The results of the endurance tests gave the impression that an increasing hypoid offset would reduce the loadability of the gears which can be regarded as contradictory to the general assumptions. It still remains difficult to separate purely the influence of hypoid offset, because next to it also other geometry parameters have been changed. It was however the first noticeable indication that a hypoid offset would not clearly lead to an increase of load capacity. These conclusions are more or less in line with the calculation method according to Niemann/Winter [2.5]. Here the influence of hypoid offset on tooth root stress is more flattened out mathematically by the choice of the virtual bevel gears.

Vollhüter [3.10, 3.11, 3.12] performed life tests and strain measurements on bevel and hypoid gears in order to establish the influence of hypoid offset. For the endurance tests the crownwheel diameter was 170 mm and the values of relative offset were 0-15-18-26%. The results of both tests and measurements showed that hypoid offset does reduce the tooth root stress at a given torque. The type of failure on the endurance tests changed from tooth fatigue breakage to surface fatigue failure at an increasing hypoid offset. The results of the endurance tests are summarised in fig.3.7.

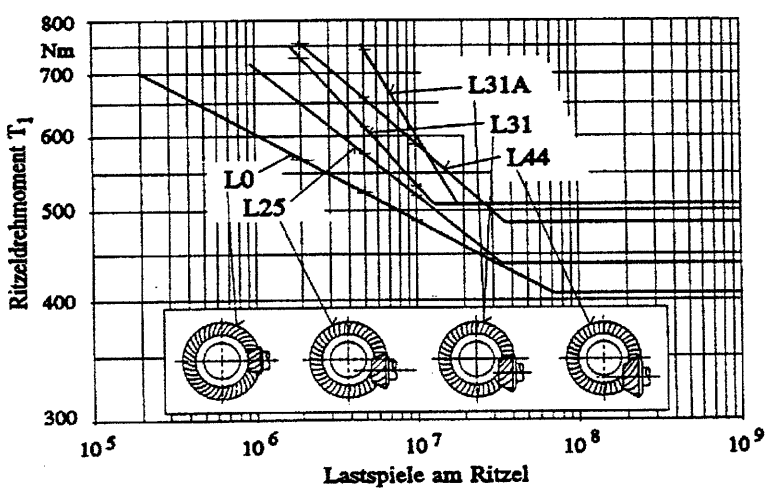

Fig 3.7 Results of Investigations by Vollhüter [3.10]

The following remarks can be given on this work.
The teeth number of the crownwheel is 39. This leads to a relatively large module, meaning that tooth breakage will not likely appear. To substract from these results fully the influence of hypoid offset on tooth breakage is not clearly possible. A teeth number of 41 to 46 would be more in the automotive range; than also the chance of tooth breakage would be higher due to the lower modulus.

The results of the endurance tests showed breakage at zero offset, while hardly any breakage occurred when an offset was introduced. This is only a quantative indication that a hypoid offset increases the tooth root strength; the endurance lifes for pitting only give the minimum increase on tooth root strength.
The loading level of the endurance tests was about 60% of the maximum torque according to the definition of chapter 6.2, based on the crownwheel outer diameter of 170 mm . This does not directly provoke tooth breakage. A crownwheel output torque of about 2000-2500 Nm for these tests would have been more appropriate in order to provoke more dominantly a root fatigue breakage in all variants. The variants had, next to the hypoid offset, also other gear geometry parameters changed, such as pressure angle, profile shift and tooth thickness correction. It appears however that the strategy of constant sum of spiral angles has been used. Some of the geometry changes are inevitably but the influence of hypoid offset is not purely to be separated from these results.
The investigations of Vollhüter cover a range of 15-25% relative hypoid offset. The most interesting range of relative hypoid offset for automotive rear axle gears however is 5-15%.
From the endurance tests, SN-curves were drawn on basis of a 50% failure probability, bearing in mind that a mix of failures has occurred. Out of these curves it is possible to substract at least the minimum change in tooth root bending stress that has occurred, since at any hypoid offset hardly fatigue breakage occurred. For a given number of cycles, namely 2 x 10^6, 5 x 10^6 and 7 x 10^6 , a region of relative loadability can be derived, based on an assumed linear relation between torque and bending stress. The relative tooth root stresses are then determined by the ratio of attainable torques at the indicated numbers of cycles. There is then a linear relationship assumed between root stress and torque. The strain measurements give stress values that can directly be related to relative stress decrease as a result of hypoid offset (see fig. 3.10).

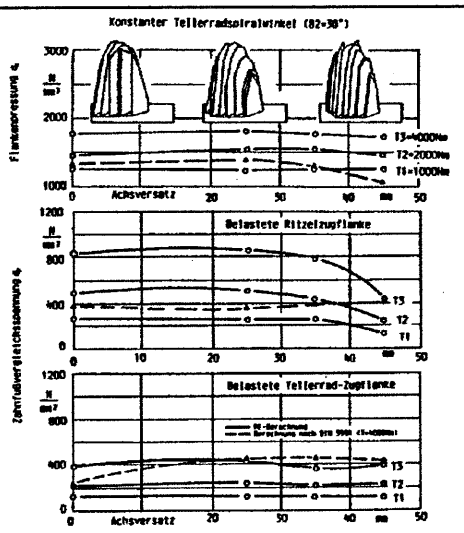

Fig. 3.8 Results of Numerical Calculations [3.14]

Theoretical investigations have also been performed on the influence of hypoid offset. This implies numerical calculations with the computerprogram "Kegelradkette", that was originally developed at the University of Aachen [3.13].
Stadtfeld [3.14, 3.15] performed series of calculations with one of the first versions of this program. The conclusion of his work with regard to hypoid offset was that there is a large difference between the three different stategies for spiral angles (figure 3.8).

At a constant crownwheel spiral angle, the tooth root stress on the crownwheel remains almost constant when the hypoid offset increases. The tooth root stress for the pinion decreases for hypoid offsets up to 10%. At larger offsets a very unusual pinion tooth form is produced because of the large pinion spiral angle. At a constant pinion spiral angle, the unfavourable contact pattern and crownwheel geometry leads to flat contact lines. This increases the root stress at both pinion and crownwheel at increasing hypoid offset. At a constant sum of spiral angles, the root stress on the gear remains more or less constant. The root stress at the pinion decreases until an offset of about 12%, caused by the increasing pinion diameter. At larger offsets there was an increase of root stress on the pinion.

Schweicher [3.16] made some specific investigations purely on the influence of hypoid offset with later versions of the "Kegelradkette", where in principle the results of FEM-calculations were considered. He calculated that in general the tooth root stress on the pinion decreases at increasing hypoid offset, whereas the stress increases on the crownwheel. Only the amount of stress change depends on the stategy for the spiral angles (fig. 3.9).

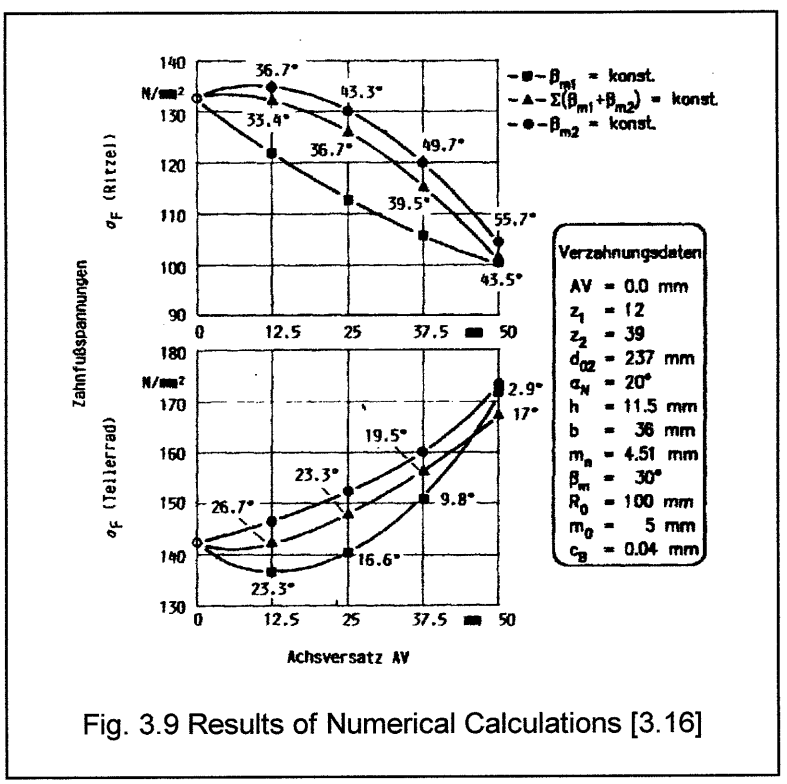

Fig. 3.9 Results of Numerical Calculations [3.16]

He found that, when introducing a hypoid offset, there are two effects that explain for the change in tooth stress. First there is the increasing pinion diameter and tooth thickness which decreases the stress. Secondly there is the effect of the increasing screwform of the teeth by which the contact pattern changes its form and the contactlines become shorter, which plays a role at large offsets. Both effects act simultaneously and countereffective with different sensitivities, depending on the spiral angle strategy and the gear geometry.

In a combined publication [3.17] of the FZG at Munich and the University of Aachen, a comparison has been made between theoretical calculated and experimental established stress changes at increasing hypoid offset. The calculations and measurements for the crownwheel correlated very well, but there was still a large difference for the pinion.

According to the authors, a more refined meshing of the pinion model is required in order to minimise the difference between measured and calculated root stress. From this conclusion one might get the impression that the results of the strain measurements, also the tendency with offset, may be regarded as fairly reliable.

3.5 Summary of Results on Hypoid Offset

From the investigations that have been discussed here, a summarising graph has been derived on the stress decrease resulting from hypoid offset. For this, the results of all different investigations have been analysed and compared. This diagram is given in figure 3.10, where the stress decrease for the pinion tooth root is given when loaded in the Drive Side at increasing hypoid offset. There it can be seen that in specific area's the theoretical derived values of some investigations coincide reasonably well with experimental findings of other investigations.

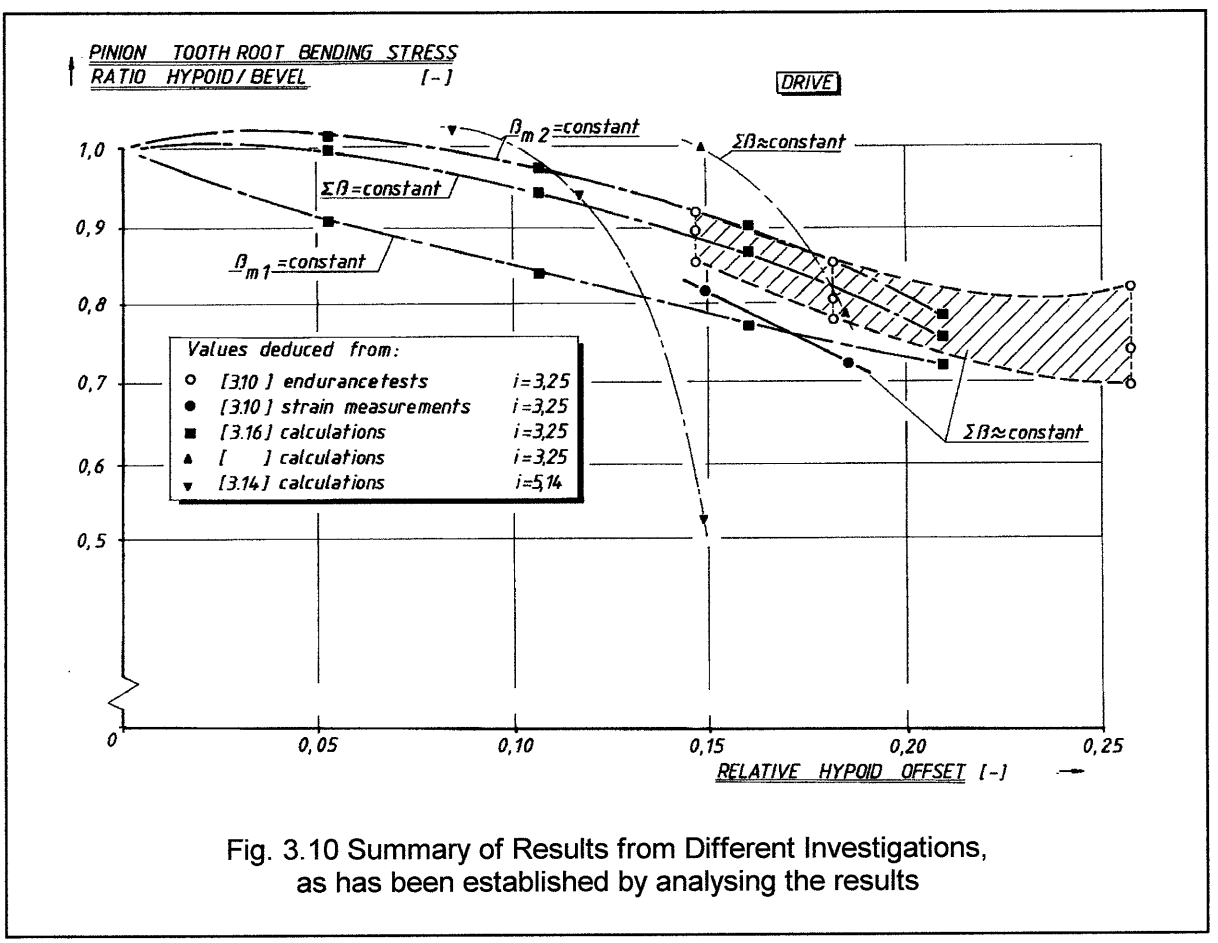

Fig. 3.10 Summary of Results from Different Investigations, as has been established by analysing the results

For hypoid offset larger than 15% and the stategy of constant sum of spiral angles, the theoretical calculations of Schweicher and the endurance testst of Vollhuter coincide even very well. Considering the fact that the values from the endurance tests only represent a minimum stress decrease, it seems that the theoretical calculations indicate a relatively mild influence of the hypoid offset to tooth root stress reduction.
A further conclusion that may be drawn, is that in general the pinion tooth root stress decreases at an increasing hypoid offset. The rate is about 10% stress decrease at 15% relative hypoid offset. At a 20% relative offset, the stress decrease is a mere 20%. It may well be possible to

assume a more or less straight line between these points. The root stress change for the crownwheel is different from this, although it is not given in the graph. Figure 3.10 can directly be compared with figures 3.5 and 3.6.

They are combined in figure 3.11, where the following conclusions may be drawn:
* The influence of hypoid offset on the tooth root stress, calculated analytically according to Oerlikon and Gleason is larger than the different investigations. A factor 2.5 - 3 larger stress decrease is calculated here than the investigations show.
* The calculations according to Winter coincide very well with the latest findings, at least for hypoid offset smaller than 10%. For offsets larger than 12%, the difference increases although it is always smaller than the Oerlikon or Gleason based calculations.
* The virtual bevel gear geometry according to the procedure of Winter may be considered as being very realistic in this respect up to a relative hypoid offset of 10-15%. The limitation is that it is valid for a gear ratio of about 3 - 3.5 and a constant sum of spiral angles strategy.
* For hypoid offsets larger than 15%, the stress decrease seems to become more sensitive for offset, as the slope is larger.

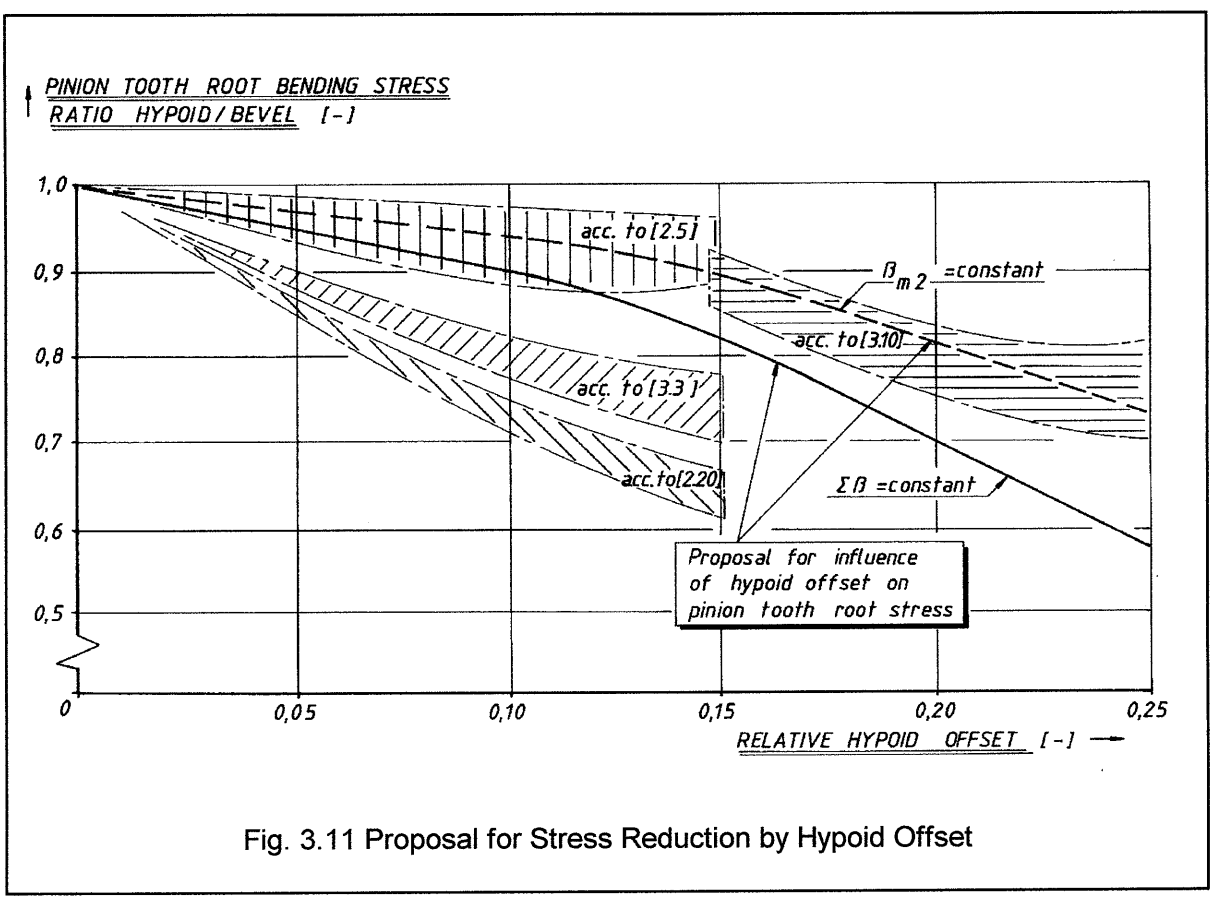

Fig. 3.11 Proposal for Stress Reduction by Hypoid Offset

According to this, a proposal may be derived to determine the effect of hypoid offset on tooth root stress for the Drive Side of the pinion, as indicated by figure 3.11.
Another aspect is that for a respective stress decrease, a far larger hypoid pinion offset is required than is commonly used in automotive applications. The greater part of automotive applications use a relative hypoid offset of 5-15%, whereas only from 15-20% offset a substantial decrease in pinion tooth root stress can be expected, as indicated by the diagram of fig. 3.10.

3.6 Resumee

For tooth root stress calculations of hypoid gears, a comparison has been made on several standards that are used by gear machine manufacturers.
In all considered standards, the geometry of hypoid gears is described by virtual bevel gears that substitute the hypoid gears. This principle is identical to the geometry calculation of bevel gears, which are substituted by virtual helical gears.
There are different ways of calculating the geometry of the virtual bevel gears for the given hypoid gears. The main differences are determined by the assumption of the spiral angle and the face width of the virtual bevel gears.
The mean spiral angle and the facewidth of the pinion both form the basis for the virtual bevel gears according to Oerlikon. The method according to Winter uses the mean spiral angle and the facewidth of the crownwheel as the basis for the virtual bevel gears. The virtual bevel gear geometry according to Gleason uses the crownwheel facewidth and the average of the sum of the mean spiral angles for pinion and crownwheel.

Analytical calculations on the pinion tooth root stress according to Gleason, Oerlikon and Winter have been performed for the calculation examples of chapter 3. The root stress was calculated as a function of the hypoid offset. Three different strategies for the spiral angles have been used. All standards calculated a decreasing tooth root stress at an increasing hypoid offset.
Generally the influence calculated by Oerlikon is much larger than the one according to Winter; Gleason here takes an intermediate position.

Other investigations, based on FEM-calculations and practical measurements of endurance life and tooth root strain have also indicated a decrease of tooth root stress at increasing hypoid offset.
For hypoid offsets larger than 15% of the crownwheel outer diameter and a constant sum of spiral angles, there is a good correlation between the theoretical calculated and experimental determined decrease of tooth root stress. Only the FEM calculations show a milder decrease for the root stress than experiments indicate.

If the results of these investigations are compared to the stress calculations of Oerlikon, Gleason and Winter, a relatively large difference is obtained between the Oerlikon and the Gleason methods on one hand and experimental findings on the other hand.
The stress decrease according to Oerlikon and Gleason is about 2.5 - 3 times larger than the experimental findings.
The difference between the Winter method and the investigations is very small.
Therefore it is concluded that the procedure for calculating the pinion gear geometry and the tooth root stress of hypoid gears according to Winter gives the best description of the influence of hypoid offset on tooth root stress of hypoid pinions.

For the pinion tooth root stress, a reduction of 10% on tooth root stress at a 10% relative hypoid offset may be expected for a constant sum of spiral angles. For a constant spiral angle of the crownwheel, a larger relative hypoid offset of 15% is required for the same reduction of 10% in tooth root stress. At larger hypoid offsets, the decrease in tooth root stress is higher.

4 ENDURANCE TESTS ON HYPOID GEARS

4.1 Introduction

In automotive industry, at least for gear drives in rear axles, the determination of tooth root stresses at static loading with the required safety factor is one aspect. The other, in fact even more important issue for automotive rear axle drive gears, is the endurance life of the rear axle gears, depending on the vehicle application. The accompanying failure probability also is important if a large number of vehicles is manufactured with a very wide variation in application and different driveline loading. A 44 tonne vehicle used for long distance haulage will run in its technical lifespan about 800.000 - 1.000.000 km or even more, with the greater part of the loading conditions to be characterised by a constant and relatively low torque at high speed. On the other side of the vehicle range, a distribution vehicle for mainly inner city or even inter urban traffic, will travel about 300.000 km in its life, where the amount of relatively high torques and low speeds will prevail. This will have a large influence on the expected service life for the rear axle gears.

Dimensioning automotive rear axle gear drives, based on the life expectancy, therefore is at least equally relevant as designing on a specific safety factor as is the case with international standards such as ANSI/AGMA, DIN and ISO. In order to predict the life expectancy of a rear axle gear for a given vehicle application, a practical endurance calculation method should be available, that has been verified with actual gear endurance life tests.
This method for dimensioning rear axle gears normally contains the following items:
* A calculation method for tooth root stress when geometry and applied torque are known.
* Allowable endurance strength values and data on the fatigue characteristics of the gears.
* Life data of endurance tests on rear axle gears.

Apart from this, additional knowledge is necessary on those factors in the stress calculations, that up to now give a considerable difference in values, when the different calculation standards are compared. This means that especially for rear axle gears, the Face Load Distribution Factor and the Application Factor will have to be detemined.

In order to obtain actual gear endurance life data, test rig fatigue life tests have been performed on rear axle gears at a constant amplitude loading. The gears have been operated under conditions that are close to vehicle conditions. This means that they are assembled in the actual rear axle casing, where actual deflections are likely to occur. The results of these tests are analysed statistically, in order to determine their failure probability. These registered endurance test results are then compared with the calculated gear life expectancy. Both calculations and test results are then fitted by adapting the calculations of root stress and service life,.
Depending on the difference between both, some adaptions will be made on the calculations in order to match calculated and measured life. Special care has to be taken to ensure that the correlation factors that are introduced to numerically fit the test and the calculation results, these corrections are to be physically correct. In this way, a practical method is then derived to determine new rear axle gear designs in similar applications.

4.2 Results of Constant Amplitude Endurance Tests

Life tests on a rear axle test rig have been performed on four different types of truck rear axles, that are designed for 11 and 13 tonne axle load. The vehicle weight varies from 30 to 45 tonne. The rear axles are equipped with different rear axle gears in terms of ratio and gear geometry. In order to distinguish the different types, they will be referred to by the gear outerdiameter. For each of the four different axle types, several ratios have been tested. For each ratio several gears have been used on the endurance life tests. The tests have been performed on complete rear axles, in order to incorporate realistic built in situations such as pinion and gear deflections under load.
All tests have had a constant amplitude loading of the gears; both the output torque and input speed were kept at a constant level. From these endurance tests, specific data are obtained on the actual fatigue characteristics of the complete assembled gear sets.

4.2.1 Geometry of the Tested Rear Axle Hypoid Gears

General data of the gears in terms of crownwheel outerdiameter, gearing type and axle ratio, are given in table 4.1. All rear axle gears are hypoid gears with one and the same absolute value of hypoid offset of 41 mm. This means that the relative hypoid ranges from 8-10%.

Crownwheel Outerdiameter [mm]	Gearing type [--]	Axle ratio's [--]	Number of Testsamples [--]
485	Oerlikon	2.93 - 5.63	22
445	Oerlikon	2.93 - 5.63	28
425	Gleason	3.31 - 6.14	19
410	Oerlikon	3.31 - 5.63	17

Table 4.1 General Data of Tested Rear Axle Hypoid Gears

Axle Ratio	2.93	3.31	3.73	4.10	4.56	5.13	5.63	6.14
Teeth Numbers	14/41	13/43	11/41	10/41	9/41	8/41	8/45	7/43

Table 4.2 Teeth Numbers and Rear Axle Ratio's

The tested rear axle gears with different diameters have identical teeth numbers and ratio's. The teeth numbers of both pinion and crownwheel as well as the gear ratio's are given in table 4.2. The axle with 410 mm crownwheel diameter was an experimental one; it was not released for production. The other three rear axle gear types are in production since the late eighties and still operate without any problems. The most important geometrical data are given here in terms of the gear outerdiameter, the mean normal module, the gear mean spiral angle, the gear facewidth and the cutterradius, which are given in table 4.3.

Crownwheel Outerdiameter [mm]	Mean Normal Module [mm]	Spiral angle [°]	Face width [mm]	Cutter radius [mm]
485	8.2 - 8.6	32-35	75	140
445	7.3 - 7.6	34-38	65	140
425	7.0 - 7.7	29-32	60	6"
410	6.9 - 7.1	33-36	60	140

Table 4.3 Most important General Geometrical Data of Tested Rear Axle Gears

All gears have basic geometric characteristics resembling current state of the art and are representative for nowadays truck rear axle design. Several geometry data are in line with Gleason and Oerlikon recommendations and guidelines. These include:
* profile shift for preventing undercut on the pinion,
* tooth thickness correction for equal life,
* standard pressure angle of 22.5^0,
* standard pressure angle correction between Drive and Coast sides,
* standard helical crowning,
* cutter geometry according to general recommendations,
* non generated teeth on the crownwheel (Gleason Formate and Oerlikon Spirac).

The gears have been manufactured with normal state of the art manufacturing methods and normal production installations, that are commonly used in the automotive industry for large scale production. Soft machining of the gears takes place on Oerlikon and Gleason bevel and hypoid gear cutting machines. Pinions and crownwheels are both case carburised in large volume production heat treatment furnaces with state of the art control systems for the carburising process. After carburising, the pinions are direct hardened; the crownwheels are heated to austenite temperature and then hardened under a quenching press. Finally both members are lapped on Oerlikon and Gleason lapping machines according to standard procedures. The general gear quality is according to standard gear production techniques and may be regarded to be representative for normal truck applications.

The material for the pinion and the crownwheel is a case-carburising steel, as normally in automotive rear axle gears. In this case 23CrMoBS3.3, W.St.Nr 1.123.456 is used. The most important characteristics of the chemical composition are 0.20-0.25% Carbon, 0.70-0.90% Manganese, 0.70-0.90% Chromium, 0.30-0.40% Molybdenum and a small fraction of Boron for increased hardenability.

The gearsets of each axle type that has been tested, were produced within a limited time period of half a year maximum. The testresults of the gears with crownwheeldiameter 445 mm covers a longer timespan; some of the gears were tested three years after the first tests. This means that the variation in different material and heat treatment batches covers a limited time peroid. Over a longer period however, the variation of material and production related endurance characteristics will not significantly increase due to strict quality requirements and control of the manufacturing and heat treatment processes.

4.2.2 Test Rig and Test Conditions

The test rig is a so called open type. It consists of three electric motors, one for driving and two for loading the axle; each motor is equipped with gear boxes to cover a given range of speeds and torques. With the electronic control system, several vehicle conditions such as Drive and Coast loading of the axle gears can be simulated. The maximum attainable power output amounts to 350 kW. A view of the test rig is given in fig.4.1 on the next page.

During the endurance tests, a mineral oil of API-GL5 quality and a viscosity range of 85W140 is used. This is a standard oil that is normally used for these types of rear axles. Normal splash oil bath lubrication is used in the rear axle.
During the tests, the oil was maintained at a constant temperature of about 80^0 - 90^0C by means of a closed loop cooling system. This oil temperature corresponds to stationary vehicle conditions as has been measured on Long Distance Haulage operations.

During each test, the torque and the rotational speed were kept at a constant level as these were constant amplitude tests. Most of the test have been performed at the "Maximum Torque", of which the definition in relation to the crownwheeldiameter is given in chapter 6.2.1. A smaller part of the tests were performed at about 50% of this value; the rest of the tests have been conducted at a torque level that is in between both levels.
Several loading conditions and the number of test samples used during the tests are given in Table 4.4. The crownwheel output torques of 47 kNm for the axle with 485 mm outerdiameter, 39 kNm for the 445 mm diameter and 32 kNm for both axles with 425 and 410 mm correspond to the term "Maximum Torque".

In the first place a relatively large variation in stress level is thus obtained, in order to minimise the error at determining the slope of the SN-curve. Secondly the tests at half the maximum torque level give a possibility for establishing the endurande limit value for the gears. The failure criterium of all tests was a reproducable and constant automatic shut down of the test rig when the measuring equipment registered a variation on the input torque that exceeded +/- 5% of the actual torque value.

Crownwheel diameter [mm]	Output Torque [Nm]	Input Speed [rpm]	Testsamples [--]
485	47.000 23.500	242 605	11 7
445	39.000 19.500	242 605	16 8
425	32.000 16.000	242 605	11 7
410	32.000 16.000	242 605	11 14

Table 4.4. Test Conditions of Endurance Life Tests

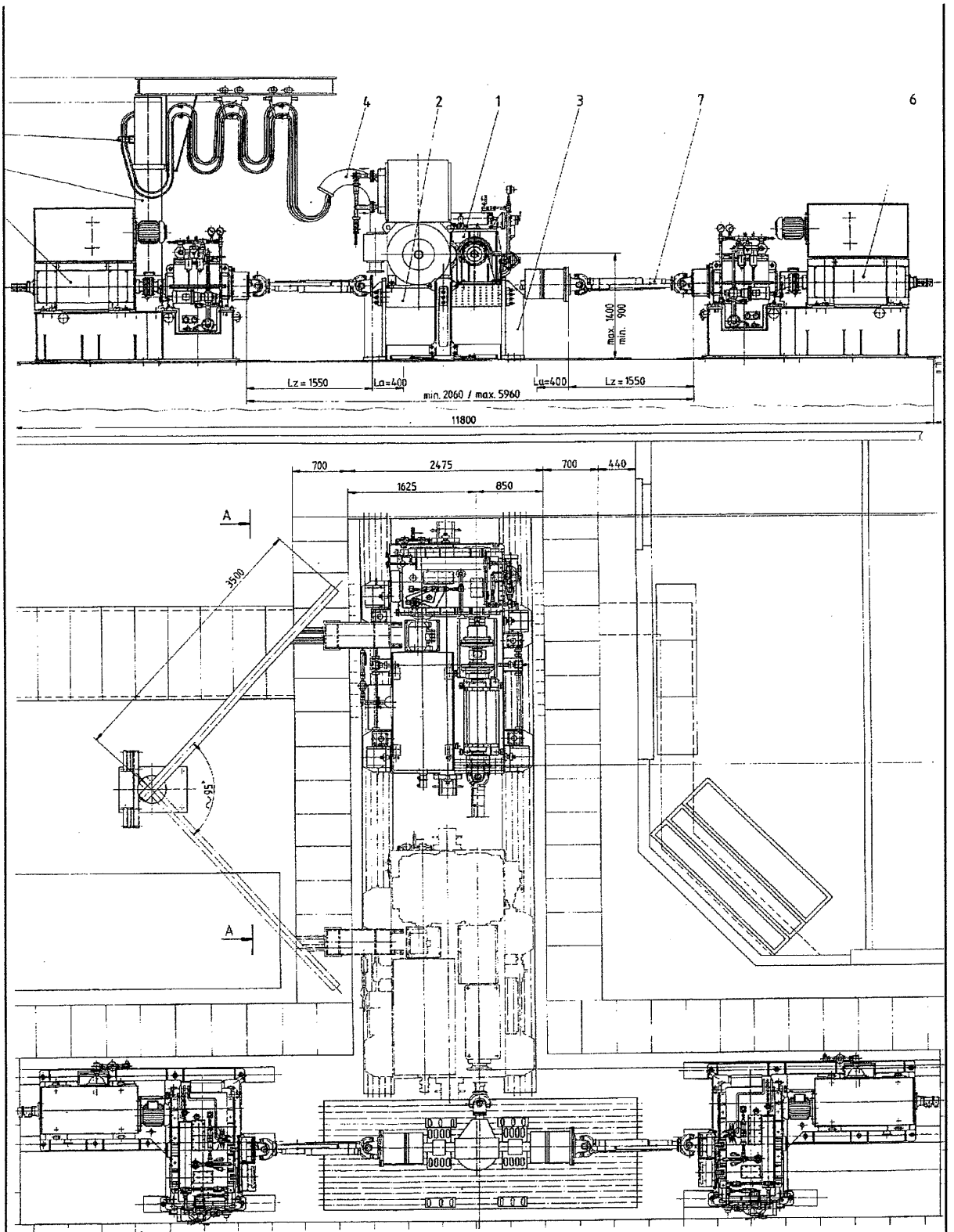

Fig. 4.1 Test Rig Lay-Out (Front and Top View)

4.2.3 Results of Constant Amplitude Tests

At the maximum torque level, the type of failure practically always was very clearly fatigue breakage of the pinion tooth root. The reason for this is threefold:
1. The relatively high stress level on the gears promotes tooth root fatigue breakage.
2. A very constant and reproducable loading level during the entire course of the tests.
3. A uniform and identical stopping criterium for all tests.

On all tests, the pinions failed. The registered endurance life values are therefore determined by the pinions. The only difference between several results was the number of teeth on the pinion that had been broken or the severeness of the broken parts. In some cases not only the teeth had been broken; also a relatively large part of the pinion cone shaped body was broken. The influence of this aspect on the endurance life evaluation has not been taken into account, as it is considered to be a consequence damage resulting from the original tooth breakage. On some occasions also parts of some crownwheel teeth had been broken. As these were beleived to be the result of broken pinion teeth coming entrapped in the gear mesh, they were considered to be a consequence damage that does not influence the result of the endurance tests.

Most of the tests that were performed at half the maximum torque level, were stopped after about $3x10^7$ revolutions when the stopping criterium of variation in torque had not come into action. In that case, mostly a slight form of surface pitting could be observed. Only in some cases there was a fatigue breakage of pinion teeth at which the test was automatically stopped. The results of these tests have been used in order to determine the endurance strength for the tested gears.

4.2.3.1 Statistical Analysis of Endurance Results

The results of the four different series of endurance tests have been statistically analysed. The statistical life results at one torque level, namely the maximum output torque, have been determined for 10%, 50% and 90% cumulative failure probability, assuming a 2-parameter Weibull and a Lognormal distribution. Table 4.5 gives the statistical results for a 2-parameter Weibull distribution and table 4.6 gives the results for an assumed Lognormal failure distribution.

Crownwheel Outerdiameter [mm]	N (f.p.=10%) x 10^5 [--]	N (f.p.=50%) x 10^5 [--]	N (f.p.=90%) x 10^5 [--]	Ratio N90 / N10 [--]
485	1.65	2.53	3.70	2.4
445	0.77	1.09	1.49	1.9
425	1.21	1.93	2.75	2.3
410	0.72	1.12	1.57	2.2

Table 4.5
Registered Number of Pinion Load Cycles at Maximum Torque for Failure Probability of 10, 50 and 90% when 2-parameter Weibull Failure Probability Distribution is assumed

Crownwheel Outerdiameter [mm]	N (f.p.=10%) x 10^5 [--]	N (f.p.=50%) x 10^5 [--]	N (f.p.=90%) x 10^5 [--]	Ratio N90 / N10 [--]
485	1.56	2.67	4.47	2.8
445	0.80	1.09	1.52	1.9
425	1.32	1.99	3.03	2.3
410	0.78	1.19	1.79	2.3

Table 4.6
Registered Number of Pinion Load Cycles at Maximum Torque for Failure Probability of 10, 50 and 90% when a Lognormal Failure Probability Distribution is assumed

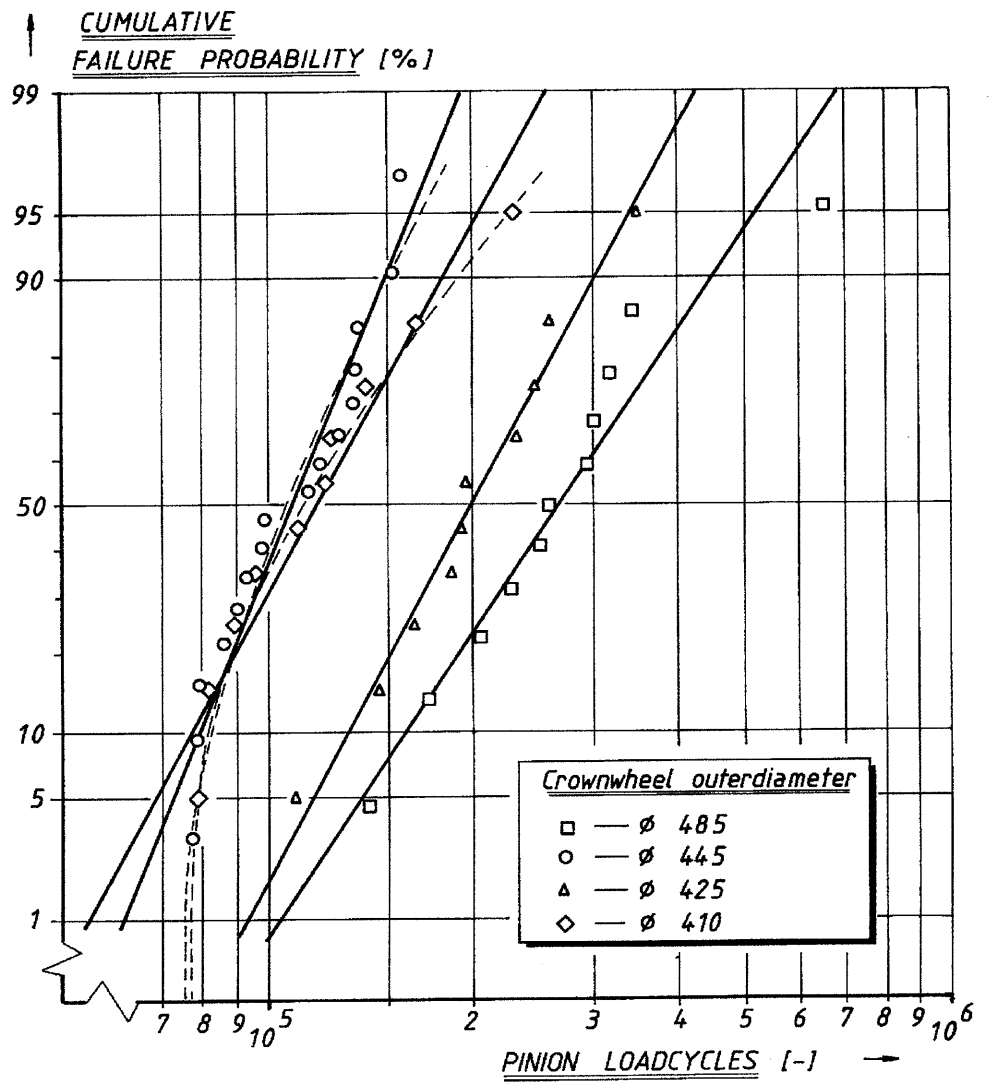

Fig. 4.2 Lognormal Representation of Test Results at Maximum Torque

In fig. 4.2 the testresults are plotted for an assumed Lognormal failure distribution.
The endurance results of the four different types show very clearly statistical differences, although the difference between the axle types with 445 mm and 410 mm diameters is very small, as the calculated tooth root stress of both types only differs little. Variation in endurance life between the 10% and the 90% failure probability ranges from 2 to 3 for the tested axle gears. This is a realistic value in view of the limited number of test samples and the limited number of material charges and different heat treatment batches. It is comparable to the results of other investigations, as indicated by [4.2] to [4.5], [4.7] and [4.11]. Based on the ratio of endurance lifes at 90% and 10% failure probability, the results of the rear axle endurance tests may be considered to be reliable.
Only the axle type 445 covers a larger variation in material and heat treatment batches over a longer time period of about three years. Still the results of these gearsets fit very well in the statistical analysis without any noticeable increase of the ratio N(90)/N(10). Therefore it is concluded that the variation of all tests can be regarded as being representative for a production time of three years. The variation in life over a longer period will hardly be larger than in this case because the variation in material and heat treatment properties will not be significantly higher. The difference however is expected to be not very large. High stress levels generally lead to a small variation in endurance lifes. At lower stress levels, the variation in fatigue life will increase.

4.2.3.2 Crack Investigations

Crack investigations have been performed on some of the tested rear axle gears. On some teeth, cuts have been made of the normal tooth section and the following was investigated:

* crack initiation and propagation at the tooth root in the tooth normal section
* crack propagation in direction of the face width.

Figure 4.3 gives some of the most representative and first visible cracks in the tooth root.

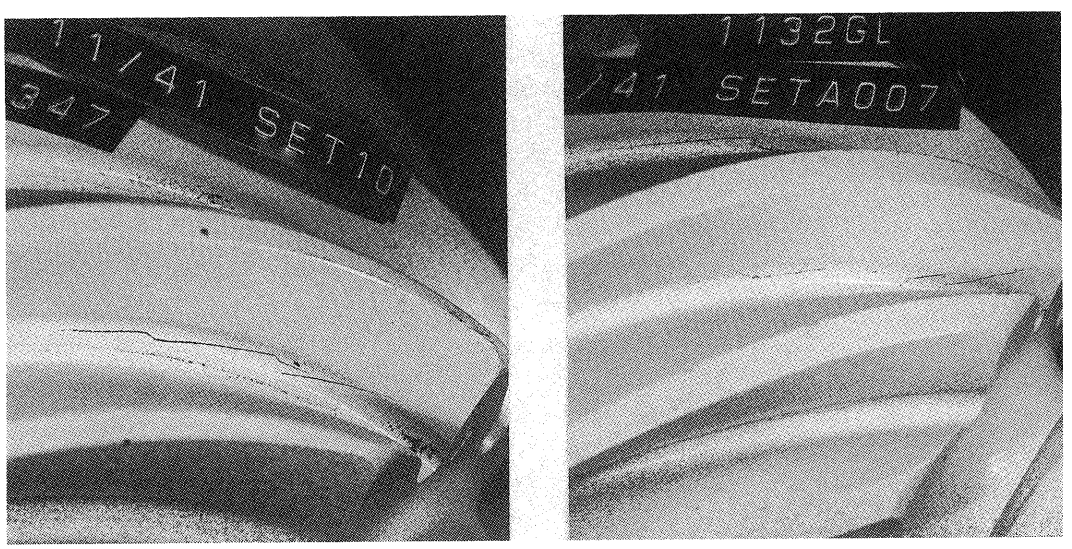

Fig. 4.3 Crack Initiation in the Middle-to-Toeside of the Facewidth

Figure 4.4 gives two examples of these cuts in the normal tooth section. On almost all pinions that have been investigated, the position of the crack initiation in the root and the direction of the crack propagation was similar to those shown in fig. 4.4.

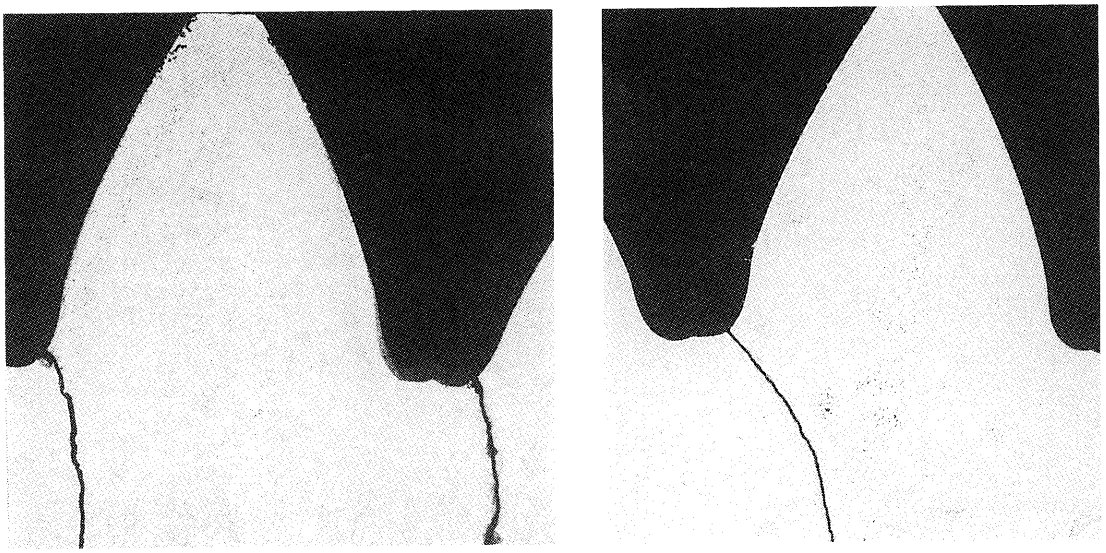

Fig. 4.4 Examples of Cracks in the Normal Section at the Middle of the Facewidth

The angle of the first section of the crack, which is supposed to be initiated at the outer surface of the tooth root, has been determined. This has been done by measuring the inclination of the crack at the outer surface to the tooth centre line in the normal section, as indicated by figure 4.5. As for this the test pinions had to be grinded into pieces, therefore the inclination angle has been measured only on a limited number of test samples.

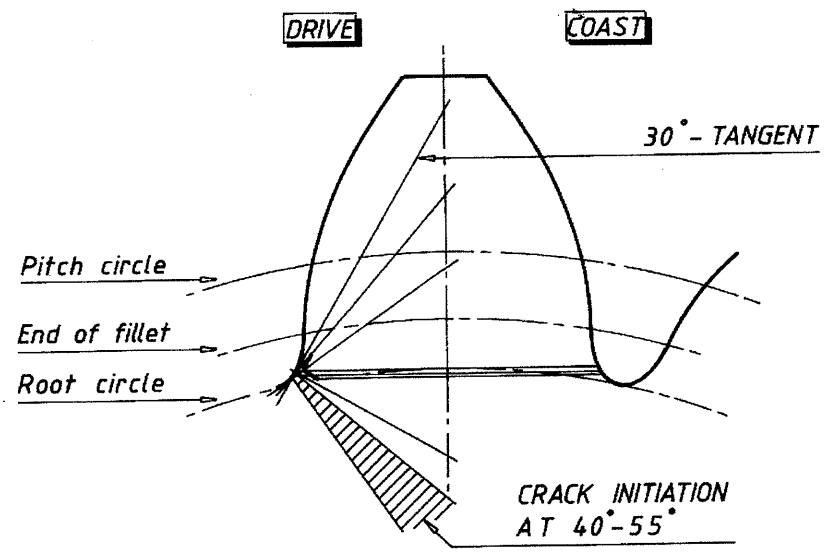

Fig. 4.5 Angle of Crack initiation at Tooth Root in Normal Section

The results of measurements on the angle of crack initiation are summarised in figure 4.6. There it can be seen that there is hardly any influence of gear ratio and gear type. The measured angle of crack origination at the tooth root in the middle of the face width ranges from 40 degrees minimum to 55 degrees maximum. Now it may be assumed that at that point, also the maximum stress would have occurred. This perception does not coincide with the general accepted 30^0-tangent; the angle is significantly higher than 30^0. In fact it appears to come more in the range of the intersect of the Lewis-parabola.
The difference with the 30^0 -tangent is not so surprisingly. In other publications of measurements on tooth root stress, similar results have been found. Therefore it can be concluded that in this aspect, hypoid gears do not differ from other gear types. This is valid for all the tested gear types. The actual value of the angle of maximum root stress may vary according to the gear geometry, but in general it differs from the assumed 30^0-tangent. This difference is acceptable because of the fact that the assumptions and the modelling the gear teeth as a cantilever beam, and only taking into account the tensile stress or a sum of different principal stresses, is also tantamount to some criticism. Like other publications, this will not be taken into account for the stress calculations.
The 30^0-tangent is a generally accepted convention that makes it easy to calculate the tooth form factor. It seems, however, that the position of crack origination corresponds more to the assumption of the Lewis parabola for the critical root thickness.

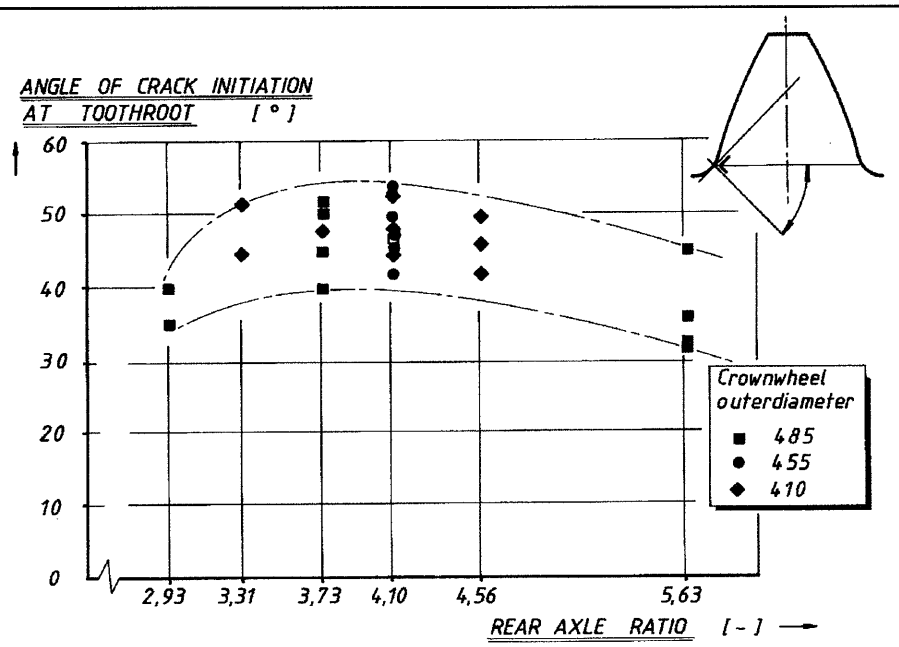

Fig. 4.6 Measured Angle of Crack Initiation at the Middle of the Facewidth

The crack propagation in the normal tooth section has further been studied. After being initiated at the outer surface of the tooth root, the cracks grow inward into the direction of the pinion centre line. This appeared to be the case on all pinions that have been investigated after the tests. Therefore it is assumed that this type of crack propagation is representative for all tested gears. This however differs from what normally can be observed at fatigue tooth breakage on helical gears, where propagation of the crack mostly is directed to the other side of the tooth.
The more complex stress situation in the tooth root resulting from the tooth curvature on bevel

and hypoid gears may well cause this effect. The forging texture of the material will possibly also play a role in determining the direction of the crack propagation. As all investigated pinions have a similar direction of the crack propagation, the influence of this on the life results has not been taken into account here.

On most of the broken pinion teeth, the angle of the crack initiation at the tooth root changed when proceeding in the lengthwise direction of the facewidth. Starting from the middle of the face width to both ends of the tooth, the position of the crack at the root moved out of the tooth root and upward towards the tooth tip. Investigating further the angle under which the crack proceeds into the teeth, the following could be observed.
Towards toe side, the initiating angle decreased; at the face end at toe side it mostly was about zero degrees, more or less horizontally. Towards heel side the angle however first increased and then it decreased only a small amount in the last part of the face width. This seems to be an indication that the concept of effective face width in the AGMA standard might play a role here.

On some occasions one could observe that only a part of the teeth had been broken. This probably was a result of a shifting of the contact pattern over the face width towards toe side. This effect did not indicate to lead to a smaller life; the crack origination always was in the middle of the facewidth.

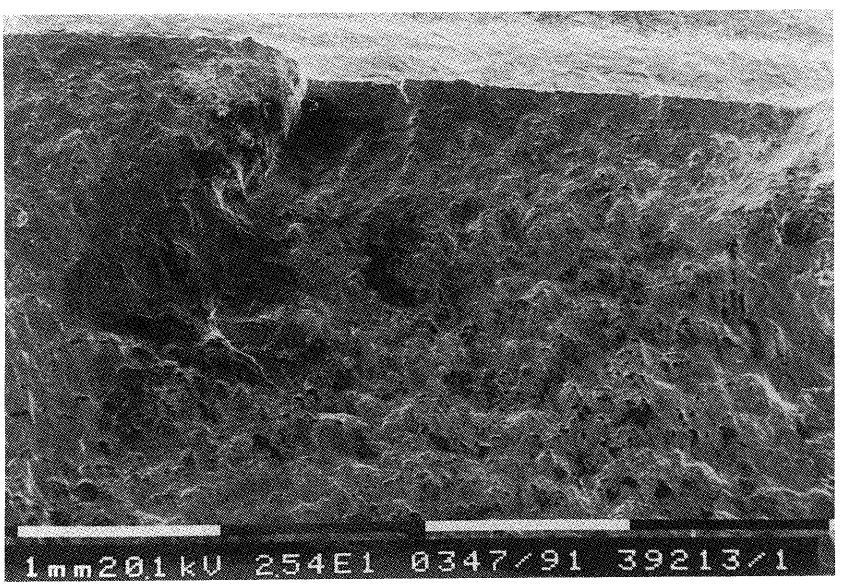

Fig. 4.7 “Steps” at the Cracks on the Root Surface

The cracks in the middle of the facewidth always show several "steps" which are normally present in fatigue cracks at case hardened parts. They are a result of several small initiating cracks at different places, growing in the lengthwise direction to meet each other. At these positions, the "steps" occur. This was observed on the major part of the test pieces. This may be the result of a relatively high stress level during the endurance tests, which promotes the initiation of several cracks at different positions. The relatively low ductility of the case hardened layer will also promote this. At lower stress levels, the number of different initiation locations generally will be lower. This aspect is only refered to as an indication that the failure phenomena correspond to fatigue failures. It does however have hardly any influence on the actual life.

From this analysis, the follwing conclusions can be drawn.
* At some pinions the origination of the cracks could be observed, as these tests were stopped during the first part of the lifetime. At these examples, it has consistently been shown that the first visible cracks on the surface of the tooth root were located in the middle of the facewidth to the toe side of the facewidth, as indicated in figure 4.3.
* The assumption that the middle of the face width of the pinion is the reference position for calculating the maximum tooth root stress, can therefore be considered to be correct.
* For the position of the crack initiation in the normal section of the root, there is however a difference between general calculating practice and observations of the test samples. The angle of crack initiation lies in the range of 30^0 - 50^0 tangent to the tooth root.

4.2.3.3 Endurance Life and Heat Treatment

The following material structure and heat treatment parameters will be responsible for a variation in fatigue characteristics:

* core strength
* surface hardness
* case carburising depth (Eht)
* amount of retained austenite / free ferrite
* surface oxydation and decarburisation
* possible carbides and precipitations.

Afer the tests, only data on the first three heat treatment parameters have been determined on a limited number of the tests pinions. The other three parameters can only be determined by extesive laboratory investigation; this has not been done here.
No significant correlation has been found between registered endurance life and the surface hardness or the core strength, under the condition that the minimum value is 1100 N/mm^2. Physically this would be expected, since these aspects are beleived to be more related to the appearance of surface fatigue or case crushing failures than with tooth root fatigue breakage. However there appears to exist a correlation between the case depth and the registered endurance life, based on the limited number of investigated pinions.

This tendency (fig. 4.8) is based on only a limited number of samples. There is a tendency of increasing endurance life with an increasing case depth. Two different regions can be distinguished between the largest and the smaller axle types. This difference is however caused by the different stress levels resulting from the differences in gear geometry. To ensure and verify this relation, further work will be necessary.

The observed tendency here corresponds partially to [4.13] where a correlation between case depth and fatigue strength is observed. When the case depth is higher than a minimal required value, however, there will hardly be any increase in fatigue strength to be expected, as is also indicated in [2.5]. In [4.14] there appears however to be no correlation between case depth and life, which is however contradictory to the here observed impression.
For a large scale production of rear axle gears, some amount of variation in several heat treatment parameters inevitably will occur. Fig.4.9 gives the variation of the hardening profile for most of the tested pinions. These values are attained with conventional manufacturing methods under normal production conditions; it is representative for the production process of the gears that have been investigated. The case depth in the tooth root is smaller than at the tooth midheigth, which is normally to be expected.

The actual measured case carburising depths of the tested gears at the middle of the tooth height correspond very well with the general guidelines of the ANSI/AGMA, Winter-Niemann and Oerlikon standards, that give a required case carburising depth of about (0.12 -0.25)*m_n.
If the relation between the endurance life and the case depth would be valid here, than this would mean that most of the variation in registered life for one gear type and under a constant and reproducable loading would be caused by the variation in case depth. This also could be an indication that the greater part of endurance life would be determined by the crack initiation and

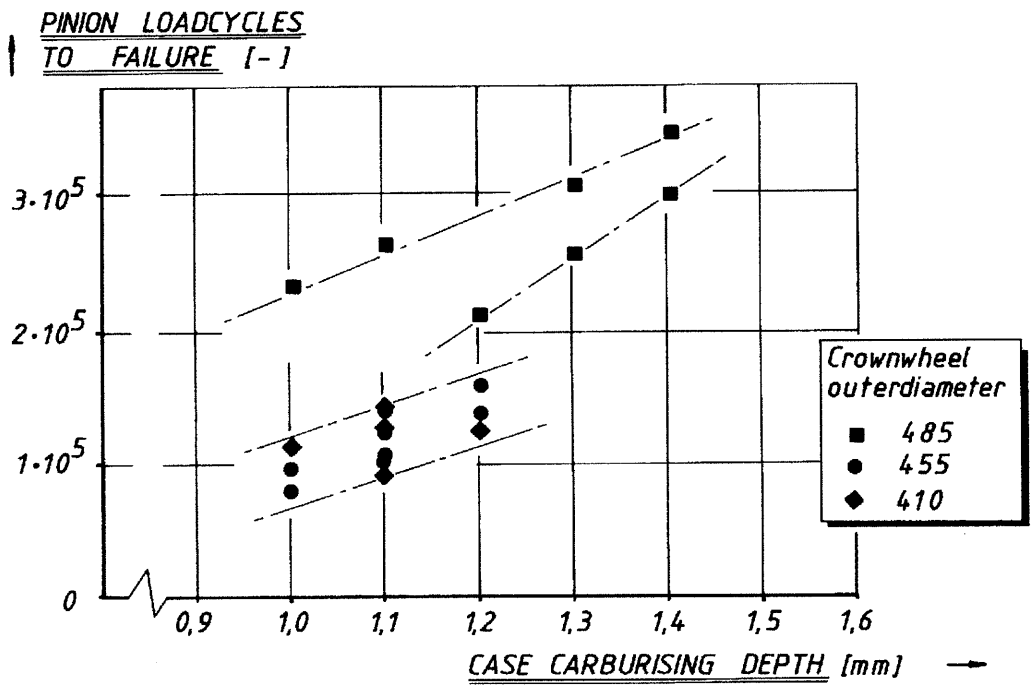

Fig.4.8 Correlation between Endurance Life and Case Depth

propagation in the case hardened layer. Once the crack is propagated beyond the case hardened surface layer into the core material, the fatigue characteristics would be determined by the material structure of the core. It would appear that here the variation in fatigue life is partly influenced by the variation in case depth.

It appears that a variation in the registerd life for the pinions with a value of about 2 would be minimal. This will be only achieved when the gears are:

- from one and the same material and forging batch
- from one and the same heat treatment batch
- tested on one and the same test rig at a very constant loading.

When testing under the same conditions but only over a longer period, two to three years for one axle type, one would expect a larger variation in endurance life because of the larger variation of material characteristics. If on the other hand the variation in casedepth is limited to a specific value by means of manufacture control, the anticipated spread in pinion endurance life may be also restricted to a maximum value. In real vehicle application,where generally there is a large difference in loading conditions, the variation in registered life wil increase, as indicated in the chart of figure 2.20.

Finally, the estimated stress under the tooth root surface at the "Maximum Torque" for all ratio's is drawn in fig. 4.9. From the comparison of allowable to actual stress, the critical point of crack initiation may be considered to be located at the surface of the pinion tooth root and not under the surface. Because of the stress concentration in the tooth root, which has a value of about 2.0, the sub surface hardness profile of the pinion here will not likely be the cause of sub surface crack initiation.

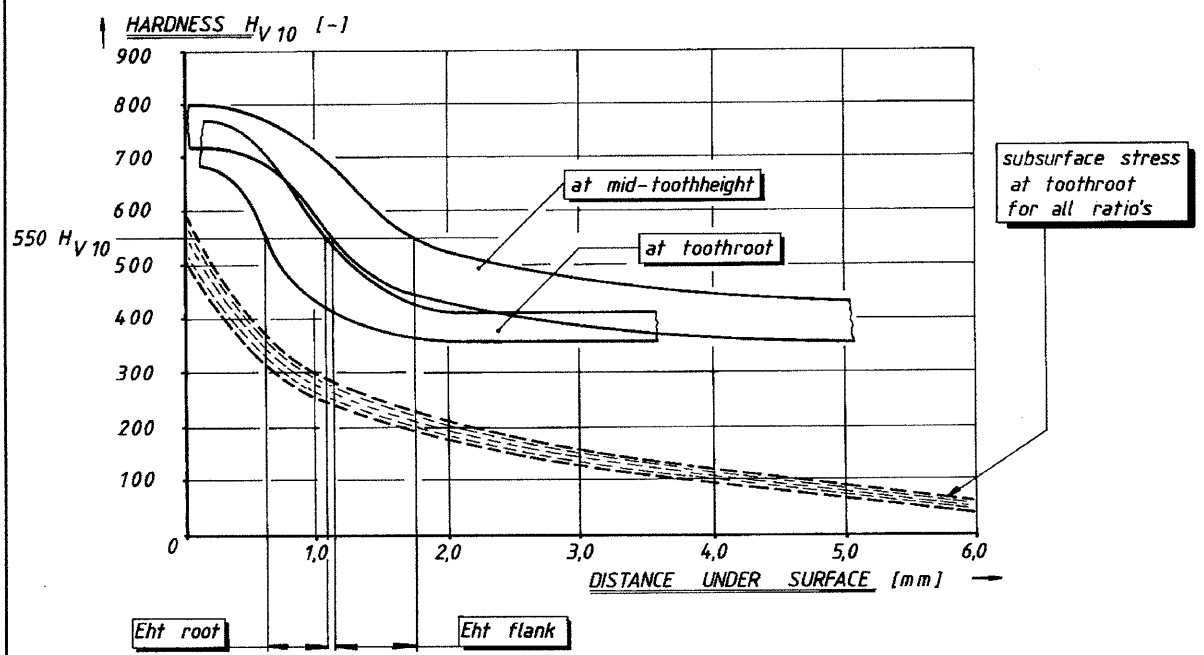

Fig. 4.9 Variation of Measured Hardness Profiles for several Pinions and estimated Subsurface Stress due to Tooth Root Bending

It is always possible that the real crack origination was situated under the surface and not at the root surface, as sometimes is possible at case hardened parts. On basis of this estimated sub surface stress, that is compared with the measured hardness profiles, it is concluded that most cracks will have been initiated at the surface.

* *Constant amplitude fatigue test have been preformed on actual rear axle gears,* *
* *built in rear axle casings. The test were run at a relatively high and reproducable* *
* *torque level, so that tooth root breakage was clearly promoted.* *
* *The tests showed statistically reliable results, that could well be described* *
* *by a Weibull or a Lognormal failure distribution.* *
* *The first visible cracks on the root surface were in the middle of the facewidth* *
* *to the toeside. The angle of the crack propagation from the root surface into* *
* *the material was about 30^0 - 50^0.* *
* *There appears to be a correlation between endurance life and casedepth,* *
* *although this is determined on a limited number of testsamples.* *

4.3 Verification of Calculated and Measured Life

For a comparison of the actual recorded pinion endurance life of the test axles and the theoretical calculations, only the tooth root stress calculations according to DIN 3991 for the virtual bevel gears will be used.The reason for this is the fact that the author did not have the same possibilities of performing extensive calculations according the other methods. This also means that no comparative quality remark iwill be given on the different stress calculation methods. The results of the constant amplitude tests are used for comparing the actual measured and calculated endurance life of the rear axle gears. Based on the assumption of a statistical endurance life distribution, a synthetic SN curve was established for the actual measured endurance life values. Also some of the most important material endurance characteristics have been determined.

The following **procedure** was used:

1. The tooth root stress of the hypoid pinions is calculated using the DIN 3991-method.
2. The extension for hypoid gear geometry according to Winter is applied.
3. A value for $K_{f\text{-}beta} = 1.30$ is used. For the investigated axles this factor is considered to be constant and independent of the torque.
4. A linear relation between calculated tooth root stress and torque is assumed.
5. At each torque level, the registered pinion load cycles for a 10%, 50% and 90% failure probability have been determined statistically. No distinction has been made for the axle ratio at each axle type.
6. Straight lines were then drawn through these points on a dubble logarithmic stress-cycles diagram. The stress is calculated, the number of pinion load cycles are the actual registered cycles of the endurance tests.

The following **criteria** had to be fulfilled:

1. The difference between the endurance lifes at 10% and at 90% failure probability at the maximum torque level should be about 2 to 3.
2. The assumed SN-line for the material will have a static limit at 10^3 cycles.
3. The difference between calculated- and measured life for 10% failure probability should be minimal, at least less than 10% difference. For larger failure probabilities, the difference may be larger, however it should also be as minimal as possible.

With these restrictions, it was possible to draw SN-curves, based on the results of the rear axle endurance tests and fullfill the criteria mentioned above. The resulting SN diagram is given in figure 4.10. Based on this figure, specific fatigue values, such as the endurance limit, the slope of the SN curve and the number of limit cycles for the rear axle gear material have been determined. Table 4.6 gives the typical fatigue data that have been established in that way. Here, the endurance limit and the knick point are given as well as the slope of the limited life line for several failure probabilities.

Figure 4.11 shows the relation between the endurance strength and its cumulative failure probability. Note that the scale for the endurance strength is linear; this is not for the scale of the cumulative failure probability. The points for the 10, 50 and 90 % failure probability have been calculated, based on the registered number of cycles in the rear axle endurance tests. As they are assumed to coincide with a Lognormal or a Weibull distribution for the endurance strength,a straight line can be drawn through these points.

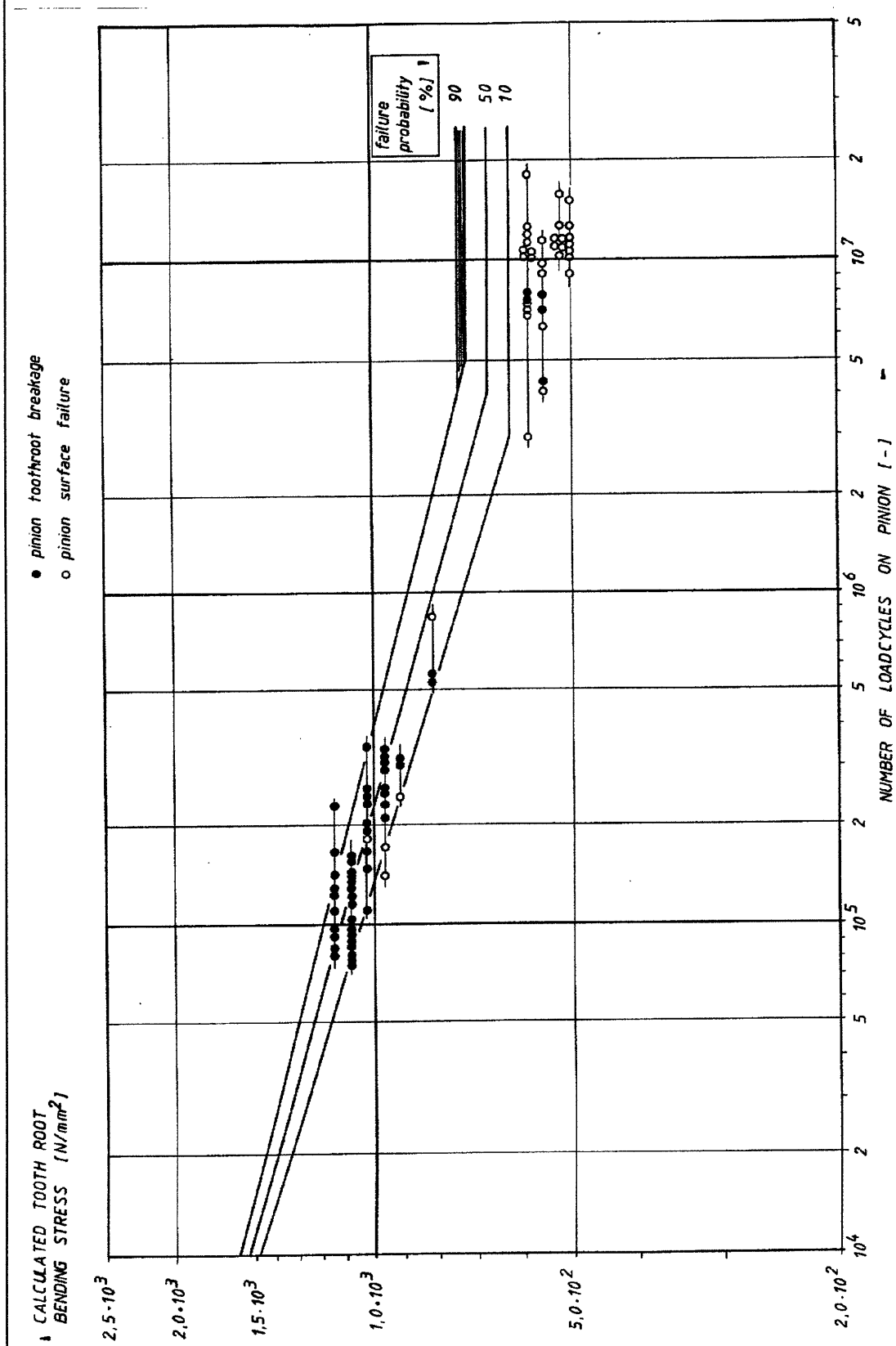

Fig. 4.10 SN Curves based on Registered Number of Load Cycles and Calculated Tooth Root Stress

Failure Probability [%]	Endurance Limit [N/mm2]	Slope SN-curve [-]	Knickpoint N_w [-]
1	595	6.00	$3 * 10^6$
5	615	6.25	$3 * 10^6$
10	625	6.50	$3 * 10^6$
50	670	7.25	$4 * 10^6$
90	705	7.75	$5 * 10^6$
95	720	8.15	$5 * 10^6$
99	740	8.50	$5 * 10^6$
Static Limit	2125	-	$1 * 10^3$

Table 4.6 Endurance Data established from Testresults

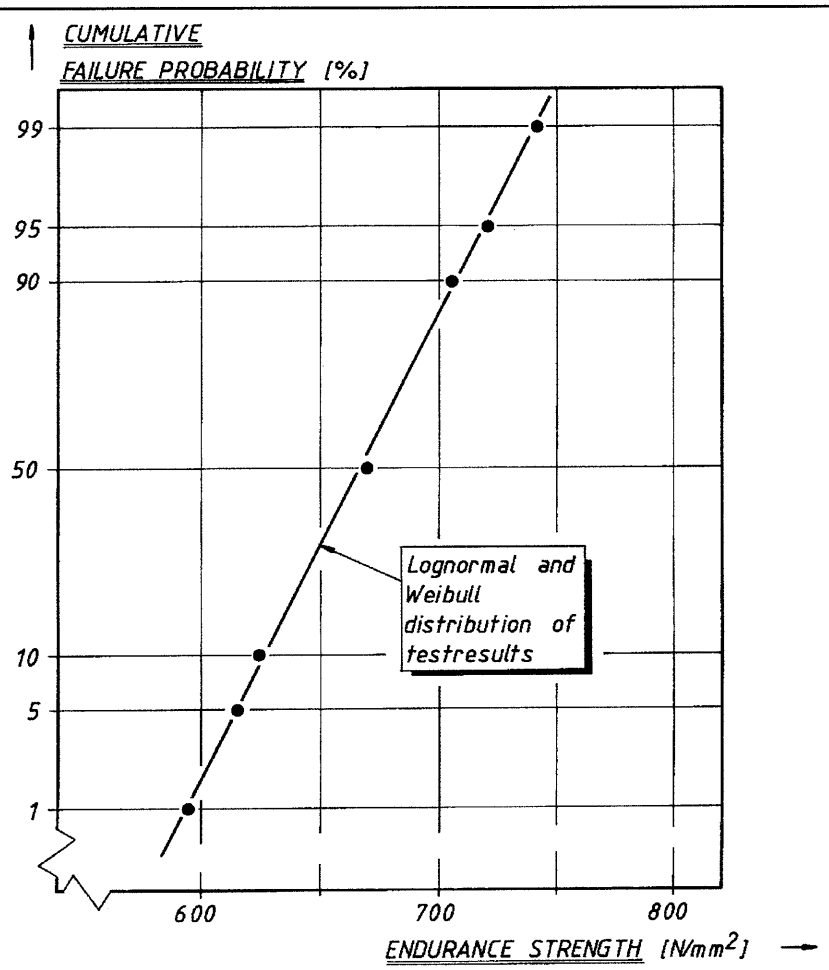

Fig. 4.11 Endurance Strength and Failure Probability

The values for 1, 5, 95 and 99% failure probability have not been calculated on basis of the registered gear life. They have been determined by assuming a straight line between failure probability and endurance strength. The difference between several distribution functions such as a normal, a lognormal, a 2 and a 3-parameter Weibull failure distribution may become very large for regions outside the 10-50-90% failure probability, as indicated in [4.6]. Therefore these last values should be used with care. Table 4.7 and 4.8 give the difference in % between the calculated and the measured pinion endurance lifes at the maximum output torque level for 10, 50 and 90% failure probability. From this it can be seen that generally the differences between calculated and registered life for the 10% probability are the smallest. For a negative value of the difference, the calculated pinion life is smaller than the actual one.
The region of 10 % failure probability is the most important area for designing automotive rear axle gears. Therefore larger differences between calculated and registered life for higher failure probabilities are acceptable. As can be seen from both tables, the difference between calculated and actual gear life depends on the assumed failure distribution. The values differ only to a small extent.

Crownwheel diameter [mm]	Failure Probability f.p. = 10 %	Failure Probability f.p. = 50 %	Failure Probability f.p. = 90 %
485	-0.03	-8.34	-16.25
445	3.98	11.38	16.42
425	-2.78	-1.06	-2.08
410	-18.11	-24.01	-27.85

Table 4.7. Difference in % between calculated and actual pinion life (Lognormal Distribution)

Crownwheel diameter [mm]	Failure Probability f.p. = 10 %	Failure Probability f.p. = 50 %	Failure Probability f.p. = 90 %
485	-5.48	-3.27	1.18
445	8.03	11.38	18.76
425	6.05	2.02	7.89
410	-11.28	-19.26	-17.74

Table 4.8. Difference in % between calculated and actual pinion life (2-par. Weibull Distribution)

For the 10% failure probability the difference between calculated and actual life is equal to or less than 10 % for three largest axle types and for both failure distributions. This is an acceptable error for designing and calculating rear axle hypoid gears. For the 50 % failure probability the maximum difference is just over 10 %. Only for the smallest axle type however, the difference between calculated and actual life is significantly larger than 10%, in this way that the actual life is always larger than calculated. These findings are graphically represented in figure 4.12.

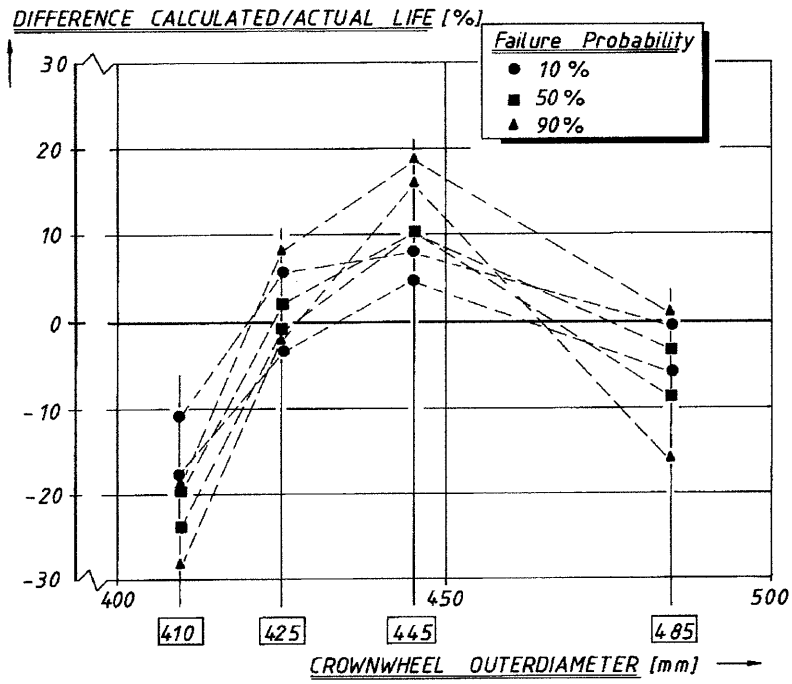

Fig. 4.12 Difference between Calculated and Actual Endurance Life of Pinions

4.4 Discussion of Test Results: Material Related Aspects

Based on the testresults, an SN curve has been established for tooth root fatigue failure of hypoid gears in rear axles. The most important fatigue related aspects that can be derived are:

* Relation of endurance strength with failure probability.
* Slope of the SN curve, k-factor.
* Ratio of static to endurance strength.

These three aspects, for different cumulative failure probabilities, have been established from the testresults and are compared with data from different sources.
In fig. 4.13 the ratio of endurance strength for several failure probabilities is given, in which the black dotted points are the results of the endurance tests. They are in line with the range according to DIN 3990 for helical gears. The fact that the stress calculations are based on the DIN 3991 standard only partially accounts for this correspondence. They also correspond to the results of rotating bending fatigue tests on unnotched samples from the same material as where the testgears were made of [4.18]. It differs however clearly from the values according to Gleason [2.6] and ANSI/AGMA [2.3].
In fig. 4.14 the slope of the resulting SN-curve is drawn; it varies between 6.5 and 8 for 10% to 90% probability. With an assumed SN-curve that has only one value of a static allowable stress at $1*10^3$ cycles, the value of the slope depends on the failure probability. This is purely a result from the varying endurance strength with failure probability, whereas the static strength is assumed to be independent of the failure probability. The values for the slopes of the SN curve, the k-factor, have been compared with other data, as indicated in fig. 4.14. From this, it can be seen that there are two different regions of the k-factors for helical and bevel/hypoid gears. The data of bevel and hypoid gears are derived from [2.6] - [2.19]; the helical gears from [4.2] to [4.7].

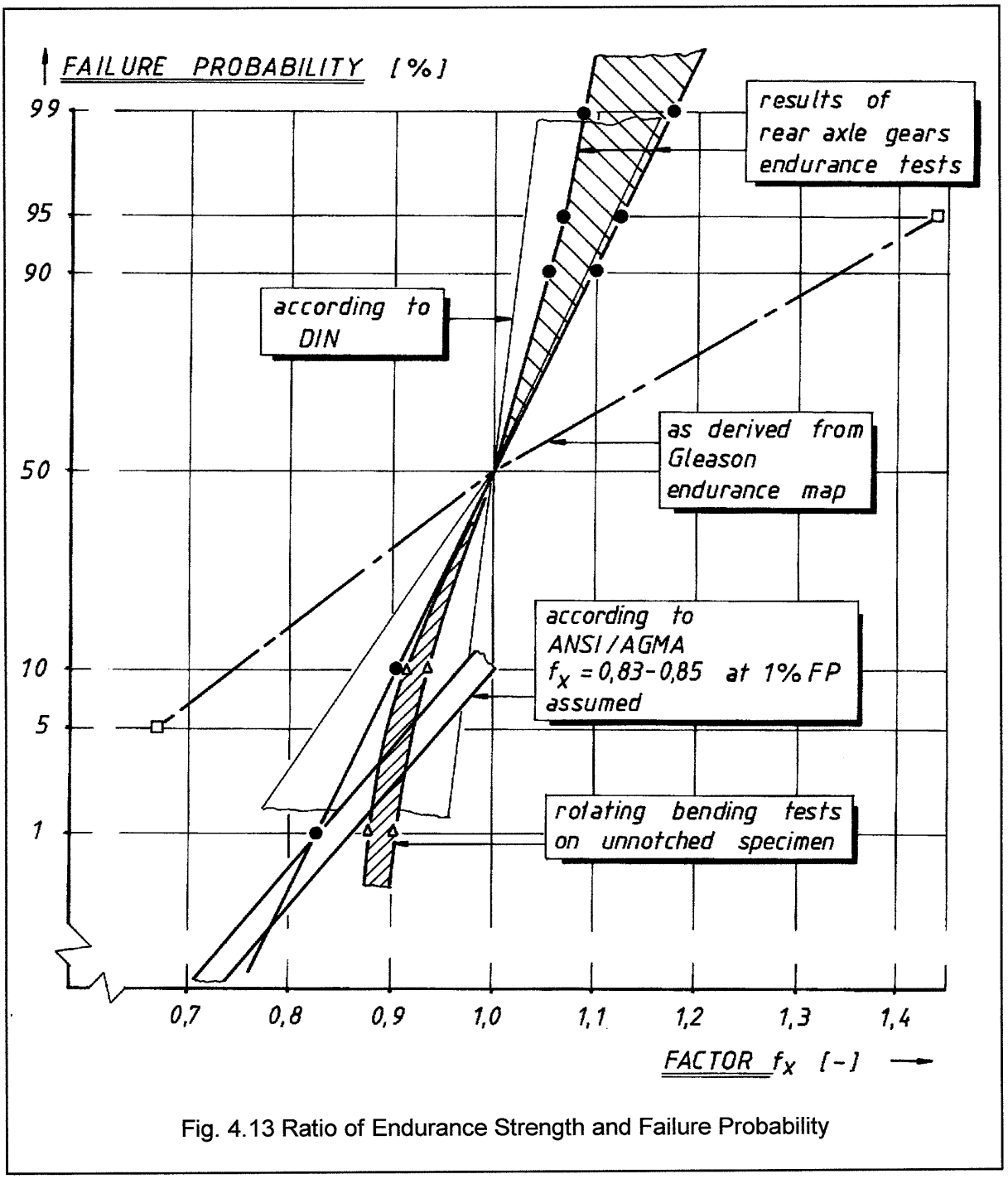

Fig. 4.13 Ratio of Endurance Strength and Failure Probability

It appears that for a given failure probability, the slope of the SN curve for helical gears is lower than for bevel/hypoid gears. For helical gears the value is 7.5 to 10, whereas this value ranges from 5.5 to 8.0 for bevel/hypoid gears.

The values for the k-factor for hypoid gears are determined on the results of the endurance tests. Here, a linear relationship is assumed between tooth root stress and applied torque. This is also the case for helical gears, where identical case carburised gear materials are used.

This difference of the k-factor between helical and hypoid gears with comparable material is a point of concern, as the slope of the SN curve should mainly be determined by material characteristics. Hardly any differences in k-factors should therefore be expected.

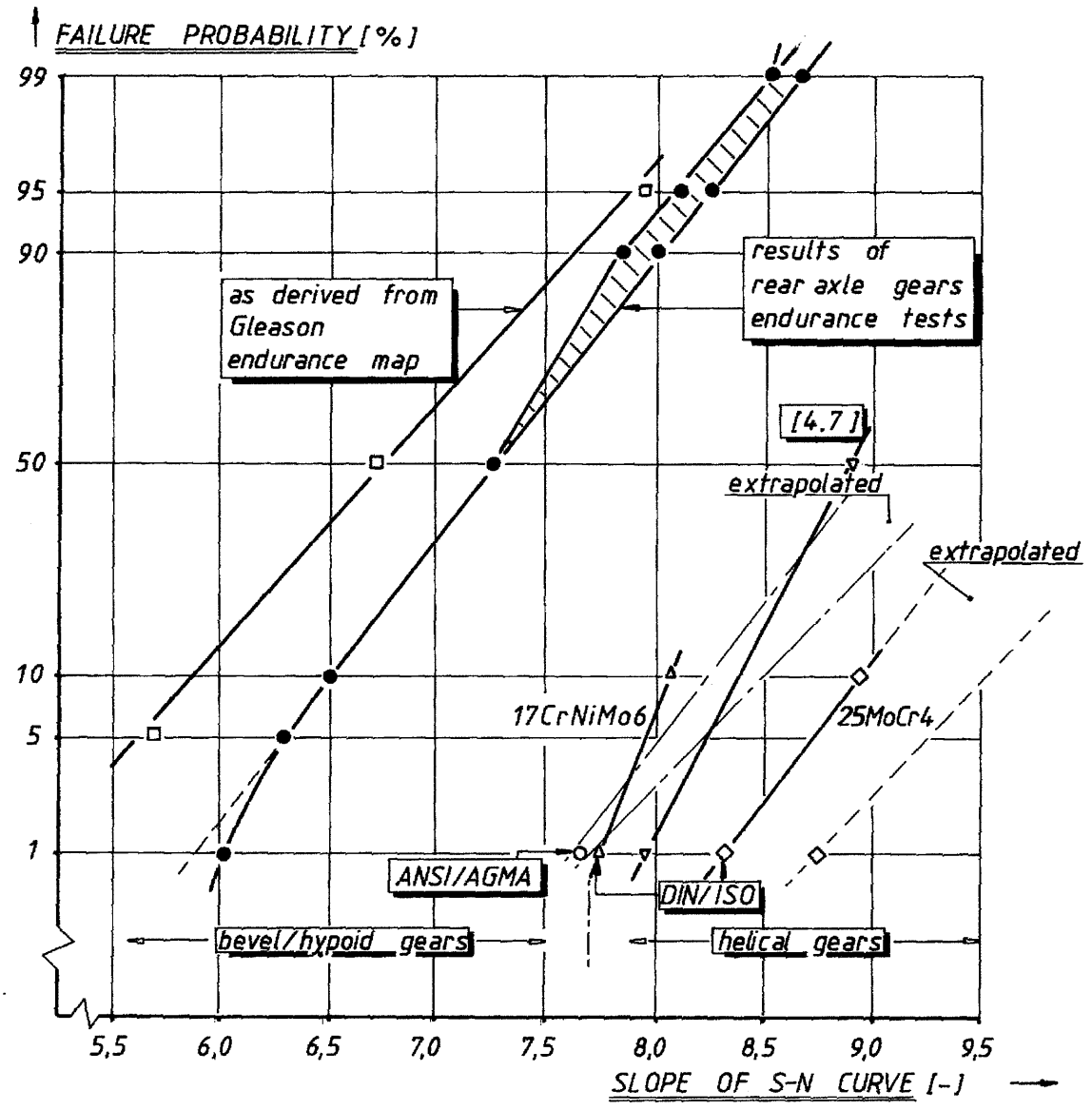

Fig. 4.14 k-factor of SN Curve and Failure Probability

Fig.4.15 shows the ratio of the static to endurance strength for several failure probabilities. Also here a striking difference appears in this ratio as a function of failure probability, between bevel/hypoid and helical gears. This aspect appears to be strange because spur/helical and bevel/hypoid gears, manufactured from the same material with equivalent heat treatment and thus comparable material behaviour, are expected to exhibit one and the same slope of the SN-curve as well as the same ratio of static stress to endurance limit.

The difference in k-factor and ratio static/endurance strength between helical and hypoid gears might be determined by the difference in crack growth between both types of gears.

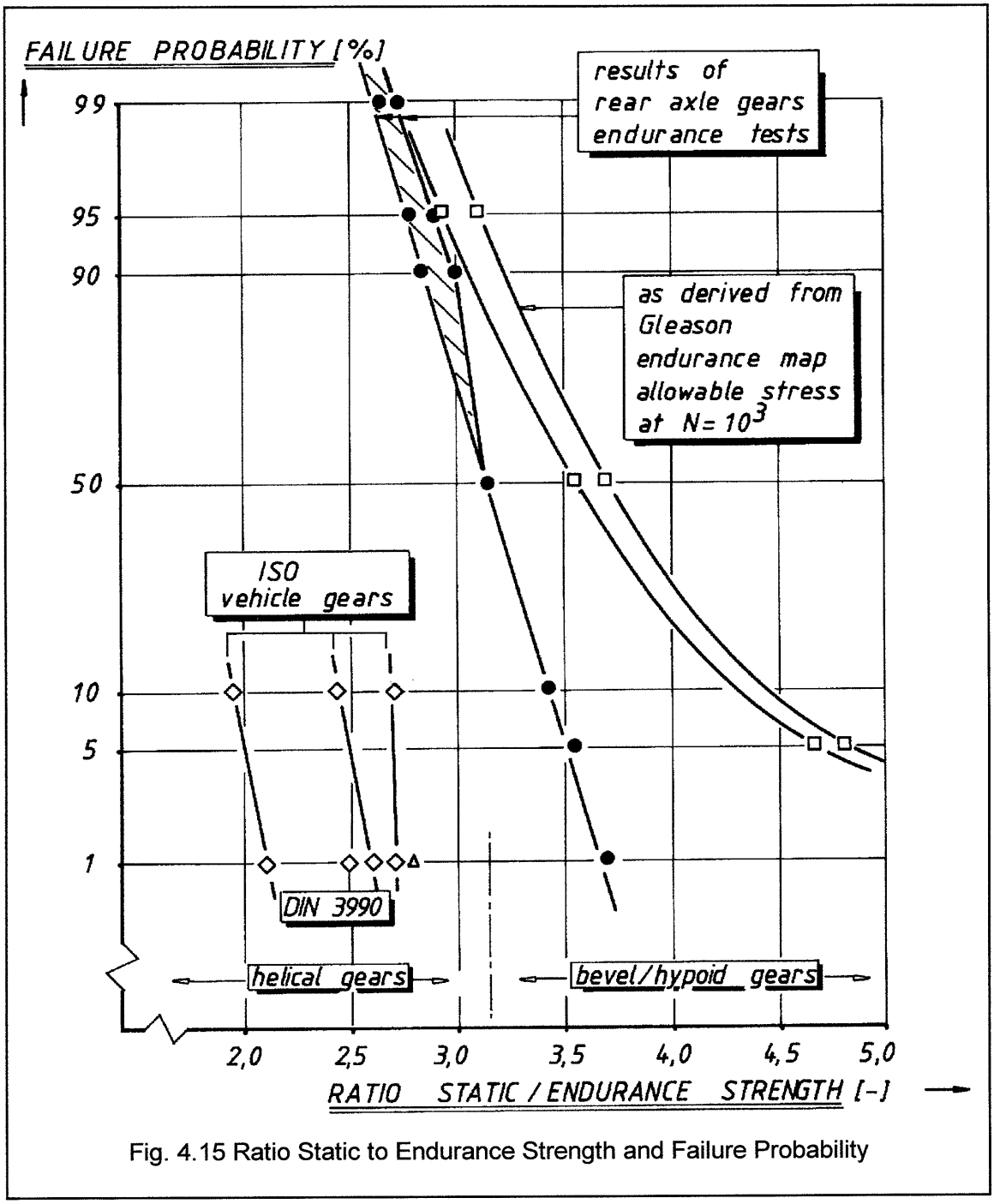

Fig. 4.15 Ratio Static to Endurance Strength and Failure Probability

As already indicated, there appears to be a distinct difference in the observed direction of crack propagationbetween the tested gears and what is normally to be expected for helical gears. In that way the difference in stress complexity between helical and hypoid gears as well as the forged material may cause the observed phenomena.

For helical gears there is however no relation observed between the slope of the SN curve and the forging of the material. Also no difference is made in the stress calculation with regard to the influence of a complex stress situation, for spur and helical gears with straight teeth, as well as helical gears with curved teeth. This means that these just mentioned aspects will hardly play a role in the observed different fatigue characteristics between the helical and hypoid gears.

In this way, a quite different aspect may play a much more important role here, namely the fact that the relation between stress and torque for bevel/hypoid gears principally is not linear, whereas it is linear for helical gears. Tooth root stress calculations for spur/helical gears and bevel/hypoid gears all assume a linear relation between applied input torque and tooth root stress. If the actual relation indeed would be a linear behaviour, than endurance tests should give one and the same slope of the SN-curves for helical as well as bevel/hypoid gears for the same material and fatigue failure mode. If the root stress however would not be linear with torque for bevel/hypoid gears, then a difference might be expected in fatigue related values.

Several measurements [3.8] to [3.12 have shown that the relation between pinion tooth root stress and torque level is not linear for bevel/hypoid gears. With an increasing torque, the slope of the root stress versus torque relation gradually decreases. This value is of course influenced by gear geometry, of which the width of the contact pattern and the load sharing during increasing torque are the dominant parameters. Fig. 4.16 gives the relation between tooth stress and torque, as can be derived from [2.41] to [2.43]. In this graph, the stress at the maximum torque was taken as the reference. Then, for lower torques, the ratio of the stress to the stress at maximum torque was calculated. It shows that at about 50% of the maximum torque, the actual root stress is about 15-20% higher than when a linear relation is assumed.

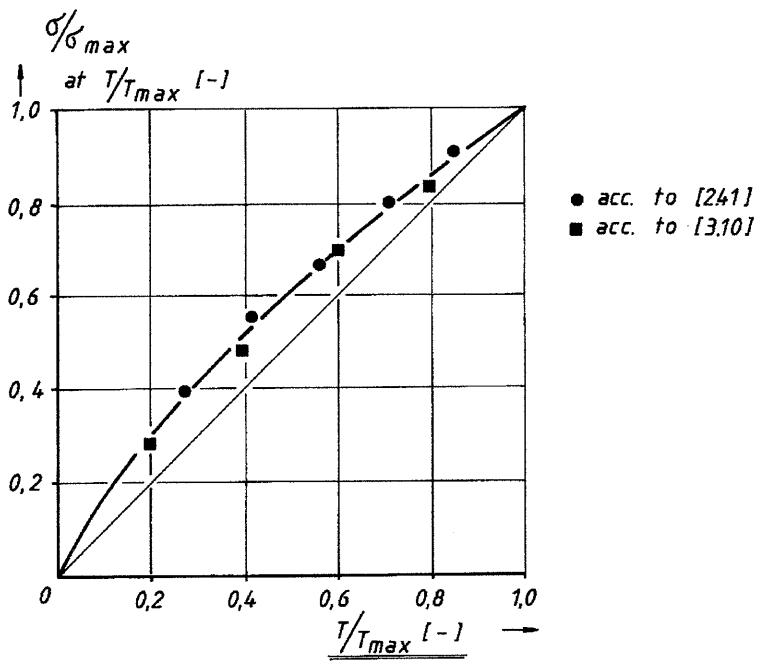

Fig. 4.16 Tooth Root Stress versus Torque as measured in [2.41] and [3.10]

In the analysis of the endurance test results, the vertical scale holds the calculated stress which is based on a linear relation between stress and torque. The slope of the SN curve for a non linear stress/torque relationship, then will differ from the slope for a linear stress/torque relation. Starting from a given stress at a maximum torque with a maximum width for the contact pattern, the calculated root stress at lower torques will be slightly higher for a non linear relation between stress and torque. This would mean that the slope of a well fitting SN curve will then be lower and hence the value for the k-factor will be higher for a linear relation between stress and torque.

This means that a non linear relation between stress and torque should actually be present in the calculations. If this would be the case, then the same endurance material characteristics such as the k-factor or the slope of the SN curve as well as the ratio of static strength to endurance limit for case hardened helical gears, could be applied to both bevel and hypoid gears. In that way, no difference would be required for specific material values between bevel/hypoid and helical/spur gears. Physically this would be correct as a given material will have one and the same fatigue behaviour, irrespective of the gear type it is used for.

The reasons for a non linearity between root stress and torque on bevel/hypoid gears are:

* The growth of the contact pattern width under increasing torque and hence an increasing effective face width of the tooth load at increasing load.
* A shift of contact pattern under increasing load and hereby loading a larger tooth section.

Generally this non linearity between root stress and torque may be considered as being structural for bevel and hypoid gears. For helical and spur gears the relation between root stress and torque is in almost all cases linear. This would mean that a new factor should be introduced in the stress calculations for bevel and hypoid gears, that takes account for this non linearity.
In this factor, the influence of the contact pattern on the non linear relation between root stress and torque will have to be embodied. First the growth of the contact width and the contact height are involved. Secondly the shift of the contact pattern in combination with variation of the tooth root section over the face width are to be taken into account.
Even in the ANSI/AGMA standard, a special remark is made on this aspect. Here the difference between the slope for helical and bevel gears is thought to be caused by the shifting of the contact pattern towards the heel side, where for tapered tooth heights the root section is wider and hence the stress will be lower.

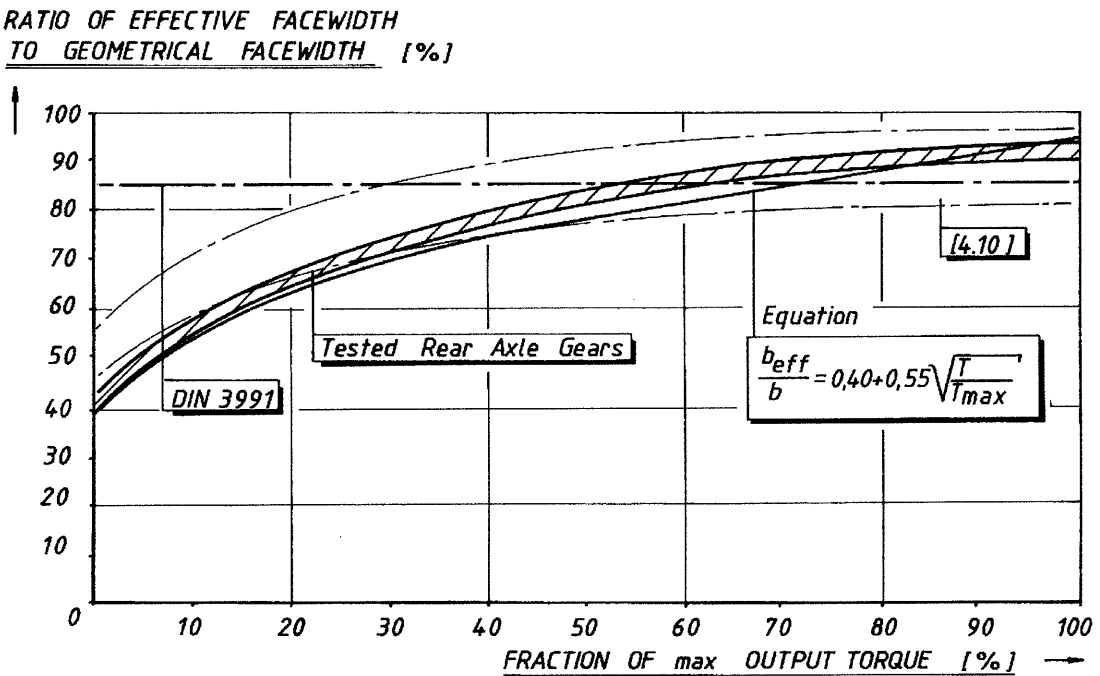

Fig. 4.17 Development of Contact Width for the Tested Gears

In fig.4.17 a summarised graph is given on the growth of the contact width under increasing input torque, as measured on the tested rear axle gears. The contact pattern development of the four investigated rear axles are all situated within the indicated bandwidth. At low torques the contact width increases very quickly, whereas at about 70-75% of the Maximum torque the contact pattern almost completely covers the entire facewidth. A similar characteristic for the contact height may be drawn, although the maximum value is attained at a much lower torque, because of the much smaller crowning in the profile direction than in the lengthwise direction.
Based on the actual measurements of the increase in contact pattern width from fig. 4.17, it can be derived that the effective face width limited by the contact pattern at 50% of the maximum torque is about 15 to 20% smaller. This would mean that at 50% of the maximum torque the tooth root stress will be about 15 to 20% higher than when a linear relation is assumed.

Life calculations have been performed with a non linear relation between root stress and torque. The endurance strength ranged from 710-730 N/mm^2 for the 10% failure probability and the root stress at maximum test torque was 5% higher than when calculated with a full geometric facewidth, because of the maximum effective facewidth being 95% of the geometric facewidth. In that situation the ratio of calculated to realised endurance life for three axle types also appeared to be less than a 10% deviation. The value of the k-factor for the 10% failure probability was 8.50. This would come more in line with the already existing values for helical gears in the same material.
Therefore, it is well advisable to apply a non linear behaviour between the tooth root stress and the torque at the tooth root stress calculations and to subsequently adapt the material fatigue data. This means an alteration of the endurance limit and the slope of the SN-curve to values that are more in line with already existing data for helical gears in case hardened materials.

4.5 Proposal for Improved Calculation Method: Introducing a Non Linear Stress-to-Torque Relationship

The influence of the non linearity between tooth root stress and torque is mainly caused by the behaviour of the contact pattern when the torque is varied. This behaviour of the contact pattern can be described in two different ways:

* change in size of contact pattern
* change of position of contact pattern.

The size of the contact pattern can be expressed in the direction of the facewidth (contact pattern width) and in the direction of the tooth profile (contact pattern height). The width of the contact pattern generally increases at an increasing torque. As a result, the gear unit load, F_{mt}/b will not increase in a similar way as the gear load does. The effective facewidth also increases at an increasing contact pattern width, hereby increasing the effective face contact ratio. This in it's turn has a positive effect on the load sharing of the gear load as theoretically more teeth are engaged. Both effects act together thereby ensuring a non linear behaviour. The height of the contact pattern, of which the growth is mostly much smaller than in the direction of the facewidth, influences the effective profile contact ratio. In it's turn it influences the amount of tooth load sharing. A larger contact pattern height leads theoretically to a larger load share.
The position of the contact pattern can also be expressed in the direction of the facewidth and in the direction of the tooth profile. When the mean position of the contact pattern changes in the direction of the facewidth, generally a different normal section of the gear tooth will be loaded. This will result in a change of the tooth form factor thereby changing the tooth root stress.

The mean normal section may however vary over the facewidth of the gear. This mostly depends on normal gear data such as mean cone distance and cutter radius, as well the tooth form (tapered or costant tooth height) and the actual deflections of both gears relative to each other in the driving head. A shift of the contact width in profile direction will lead a change in the point of load application or in the bending arm of the tooth load. This also influences the root stress. Therefore a new geometry factor is proposed, that accounts for the influence of the contact pattern on tooth root stress. This factor is called the Contact Pattern Factor Y_{CP}. In this factor, both the influences of the size as well as the shift of the contact pattern on the tooth root stress are incorporated. This Contact Pattern Factor thus is the product of the Contact Pattern Factor for Shift $Y_{CP\text{-}shift}$ and the Contact Pattern Factor for Size $Y_{CP\text{-}size}$.

The Contact Pattern Factor for Size $Y_{CP\text{-}size}$ is influenced by the following parameters:

* Output torque, relative to $T_{2\,max}$
* Amount of gear crowning in direction of facewidth and in profile direction
* Gear geometry.

The Contact Pattern factor for Shift $Y_{CP\text{-}shift}$ is influenced by the following parameters:

* Gear deflections under load in driving head,
* Tooth type, constant or tapered tooth height; m_{nm} = f (cone distance, facewidth),
* Ratio of gear curvature to mean cone distance.

The following expressions for the Contact Pattern Factor are proposed:

$$Y_{contactpattern} = Y_{CP} = Y_{CP\text{-}size} * Y_{CP\text{-}shift} \tag{4.1}$$

$$T_{max} = \Gamma * GVW \quad resp \quad T_{max} = \left(\frac{d_{e2}}{12.5-14.5}\right)^3 \tag{4.2}$$

$$\left(\frac{b_e}{b}\right) = 0.40+0.55*\sqrt{\frac{T_2}{T_{max}}} \quad for\ L_b=(0.01-0.02)*m_{mn} \tag{4.3}$$

$$Y_{CP\text{-}size} = \frac{1}{\left(\frac{b_e}{b}\right)} = \frac{1}{0.4+0.55*\sqrt{\frac{T}{T_{max}}}} \tag{4.4}$$

$$Y_{CP\text{-}shift} = f\left[T_2,\ T_{max},\ \frac{r_c}{R_m},\ m_n=f(r)\right] = 1.0 \tag{4.5}$$

The definition of the maximum output torque is based on the method of chapter 6.2. As the change in contact pattern size in the direction of the facewidth is much more pronounced than in the direction of the tooth profile, the change of the contact pattern in the facewidth direction may only be used for a first order definition of the factor for contact pattern.

Also here, the changes in the position of the contact pattern in the direction of the facewidth are much more pronounced than in the tooth profile direction. As this strongly depends on the gear type and geometry, it is very difficult to give an approximation of this effect on the tooth root stress. Therefore, the value for this factor has been set to unity. Further investigations are required to determine an expression for this Contact Pattern factor for Shift $Y_{CP\text{-}shift}$.
Two very important aspects should however be mentioned here.
First the fact, that all geometry factors and the unified tooth root stress should be expressed in the nominal gear geometry values. This means that these factors are only determined by the gear geometry and hence they are constant values at a given gear geometry, irrespective of the output torque. The only geometry factors that depend on the output torque, is the just proposed Contact Pattern Factor. It may therefore be also appropriate to position this Contact Pattern Factor in the row of Load Factors.
Second is that when this Contact Pattern Factor is used, the non linearity of the stress-to-torque relationship is automatically accounted for. This means that the same material fatigue data, more particular the slope of the SN curve, for case carburised helical gears now can be used for bevel and hypoid gears. In this situation, there will then be no or hardly any difference in the applied material fatigue data between spur/helical gears and bevel/hypoid gears of the same material.

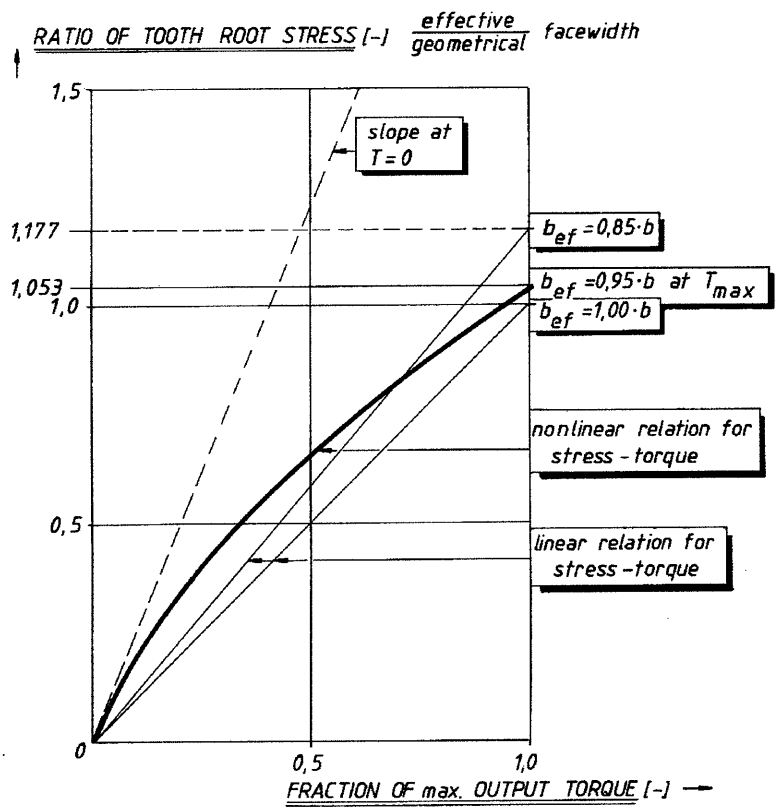

Fig. 4.18 Proposed Non-linear Behaviour of Stress-to-Torque

The equations, used for determining the non linear pinion tooth root stress are as follows:

$$\sigma_F = \sigma_F|_{lin\ @\ T_{max}} * \frac{T_i}{T_{max}} * \frac{1}{Y_{CP}} \tag{4.6}$$

$$Y_{CP} = 0.4 + 0.55 * \sqrt{\frac{T_i}{T_{max}}} \rightarrow for\ \frac{T_i}{T_{max}} \leq 1.0$$

$$Y_{CP} = 0.95 \rightarrow for\ \frac{T_i}{T_{max}} \geq 1.0$$

$$\sigma_F|_{lin\ @\ T_{max}} = \sigma_F\ (\sigma/T\text{-}linear,\ T_{max},\ b_{eff} = 100\%)$$

Fig 4.18 shows the principal relation between tooth root stress and torque for bevel and hypoid gears, when a non linearity is present. At the maximum torque T_{max}, the stress is 5% higher than originally calculated with a linear relation and for a full geometric facewidth. In the non-linear stress-torque relation, the maximum effective facewidth is limited to a maximum of 95% of the full geometric facewidth. The minimum effective facewidth is 40% of the geometric facewidth; this means that the slope of the stress-torque curve at zero torque is a factor 2.5 higher than if the full facewidth is assumed. At torques higher than T_{max} the root stress behaviour is again linear with torque, but it always remains 5 % larger than for a linear relation.

Failure Probability [%]	Endurance Limit [N/mm2]	Slope SN-curve [-]	Knickpoint N_w [-]
1	690	7.50	$3 * 10^6$
5	710	7.75	$3 * 10^6$
10	720	8.00	$3 * 10^6$
50	757	8.75	$4 * 10^6$
90	790	9.50	$5 * 10^6$
95	800	9.75	$5 * 10^6$
99	820	10.0	$5 * 10^6$
Static Limit	2125	-	$1 * 10^3$

Table 4.9 Endurance Data established from Testresults for a Non Linear Stress-Torque Relation

With this non linear relation between root stress and torque, the endurance material related data from table 4.9 have been established in the same way as chapter 4.3.
The endurance data of the three characteristic failure probabilities of 10, 50 and 90 % have been established by comparison of the calculated and the actual registered pinion life cycles. The endurance data for the other failure probabilities have been determined only by assuming straight lines in the graphs of figures 4.13 to 4.15; therefore these data are not verified.
Especially the k-factor for the slope of the SN curve comes very well in line with those from helical gears of comparable gear material. With these values for endurance chararcteristics, the ratio of calulated to realised pinion load cycles for the 10, 50 and 90% failure probability becomes as indicated in tables 4.10 and 4.11.

Crownwheel diameter [mm]	Failure Probability f.p. = 10 %	Failure Probability f.p. = 50 %	Failure Probability f.p. = 90 %
485	+ 5.47	- 2.97	- 14.06
445	- 5.06	+ 2.05	+ 0.92
425	- 4.47	- 2.68	- 7.56
410	- 30.93	-35.80	- 43.00

Table 4.10. Difference in % between Calculated and Actual Pinion Endurance Life for a Lognormal Failure Distribution and a Non Linear Stress-Torque Relation

Crownwheel diameter [mm]	Failure Probability f.p. = 10 %	Failure Probability f.p. = 50 %	Failure Probability f.p. = 90 %
485	- 0.28	+ 2.40	+ 3.82
445	- 1.36	+ 2.05	+ 2.95
425	+ 4.21	+ 0.34	+ 1.85
410	- 25.17	- 31.78	- 35.01

Table 4.11. Difference in % between Calculated and Actual Pinion Endurance Life for a 2-parameter Weibull Failure Distribution and a Non Linear Stress-Torque Relation

Both tables show that for the three largest axle types, the difference between calculated and actual pinion load cycles very clearly lies between plus-minus 10% and this for all three failure probabilities of 10, 50 and 90%. These differences are significantly smaller than for those, calculated with a linear stress/torque relation, as can be sen in fig. 4.19.
Only for the smallest axle type, the difference between calculation and realisation is relatively large for all three failure probabilities. Here the difference between calculated and actual pinion load cycles is about 30 -40 %. Roughly estimated this would mean a difference in actual or allowable pinion root stress of about 3.5 % at all three failure probabilities. The reason for this difference has not been investigated as this axle type is not in production.

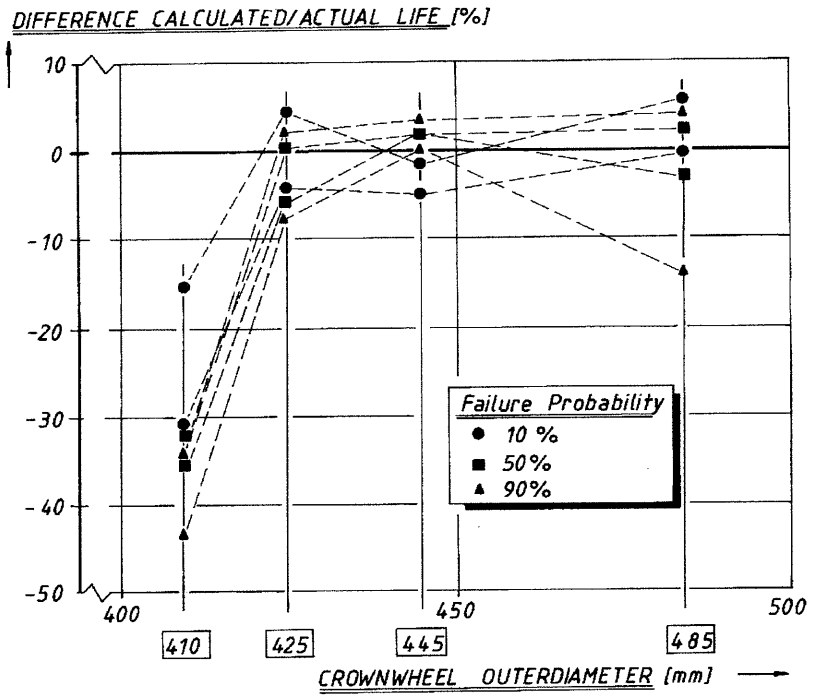

Fig. 4.19 Difference between Actual and Calculated Endurance Life of Pinions

The calculated pinion tooth root stress for the different axle types may attain a specific stress value at the characteristic output torque T_{max}. This maximum output torque was determined according to the definition of equation (4.2), where a value of 13.12 is assumed for the constant coefficient in the expression for crownwheel outerdiameter and maximum output torque. Table 4.12 gives a summary of those characteristic calculated root stress values for the pinion. These values give the calculated pinion load cycles when the endurance values for a non-linear stress-torque relation of table 4.9 are used.
This means that when the definition for the maximum output torque T_{max} is applied according to equation (4.2), the calculated pinion root stresses for all four axles appear to lie within the range of 1135 to 1140 N/mm^2, which resembles a tolerance of less than 0.5 %. These data may well be considered to be characteristic design values for the tested vehicle rear axle gears.

Crownwheel Outer Diameter [mm]	Maximum Output Torque [Nm]	Calculated Pinion Root Stress [N/mm^2]
485	50.500	1135
445	39.000	1140
425	34.000	1135
410	30.500	1135

Table 4.12. Characteristic Data for Tooth Root Stress Calculations for Constant Amplitude Loading, when a Non Linear Stress-Torque Relation is assumed

4.6 Resumee

Constant Amplitude Load endurance tests for tooth breakage on four different types of hypoid rear axle gears have been performed. The results for constant amplitude loading at maximum torque have been statistically analysed. All show defined failure modes, which are clearly tooth root fatigue breakage.
The variation in registered cycles for 10- and 90%-failure probability is 2 to 3. This is relatively small, mainly because of the high tooth root stress value which provokes evidently fatigue breakage and the relatively acurately torque level that was maintained during the tests.

The results of the endurance tests have been described by a 2 parameter Weibull and a Lognormal failure distribution with a relatively good correlation factor.
Therefore the results of the endurance tests may be considered to be reliable.

A correlation of the actual measured endurance lifes and the calculated lifes has been performed. The root stress calculations were performed with DIN 3991 for the virtual bevel gears. The virtual bevel gears were calculated according to the method as given by Winter. The Faceload Distribution Factor for the tested rear axle gears was set equal to 1.30. This value is only valid for the axle types that have been tested with a straddle mounted pinion.

Based on this correlation, material fatigue data have been established for the gear material. The endurance limit and the slope of the SN-curve that have been established give lower values than for helical and spur gears of comparable material. For the hypoid gears first a linear relationship was assumed between calculated stress and torque, just as is the case with other gear types.
With this correlation, it was possible to reduce the difference between actual and calculated gear life for three axles within plus-minus 10%, for a 10% failure probability.

A non linear relationship has been introduced between tooth root stress and input torque. This non linearity between torque and tooth root stress for bevel and hypoid gears is mainly caused by the variation on the width of the contact pattern when the outpu torque is varied. This is a normal phenomena for bevel and hypoid gears.
With this non linear stress-torque relation, a second correlation between measured and actual lifes has been performed. Now the value for the endurance limit and the slope of the SN curve clearly come much more in line with those of helical gears of the same material.

Two factors have therefore been proposed in order to accomodate for the non linear stress-to-torque relation. These factors incorporate the size and the position of the contact pattern. The contact pattern position factor was set to unity. When using the factor for contact pattern width, the geometry factors and the gear unit load may then be based on the nominal geometric data of the gears. The maximum effective gear facewidth here is assumed to become 95% of the full geometric value for the facewidth.

With this, a non linear relation between tooth root stress and torque is assured. Then the slope of the SN curve and the ratio static to endurance stress of bevel and hypoid gears come close to the values for spur and helical gears of identical material.
With this non linear relation between stress and torque, the difference between calculated and actual pinion life for the three largest axle types becomes distinctively smaller than with a linear relation. In this way, a non linear stress-torque should be used for calculating tooth root stress on bevel and hypoid gears.

5 DRIVELINE LOAD SPECTRA FOR TRUCK APPLICATIONS

5.1 Introduction

In the previous chapter a method has been developed to predict the expected life for rear axle gears under a constant amplitude loading. In actual vehicle application, automotive rear axle gears are typically loaded under varying conditions. These loading conditions, described in terms of input torque, speed and oil temperature are constantly changing during actual operation. The oil temperature hardly has any influence on teeth breakage failures, when a maximum value is not exceeded to prevent annealing effects of the gear material. Then gear loading conditions are sufficiently described by torque and speed [5.1].

In order to make a reliable prediction of the expected gear service life in actual vehicle operation, the influence of varying loads on endurance behaviour will have to be taken into consideration. The service loads during actual operation can best be described by a load spectrum, sometimes refered to as loadcycle history or load histogram. When a load spectrum is combined with the known stress-to-torque relation of the gears and a damage accumulation theory, it then is possible to give a prediction on the expected service life for rear axle gears at variable amplitude loading [5.2].

In this chapter, some representative load spectra for rear axle gears will be discussed. These will be compared with calculated load spectra. Then, calculated load spectra for some representative vehicle applications will be analysed. On basis of this, they will be approximated by two descriptions of a continuous spectrum. With these two spectra, that are in fact simplifications of the calculated torques, expressions for the equivalent torque will be developed. In this way a simplified method is then available for determining the expected equivalent torque on rear axle gears for some representative vehicle applications.

5.2 Measured Load Spectra

Loading spectra have been determined for some vehicle applications, typical testing routes that are mostly used by proto vehicles. The gross combination weight GCW varies from 38 to 41 tonnes, the engine power ranges from 230 kW to 375 Kw. Two specific types of routes have been selected, namely typical Test Routes and Transport Routes.
The Test Routes are representative for International Transport or Long Distance Haulage with a relatively high to severe loading on the driveline components. In this way, much information on the driveline capabilities can be gathered in a relatively short time. These routes are:

-"LuO"-Route or the "Lastauto und Omnibus"-Route,
-"Fulda"-Route.

The name of the last route refers to the city in the region where the testroute is situated. Both routes are used for testing purposes and are situated in Western Germany.
The Transport Routes that have been measured are representative for National Transport. Typical parts of these types of route are:

-"Secundary"-Road,
-"Distribution"-Route, in between several cities,
-"Inner City"-Route with intensive city traffic.

The driveline torque and speed are measured during actual vehicle operation. After the data aquisition, the measured values are counted and classified according to a specific method and represented in load histograms, where the measured rear axle input torque and speed are given in the form of a table. Both torque and speed are divided into different classes of a predetermined value. Different class values may be used for torque and speed. At all measured torque/speed combinations, the time of occurence is registered. It may also be possible to indicate the total number of driveshaft revolutions at each specific torque/speed combination. These histograms then may be modified into a continuous diagram, which then becomes the load spectrum. This is a standard method to determine the load spectrum.

In a loading spectrum the value of the torque is given as a function of its cumulative fraction of loading cycles. The fraction mostly ranges from 10^{-6} to 1. The latter coincides with 100% of all registered loading cycles. Because of limitations of the measuring equipment, in some cases the minimum fraction is limited to 10^{-6}. As the torque values are both positive and negative, the scale of torque mostly is linear although in some load spectra a logarithmic scale is used for the torque. For the number of loading cycles, in almost all cases a logarithmic scale is used, because of the relatively large number of load cycles. A continuous load spectrum may be established for the Drive and Coast loading condition separately.

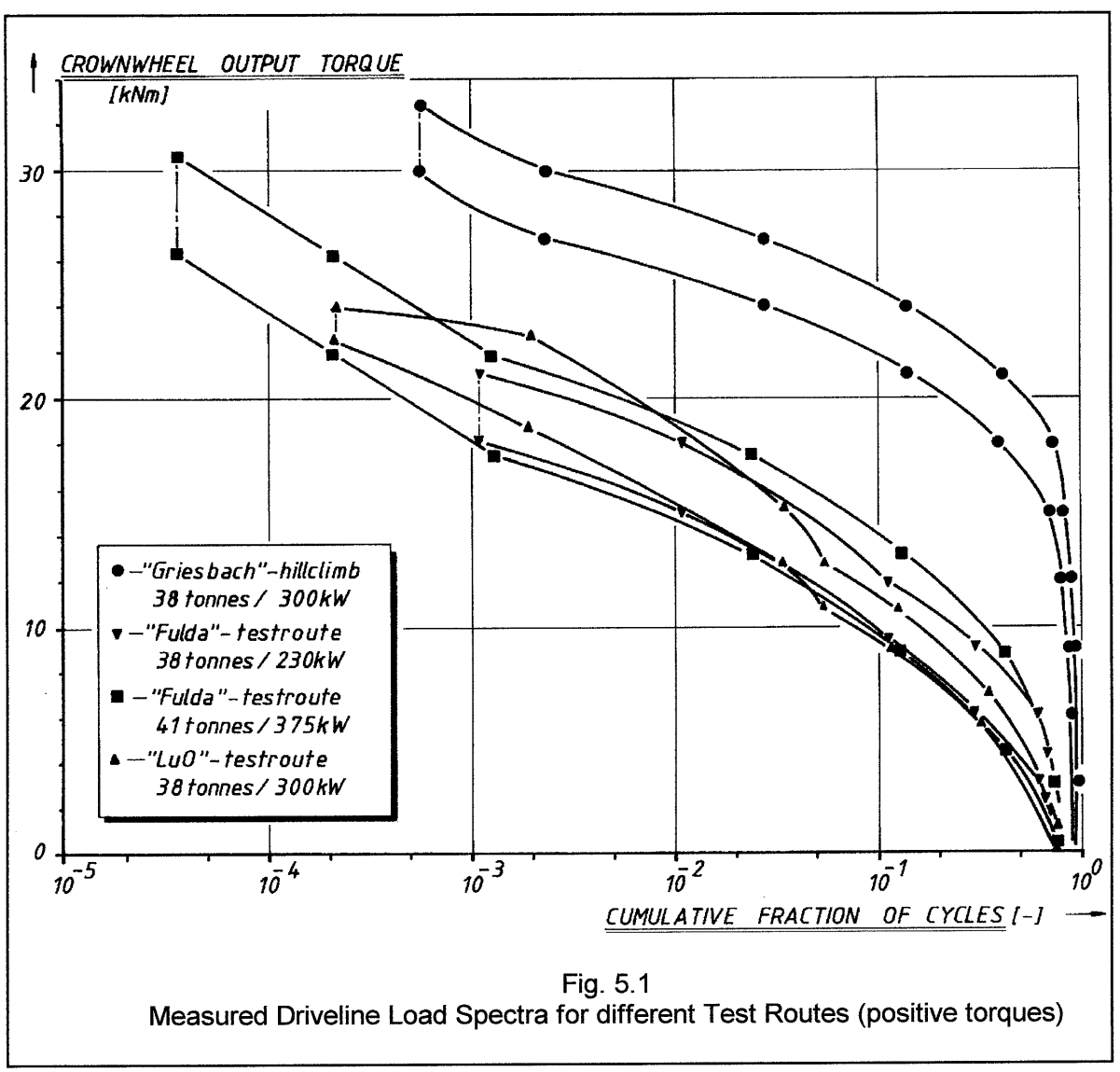

Fig. 5.1
Measured Driveline Load Spectra for different Test Routes (positive torques)

Depending on the maximum frequency of measured torques, the actual maximum value that occurred during driving may have been higher than given in the spectrum. The duration of high peak torques is very small, so these may not always be registrated in the measured load spectrum. Mostly a very long duration of the test is required for determining torque values that occur only incidently. The width of each measured torque-class may vary according to the possibilities of the measuring equipment.

Fig. 5.1 gives the results of measured load spectra for the rear axle output torque, for some Test Routes that are typical for Long Distance Haulage or International Transport. For these Test Routes, about 65-70% of the number of load cycles is in Drive condition, whereas the remaining 30-35% of the registered cycles is in Coast condition. This is an extra indication that the routes are relatively hilly, since on a flat route or with an unloaded vehicle, the Driving side of the gear flanks will be loaded during about 90% of the time.

Fig. 5.2 shows measured load spectra of rear axle output torque for some typical Transport Routes. The general appearance of these spectra is more severe for the driveline than the spectra of fig. 5.1. This would also be expected in view of the typical loading conditions that will prevail on these routes. The load spectrum for a 38 tonne / 230 kW vehicle on National Transport is more severe than the load spectrum for a 41 tonne / 375 kW vehicle on an International Transport Route. A large amount of vehicle acceleration and gear shifts because of traffic situations in National Transport are the main cause for these differences.

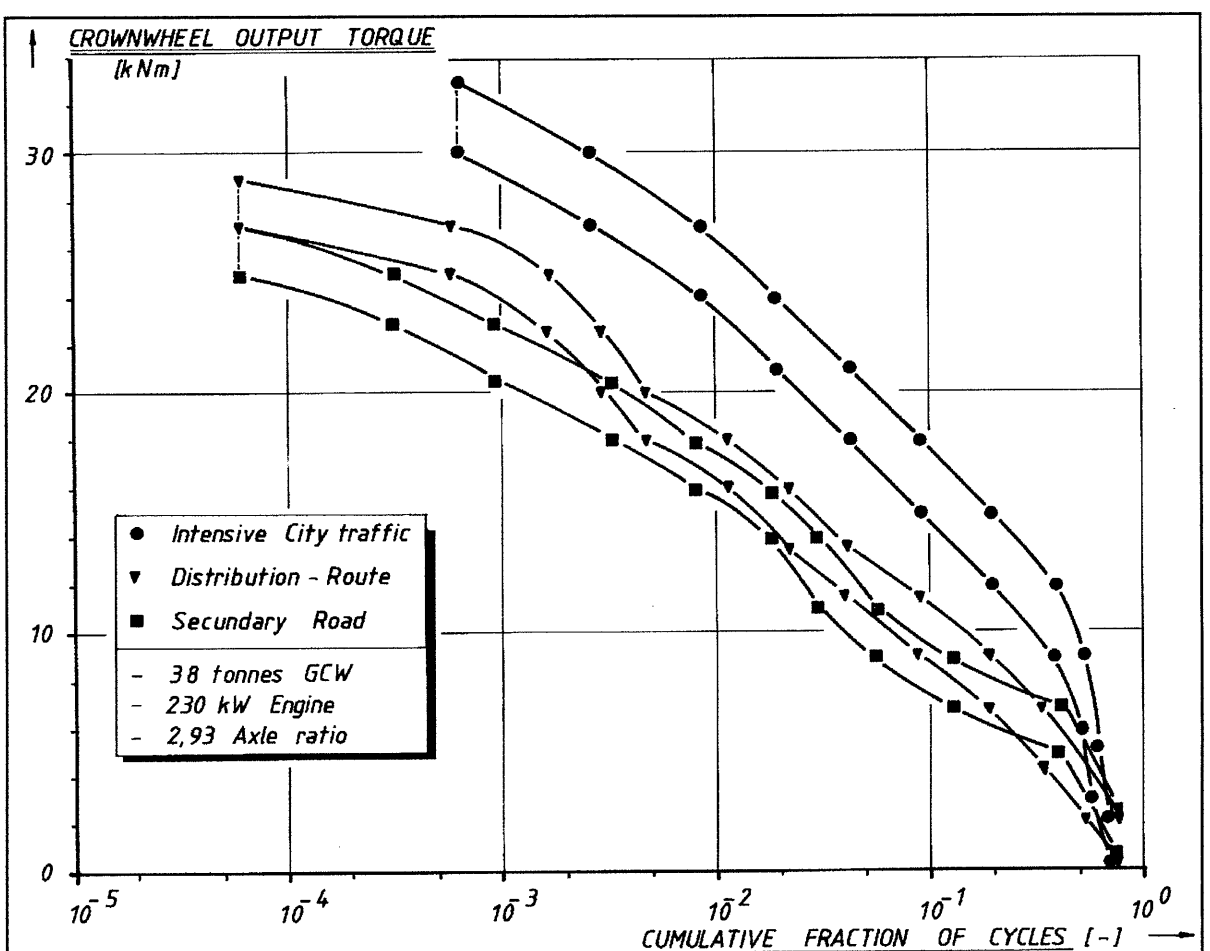

Fig. 5.2
Measured Driveline Load Spectra for different Transport Routes (positive torques)

Extreme high torques that occur only during a very limited time, are not recorded here since the measured minimum fraction is not less than 10^{-5} to 10^{-4}. Torques on the Drive side occur during about 80% of all cycles on the Distribution and Secundary road, whereas this value reduces to 70% in City Traffic. As these test have been performed with one and the same vehicle and driver, these differences may be seen as representative for different route types.

The representative or equivalent speed of the driveshaft at each torque level has been determined for all these measured loading spectra. This representative speed is calculated by adding the individual products of the time of occurence with speed (time * speed) at every torque level and dividing this summation by the total time of occurence at this particular torque level. In this way, each torque level may be seen as being operated at one constant and equivalent driveshaft speed. In this way an impression may be obtained at what representative power level the torque value has been applied. The representative combinations of driveshaft speed and torque that have been determined in this way on different Routes for one and the same vehicle, are given in figure. 5.3. For each torque, a specific fraction of the installed engine power can be considered to be representative for a vehicle application. For higher vehicle speeds, a constant power may be regarded to be representative for vehicle use. For the higher torques at City, Distribution and Secundary Roads, torque is more required than power as these are mostly stop-and-go accelerations. For Hillclimb, which is high torque / low speed, about 80% of the engine power is used.

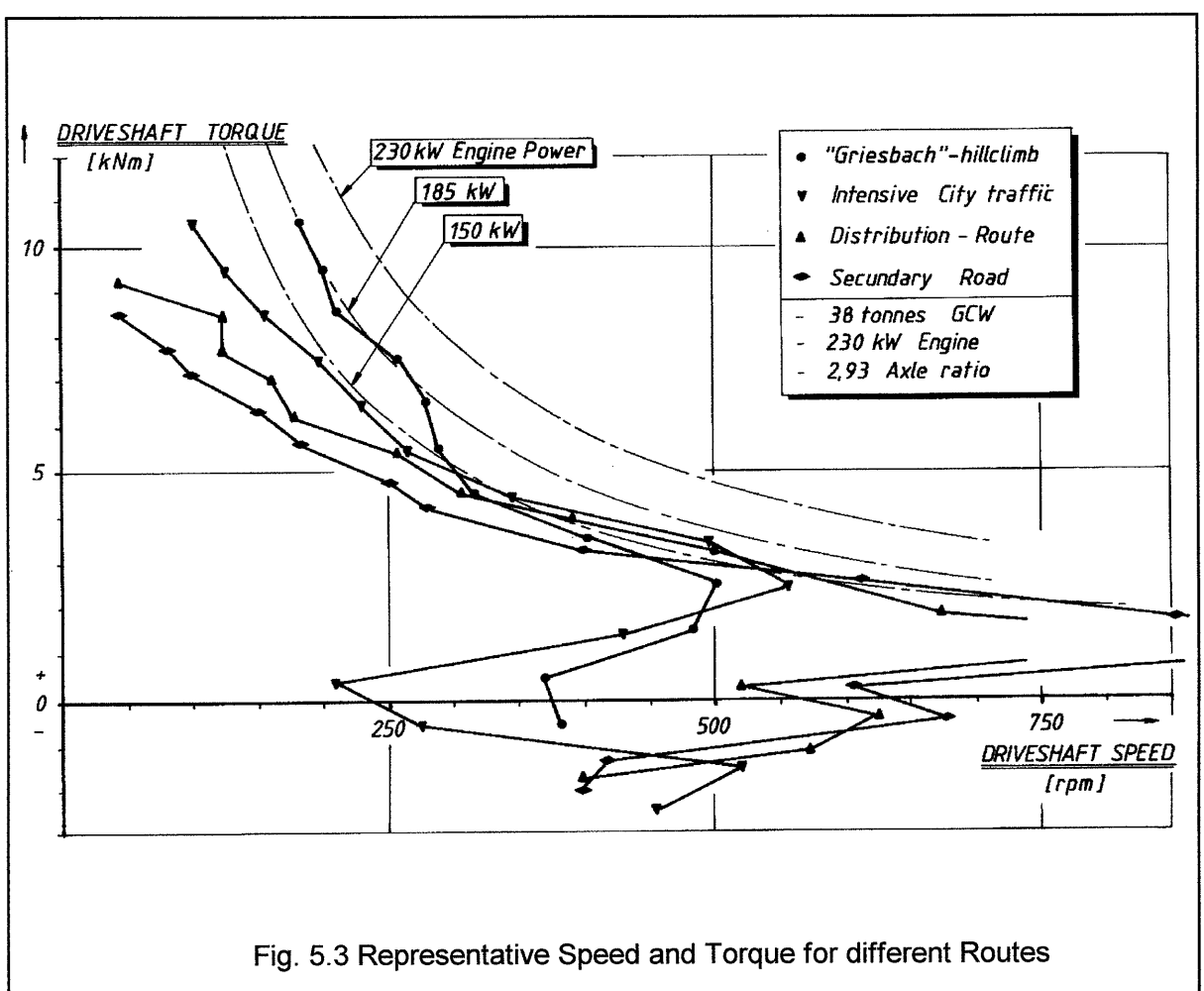

Fig. 5.3 Representative Speed and Torque for different Routes

At intensive city traffic this fraction is about 65%. For a Distribution Route and a Secundary Road, the fraction of applied engine power at the high torque / low speed range is about 50%. On both routetypes, however, the maximum measured torques are identical. The required torque for accelerating a vehicle in city traffic may be comparable to a hillclimb with a constant speed. For the low torque / high speed range, about 65% of the maximum engine power is applied up to the point of maximum speed, irrespective of the route type.

This would mean that for design purposes, the installed engine power or a given fraction of this may be regarded to be one of the most dominant parameters for determining the significant torque/speed combinations of the load spectrum, next to the vehicle weight GVW/GCW and the routetype. A value of 80% of the installed power may be assumed for International Transport. For National Transport about 65% of the engine power may be considered to be representative for the driveline loading spectrum. For the high torques, a smaller amount of the engine power is used, as in these regions the torque will prevail rather than the required power. For this maximum torque, the vehicle weight GVW/GCW will be the main determining factor. The maximum rear axle input speed is limited to a vehicle speed of about 1.20 times the average vehicle speed. These considerations will only be valid for trucks where the ratio of engine power to vehicle weight has a value in the range of 6 to 9 kW/ton. As the specific power for passenger cars is much higher, the use of the available engine power will be quite different there.

Therefore it can be stated that for initial design purposes, the installed engine power, the vehicle weight and the route type are the three variables that will mostly determine the representative loading spectrum of rear axle gears for truck applications.

5.3 Comparison of Measured and Calculated Load Spectra.

A computer program called ROSI (ROute SImulation) has been created by the development department of DAF trucks [5.22]. Here the driveline loading of a vehicle can be calculated by simulation for different vehicle applications. It gives the possibility to calculate a load spectrum and load histogram of the rear axle input torque for a given vehicle with detailed specification, a route description and a driver type. In chapter 1 the required data to perform these claculations are given. The actual measured vehicle speed and slope profile for several routes is the basis of the calculation programm. The rear axle input speed and torque that are required to give the vehicle a predescribed speed profile, are calculated by simulation. Figure 5.4 gives a direct comparison of the measured and calculated loading spectrum for a test vehicle on the Fulda route [5.23]. The vehicle GCW was 41 tonne, the installed engine power 375 kW.
For the Drive side loading of the gears, there are only relatively small differences between the measured and simulated loading spectra. For low torques the correlation is very good; wheras for high torques the difference increases. Measured and calculated spectra both show hardly any influence of a secundary retarder on the load spectrum. For the Coast loading, the influence of the retarder on the measured spectrum is clearly visible.

The mean value of the measured torque lies at about 40% of the torque class values, which is a result of the probability distribution of the measured torque values within each class.
The Drive condition gives a good correlation between measurement and calculation for the low torque range. For the medium torque range of 4 to 10 kNm, the difference between

measured and calculated torque amounts to about 10%, which may be considered as relatively small. At higher torque values the difference between measured and calculated torques increases. This is caused by the deterministic character of the calculated torques that have not been measured during actual vehicle operation, because of the very small time of occurrence and the capacity of the measuring equipment. For the Coast condition, the difference between the measured and calculated spectrum is more difficult to determine. Since the measured torques only cover a small fraction of the total number of cycles, only a comparison can be made for this part. The calculated load spectrum is valid without the use of a secundary retarder. The correlation for this small part of the spectrum is relatively good. As this covers only a relatively small range of cycles, this comparison should further not been used.

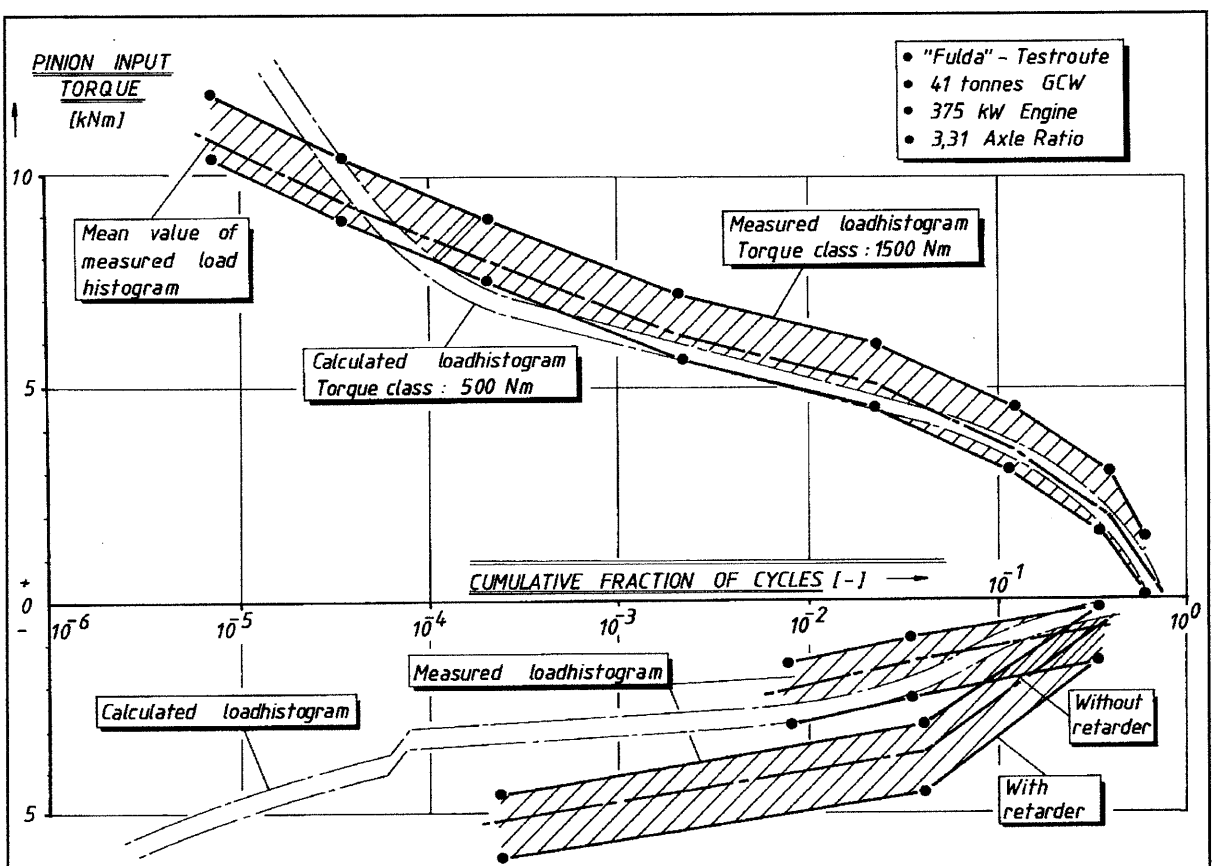

Fig. 5.4 Comparison of Calculated and Measured Driveline Load Spectra

Generally a variation can be expected between different measured spectra for one vehicle. This is the result of changing traffic conditions, different traffic situations and driver behaviour. In view of this, the correlation between calculated and measured load spectrum may be regarded as being good.

This means that with this simulation program, a good description can be given of the loading spectrum that can be expected for a given vehicle and route description on the Drive Condition. This is only valid under the condition that the route is known in terms of slope and speed profile. For the Coast condition, however the calculated spectrum without the use of a secundary retarder only is to be considered for a minimal fraction of 10^{-3} to 10^{-2}.

5.4 Some Calculated Load Spectra

Several calculations have been performed with the Route SImulation program to determine the driveline load spectrum. Two representative truck applications have been simulated, namely Test Routes and Transport Routes. Both Test Routes are described in terms of the actual measured vehicle speed and the route gradients. The Transport Routes are typical International Transport and National Transport, and they are described by characteristics as roadtype (highway / secundary road / city) and slopetype (flat / hilly / mountains).

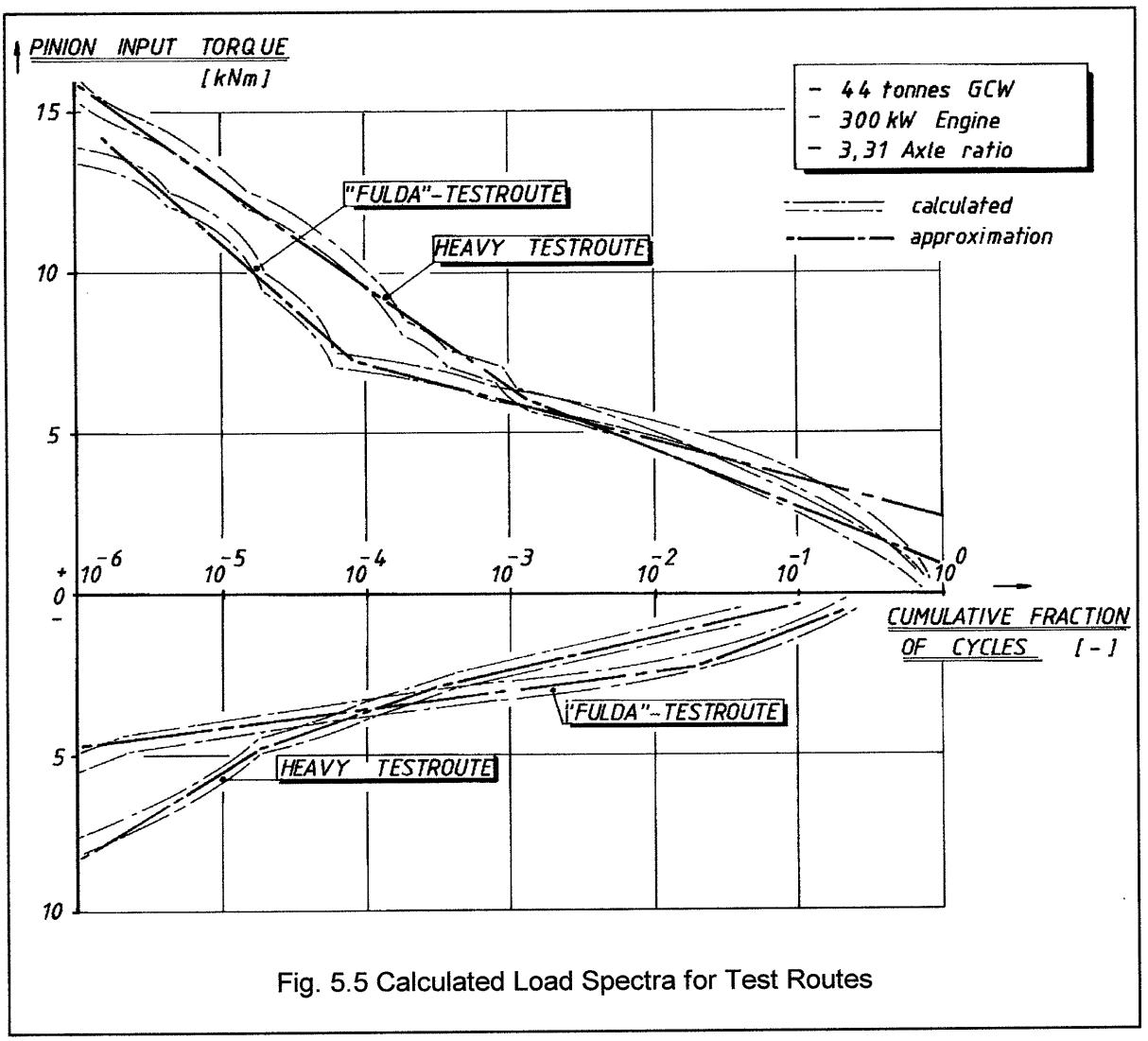

Fig. 5.5 Calculated Load Spectra for Test Routes

Load spectra have been calculated for a 44 tonne vehicle with a 300 kW engine and a rear axle ratio of 2.93. Figure 5.5 shows calculated loading spectra for both Test Routes, whereas figure 5.6 holds the spectra for two Transport Routes. In all graphs the rear axle torque is plotted on a lineair scale and the cumulative fraction of loading cycles on a logarithmic scale. Both the Drive and Coast loading are calculated.

The results of many comparable simulations show that these calculated rear axle loading spectra also can be approximated in a uniform way. This approximation is indicated by relatively thick lines in the graphs. The dotted lies are the simulated load spectra with a specific torque class, indicating the upper and lower value of the torque at each fraction of

the distance. The Drive side of both Transport Routes consist of a straight line approximation for the high torque range and a slight concave curve for the low torque range. The Coast side of the spectra for the Test Routes can be approximated by two straight lines with different slopes. The slope of the straight line approximation on the mid-to-high torque range is higher than on the low torque range. No retarder is used here. National Transport obviously gives higher torques than International Transport. Both spectra have an identical minimal torque.

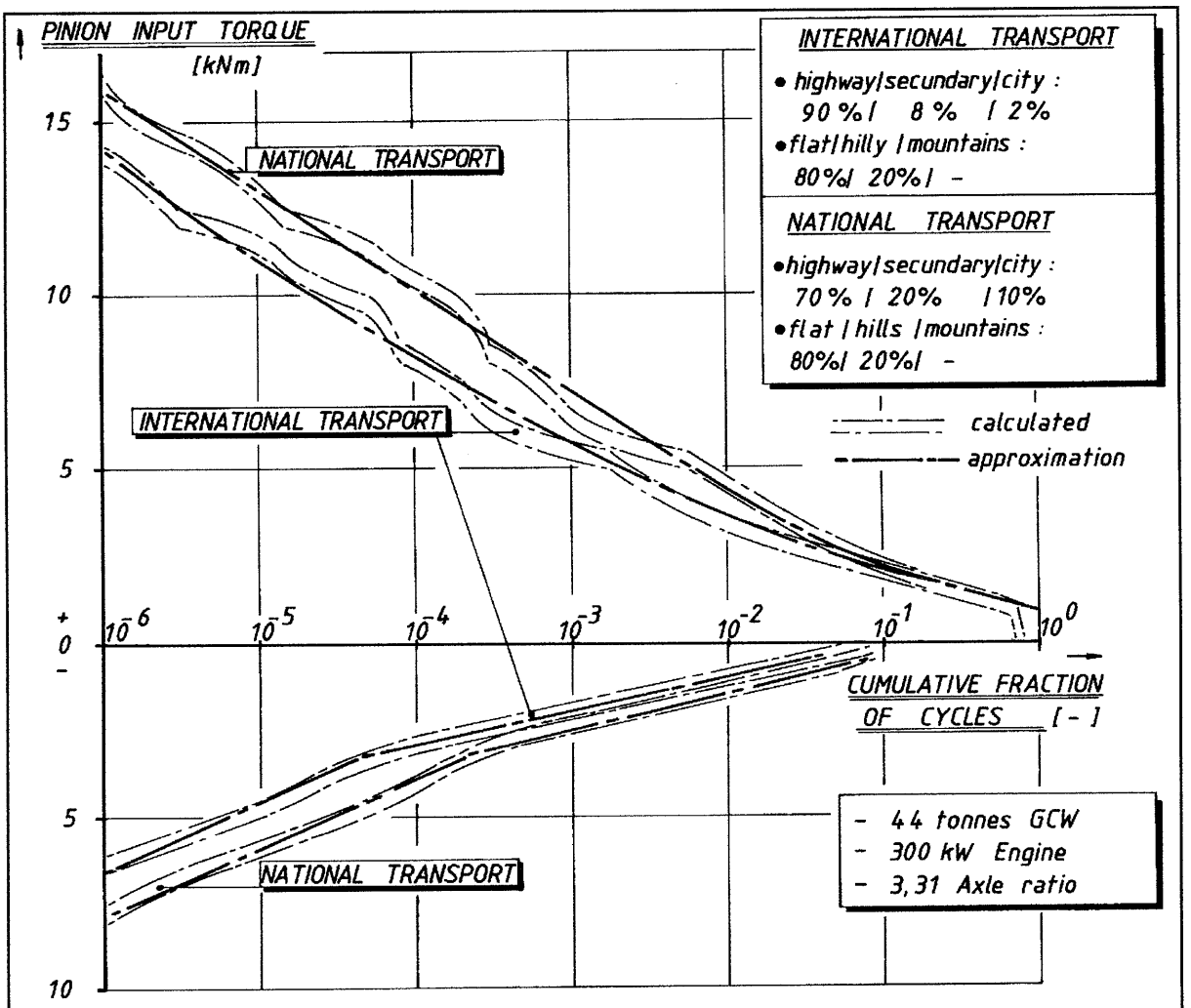

Fig. 5.6 Calculated Load Spectra for Transport Routes

This straight line shape of the loading spectrum in a diagram with lineair-logarithmic scales comes down to a stochastic behaviour of the driving torque over a longer period.
Deterministic torques that occur only during a very limited time and that are a result of specific actions of the driver, such as extreme gearshift and heavy acceleration of the vehicle, result in high torque values. They are however not indicated in the spectra, because they only take account for a fraction of the total number of revolutions that is smaller than 10^{-6}.
The minimum values of the torque in all spectra are required to drive the vehicle over a flat or slightly sloped road. The maximum theoretical value will be required to climb the steepest hill on an International Transport Route or to achieve the required acceleration on National Transport. In this way, these calculated rear axle load spectra can be simplified.

5.5 Simplification of Load Spectra

In figure. 5.7 a group of calculated and simplified load spectra is given for a 38 tonne vehicle with 230 kW engine power travelling on a standard International Transport Route. The pinion input torque is calculated here for five different rear axle ratio's. The typical curve for the Drive side loading, a part convex shaped and a part straight line for the spectrum, can clearly be seen. This type of driveline load spectrum may considered to be representative for transport in general.

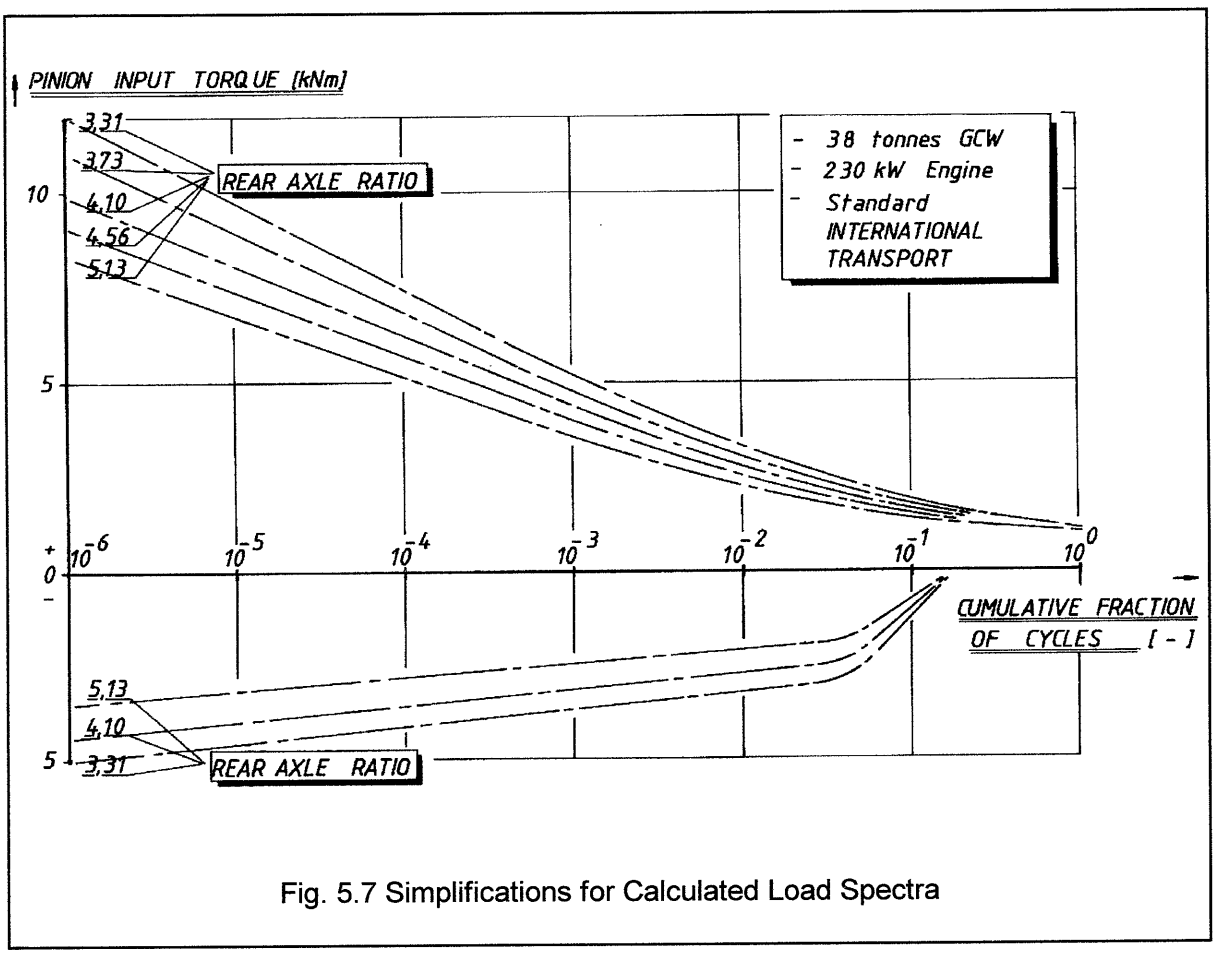

Fig. 5.7 Simplifications for Calculated Load Spectra

There are two basic types for driveline load spectra that can be distinghuished, based on the following graphical representations:

* a lineair load spectrum in a dubble logarithmic diagram: the "Log-Log" spectrum.
* a lineair load spectrum in a linear-logarithmic diagram; the "Lin-Log" spectrum.

These two basic types of driveline load spectra can be represented schematically by scaling the torque and the cumulative fraction of cycles in dimensionless units. The ratio of the actual value to the maximum value for the torque and the cumulative distance fraction are used here, as indicated in figure 5.8.

The load spectra are only given for the Drive condition; the Coast side is not considered here. It is assumed that the maximum torques will not lead to any static overloading. The cumulative fraction of the loading cycles on the horizontal scale ranges from 10^{-6} up to 1.0.

The ratio of the actual to maximum torque ranges from 0 to 1. Most of the calculated load spectra that can be regarded as representative for normal truck applications, will have a form

that is either one of two or that is situated somewhere in between both variants.
The upper graph is very close to a lognormal distribution, being the result of a stochastic driveline use. As it's representation is a straight line in a double logarithmic diagram, this is called a "Log-Log" spectrum. The lower graph is close to a normal distribution. Here deterministic effects, such as gearshift and accellerations of the vehicle resulting in high torques, are hardly taken into account. It's representation is a straight line in a linear-logarithmic diagram, therefore it is called a "Lin-Log" spectrum.

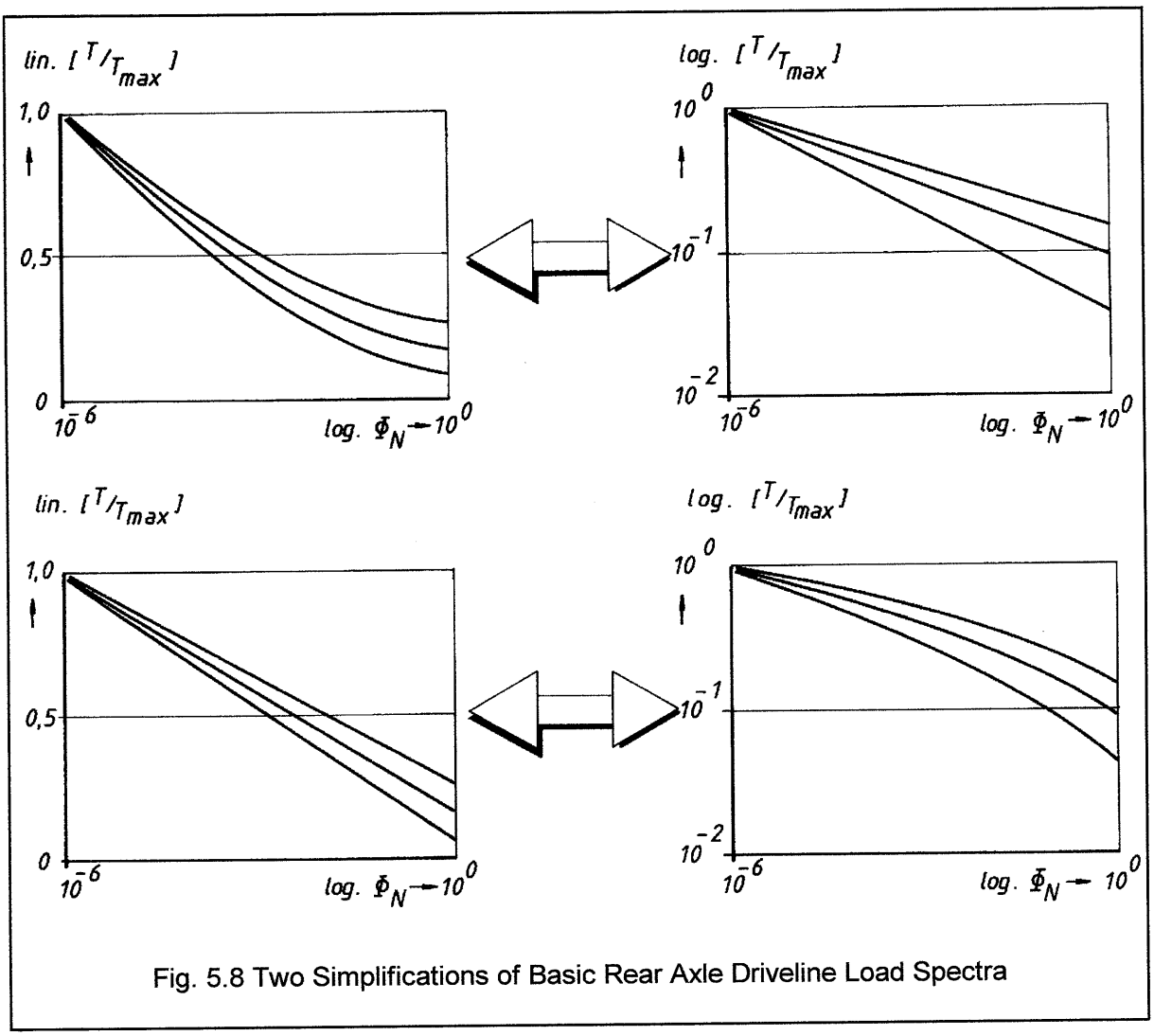

Fig. 5.8 Two Simplifications of Basic Rear Axle Driveline Load Spectra

* *Some typical load spectra for the driveline torque have been measured;* *
* *two typical routes may be distinghuished: Test Routes and Transport Routes.* *
* *A certain fraction of the engine power is applied to accomodate the spectra.* *
* *A comparison between measured and calculated spectra showed a good* *
* *correlation.* *
* *Many calculated driveline load spectra have a similar appearance; therefore* *
* *it was possible to develop two basic types of driveline load spectrum.* *
* *These two types have been styled to simple spectra, that can be described* *
* *mathematically.* *

5.6 Equivalent Torque for Simplified Load Spectra.

Both simplified and basic driveline load spectra can be expressed mathematically as a continuous loadspectrum. This mathematical expression for the driveline load spectrum can then be coupled with a given fatigue damage acccumulation theory. In this way, the severeness of the spectrum can be determined, that is expressed by the equivalent torque.

On basis of the damage accumulation theory, it is possible to determine the equivalent torque of a load spectrum that is given as a continuous function. This equivalent torque is representative for the fatigue damage of the complete load spectrum and can be used to make an estimate of the expected gear service life. It also serves as an indicator for the severeness of the loading spectrum. It can be expressed as:

$$\frac{T_{eq}}{T_{max}} = [\frac{1}{N_{\infty}} * \int (\frac{T(N)}{T_{max}})^{k} * dN]^{\frac{1}{k}} \qquad (5.1)$$

According to the theory of Palmgren-Miner, only the torque values higher than the endurance limit are assumed to have a contribution in the damage accumulation. According to Corten-Dolan, all torques have a contribution in the total damage, that are weighed by one and the same exponent that is determined by the slope of the SN-curve. Torques with values that are lower than the endurance limit, contribute in a comparable way to the cumulative damage than torques that are higher than the endurance limit. The equivalent torque that is determined in this way will generally lead to lower life estimates than when determined according to Palmgren-Miner. In other damage accumulation theories, such as Haibach-Gatts, stresses lower than the endurance limit contribute to the total fatigue damage in a restricted way.

When the mathematical expressions for the loading spectra are written in the general expression for the equivalent torque, formulations are generated by which the ratio of the equivalent torque to the maximum torque is given only as a function of the slope of the SN curve, indicated by k, and the ratio of minimum to maximum torque of the load spectrum.
The ratio of the minimum to maximum torque of the load spectrum is indicated by:

$$\varphi = \frac{T_{min}}{T_{max}} \qquad (5.2)$$

For both basic loading spectra, the “Log-Log” and “Lin-Log” spectrum, the expressions for the equivalent torque have been determined by applying the damage accumulation theory of Corten-Dolan thereby implying all torque levels.
Figures 5.9 and 5.10 show the ratio of the equivalent to the maximum torque as a function of the slope of the SN-curve. The parameter in the graphs is the ratio of the minimum to the maximum torque of the load spectrum. The damage accumulation theory according to Palmgren-Miner allows a closed analytical expression for the equivalent torque to be derived. Modifications on the cumulative damage theory, such as Haibach-Gatts, only allow relative complex analytical formulations.
The equivalent torque for the "Lin-Log"-spectrum is mathematically rather complicated; this can only be calculated using a recurrent expression [5.5] that has been derived in Appendix 5.1. The analytical expressions and it's graphical representation are given here.

5.6.1 The "Log-Log" Spectrum

The mathematical expression for the "log-log"-spectrum is:

$$\log T(N) = \log T_{max} + \frac{\log\varphi}{\log N_{\infty}} * \log N \tag{5.3}$$

The equivalent torque for the "Log-Log"-spectrum is described as (Appendix 5.1):

$$\frac{T_{eq}}{T_{max}} = \left[\frac{N_{\infty}^{a} - 1}{N_{\infty}} * \frac{1}{a}\right]^{\frac{1}{k}} \tag{5.4}$$

$$a = 1 + k * \frac{\log\varphi}{\log N_{\infty}} \tag{5.5}$$

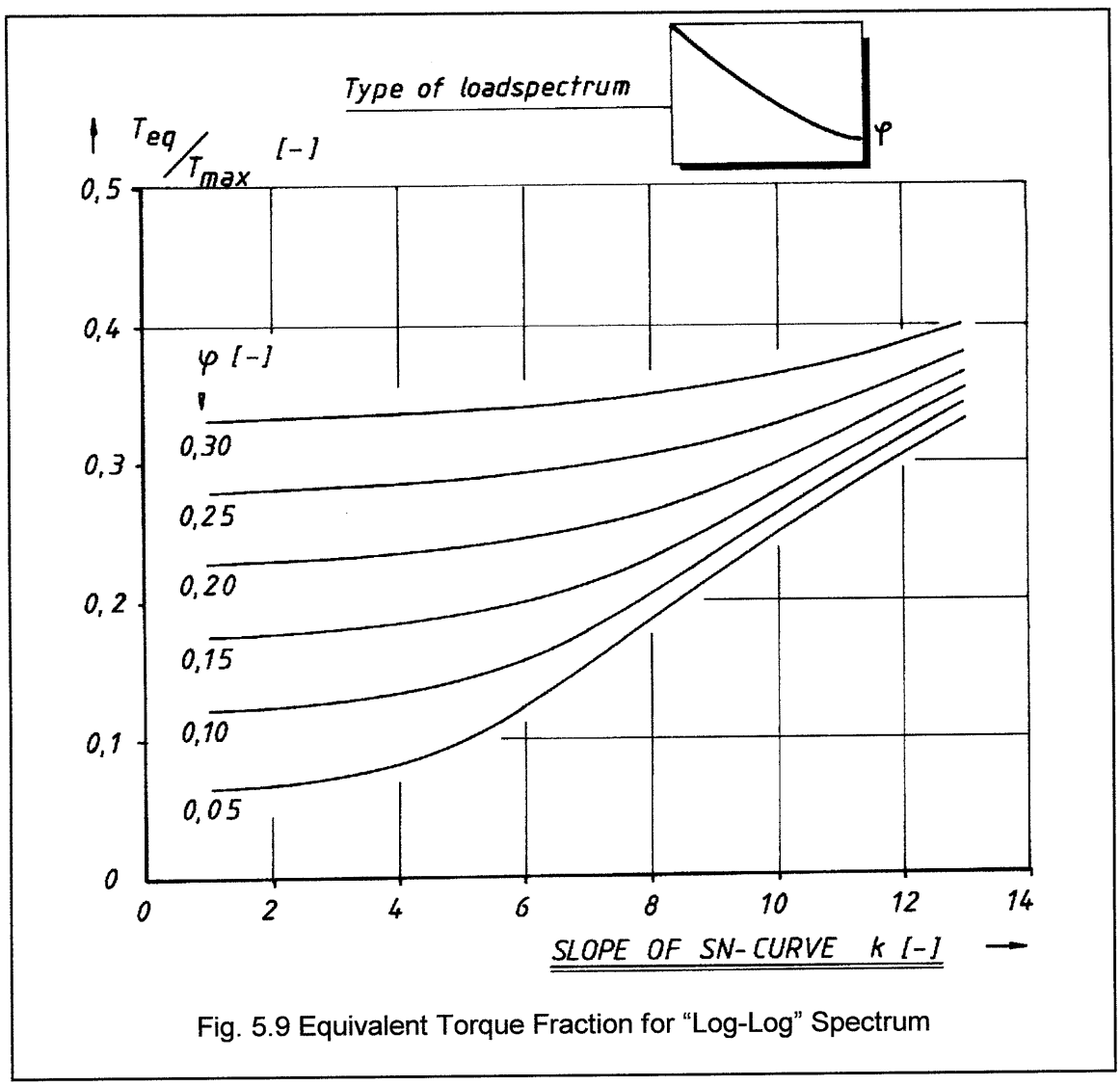

Fig. 5.9 Equivalent Torque Fraction for "Log-Log" Spectrum

5.6.2 The "Lin-Log" Spectrum

The mathematical expression for the "Lin-Log"-spectrum is:

$$T(N) = T_{max} * [1 - \frac{(1-\varphi)}{\log N_\infty} * \log N] \tag{5.6}$$

The equivalent torque for the "Lin-Log" spectrum is described as (Appendix 5.2):

$$\frac{T_{eq}}{T_{max}} = \Sigma[\frac{k!}{(k-1)!} * (-D)^i * \{(1+D*lnN_\infty)^{k-i} - \frac{1}{N_\infty}\}] + k! * (-D)^{k-1} * I_1 \tag{5.7}$$

$$I_1 = 1 + D * \ln N_\infty - \frac{1}{N_\infty} - D + \frac{D}{N_\infty} \quad where \quad D = -\frac{\varphi}{ln10} \tag{5.8}$$

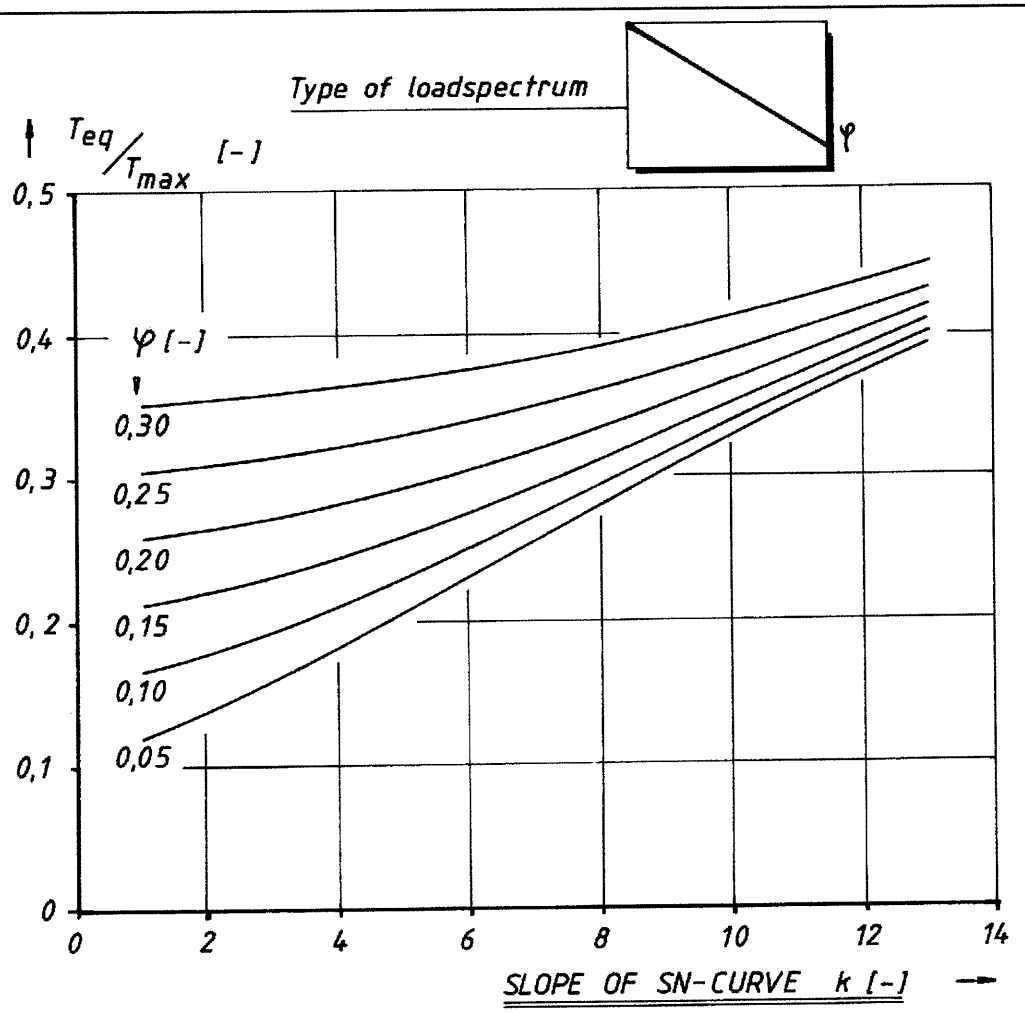

Fig. 5.10 Equivalent Torque Fraction for a ""Lin-Log" Spectrum

5.6.3 Evaluation of Equivalent Torques for Load Spectra

The values for the equivalent torques that have been determined by these two methods may be considered as an overestimate for truck applications, because the applied theory for damage accumulation also incorporates the damage of torques being lower than the endurance value. For the driveline load spectra that have been generated, the following general dimensionless values may be used:

* $\phi = T_{min}/T_{max} = 0.05 - 0.20$
* Slope SN-curve = 7 - 9.

The slope is valid for the fatigue bending failure of hardened case carburised gear materials and normal failure probabilities. The minimum torque is the required torque for a vehicle speed of about 70 km/h on a flat road. The maximum torque is required for driving the vehicle uphill along a 15% slope. This is the same value as the maximum torque that is defined in chapter 6, as being a function of the crownwheel outerdiameter.

Based on the equations of this part, the following values for the equivalent torque ratio may be used:

* International Transport: $T_{eq} = (0.20 - 0.25) * T_{max}$
* National Transport: $T_{eq} = (0.27 - 0.33) * T_{max}$.

The lower values are based on the "Log-Log" spectrum; the higher values are based on the "Lin-Log" spectrum. This means that an equivalent rear axle torque of about 20 to 25% of the maximum torque may be regarded as representative for International Transport, whereas for "National Transport" the equivalent torque is 27 to 33% of the maximum torque.

In [5.7] synthetic loading spectra have been developed that can be applied for automotive use. This type of load spectrum is described as:

$$\frac{T}{T_{max}} = \left[\frac{\log\frac{N}{N_{max}}}{\log\frac{N_{max}}{N_{min}}}\right]^{\frac{1}{m}} \qquad (5.9)$$

In the description of these spectra, m is supposed to have a constant value.
Both simplified load spectra of the previous part have been compared with this synthetic spectrum; they appear not to correlate with each other. In order to fit the simplified loading spectra with the spectrum of equation (5.9), the parameter m had to assume different values for different cumulative distance fractions. When using this synthetic load spectrum for describing several vehicle routes, the following values for m may be used then:

* International Transport: m = 0.7 - 0.9
* National Transport: m = 0.9 - 1.1
* Test Routes for trucks: m = 1.1 - 1.5
* Test Routes for cars: m = 1.5 - 2.0.

For these synthetic load spectra, also expressions are given for the equivalent torque ratio. These are however only valid for parts of loading spectra with a lineair behaviour in a dubble logarithmic diagram. The equivalent torques, calculated with the expressions of [5.7] may then be compared with the equivalent torques, calculated according to the just derived equations for a "Log-Log" spectrum. The results are given in the following table, where the slope of the SN curve is assumed to be k = 9.

For high values of T(min) / T(max) of the load spectrum, the difference in calculated equivalent torque between both methods is relatively small. For relatively light spectra, where the ratio of maximum to minimum torque is less than 0.15, the difference increases. As the self derived equations assume no endurance limit, the calculated equivalent torque will here be higher than calculated according to [5.7].

In [2.7] and [2.8] the gear performance torque may be regarded as the equivalent torque for a given vehicle specification. This gear performance torque is based on the performance ratio for vehicles; it is dependent on the vehicle gradeability and the road type. The performance ratio is based on a relation between the maximum engine torque and the vehicle weight.
In itself, a ratio between engine power and vehicle weight would be better to be expected.
The values from [2.7] and the expression from chapter 6, where the ratio between maximum output torque and vehicle weight is equal to unity, are combined here. This means that the value for the performance to the maximum torque may be written as:

$$\frac{T_{eq}}{T_{max}} = (0.20 \div 0.40) \qquad (5.10)$$

It appears that the derived equations for the equivalent torque ratio are in line with other sources, although at the last one, the variation in the numerical value is relatively large. When the recommended values for domestic or foreign highway, city or inter-urban busses are used, an expression for the required performance torque as a function of the vehicle GCW may be given. The maximum possible variation of the values of these parameters may lead to a variation of the gear performance torque by a factor of 2.5, even within every vehicle application. Therefore it will only be used as a guideline for a first order determination of the general gear dimensions.

* *Simplifications of two typical vehicle driveline loading spectra have been* *
* *developed, the "Lin-Log" and the "Log-Log" spectrum.* *
* *Both load spectra have been mathematically described.* *
* *Based on the damage accumulation theory of Corten-Dolan, expressions* *
* *for the equivalent torque have been derived.* *
* *For these load spectra and case carburised gear materials, the ratio of the* *
* *equivalent torque - to - maximum torque lies between 0,20 and 0,33.* *

5.7 Variable Amplitude Endurance Tests

5.7.1 Results of Variable Amplitude Tests.

On one axle type, crownwheeldiameter 445 and axle ratio 4.10, two series of Variable Amplitude tests based on load a spectrum have been performed. For each spectrum, a total of four gearsets has been tested. The load spectra were of the "Lin-Log"-type, although not continuous; the continuous spectra have been approximated by several discrete torque values that were kept constant during a limited time interval. Therefore the test was referred to as a "Block"-test. Only one basic type of loading spectrum has been used; both spectra had different values for the torques, although they differed only slightly. They are indicated by LOW and HIGH, referring to the level of the torque. The LOW spectrum consists of 5 torque levels, the HIGH spectrum has 7 levels with each torque level a small variation of the actual torques to about maximum 5% of the actual value. The graphical representations of the load spectra are given in figure 5.11.

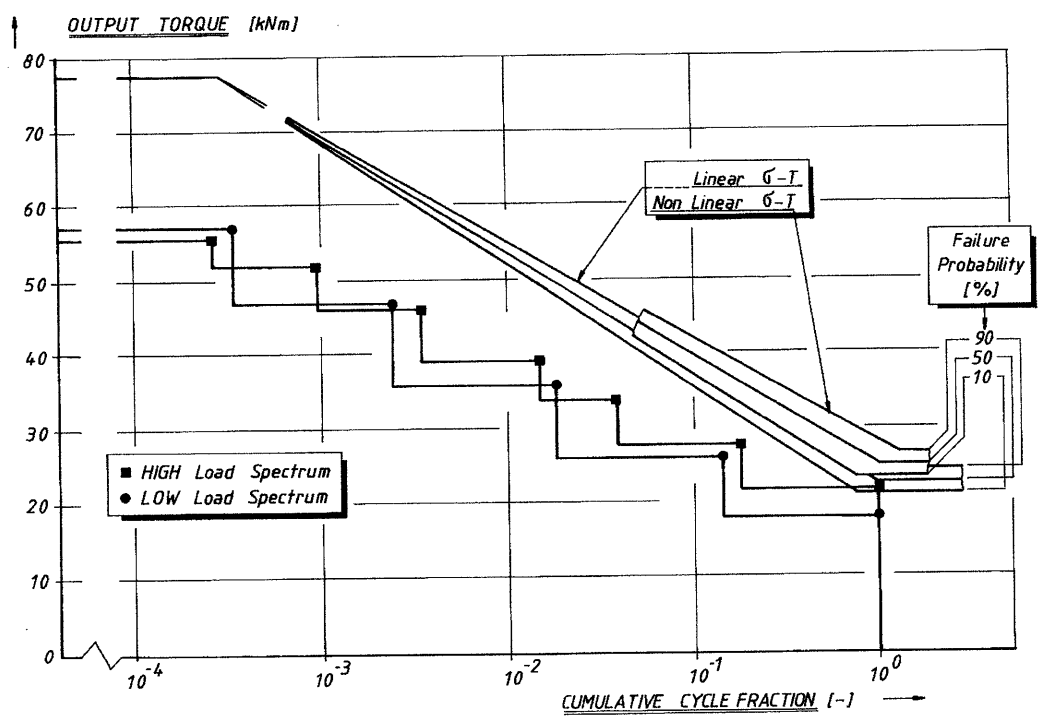

Fig 5.11 Load Spectra in Block form for Variable Amplitude Loading

Three gearsets of both series have been running until the same testrig stopping criterium of the constant amplitude tests became active. Out of each serie one set was stopped earlier for inspection purposes, which also would give some indication on the crack initiation. The general level of the testing spectra was such that failures were to be expected within a limited time, as the major part of the spectrum torques is higher than the endurance torque. The general level of both loading spectra is appreciably larger than what is to be expected under normal or even heavy vehicle conditions. This has been done in order to provoke tooth root fracture, similar to the constant amplitude tests. The results of the variable amplitude tests are summarised in Attachment 5.7, together with the actual torque values.

As can be seen in the table of the testresults, the failuretypes of the Variable Amplitude tests differed from the failuretype of the constant amplitude tests. Whereas the Constant Amplitude tests at high torque level showed very predominantly tooth root fatigue failures on almost all samples, the results of the Variable Amplitude tests showed a mix of principal gear failures. Here a beginning type of surface failure in the form of pitting or even spalling could clearly be examined. On several pinions, breakage of the upper part of the tooth and even cracks in the root could be observed. A type of surface failure may have been generated by the lower torque part of the spectrum. As a result of the stress rising effects of failures on the tooth surface, part of the teeth have been broken when larger torques are applied. These large torques would normally give lesser damage if the teeth had not partly been damaged by surface failure at an earlier stage. Both torque levels next higher to the endurance torque are responsable for more than half of the calculated damage at the HIGH load spectrum. The statistical representation of the results for both variable amplitude tests with LOW and HIGH Load spectra are given in fig. 5.12, for an assumed lognormal failure probability distribution. Because of the limited number of samples, these values should be considered with care.

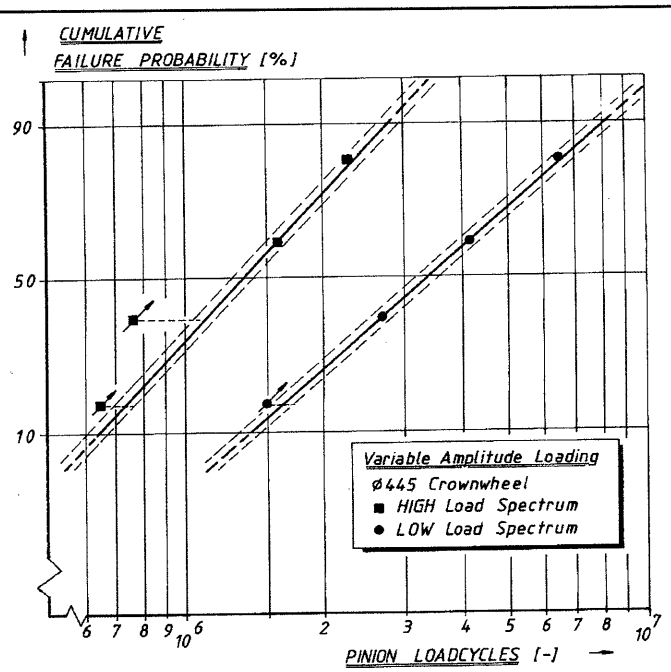

Fig 5.12 Statistical Evaluation of Variable Amplitude Tests

It has been observed that the point of crack initiation lies at about 75-80% of the total registered number of test cycles. This percentage of crack initiation relative to the gear life only counts for small cracks that are visible. The actual occurence of crack initiation will be on a smaller number of cycles. This fraction has not been determined, as this goes beyond the scope of this work. The fact that a clearly and visible crack could be observed at less than about 75 % of the total endurance life, is consistent with the findings during the Constant Amplitude tests. There the impression existed that at about more than 65% of the registered endurance life, a visible crack initiation had been taken place. This was found by using an endoscope to examine the gear surface during intermediate inspections.
The ratio of the cycle numbers at 90 to 10% failure probability of these tests has been given in fig. 5.13, together with data for the Constant Amplitude load tests of the four axle types.

In this diagram, other data are also given for reasons of comparison. These data have been derived form [4.7], [4.10] and [4.11]. It shows that for the very limited number of test samples for the Variable Amplitude tests, the ratio of cycle numbers for 90% to 10% failure probability lies well within the range of other endurance tests.
As the variable amplitude tests have only been performed with a very limited number of 4 test samples each, the statistical evaluation is to be considered here with some caution.
Nevertheless the results are considered to be statistically viable and they are therefore used for further analysis and comparison with calculated endurance data.

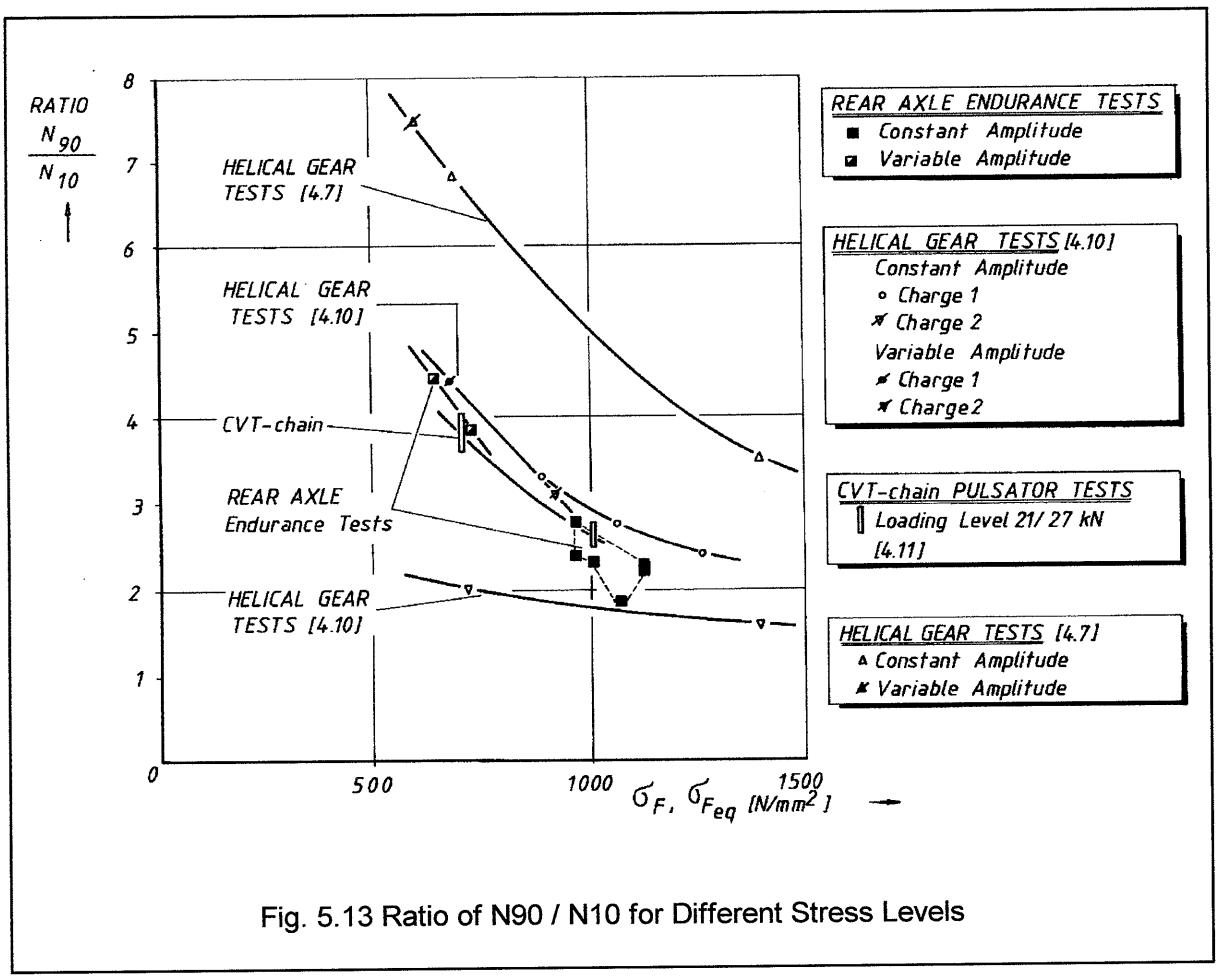

Fig. 5.13 Ratio of N90 / N10 for Different Stress Levels

5.7.2 Verification of Measured and Calculated Life at Variable Amplitude

The expected pinion life has been calculated for both loading spectra of the Variable Amplitude tests. Both the linear and the non linear stress/torque relations, together with the accompanying endurance values of the Constant Amplitude tests have been used here. The life calculations have been performed for three well known cumulative damage theories, namely according to Palmgren-Miner (PM), Corten-Dolan (CD) and Haibach-Gatts (HG).
Generally these theories will lead to differences in calculated pinion life. As the theory according to CD includes all loading levels, the calculated endurance life will be lower than the calculated life expectancy according to PM, which only accounts for torques higher than the enduarnce limit. Calculated load cycles according to HG will lie in between the results ofboth mentioned theories.

The results of the calculated life expectancy for both spectra HIGH and LOW are given in figures 5.14 and 5.15, together with the actual realisations of the tests. The calculated values are given for three failure probabilities, 10, 50 and 90 % as well as for the three applied damage accumulation theories CD, HG and PM. In these graphs, also the distinction is made between the linear and the non-linear stress/torque relationship. For the linear stress/torque relation, the material values of Table 4.6 have been used. For the non-linear srtess/torque relation, the values of Table 4.9 have been used. These data are based on the results of the constant amplitude tests. The relatively small difference in the calculated endurance lifes for the three theories is mainly a result of the spectrum, of which allmost all torques are higher than the endurance torque of the gears.

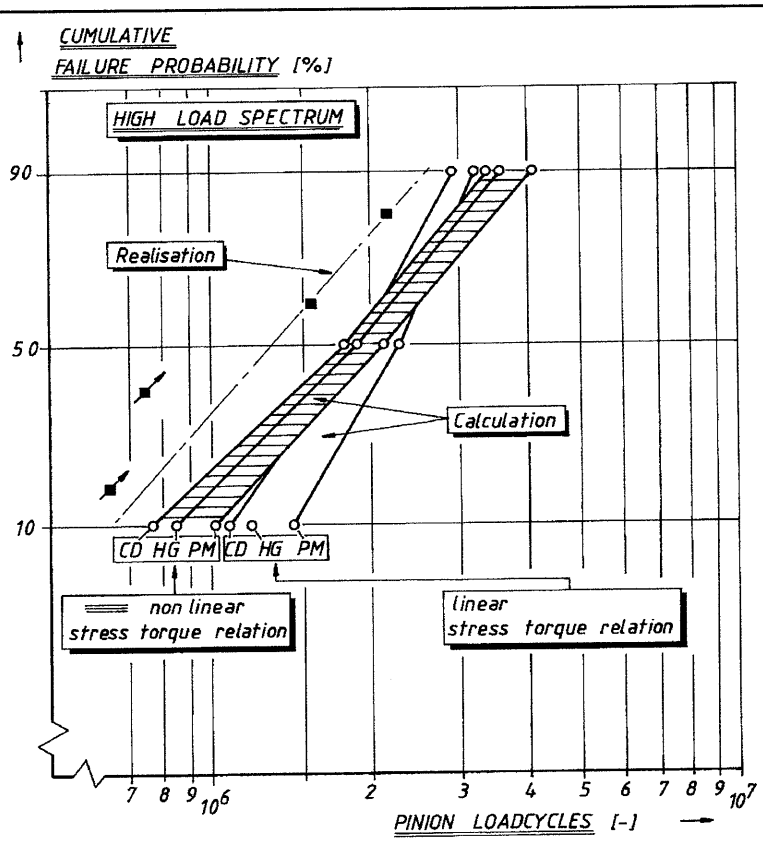

Fig. 5.14 Calculated and Actual Results for "High" Load Spectrum

For both spectra, the actual registered lifes are lower than the calculated ones, for both the linear and non-linear stress/torque relationship. The non-linear stress/torque relation however gives the best correlation between calculated and registered pinion lifes for the 10% failure probability for both spectra of the Variable Amplitude tests. In this way, the non-linear stress/torque relation gives an improvement compared to the linear relation. These results confirm the preference for a non-linear relation in stress/torque. For the 90% failure probability the difference between linear and non-linear torque/stress relation is small. This is however a probability value that is not interesting for design purposes.
The damage accumulation theory according to Corten-Dolan (CD) here gives the best fits for all three failure probabilties of 10% and 50%. This has also been observed by [4.7].
For the Constant Amplitude loading, the difference between calculated and actual pinion lifes for the 445 axle are lower than plus/minus 5% for the 10, 50 and 90 % failure probabilities,

when a non linear stress/torque relation is assumed. For the linear relation, the difference between calculated and actual pinion life is less than 8% only for the 10 % failure probabilities; it is between 10 to 20 % for higher failure probabilities.
For the Variable Amplitude loading of this axle, the differences between calculated and actual gear life are about 13% for a 10% failure probability and a non-linear relation between stress and torque. The differences between calculated and actual pinion life are larger for the variable amplitude loading cases than as for the constant amplitude loading. The reason for this may be decrease in the fatigue behaviour of the material.

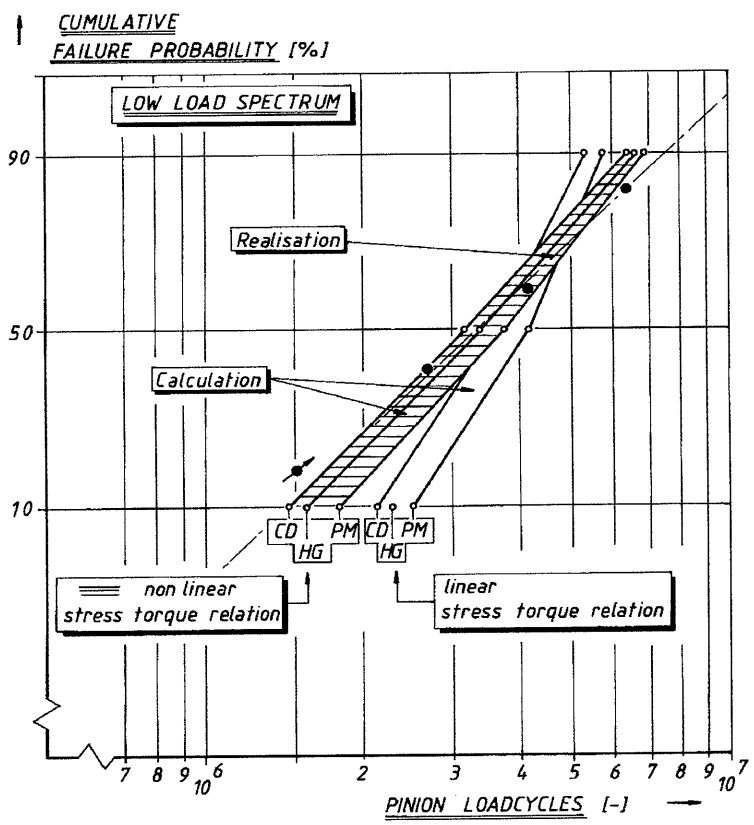

Fig. 5.15 Calculated and Actual Results for "Low" Load Spectrum

Generally it can be said that for variable amplitude loading, a mix of pinion failure may be expected. This is at least valid for the case of relatively high load spectra. Mostly some kind of surface failure will first be generated, in the form of pitting or spalling. This will hardly have any noticeable detrimental effects on the gears, but it will be an premature initiation for other failures such as root breakage. In some cases they may be combined with partially tooth tip breakage, caused by the stress effect of pittings at high torques.
These effects will lead to a reduction of the endurance values that have been established during constant amplitude load testing. This means that the actual registered fatigue life at variable amplitude loading will be smaller than when calculated by using the endurance values of constant amplitude loading. For the "LOW" spectrum, the required decrease in endurance strength would be relatively low with about 2.5%. For the "HIGH" spectrum, the reduction in the endurance fatigue limit would be about 5% for a 10% failure probability and about 10% for 90% failure probability.

It would mean that for Variable Amplitude loading, the endurance limit of the gear material that has been established at Constant Amplitude loading, would require a correction to account for this reduction in endurance strength. The results are given in Table 5.1.
When comparing this table with the endurance data from the earlier established tables, it is striking that for the 10 % failure probability, the values are identical. This is an indication that the non-linear stress/torque relation is valid for a Constant and a Variable Amplitude loading.

Failure Probability [%]	Endurance Limit [N/mm2]	Slope SN-curve [-]	Knickpoint N_w [-]
1	665	7.50	$3 * 10^6$
5	700	7.75	$3 * 10^6$
10	720	8.00	$3 * 10^6$
50	790	8.75	$4 * 10^6$
90	850	9.50	$5 * 10^6$
95	870	9.75	$5 * 10^6$
99	900	10.0	$5 * 10^6$
Static Limit	2125	-	$1 * 10^3$

Table 5.1
Endurance Data as established from Variable Amplitude Testresults
for a non-linear stress / torque relation

In fig. 5.16 the values for the endurance limit in relation to the failure probability are graphically represented. It shows the change in endurance value when going from a linear to a non linear stress/torque relation at Constant Amplitude loading, as has been derived in the previous chapter 4. Included are also the values for the endurance limit for a non linear stress/torque relation at Variable Amplitude loading. This is mostly a result of the variation in service life for the 90 and 10% failure probability, that differs between the constant and variable amplitude load tests. Further tests are required however in order to statistically establish if a correction is required for a higher number of testsamples.

In fig. 5.17 the values for the slope of the SN-curves are represented. It shows quite clearly that for a non linear stress/torque relation, the k-factors come much more in line with those from helical gears of the same material. When fitting the calculated with the registered service life for Variable Amplitude loading, the k-factors for variable and constant amplitude loading could remain unchanged. As this was only possible with a non linear stress/torque relation, this non linearity gives mathematically and physically a far better agreement .

The reduction in endurance strength might be the reason for the fact that here the damage accumulation theory of Corten-Dolan CD gives the best correlation between calculated and actual pinion life. Normally for gear applications the Haibach-Gatts theory is applied.

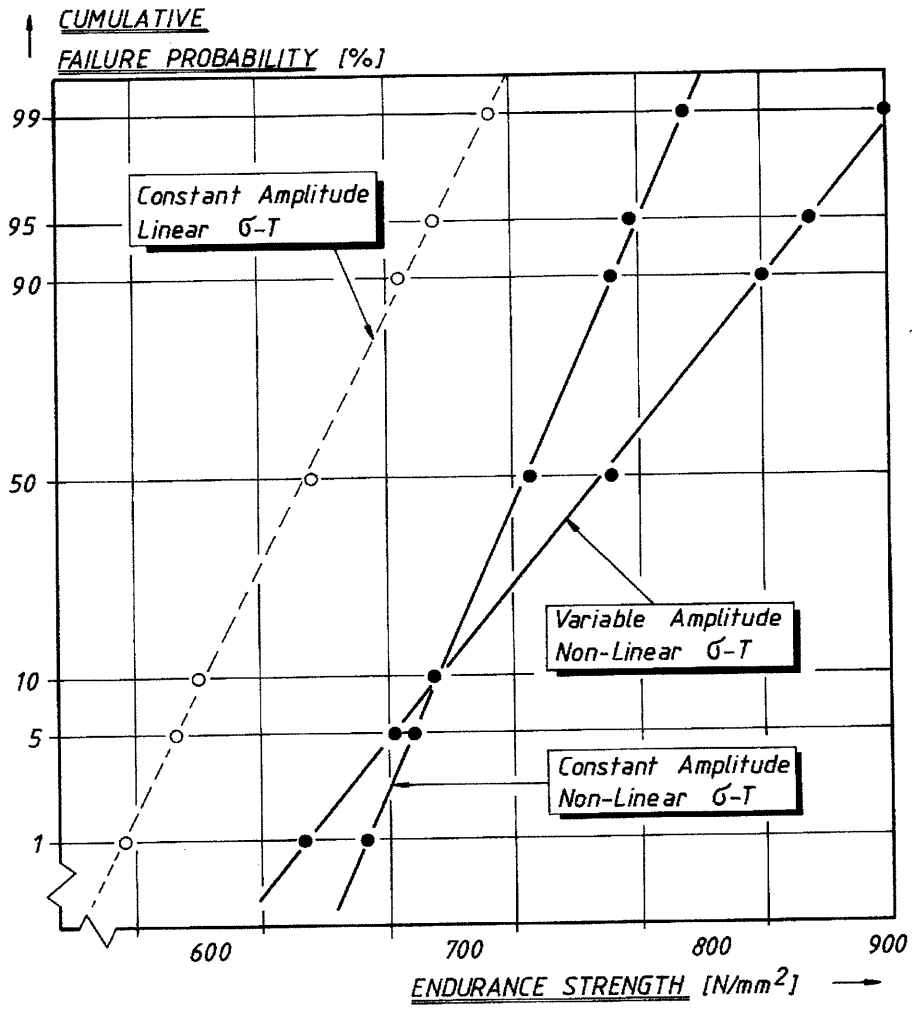

Fig. 5.16 Values of Endurance Limit

It may well be that in some cases the theory of Corten-Dolan gives the best correlation between measured and calculated life cycles, whereas in other cases the theory of Haibach-Gatts gives the best results. This may well depend on how the load spectrum is situated in relation to the SN-curve, more precisely to the endurance limit.

Some loading spectra may have theoretically by far the most damage for root fatigue than for surface fatigue and are thus very heavy with regard to root fatigue failure. This may be the case when gears have a relatively small module and large teethnumbers, for reasons of noise production. These gears may obtain easily premature gear flank surface damage by some loads of the spectrum. This may reduce the root fatigue endurance values determined at Constant Amplitude loading. In that case the theory of Corten-Dolan may give the best correlation between calculations and tests. Still then, an additional reduction of the endurance limit may occur. This may be different for loading spectra that theoretically have for instance comparable damage contents for root and for flank fatigue. Here the theory of Haibach-Gatts may well be suited the best.

In general it may be stated that the severeness of a loading spectrum in relation to the endurance limits of the gear geometry and the material, will determine what damage accumulation theory is the best suitable for life predictions.

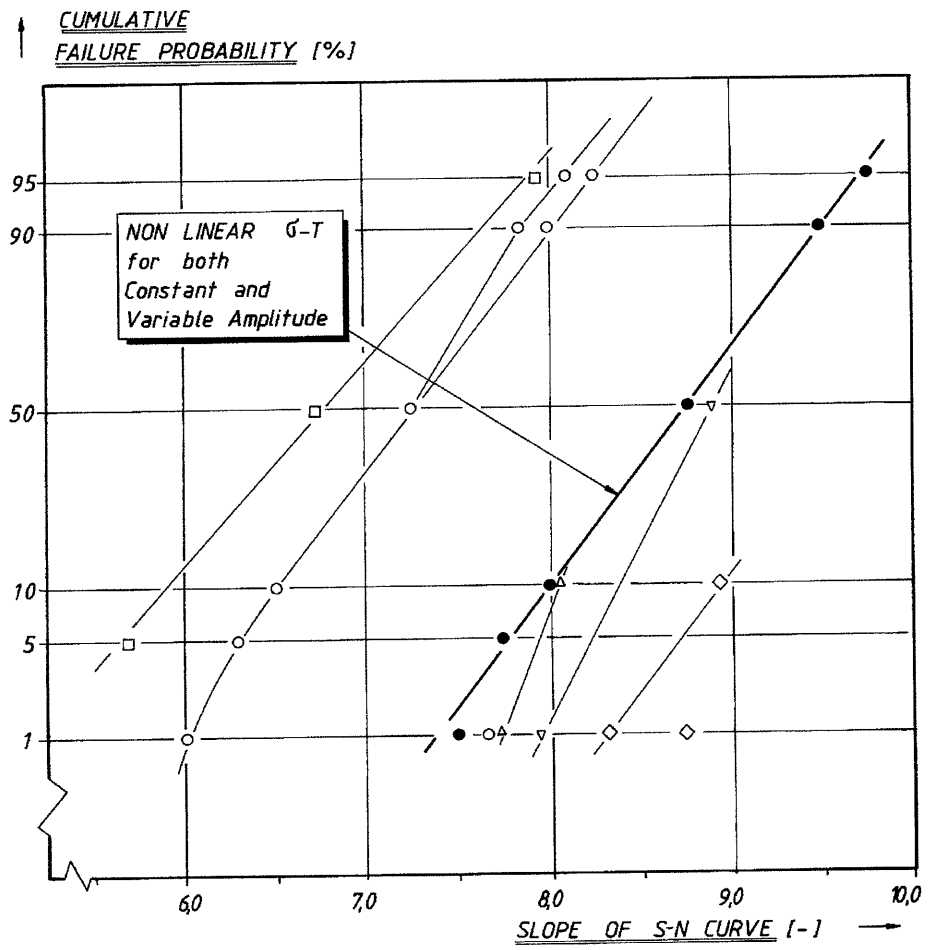

Fig. 5.17 Values for Slope SN for Non Linear Stress Relation

* *Although there is only a little difference in the torque values between both* *
* *spectra HIGH and LOW, both calculated and registered lifes indicate a* *
* *significant difference.* *
* *The actual life is less than the calculated pinion life; about 15% lower* *
* *values for both the LOW and HIGH at a 10 % failure probability.* *
* *The life expectancy calculated according to the theory of CD gives a better* *
* *correlation to the test results than the PM and the HG theory.* *
* *Early surface failures at variable amplitude loading may lead to a reduction* *
* *in the endurance limit that has been established at a constant amplitude loading.* *
* *This effect of different failures accelerating the dominant failure type is* *
* *designated here as "failure interference".* *
* *The effect will depend on the severeness of the load spectrum in relation* *
* *to the endurance limits of the gears.* *
* *A non linear stress-torque relation gives remarkedly smaller differences* *
* *between calculations and realisation also for Variable Amplitude loading.* *

5.8 Resumee

Several measured driveline loading spectra for rear axle gears have been discussed and evaluated. Generally two types of driveline load spectra can be distinguished: Transport Routes and Test Routes. For heavy and hilly Test Routes about 65-70% of all load cycles is on the Drive Side of the gears, whereas this amounts to about 90% for Transport Routes.

The engine power, or a fraction of this, can be seen as representative for determining the loading spectrum. With this the dimensioning of rear axle gears at the initial design may be simplified when the vehicle GCW/GVW and the engine power are known.

The comparison between a measured and a simulated load spectrum shows a difference in driveline torque of less than 10 % for normal torque values. For large torques, the difference increases. In view of the variation in measured load spectra, this difference is acceptable. Here, deterministic actions such as gear shift and accelerations with smaller occurrences than 10^{-4} to 10^{-5} distancefractions are not measured.

Calculated driveline load spectra for most truck applications may be simplified by two basic forms. These are the "Log-Log" and the "Lin-Log"-spectrum. The first one is suitable for Transport Routes, whereas the second describes Test Routes.
Both spectra have been described mathematically and expressions have been established for the equivalent driveline torque. The equivalent torque for International Transport Routes is about 20 to 25% of the maximum torque. For National Transport this value is about 25 to 30%.

Endurance life tests with Variable Amplitude load have been performed on a limited number of sample gears of one axle type. The damage type that occured with these Variable Amplitude loading differs from the damage at Constant Amplitude loading. At Variable Amplitude loading generally a mix of failures can be expected, where one failure type may accelerate another failuretype. In this case the appearance of light surface damage may well have accelerated tooth root fatigue. This aspect, which is defined as "failure interference" may be the cause for a reduction in the endurance limit that has been established at a Constant Amplitude loading.

Pinion life calculations for Variable Amplitude load spectra, with a non linear relation between stress and torque assumed, showed a far more better agreement between calculation and realisation than with a linear stress/torque relation, especially for the 10% and 50 % failure probability.
At 10 % failure probability the calculated pinion life is about 15 - 20 % higher than the actual realisation, when the non linear stress-torque relation is applied. For a linear stress-torque relation, the difference between calculated and actual pinion life is about 75 - 100 %.
This shows that also here the non-linear stress/torque relation gives a clear improvement in the predictability of life calculations.
The damage accumulation theory according to Corten-Dolan gives the best agreement between the actual registered life and the calculated life. A reduction on the endurance fatigue limit, established at Constant Amplitude load, would then still be required in order to match calculation and realisation.

These results are based on a very limited number of test samples, therefore the conclusions should be considered with care and further investigations are required.

6 SCALE LAWS AND GENERAL DESIGN FOR REAR AXLE GEARS

6.1 Introduction

Mostly rear axles are manufactured in a range of dimensions in order to cover a wide field of applications. It would be very helpfull if a range of axles could be designed, using a scale law for automotive rear axle gears. In the general applications of technical products, produced and manufactured by man, one can distinguish a relatively large scale of dimensions. For these technical products, in particular mechanical engineering elements, the dimensional scale ranges from several millimeters for the so-called fine mechanical elements to several tens or hundreds of meters for large oilrig platforms or supertankers.

In the first part of this chapter, an analysis will be given on the characteristic dimension of rear axle gears, the gear diameter, and its dependency on a vehicle related value. A study will be performed to determine a simplified scale law for a wide range of rear axle gear dimensions. Secondly, a comparative analysis will be given on other mechanical parts that transmit torque or power. Here it will be shown that in principle the same scale law is valid as is for automotive rear axle gears. In the third part, a comparison with Nature will be made, where some scale laws are considered and compared with those of rear axle gears.

Finally a short review will be given on a general design procedure that may be used for the preliminary design of rear axle gears. On basis of the aspects that have been delt with in the previous chapters, it is possible to give some directives or guidelines for a general gear lay-out. General dimensionless factors can be used to determine the basic gear geometry data, for a given vehicle- and application description is the starting point. Secondly, a further specification will be required in terms of fine tuning the gear design for customary automotive design practice.

6.2 Scale Laws for Bevel and Hypoid Rear Axle Gears

6.2.1 Gear Diameter versus Output Torque

For single stage gear drives with cylindrical or helical gears, the centredistance is the main and governing feature that determines the general dimensions [6.1]. For bevel and hypoid gears the gear outer diameter is the determining value for the overall dimensions. Not only does this diameter determine the overall rear axle lay-out, the dimensions of the rear axle casing are also determined by it. As a result of this, the axle weight and costs mainly will be governed by the choice of the gear outerdiameter. Also, important vehicle features such as ground clearance, vehicle suspension dimensions as well as restraints are determined by this overall gear dimension.
It is possible to derive, purely on a theoretical basis, a relationship between the gear outer diameter of bevel and hypoid gears and the output torque. This can be done by rewriting the basic formulations for the strength calculations. Here, a geometrical similarity of the gears is assumed which means that the ratio of facewidth to gear outer diameter is constant. Also, the ratio of vertical pinion offset to gear outer diameter is considered constant, as is the teeth number of the gear.

Then the following relationship between gear outer diameter and output torque can be established:

$$d_{e2}=c_m*c_g*c_l*T_2^{1/3} \qquad (6.1)$$

In this expression, c_m is a material related parameter that is determined by the type of the gear material and its heat treatment. The parameter c_g is geometry related and its value is determined by gear geometry data such as facewidth, spiral angle and teeth numbers. The value c_l is load related and depends on dynamic effects and actual service loads. These constants can be specifically dedicated to tooth root failure and tooth surface failure, leading to the following expressions:
For Tooth Surface Failure:

$$d_{e2}=c_{m_H}*c_{g_H}*c_{l_H}*T_2^{1/3} \qquad (6.2)$$

For Tooth Root Failure:

$$d_{e2}=c_{m_F}*c_{g_F}*c_{l_F}*T_2^{1/3} \qquad (6.3)$$

Attachment 6.2.1 gives the derivation of the above expressions. The values of all parameters are different, depending on tooth root failue or tooth surface failure. Also for a static or a continuous loading they will differ.
When a minimum/maximum analysis on specific gear geometry and material data is applied, it is possible to determine the range of the constants. This analysis is based on the general variation of gear geometry data in terms of teeth number, gear ratio, spiral angle and facewidth, that may be encountered on typical automotive rear axle gears. The material under consideration is case carburised gear steel, since for highly loaded gears this type of material is commonly used in automotive applications.

Tooth Surface Failure.
For the surface failure mode, the generalised expression becomes:

$$d_{e2}=12.6*\left[\frac{S_H}{\sigma_H*\Pi Z_{mat}}\right]^{2/3}*\left[\frac{(\Pi Z)^2*\sqrt{i^2+1}}{\xi(1-\xi*\sin\delta_2)^2*\phi}\right]^{1/3}*[\Pi K]^{1/3}*T_2^{1/3} \qquad (6.4)$$

At a static maximum torque, with plastic deformation on the tooth surface, the expression yields:

$$d_{e2}=(7 \div 17.5)*T_{2_{max}}^{1/3} \qquad (6.5)$$

At the endurance or continuously applied torque, where fatigue of the surface layers may occur in the form of pitting:

$$d_{e2}=(8.5 \div 21.5)*T_{2_{cont}}^{1/3} \qquad (6.6)$$

Tooth Root Failure.

For the tooth root failure mode, the generalised expression is:

$$d_{e2}=12.6*[\frac{S_F}{\sigma_F*\Pi Y_{mat}}]^{1/3}*[\frac{\Pi Y*z_2}{\xi*(1-\xi*\sin\delta_2)^2*\cos\beta_{m2}}]^{1/3}*[\Pi K]^{1/3}*T_2^{1/3} \qquad (6.7)$$

At the static maximum torque, where mostly a brittle fracture of the teeth may occur, the expression is:

$$d_{e2}=(11.5\div16)*T_{2_{max}}^{1/3} \qquad (6.8)$$

At the endurance or continuously applied torque, where fatigue breakage of the gear teeth may occur, it is expressed as:

$$d_{e2}=(15.5\div21)*T_{2_{cont}}^{1/3} \qquad (6.9)$$

A comparison of the required diameter at a given output torque for the surface and the root failure mode, shows that the largest diameter is required for tooth root failure.
This seems to be the determining gear failure, at least in the use of case carburised gears with geometries as determined in Attachment 6.2.1. The only exception are gears very small teeth numbers and small spiral angles.

Having established that tooth breakage is the determining criterium for the gear outer diameter on basis of this analytical exercise, it still remains to be established whether a static or a continuous loading is the decisive loading situation for gear dimensions. As has been shown in chapter 5.6.3, the average ratio between the continuous or equivalent torque and its maximum value for generalised rear axle gears load spectra in automotive applications can be described by the following expressions:

$$\frac{T_{eq}}{T_{max}} = 0.20 \div 0.25 \quad \textit{for International Transport} \qquad (6.10)$$

$$\frac{T_{eq}}{T_{max}} = 0.27 \div 0.33 \quad \textit{for National Transport} \qquad (6.11)$$

The ratio of the static allowable stress to the endurance limit for case carburised steels is about:

$$\frac{\sigma_{F_{cont}}}{\sigma_{F_{max}}} \geq 0.35 \qquad (6.12)$$

It is obvious that in the cases considered, the ratio for torques is always lower than the ratio for stresses. This would mean that for case carburised materials the gear outer diameter may considered to be mathematically determined by the failure mode of static tooth breakage of the pinion at the rear axle maximum output torque.

The values of the gear geometry data on which equations 6.4 to 6.9 are based, are extremes for the minimum-maximum analysis. If several gear geometry variables are limited to those values that are more likely encountered in automotive industry, than equation 6.8 will yield a smaller variation:

$$d_{e2}=(12 \div 14)*T_{2_{max}}^{1/3} \qquad (6.13)$$

The lower values of the constants are for hypoid gears; the larger ones are for bevel gears. Here, the maximum gear outerdiameter of a bevel or hypoid gear set is directly determined by the value of the maximum gear output torque.

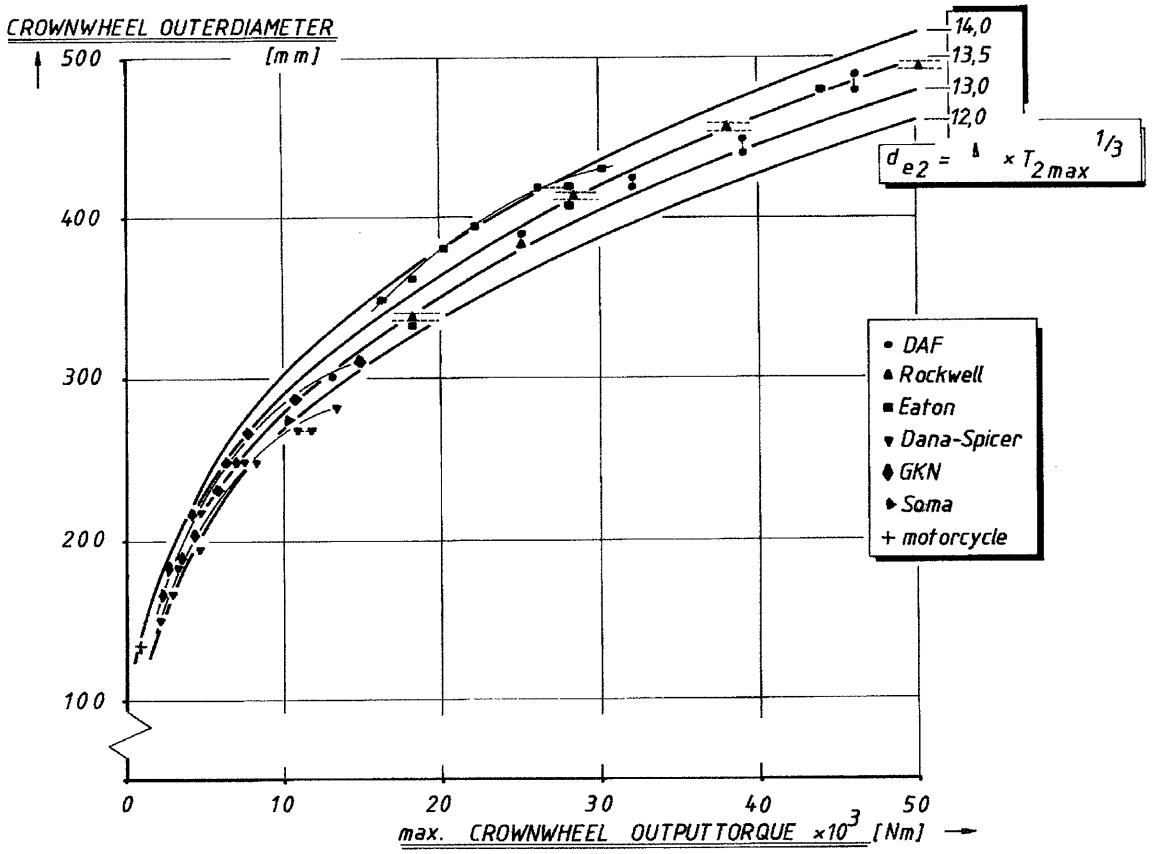

Fig. 6.1 Gear Outer Diameter and Maximum Output Torque for Rear Axle Gears

Fig. 6.1 shows the relationship that **CAN** be drawn between gear outer diameter and maximum gear output torque for several axles. The dimensions of the gears range from about 130 mm to 500 mm, which is a variation of about 1:4. It is valid for vehicles, equipped with single driven rear axles. This graph is based on data that can be derived from information leaflets of several rear axle manufacturers [6.2] and cover the period 1990-1995. As can be seen, almost all data lie well between the theoretical established relationship between gear outerdiameter and maximum gear output torque. Therefore it may be concluded that this theoretical relationship may be considered as reliable and representative.

Most of the rear axle data refer to the vehicle weight, indicated by Gross Combination Weight GCM or Gross Vehicle Weight GVM. In that situation a translation has been made from GCM/GVM to maximum output torque. It appeared that is was possible to derive the following relationship between maximum output torque and vehicle weight:

$$T_{2_{max}} = \Gamma * GCW/GVW \qquad (6.14)$$

This implies that the maximum output torque for a solo rear axle, that is required to determine its gear outer diameter, **CAN** directly be related to the vehicle mass. For trucks, the value of this coefficient is about unity; in other words for each tonne vehicle weight 1 kNm of output torque is required at the wheels. For hubreduction axles, the wheel torque needs to be divided by the ratio of the hub reduction, in order to obtain the gear torque. Note that the influence of wheelspin is not included here. For busses and coaches, the value of Gamma is about 0.85. For small commercial vehicles and vans, the value of Gamma lies between 1.10 and 1.35. Fig. 6.2 gives a representation of this relationship.

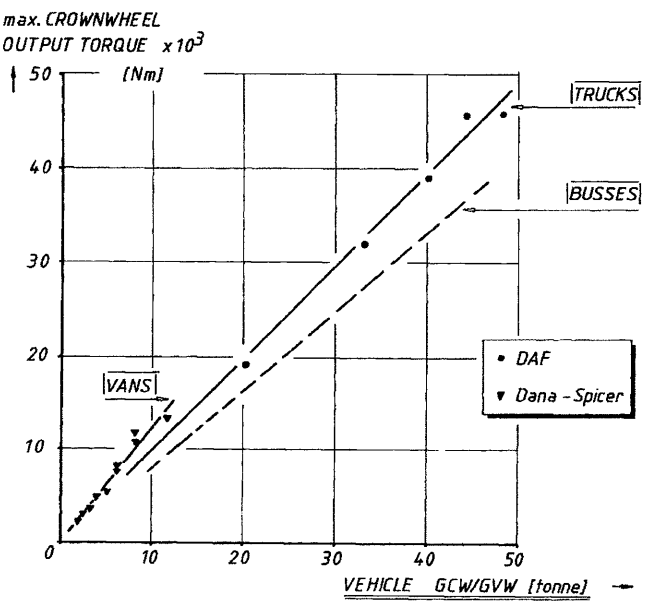

Fig. 6.2 Relation between Gear Output Torque and Vehicle Weight

In general terms, this comes down to a rear axle output torque for driving a vehicle upgrade on a slope of 15%. Then a calculated safety factor of 2.0 to 2.5 for static breakage of the gear teeth will prevail in this situation. No influence is required here on the vehicle application, the required endurance life as well as the reliability and it's failure probability. These factors, of course will have to be taken into account by fatigue calculations at the final design for Proto Release. The relationship introduced here is only based on general data; therefore it only represents a general view. Aspects as axle standardisation and use of one and the same driving head for different vehicle types, may cause individual designs to deviate from this relationship.
It is **NOT** concluded that all gear diameters **ARE** designed on this base, but it is striking that this simple relationship **CAN** be drawn for such a wide variety of gear dimensions and rear axle manufacturers and vehicle applications.

6.2.2 Comparison with Existing Design Guidelines

In order to verify this striking simple relationship between gear outer diameter and maximum output torque for a large variety of dimensions, a comparison may be required with existing design rules. In order to make sure that a reference still exists with actual practice, the general guidelines, as used by two well known companies in the manufacture of automotive bevel and hypoid gears, will be compared.

Gleason

Several design directives published by this company for the preliminary design of automotive vehicle rear axle gears [6.3] to [6.6] give a graphical representation between gear outer diameter and an endurance torque. From the graphs where tooth root breakage is involved, the following mathematical relationships can be established.
For bevel gears:

$$d_{e2}=(19.0\div 21.5)*T_{2_{cont}}{}^{1/3} \qquad (6.15)$$

For hypoid gears:

$$d_{e2}=(18.0\div 19.0)*T_{2_{cont}}{}^{1/3} \qquad (6.16)$$

Here, the relation between gear diameter and torque is based on a continuous torque or a gear performance torque, where it seems that endurance loading may be determining the failure rather than an overloading only occurring once. This gear performance torque is based on a so called performance ratio for vehicles [6.4]. It is dependent on the vehicle gradeability and the road type.

When the recommended values of this guideline for domestic or foreign highway and city or inter urban busses are used, it is possible to give an expression for this required performance torque as a function of the vehicle GCW. The continuous torque may be rewritten into a maximum torque, which leads to:

$$T_{2_{cont}}=(0.20\div 0.60)*T_{2_{max}} \qquad (6.17)$$

As can be seen, this leads to a variation by a factor 2.5 to 3.0 for the gear performance torque within every vehicle application. This variation is too large for a good comparison with the equations that have been derived. It is only used as a guideline for first order determination of the gear outer diameter.

As has been shown in chapter 5.5, ratio between the maximum and the continuous or equivalent torque can be establish, based on a general pattern of loading cycles for automotive applications and a constant slope of the SN-curve for the gear material.
This relation is:

$$T_{2_{equivalent}}=T_{2_{cont}}=(0.20-0.25-0.30)*T_{2_{max}} \qquad (6.18)$$

If the mean value, namely 0.25 is substituted in expressions 6.15 and 6.16, these equations can be rearranged in the following manner:

For bevel gears:

$$d_{e2}=(12.0-13.5)*T_{2_{max}}^{1/3} \quad (6.19)$$

For hypoid gears:

$$d_{e2}=(11.0\div12.0)*T_{2_{max}}^{1/3} \quad (6.20)$$

Oerlikon

Here, also several diagrams are given that are intended specifically for vehicle applications and may only serve as guidelines for a preliminary design [6.7] . If gear teeth numbers of about 40 are assumed, which is normally the case for automotive applications, the following relationships can be determined from these diagrams. For bevel gears in commercial vehicles, based on a torque that is representative for required gradeability:

$$d_{e2}=(20\div25)*T_{2_{cont}}^{1/3} \quad (6.21)$$

Hypoid gears for passenger cars, based on the same continuous output torque, yield:

$$d_{e2}=(18\div20)*T_{2_{cont}}^{1/3} \quad (6.22)$$

If the same value for the ratio of continuous to maximum torque, 0.25, is substituted in both equations according to Oerlikon, then they become:
For bevel gears:

$$d_{e2}=(12.5\div13.5)*T_{2_{max}}^{1/3} \quad (6.23)$$

and for hypoid gears:

$$d_{e2}=(11.5\div12.5)*T_{2_{max}}^{1/3} \quad (6.24)$$

It becomes obvious that there is a good agreement between both design guidelines and the theoretical estimated relationship between gear outer diameter and output torque. Furthermore, it can be seen that there is hardly any difference in gear dimensions, when they are designed according to the considered guidelines. This is an indication that the derived relationship can be considered as a fair accurate and a practical way of determining the gear outer diameter for solo rear axle gears.
In general there is a difference between hypoid and spiral bevel gears. For a given loading, the gear outer diameter for bevel gears is about 10-15% larger than for hypoid gears, if the same loadability is assumed. For a given dimension, hypoid gears would have a 12% higher torque capability than spiral bevel gears. The difference in torque capacity between Gleason and Oerlikon guidelines may be considered to be minimal. If also the variation for safety factors and definition of output torque is taken into consideration, one may state that both type of gears will have comparable loadability. This is of course valid for gears with identical gear quality, heat treatment, material and geometry. The guidelines of Klingelnberg are not used in this comparison, since these are not directly comparable to the same standard as the others do.

6.3 Scale Laws in General

For rear axle gears, a relationship has been established between the outer diameter and the vehicle mass. The question may rise whether this can be considered as a unique situation or that more and comparable relationships do exist where the independent variable is output torque? In order to answer this question, further similarities will be investigated on other gear drives.

6.3.1 Scale Laws for Gear Drives

For gear drives with spur or helical gears, the most characteristic dimension is the centre distance, that is determined by the gear ratio and the diameter of the largest gear. Jaskiewicsz [6.1] has shown that a typical relationship can be drawn between centre distance and maximum attainable output torque for a range of Eastern European automotive gear boxes. In practical applications, one may expect a certain variation on a theoretical derived relationship. Normally, the choice of the value of centre distance will also depend on manufacturing or casting restraints or even vehicle related packaging requirements.
In order to cover a wider field of applications, a survey has been made on several general catalogues of gear-drive manufacturers. These are considered as being representative for transmissions for automotive, marine and general industrial applications [6.9] and [6.10].
They consist of gear drives for:
* Automotive applications: gearboxes for passenger cars, medium and heavy road transport.
* Marine applications: gear drives for sea going vessels and river vessels.
* Industrial applications: highspeed gear drives and standard industrial drives.
When an extensive analysis is performed on the data, extracted from those catalogues, the following relations can be drawn between the centre distance and the maximum output torque for some typical gear drives [6.8].
Gear boxes for commercial vehicles / road transport:

$$a = (4.5 \div 7.5) * T_2^{1/3} \qquad (6.25)$$

Gear boxes for passenger cars:

$$a = (8.0 \div 9.0) * T_2^{1/3} \qquad (6.26)$$

Industrial high speed gear drives:

$$a = (9.0 \div 10.5) * T_2^{1/3} \qquad (6.27)$$

Industrial heavy duty:

$$a = (12.0 \div 13.0) * T_2^{1/3} \qquad (6.28)$$

Gear drives for sea going vessels

$$a = (14.0 \div 15.0) * T_2^{1/3} \qquad (6.29)$$

Gear drives for river vessels:

$$a = (17.0 \div 18.0) * T_2^{1/3} \qquad (6.30)$$

These relations have been derived from representative manufacturer catalogues that cover the period of 1985 to 1993 [6.10]. These equations may however only be seen as generalised indications for dimensions; they are comparable with the expressions of the preceeding chapters (fig. 6.3). Despite these facts, some differences may however occur in the definitions for the values of the maximum or the nominal output torque.

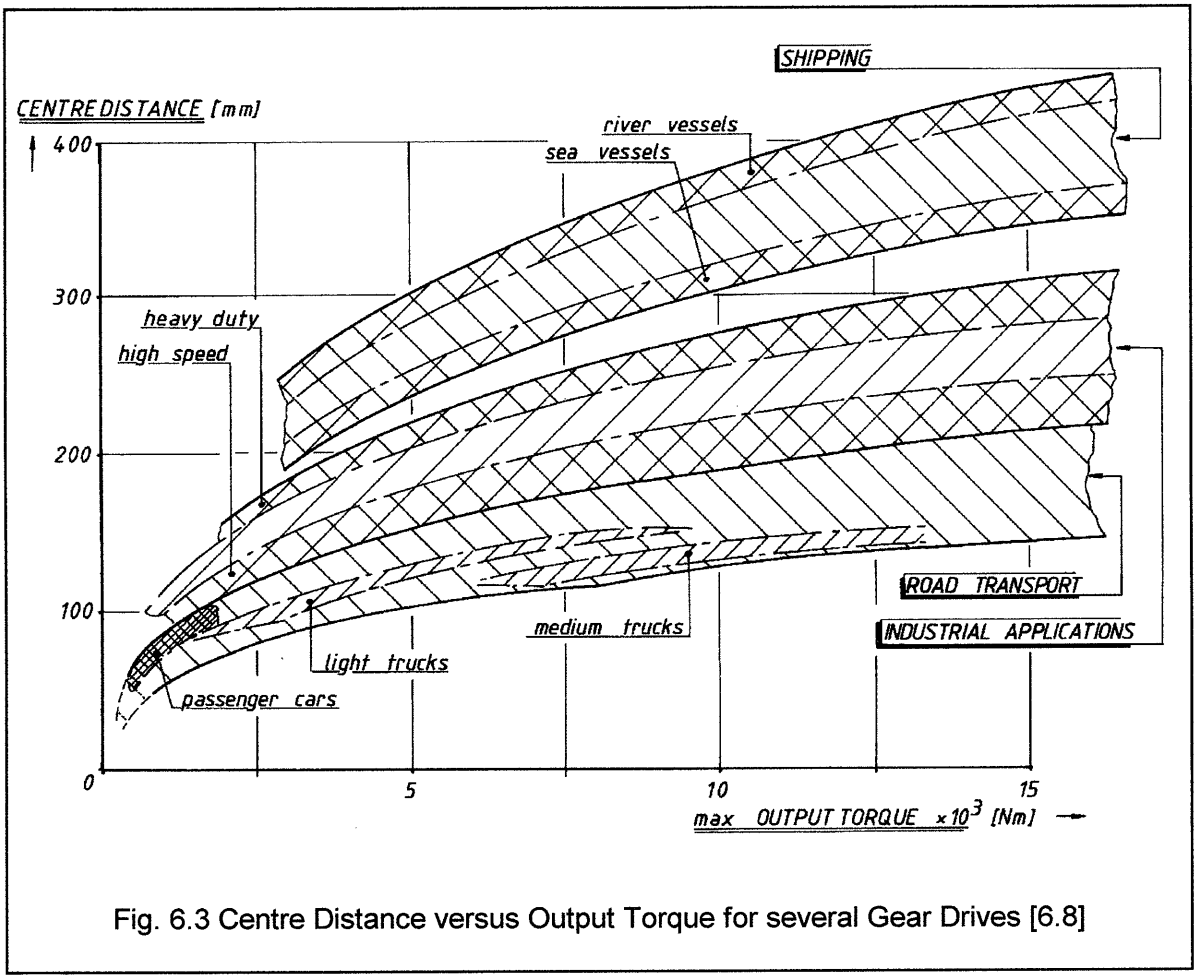

Fig. 6.3 Centre Distance versus Output Torque for several Gear Drives [6.8]

They are only valid for one-stage gear drives with a ratio of about i=2. For vehicle gearboxes, the ratio of the so called "Konstante" of the intermediate shaft is about 2.5 to 3.5. Not only the values of the constants in the above equations, but also the differences in the several regions of the gear drives in fig. 6.4 indicate a relatively large variation in power density. Gear transmissions for road transport in general have the highest power density. Because weight is an important phenomenon in this application, extensive testing renders the possibilities of reaching the design limits. Industrial gear drives, however do not have the same strict needs for weight; here service and safety factors will be largely greater. Gear drives for ships will have to meet the regulations of several classification companys such as Lloyds Register of Shipping, Det Norske Veritas etc.

The following theoretical and general relationship can be derived for all just investigated gear drives between centre distance and output torque:

$$a = (5.0 \div 18.0) * T_2^{1/3} \qquad (6.31)$$

In this case the determining failure mode is tooth breakage for static loading of case hardened gear steel. The range in the value of the constants is achieved by a minimum/maximum analysis. All these values are related to practical data, and it is striking to see that it covers almost completely the entire range of gear boxes that are considered here. For reasons of comparison, a relation between the output torque and the large gear diameter is required. Therefore the expressions (6.25) to (6.30) will have to be rewritten. This is done by deriving the diameter of the largest gear from the centre distance and the gear ratio. In this way a relation is obtained similar to the expressions for bevel and hypoid gears in the previous chapter.

Gear boxes for commercial vehicles / road transport:

$$d_2=(6.5\div11.5)*T_2^{1/3} \tag{6.32}$$

Gear boxes for passenger cars:

$$d_2=(12\div13)*T_2^{1/3} \tag{6.33}$$

Industrial high speed gear drives:

$$d_2=(13.5\div15.0)*T_2^{1/3} \tag{6.34}$$

Industrial heavy duty:

$$d_2=(16\div17.5)*T_2^{1/3} \tag{6.35}$$

Gear drives for sea going vessels

$$d_2=(18\div20)*T_2^{1/3} \tag{6.36}$$

Gear drives for river vessels:

$$d_2=(22\div24)*T_2^{1/3} \tag{6.37}$$

Planetary gear drives (last stage) for industrial applications:

$$d_2=(13\div14)*T_2^{1/3} \tag{6.38}$$

6.3.2 Scale Laws for Mechanical Components

Similar to these gear drives, the survey has been extended to several mechanical components that are used for power transmitting functions, such as couplings, shaft connections and low speed hydraulic motors. The relevant data have been obtained from company's leaflets on dimensions and allowable torques, that were published in a comparable period, of which the relations between torque and gear diameter for gear drives have been established [610]. The following equations have been derived.
Clutch plates for automotive couplings:

$$d=(40\div46)*T_2^{1/3} \tag{6.39}$$

Low speed hydraulic motors:

$$d=(20\div25)*T_2^{1/3} \tag{6.40}$$

Flexible couplings for industry:

$$d=(14\div21.5)*T_2^{1/3} \tag{6.41}$$

Geared couplings:

$$d=(9\div11)*T_2^{1/3} \tag{6.42}$$

Cardan couplings:

$$d=(6\div10)*T_2^{1/3} \tag{6.43}$$

Shaft-hub pressing connections:

$$d=(3\div4.5)*T_2^{1/3} \tag{6.44}$$

These relationships have been based on information from general brochures of several component manufacturers [6.12], in a similar way as has been done by the gear drives. It may well be possible that data of other manufacturers may differ from these expressions. This will then be a result of differences in the designation of the output torque and the maximum diameter [6.13] to [6.15]. The ratio of transmittable torque over the outer diameter gives an indication on the torque density of the components. This ratio is calculated for all here considered mechanical components, and given in fig.6.4, showing roughly a range of about 1000 in torque density.

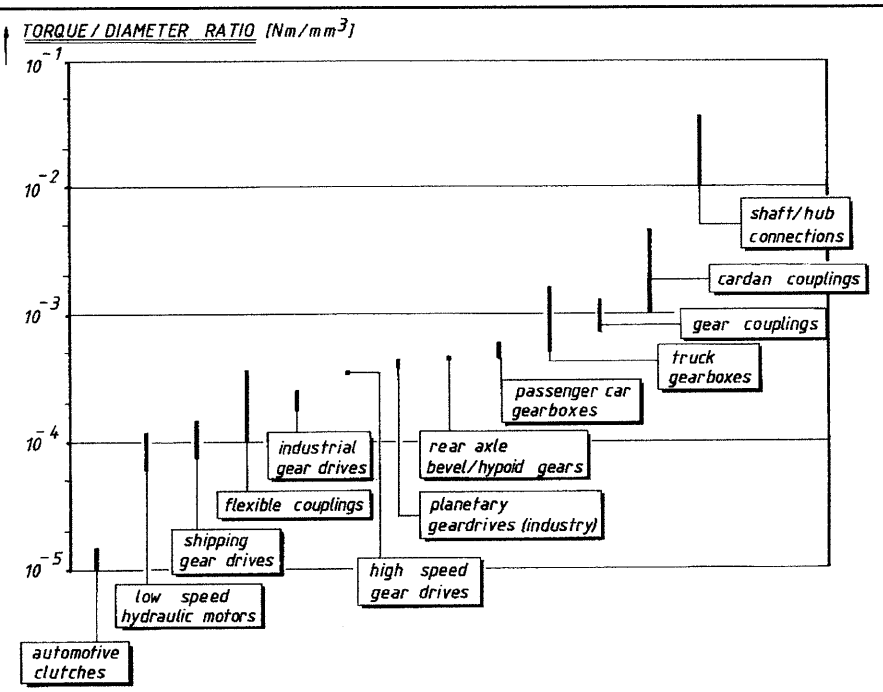

Fig. 6.4 Output Torque to Outer Diameter for several Transmission Components

6.3.3 Comparison between Nature and Mechanical Components

The most interesting way of considering the influence of scale, is to study animals or mechanical components being increased in size, while their shape or form in terms of dimensional ratio's remains unchanged. Then geometric similarity, or isometry is considered. In ranges of mechanical components, mostly this kind of isometry is realised. In Nature however, and more specific in the case of land going mammals, this kind of isometry is not assured. The large diversity of several kinds of animals with their specific forms and dimensions, makes it difficult to determine scale dependent relationships on basis of geometric similarity. Only to a very limited extent it would be possible to make an analysis on the influence of scale on several mechanical and thermodynamical aspects of animals.
In the past some research has been performed into the similarity of animals in general, and more specific into mammals. Some three hundred years ago Galileo investigated scale effects [6.16]. He found that Nature has two strategies for solving problems when the size of animals increase. A change in the geometrical proportions of the animal mostly means shorter and thicker bones, as well as stronger materials for the bones. As the latter has obviously strict limits, mostly the geometry will be changed when the size of animals is increased.

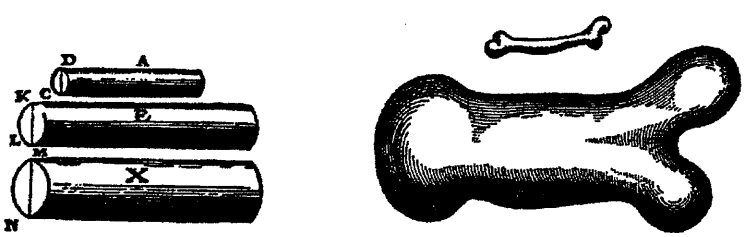

Fig. 6.5 Scale Effect on Bones as seen by Galileo [6.16]

Figure 6.5 shows two bones for a man, according to Galileo: one for the current dimension and one if that same person would be three times bigger than the current size. Generally allometry will be encountered in Nature; whereas isometry can be expected in technical components. For the best, a kind of isometry can be seen within a specific group of species. In the beginning of this century the work of D'Arcy Thompson titled "On growth and form" [6.17] appeared in which dimensional analysis and similarity criteria were introduced for general biology. Here, several scale effects are discussed for locomotion of animals, on land in the sea and in the air. Other investigations have shown several biological relations in terms of scale [6.18] to [6.22].
It appeared to be possible to mathematically describe different aspects of biological functions of several animal species. This so called allometric concept gives several life functions of animal species in the following form:

$$Y = c * M^{e} \qquad (6.45)$$

Here the body mass can be considered as the independent variable. The mass of mammals ranges from several grammes for insects to the impressive weight of several tonnes for the elephant. Fig.6.6 shows an example of an allometric expression [6.23], where the oxygen consumption is plotted against the body mass.
In [6.24] a very extended overview is given of many biological similarity functions. Out of these, two striking examples are taken that represent the most important cardio-vascular and respiratory

functions of land going mammals. The first group is the heart delivery in terms of blood volume per second and the heart power in gcm/min. The second group is the delivery of the lungs, being the amount of oxygen in ml/min and the required lung power. Equations (6.46) and (6.47) give the relationship of both groups with the body mass of animals. These expression only yield validity for landgoing mammals. Birds and fishes, as well as mammals in the sea, are excluded. One can very well see that the exponent of the bodymass M is less than unity and larger than 2/3. It appears as if this scale-influence is somewhere between the mass- and the surface determining influence. In this view, the cardio-vascular and the respiratory functions of animals are more related to the surface of the bones and/or the muscles. The pressure in the heart and in the lungs remains constant over a wide range of animal sizes.
For the heart delivery and the heart power:

$$Q_{heart}, P_{heart} = c_{a,b} * M^{0.73} \tag{6.46}$$

For the lung delivery and the lung power:

$$Q_{lung}, P_{lung} = c_{c,d} * M^{0.73} \tag{6.47}$$

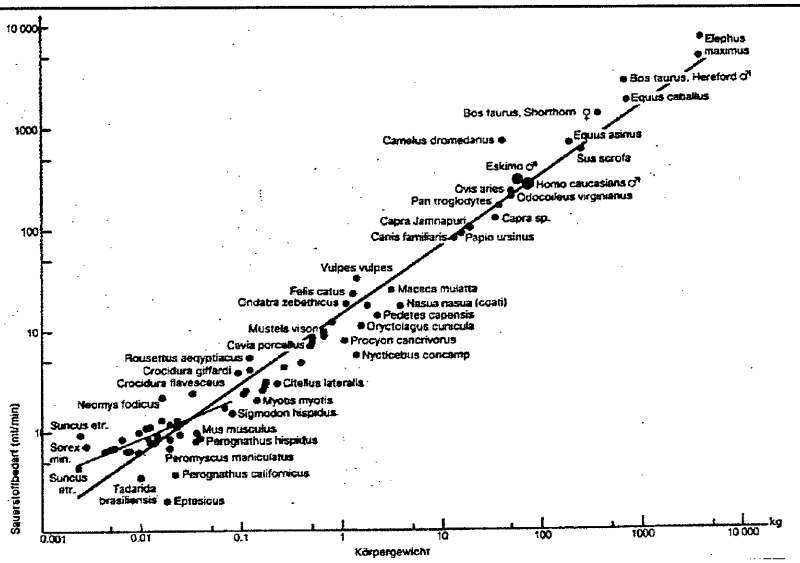

Fig. 6.6 Oxygen Consumption versus Animal Body Weight [6.20]

In Nature, however there is hardly any case of geometrical similarity, where the ratio of l/d of several important limbs remains constant over the size. Many mammals appear to maintain a constant compressive stress in their bones or a constant tensile stress in their muscles when increasing their size, by which the diamater of bones and muscles increases with the lenght $l^{2/3}$. Within one and the same group of animal species, some kind of geometrical similarity or isometry can be found. Here, the exponent of M has a value of 0.76 (=2/3). This means that the dimensions of bones and muscles can mainly be described as being directly related to the animal body mass. The stresses in bones and muscles appear to be constant and independent of the animal body mass. In some respect, this is comparable to the gear dimensions of truck rear axles in function of the vehicle mass. Here too, the stress in the gears is more or less constant, irrespective of the vehicle mass.

6.4 Basic Gear Geometry

Departing from a given vehicle application, the Functional Requirements for the rear axle gears can be established, as indicated in chapter 1. These functional rear axle gear requirements will be defined in terms of strength, noise, efficiency, weight and production costs. Together with the design features, a first order design lay-out of the rear axle gears may be generated by establishing the basic gear geometry. This basic gear geometry determines the general dimensions of the rear axle gears and the most important basic gear characteristics such as strength and noise production. The basic gear geometry can be determined by a limited number of data. They are also based on general design guidelines for rear axle gears.
The basic gear geometry principally consist of the following parameters:

* Gear system:	Gleason / Oerlikon / Klingelnberg.	
* Gear type:	Hypoid / Spiral Bevel.	
* Gear geometry:	Rear axle ratio	i
	Teeth numbers	z_2/z_1
	Gear outer diameter	d_{e2}
	Gear face width	b_2
	Gear spiral angle	β_{m2}
	Hypoid offset	a_k
	Cutter radius	r_c

To establish a reliable estimate on some of these lay-out determining rear axle gear specifications, no direct knowledge on allowable stresses and pinion loading spectra is required. Several dimensions are related to the gear outer diameter; a dimension that may be considered as important for rear axle gears as the centre distance is for spur and helical gears.

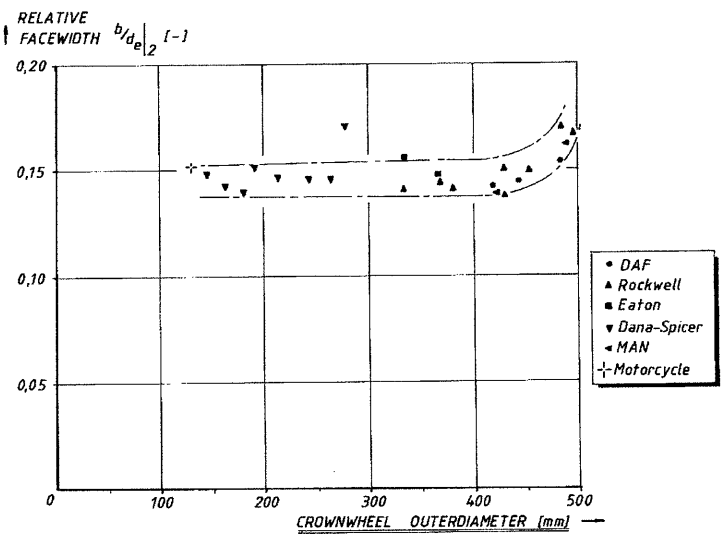

Fig. 6.7 Ratio of Facewidth to Gear Outer Diameter

First, the gear outer diameter can be established on basis of the vehicle GVW/GCW by using figure 6.1. The value for the offset may be chosen from figure 3.1, bearing in mind the relative reduction in pinion tooth root stress as indicated in that same chapter. The facewidth of the gear may be taken from figure 6.7; here the facewidth in relation to the gear outer diameter is given for some axles. As can be seen, this value is hardly independent of the gear outer diameter. In

general the maximum facewidth is limited by about 1/3 of the outer cone distance, resulting from manufacturing limitations depending on the gearing system.
The general qualification of the expected rear axle noise production generally is an important feature. For this, the profile and the face contact ratio of the gears will have to fulfill certain minimal requirements. It should be remembered that the noise generation of a gear set also is strongly influenced by it's manufacturing quality. This aspect is not taken into account here, as only geometrical requirements are to be achieved in the design phase. Figure 6.8 is a graphical representation of geometrical requirements for the profile and face contact ratio of the gear geometry, based on criteria of Gleason and Oerlikon for minimal noise requirements.
According to Gleason:

$$\sqrt{m_P^2+m_F^2} \geq 2.0 \qquad (6.48)$$

From Oerlikon directives, the following can be derived for an effective facewidth of 90%:

$$\epsilon_{v\alpha} + \epsilon_{v\gamma} * (\frac{b_{ef}}{b}) \geq 3.0 \qquad (6.49)$$

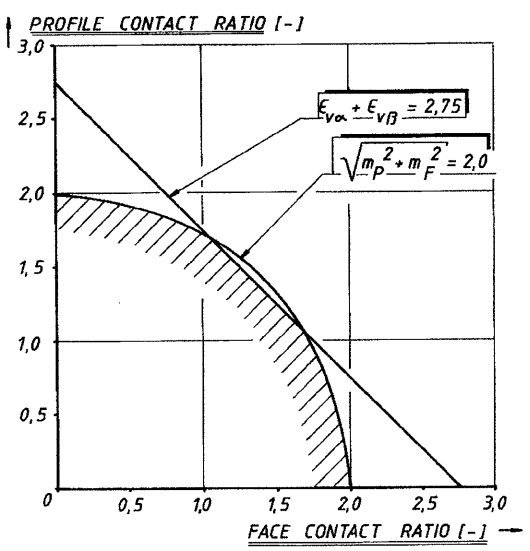

Fig. 6.8 Recommendations for Profile and Face Contact Ratio

In order to obtain a required face contact ratio, equation (6.50) may be used in which the face contact ratio is expressed as a function of the independent variables of the basic gear geometry.

$$\epsilon_{v\beta} = \frac{z_2}{\pi} * \frac{\frac{b_2}{d_{e2}}}{1-\frac{b_2}{d_{e2}}\sin\delta_2} * \frac{b_{ef}}{b} * \tan\beta_{m2} \qquad (6.50)$$

This expression for the face contact ratio as function of the mean spiral angle, the relative facewidth, the teeth number and the pitch angle of the gear, is represented in figure 6.9. The relative facewidth is taken to be 0.15, as this is the facewidth that is most likely to be expected (see figure 6.7). The gear teeth number varies between 40 and 45 teeth; the rear axle ratio varies from 3 to 5.6. These values cover most of the automotive rear axle gears for commenrcial vehicles.

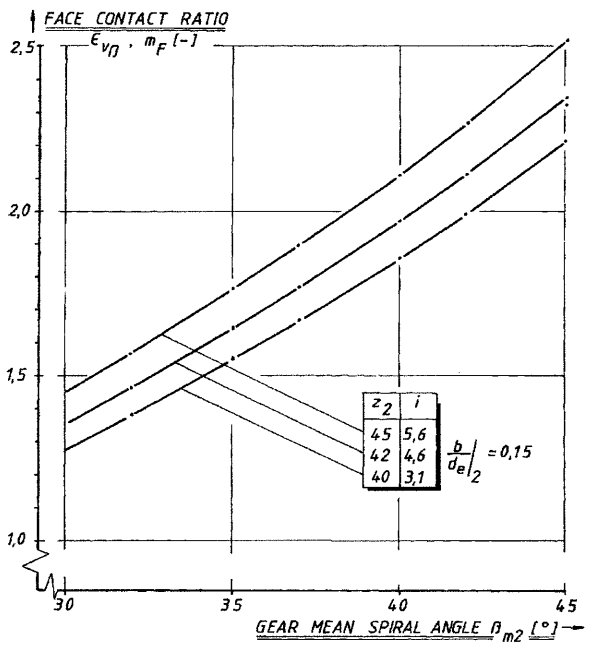

Fig. 6.9 Face Contact Ratio in function of Basic Gear geometry

Selection of the appropriate cutterhead diameter depends on the expected deflections and the required contact pattern sensitivity. Investigations have shown that a gear curvature in the middle of the facewidth, that is close to an involute spiral, generally gives the most favourable conditions for the contact pattern sensitivity. One has to bear in mind that for circular cut gears machined by the indexing method, the gear curvature is identical to the cutter head radius. For gears machined by the continous method, the gear curvature differs from the cutter head curvature. Fig.6.10 shows four different gear curvatures for a given cone distance and a mean gear spiral angle. These are approximations of a hyperbolic-, a logarithmic, an Euler- and an involute spiral. In order to achieve an involute, the following value for the cutter head radius should be chosen. According to Gleason:

$$r_c = (1.05 \div 1.25) * R_m * \sin\beta_{m2} \qquad (6.51)$$

According to Oerlikon:

$$r_c = 1.05 * R_m * \sin\beta_{m2} \qquad (6.52)$$

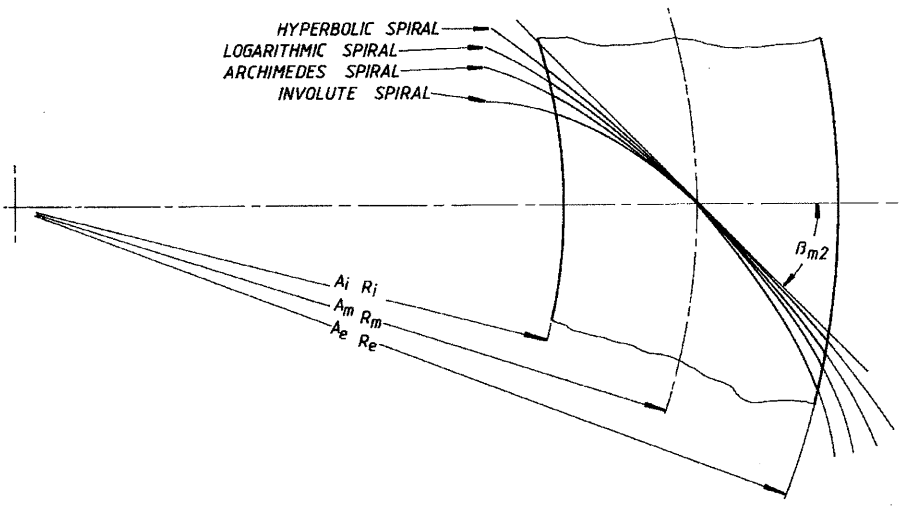

Fig. 6.10 Several Approximations of Gear Curvature

Most of the variables that describe the basic gear geometry, have restrictions in their minimum and maximum values. The maximum pinion spiral angle is limited because of maximum allowable bearing loads and deflections. The hypoid offset is limited because of restrictions in sliding speed, scoring risk and operating temperature. The minimum gear spiral angle is determined by a minimum required face contact ratio for noise requirements. This leaves only a limited region for the designer to vary basic gear geometry data, as indicated by figure 6.11.

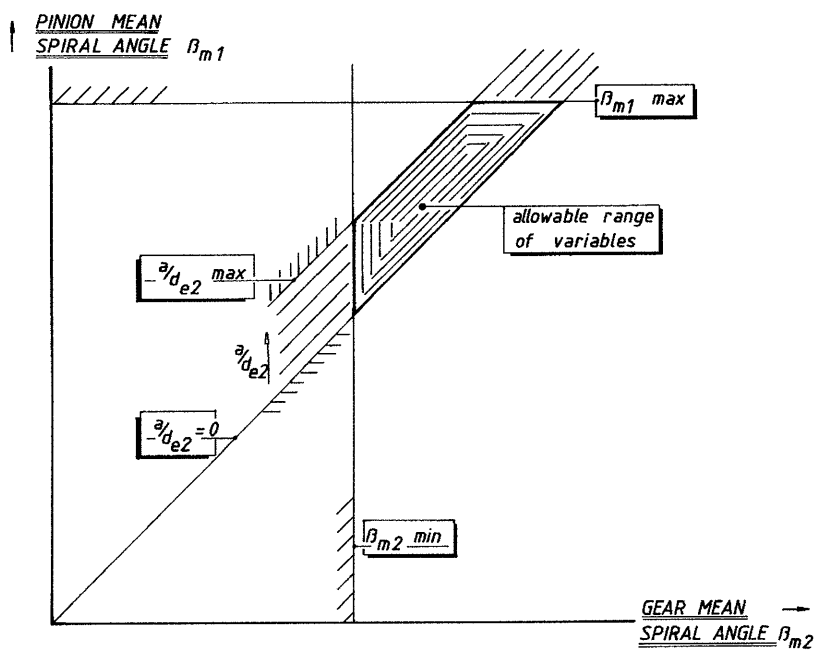

Fig. 6.11 Limits and Available Field for Variation of Basic Gear Geometry

6.5 Additional Gear Geometry

In order to determine the definite gear geometry, additional gear geometry data will have to be established. This additional gear geometry consists of:

* addendum and dedendum height
* profile shift and tooth thickness factor
* pressure angle
* blade edge radius
* profile corrections, such as Protuberance or TopRem
* lengthwise and profile crowning.

The numerical values that are more commonly used for automotive rear axle gears and thus will most probably be encountered, are summarised in figure 6.12. Here, the numerical values of several geometry variables are given, next to some other data, relative to the mean normal modulus.
The range of these values is purely to be considered as a guideline; some geometry variables may differ from the values that are indicated here. On several occasions, company's intern standardisation on tooling and manufacturing facilities may prescribe some practical values that also may deviate from the values given here.

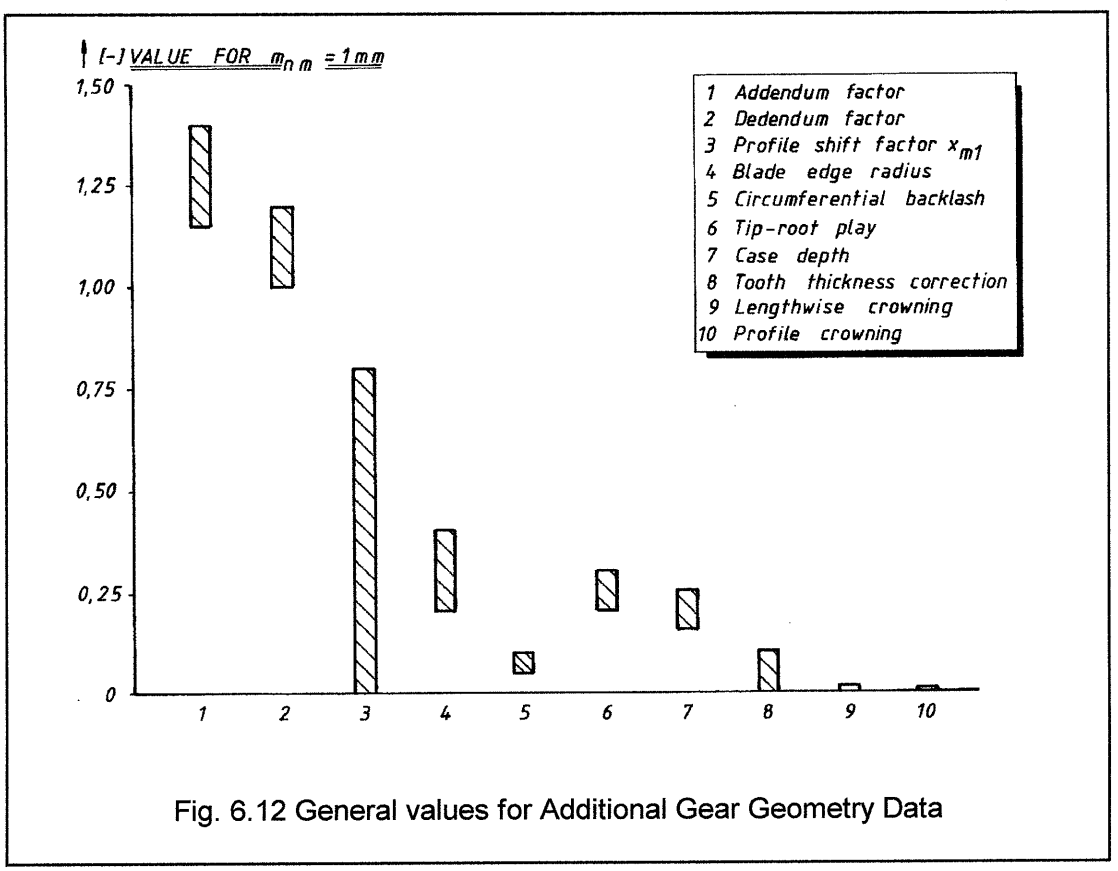

Fig. 6.12 General values for Additional Gear Geometry Data

The rear axle gear stresses that are to be aimed for, depend on the vehicle application. The most important features here are the expected vehicle travelling distance and the type of driveline loading spectrum. The latter is expressed in the expected equivalent torque. Figure 6.13 gives an indication of the general values that are to be expected for transport vehicles, as a function of the vehicle weight.

The severeness of the loading spectrum is expressed by the value of the equivalent torque. Based on the expressions of chapter 5, they can vary between 0.22 and 0.30. Although the values are only to be seen as indications; they can be considered as fairly representative values. As can be seen is the value for the equivalent torque higher for vehicles with smaller weight. These vehicles generally will have a more severe driveline loading spectrum than vehicles with a large weight. This severeness of the spectrum relates to the maximum torque and is not to be seen as an absolute value. Also low weight vehicles will travel by far a shorter technical distance than vehicles with a high weight. In this view, the numerical value for the calculated tooth root stress at the design stage of these gears will have a more or less constant value over the entire range of the vehicle weight.

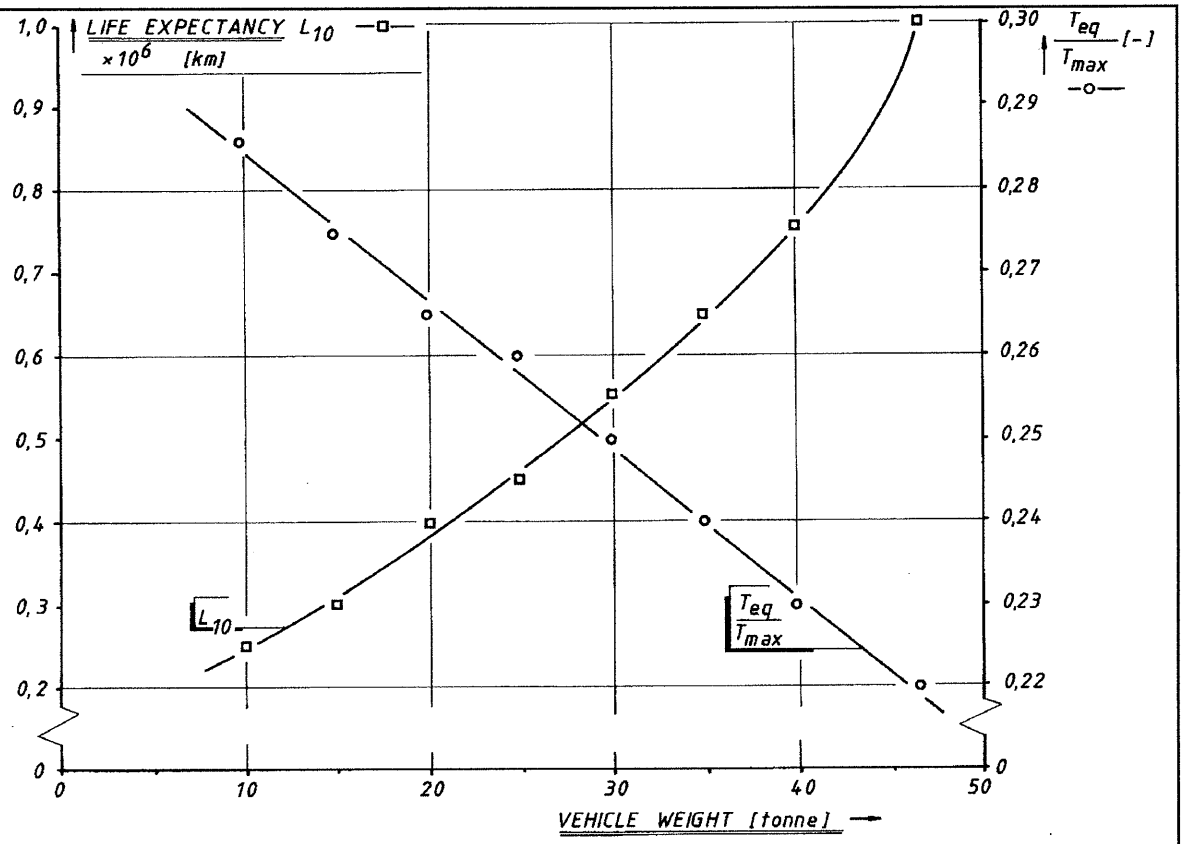

Fig. 6.13 Vehicle Travelling Distance and Indication for Equivalent Torque

An interesting remark can be made however at this point.
A clear relationship between crownwheel outer diameter and maximum output torque has been established for a relatively large range from about 100 mm to 500 mm gear outer diameter. Next to this, the gear facewidth over the same diameter range also lies within a restricted bandwidth. The results of the Constant Amplitude and Variable Amplitude Loading tests only have been established for a restricted range of 410 mm to 485 mm crownwheel outer diameter.
Because of the functional and geometrical relationships that have been established separately, it may be stated that therefore the experimental findings may be extrapolated down to diameters of 100 mm. The restrictions are of course that the driving head casing layout, driving head casing material, bearing type and arrangement as well as gear material and geometry are comparable to the rear axle gears that have been tested here.

6.6 Equal Life versus Equal Stress

In order to change the rear axle gear design in terms of required tooth root stress level for pinion and gear, the profile shift factor x_{m1} is not applied here in the same way as it is for helical gears. In many cases, it's value is restricted for hypoid and bevel gears by the following criteria:

* preventing undercut at toe side for small pinion teeth number
* limiting pinion tooth tip thickness on toe side
* optimal sliding for good lapping characteristics
* maximum allowable relative sliding for scoring.

To modify the pinion and gear root stress level on hypoid and bevel gears to a required level, the tooth thickness correction factor is therefore applied. This additional geometry variable is used for designing the pinion and gear in such a way, that either an equal stress or an equal life can be achieved for both the pinion and the gear.

For relatively low loaded gears with a high safety factor and a high endurance life requirement, such as industrial applications, it is common to design both mating members such that equal tooth root stresses prevail. If however the gears are relatively high loaded, as is the case in most automotive applications, then it is common practice to design both members to equal life. During a given lifetime or a vehicle distance, the pinion obtains a higher number of loading cycles than the gear, depending on the axle ratio. When for both members an equal endurance life in terms of travelling distance is required, the pinion tooth root stress needs to have a smaller value than on the gear. This is achieved by modifying the tooth thickness of both members. Then a maximum life for the entire gearset will be assured. In order to design rear axle gears for equal life, it is necessary to obtain a certain ratio for the tooth root stress of the pinion to the gear.

The teeth of the pinion generally obtain a positive thickness correction, so as to reduce the pinion tooth root stress. In order to maintain the same circumferential backlash, the teeth on the gear will obtain a tooth thickness decrease of the same value, hereby increasing the root stress of the gear. This implies that the sum of both tooth thickness changes needs to be zero. This can be done without harnessing the other geometric parameters of the gears that have already been established. The manufacturing method allows very easily a small change in the position of the cutter blades on the cutter head, for both the pinion and the gear.

It can be established that for equal life in terms of distance for the pinion and the gear at a constant amplitude loading, the required ratio for the root stresses can be described as:

$$\frac{\sigma_{F2}}{\sigma_{F1}} = (i)^{\frac{1}{k}} \qquad (6.53)$$

This equation is valid when the stress level for this Constant Amplitude loading is higher than the endurance limit for both members. Both members are assumed to be manufactured from the same material with identical fatigue characteristics. The parameter k is the slope of the SN curve in the limited life region. Next to the gear ratio, this material value is the only parameter that determines the amount of required difference between the tooth root stress for the gear and for the pinion when they are to be designed to equal life.

If the stress level is lower than the endurance limit and a Haibach-Gatts modification for the SN curve is assumed here, the equation should be rewritten into:

$$\frac{\sigma_{F2}}{\sigma_{F1}} = (i)^{\frac{1}{2k-1}} \qquad (6.54)$$

This shows that the stress ratio of gear to pinion only depends on the gear ratio and the slope of the SN-curve of the gear material. Depending on the prevailing stress level at a constant amplitude loading, the value for the exponent may differ. These expressions are only appropriate for a Constant Amplitude loading of the gears. Depending on the stress level, being lower or higher than the endurance limit, a different value for the slope of the SN curve is to be used. For a Variable Amplitude loading, the form of the load spectrum with regard to the endurance limit will influence the result. Mostly a part of the load spectrum contains loads that are higher than the endurance limit and a part that is lower.

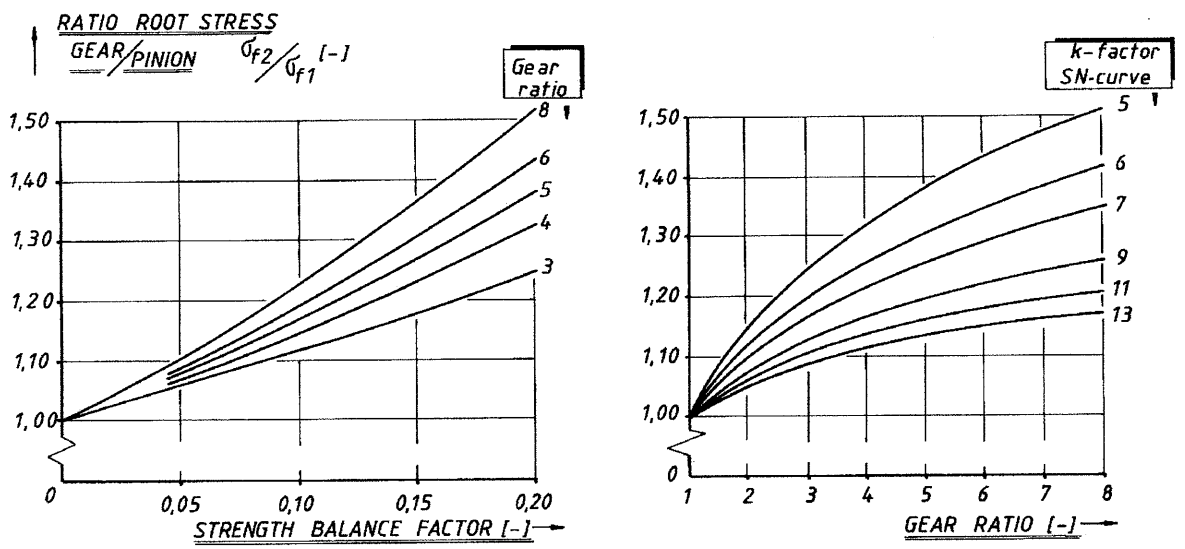

Fig. 6.14 Required Stress Ratio for Equal Life acc. to Gleason and Oerlikon Guidelines

Equations for equal life according to Gleason and Oerlikon are represented in fig. 6.14.
In the right part of this figure, the equation according to Oerlikon is drawn. Here the gear ratio is taken to be the independent variable; the k-factor or the value for the slope of the SN-curve is the parameter here. The upper three lines are according to equation (6.53) with values for the slope of the SN curve k = 5, 6, and 7. Note that the value of k = 5 for the region of limited life is conform to the design guidelines of Oerlikon. The lines according to equation 6.54, the region of semi infinite life according to the Haibach-Gatts modification are also shown here by the values of k = 9, 11 and 13.
In the left part of figure 6.14. the equation (6.55) for the stress ratio gear to pinion according to the Gleason Design Guidelines is graphically represented. Here the strength balance factor

according to Gleason is the independent variable; the gear ratio now is the parameter.
Gleason uses a strength balance factor for designing gears with equal life [2.6-2.8]. This strength balance factor may obtain three different values for the following design situations:

* equal stress: strength balance factor = 0.0
* equal life: strength balance factor = 0.18
* compromise: strength balance factor = 0.09 - 0.11.

It appears that the strength balance factor for equal life can be approximated by the reciprocal value of the SN-curve for a 10% failure probability, which is 5.86 according to Gleason [2.8]. The reciprocal value for the strength balance factor that is used for the compromise situation, is about 10.5. This coincides very well with the slope in the semi infinite life region of the SN curve, when a Haibach-Gatts modification is assumed. The value for the slope of the HG modification is 2k-1. Therefore it seems that the compromise is applicable to Variable Amplitude loading where the load spectrum is situated lower than the endurance limit for the material.

The expression for the stress ratio of gear to pinion for equal life, in terms of the stress balance factor according to Gleason may be expressed as follows:

$$\frac{\sigma_{F2}}{\sigma_{F1}} = (i)^{str.bal.fact.} \qquad (6.55)$$

It can clearly be seen that for a larger value of the rear axle gear ratio, a larger stress ratio is required for gear and pinion root root stress, when designing for equal life. A required stress ratio between gear and pinion may not always be assured in practical situations. Sometimes manufacturing restraints set limits to the maximum attainable stress ratio, for instance because of limited point width.

It has been shown that basically the equations for the required stress ratio gear to pinion for equal life, as used by Oerlikon and Gleason are very much comparable. This does not imply however that for a given rear axle ratio, the required tooth thickness corrections accoding to Gleason or Oerlikon will be identical. In fact they may differ very significantly, due to three reasons.
In the first place, the difference in the assumed slope of the SN curve for the material will lead to different values for the required stress ratio gear to pinion. Secondly, the change in tooth root stress resulting from a tooth thickness correction will differ, when calculated according to different standards. In the third place, the ratio of gear to pinion stress at zero thickness correction also determines the required amount of thickness correction.

In the Oerlikon calculations, a value of k=5 for the limited life region is used; the Gleason method indicates a value of k=5.56 to 5.88 for the same region of limited life. This means that for constant amplitude loading, a difference of 5% for the required stress ratio gear to pinion will exist between both methods. For the compromise in the Gleason method, a value of 9 to 11 for the slope between appears to be applied. This would mean that for this situation the required stress ratio according to Oerlikon will be 20-25% higher than the ratio according to Gleason.

The tooth form factors according to the different calculation standards show a different influence of tooth thickness on tooth root stress. The bending stress component is directly proportional to the square of the tooth thickness $(S_F)^2$. The compressive and the shear stress components are however directly proportional to the tooth thickness, therefore $(S_F)^1$.

All standards have different ways of adding stress components for the Tooth Form Factor. Therefore they all have different sensitivities to the influence of the thickness correction. The tooth form factor according to DIN will be directly proportional to (thickness correction)^2. As in the ANSI/AGMA and Gleason standards also the compressive stress is taken into account, the influence of tooth thickness correction on stress will be more pronounced here. The influence of tooth thickness correction, calculated according to Oerlikon will be comparable with the latter. For the stress ratio of gear to pinion at zero tooth thickness correction, three different situations may exist. Both stresses may be equal, the pinion stress may be larger than the gear stress or it may be lower. For these three situations, fig. 6.15 shows the differences in required thickness correction in order to attain a certain stress-ratio. When at zero tooth thickness correction, the pinion stress is larger than the gear, a larger correction is required according to ANSI/AGMA and Gleason to obtain equal life than calculated according to Oerlikon.

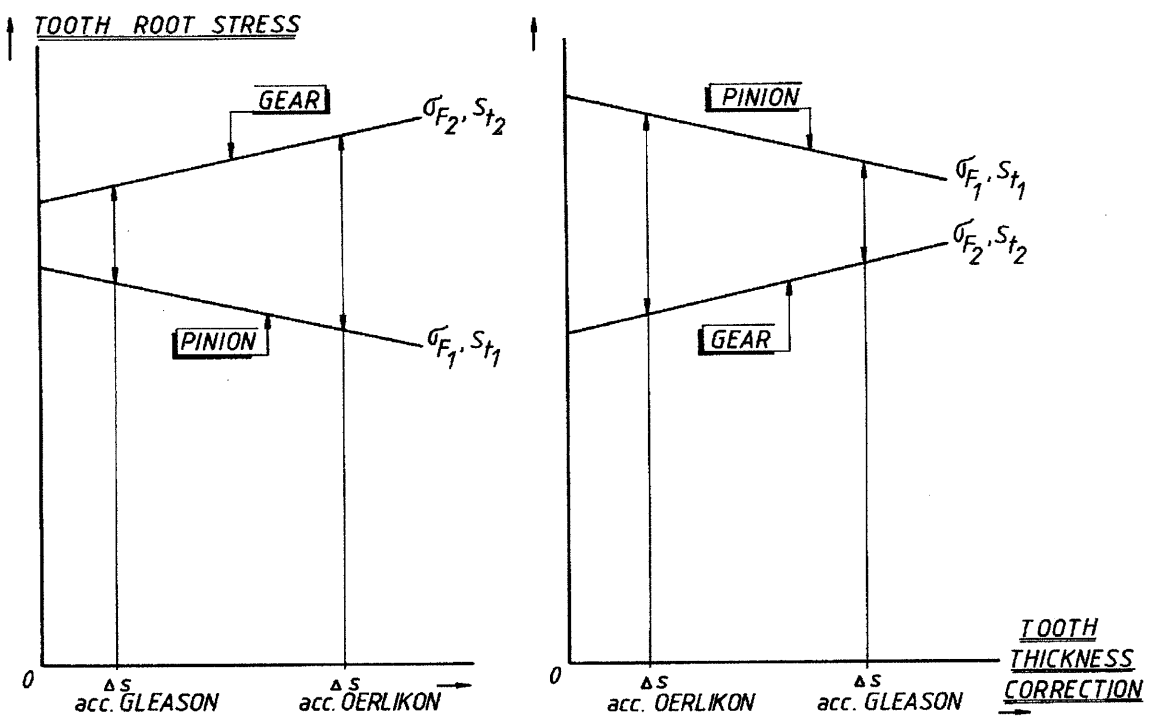

Fig. 6.15 Required Tooth Thickness Correction for Two Situations

When the pinion stress is equal or lower than the gear root stress, a smaller thickness correction is required according to Gleason. As mostly a higher stress for the pinion teeth than for the gear teeth occur at zero thickness correction, the required tooth thickness correction according to Gleason will be much higher than calculated according to Gleason, when equal life is required. In general one may assume that a set with equal life, calculated according to Gleason will require a by far larger thickness correction than calculated according to Oerlikon. In other words, Oerlikon designed sets for equal life may appear to be equal stress when calculated according to Gleason. This however strongly depends on the situation at zero thickness correction. This is a major point of interest to be taken into account when designing gears from one system to another.

6.7 Resumee

On a theoretical base, the following relationship between gear outer diameter and the maximum gear output torque for single reduction rear axles has been derived:

$$d_{e2}=(12 \div 14)*T_{2_{max}}^{1/3} \qquad (6.13)$$

This comes down to a loading situation of a vehicle driving uphill on a 15% grade. The safety factor is about 2.0 to 2.5 for static breakage of case carburised rear axle gear teeth.
This equation is valid for automotive rear axle gears of which the gear outer diameter ranges from 100 mm to 500 mm.
This equation gives a good correlation with other design directives for gear diameters, such as Gleason and Oerlikon. The differences between the design guidelines of Gleason and Oerlikon are very small. Both guidelines indicate a difference in loadability between spiral bevel and hypoid gears.

The investigation results that have been established in this thesis from test results on actual rear axles for gear outer diameters from 410 mm to 485 mm, can therefore be extrapolated to gear outer diameters of down to about 150 mm with a relative low error risk. In other words, for rear axle gears of vehicles with Gross Vehicle Weight down to 5 tonne. This is of course only valid under the premisses that the basic design of the driving head casing, gearing material and heat treatment, differential versions, bearing layout and bearing types are comparable.

For the maximum gear output torque and vehicle GVW/GCW, a linear relation may be assumed. For trucks each tonne of vehicle weight would require 1 kNm output torque.

$$T_{2_{max}} = \Gamma * GCM \qquad (6.14)$$

Both typical and very simple relationships (6.13) and (6.14) can be used for preliminary design of the rear axle gears, when only the vehicle GCW/GVW is known.
It is not concluded that all rear axle gears **ARE** desinged according to this basic relationship, but it is important is to know that rear axle gears **CAN** be dimensioned according to this simple rule. This would imply that the aspect of tooth breakage for maximum static torque can be considered to be the most determining element for preliminary design of the gear outerdiameter on case hardened rear axle gears for vehicle applications.

It has also been shown that for most other gear drives, used in different applications, a similar relationschip between a representative diameter and maximum output torque can be established. For single stage gear drives, the centre distance and output torque have mathematically a similar relationship. For most mechanical power transmitting components, the output torque can be considered as the dominant value for determining the characteristic dimensions.

In Nature, a corresponding situation may well exist. Here, the weight of land going mammals appears to be the governing variable for some important life functions and dimensioning functions such as bone thickness. For rear axle gears of commercial vehicles, the vehicle weight mostly determines the gear outer diameter.

In this way, Nature and Technique have a similar way, by keeping a maximum allowable stress constant over a range of dimensions. Hardly any difference appears to exist, whether the breakage strength of gears or the compressive strength of animal bones is considered.

Basic gear geometry may be determined by general and simple dimensionless data. With these data, a preliminary gear set may be designed that is based on only a limited number of data. The basic gear geometry parameters are teeth number, gear outer diameter, gear facewidth, mean spiral angle and hypoid offset.

The background for recommendations of the stress ratio gear-to-pinion according to Gleason and Oerlikon is comparable. The values for the slope of the SN curve differ however to a large extent, which results in significant differences in the actual tooth thickness for both systems. This is also influenced by differences in the stress ratio gear-to-pinion for a zero tooth thickness correction. The sensitivity of the tooth root stress for a change in tooth thickness correction also differs, although this influence is relatively small.
The required tooth thickness correction, that is caclulated according to both methods, for a given ratio and equal life, does differ very significantly. Generally, the required thickness correction calculated according to Oerlikon is appreciably smaller than calculated according to Gleason. A gearset with tooth thickness correction for equal life according to Oerlikon therefore appears to be an equal stress gearset in Gleason.

Gears designed according to Oerlikon or Gleason design guidelines will generally give relatively small differences in their Basic Gear Geometry, such as outer diameter, facewidth and spiral angle. The choice of these geometry values and parameters such as pressure angle and profile corrections may even be more dominated by previous experience of the designer or the availability of cutting tools. The general strength of both geartypes will also differ only to a small amount.
On the tooth thickness correction, however, relatively large differences may occur, which are the result of different SN-curve slopes and differences in the tooth root stress sensitivity to thickness variations.

7 CONCLUSIONS AND OUTLOOK

7.1 Conclusions

Four **Calculation Standards** for the tooth root stress of bevel gears have been analysed and compared. In all standards, virtual helical gears are applied in order to substitute the actual bevel gears, both for tooth proportions and gear geometry, as well as for calculating the root stress. In all considered standards, the gear mean face width is taken as the reference point for calculating the tooth root stress.
Calculations of basic gear geometry and tooth proportions in the reference point, performed by these four standards, generally lead to very small differences. The individual profile contact ratio and the face contact ratio also show very small differences in their numerical value. The total contact ratio and the modified contact ratio however may differ 15 to 30%. This is a result of differences in the definition for the total and the modified contact ratio.

The basic tooth root **Stress Equations** according to the considered standards all can and have been rearranged in one uniform way. A uniform separation between Load, Geometry and Material Factors has been introduced. By doing this, it has become clear that the basic set-up of all investigated calculation standards is very much comparable, although the original expressions do not give that impression. There are however some differences in the description of the individual factors, but basically they have a similar form.
The largest differences occur for the Tooth Form Factor, the Face Load Distribution Facor and the Allowable Material Stress. The differences in other Factors amount to a maximum of 40%. The influence of the Gear Curvature is only used in two standards. The actual curvature of the gear teeth hardly influences the tooth root stress when the tooth load position is maintained constant. The gear curvature does however influence the contact pattern sensitivity resulting from deflections; in this way the gear curvature indirectly influences the tooth root stress.

Differences in calculated tooth root stresses between the standards may even amount to a factor 2-2.5. These differences are caused by diffences in the individual Load, Geometry and Material factors and for a part by different designations of the Size Factor. The calculated Safety Factors lead to appreciably smaller differences.
A specific stress calculation method, it's accompanying allowable material stress values and the allowable safety factors are uniquely coupled to each other. This means that material stress values do not only depend on the material, but even more on the stress calculation method.

Generally the differences in general gear dimensions such as gear diameter, modulus, facewidth and spiral angle will not be large, when calculated by the different standards. The different requirements of the required safety factor, specific vehicle requirements and product liability laws may even play a larger role.
The choice of a particular standard will in principle be not of great importance; it should however always be linked with the acompanying material values and the specified safety factor for the field experience. There are hardly differences between the calculation standards in terms of quality. Therefore, gears calculated according to the different standards and for a given vehicle application, will only have small differences in their basic gear geometry lay-out.

For the **Face Load Distribution Factor** according to DIN, a smaller value is proposed for straddle mounted pinion. A value of 1.30 should be used instead of 1.50 for straddle mounted pinion and gear and for normal deflection values of pinion to crownwheel. This value of 1.30 is based on the assumption of a load distribution over the facewidth that is more flattened out than a purely elliptic load distribution function, as is assumed in the calculations according to DIN. The Face Load Distribution Factor is independent of the torque, when the deflections show a linear behaviour with the applied torque.

For the calulation of **Hypoid Gears**, some specific industrial and automotive methods have been compared. Calculations on geometry and tooth root stress on hypoid gears are performed by means of virtual bevel gears; this procedure is similar to the stress calculation of bevel gears. The differences between the several methods are mostly determined by the selection of these virtual bevel gears, that are determined by the spiral angle and facewidth of the pinion and/or gear. Depending on the calculation method, the spiral angle and facewidth of the pinion or the gear should be used.
There are relatively large differences between the Oerlikon-, Gleason- and Winter method of determining the virtual bevel gears that substitute the actual hypoid gears. As a result, also relatively large differences arise between the three possibilties in estimating the influence on hypoid offset on the tooth root stress.
In general, the influence of hypoid offset on tooth root stress as measured by means of endurance tests and strain gauge measurements from other investigations is far lesser than the influence calculated according to Oerlikon and Gleason. The method according to Winter gives the best correlation between calculations and experiments, for the influence of hypoid offset.
Generally a 10% stress decrease is to be expected at a 15% relative offset for a crownwheel constant spiral angle. The same stress decrease of 10% can already be achieved by a 10% relative offset when a constant sum of spiral angles is applied. Up to the value of 10% or 15% relative offset, the effect of stress decrease appears to be linear with increasing offset.

Fatigue Life Tests at Constant Amplitude Loading have been performed on four types of rear axle gears on a rear axle test rig. Failures were almost all fatigue breakage of the tooth root on the pinion, because of the relatively high stress level and the reproducable testrig loading conditions.
Cracks on the root surface were first visible in the middle of the face width. The assumption of a maximum tooth root stress in the middle of the face width therefore appears to be correct. During the rest of the fatigue life, the cracks grow not only inward but also towards the toe and heel side until tooth breakage occurs. The point of crack initiation in the root radius in the normal tooth section lay between an angle of 45° to 50°. This differs from the assumption of the 30°-tangent but comes more close to the Lewis parabola for the critical tooth thickness. An angle of crack initiation, different than the 30°-tangent has also been observed on helical gears.

The **Results of the Constant Amplitude Tests** on the rear axle gears could be described by a two parameter Weibull and a Lognormal failure probability distribution. The results are considered to be statistically reliable. With these test results, it was possible to calculate the gear endurance life estimate for 10-50% failure probability with an error just less than 10%.
The stress claculations according to DIN have been used with the virtual hypoid gear geometry calculated according to Winter. The Face Load Distribution Factor was assumed to be1.30.
The endurance limit, the slope for the SN curve and the ratio of static to endurance limit have been established from the testresults by matching calculated and actual life cycles.

These values are however different from helical gears in the same material. This is beleived to be caused by the non linear relation between pinion root stress and torque, which is a result of the contact pattern, of which both the width and position on the gear tooth flanks is dependent on the torque.
If a non linear relation between pinion tooth root stress and input torque for bevel and hypoid gears was assumed, especially the values for the slope of the SN curve came more close to those of helical gears of the same material. As a result, the ratio of static to endurance limit and the endurance limit also came close to helical gear related values of the same material.

Therefore, a **Load Factor** has been proposed in order to accomodate for the size and the position of the contact pattern. By applying this factor in the calculations, a **Non Linearity** is assured between tooth root stress and torque for bevel and hypoid gears.
With this Factor for Contact Pattern Size, the difference between calculated and actual endurance life was far lesser than 10% at a failure probability of 10% for three of the four tested axle types. Therefore, it can be concluded that the introduction of a non linear stress-to-torque relation for bevel and hypoid gears is required in order to use material endurance values for helical gears of the same material.

Two different types of **Driveline Load Spectra** for truck applications have been measured.
A specific fraction of the installed vehicle engine power can be considered to determine the load spectrum. This means that for the examined vehicles with representative truck applications, a specific part of the installed vehicle engine power largely determines the load spectrum.
Driveline load spectra have been calculated by using a vehicle driveline simulation program.
The difference between measured and calculated loading driveline spectra on representative applications is small.
Calculated driveline load spectra of rear axle input torque in truck applications have been generalised in two different types, the "Log-Log" and the "Lin-Log" type. Both spectra assume a straight line for the torque-to-cycle fraction. The maximum and minimum values for the torque are the two decisive parameters of these loading spectra.
Mathematical expressions have been derived to determine the equivalent torque for both load spectra. One is a simple mathematical expression, whereas the other is a recurrent expression.
Next to the form of the load spectrum, the slope of the SN curve determines the equivalent torque. The equivalent torque for general long distance truck applications, as International Transport is 20-25% of the maximum torque T-max; for Distribution Transport it is 25-30%.

Variable Amplitude Tests on a limited scale have been performed on one rear axle type with two different loading spectra. Calculated and actual life cycles also here give the best correlation between calculation and test results when the non linear stress-to-torque relation is applied.
For both loading spectra, the best correlation between calculated and actual life was realised by using the Corten-Dolan damage accumulation theory.
As here the non linear stress-to-torque relation also gives a far better correlation between calculated and actual life than a linear relation, the results of these limited number of Variable Amplitude Tests confirm the use of a non linear relation between stress and torque.
A reduction in endurance strength in comparison to the value for constant amplitude loading is still required in order to get calculation and realisation fit. The reduction of the endurance strength that is determined for Constant Amplitude loading is probably the result of additional damage phenomena that occur simultaneously under Variable Amplitude loading. This effect may be defined as "failure interference", where early occurring surface damage leads to additional cracks, thereby reducing the fatigue limit for tooth root breakage at Constant Amplitude loading.

A simple equation for the **Gear Outer diameter** has been developed, that is based on the maximum gear output torque. For many rear axle types, there appeared to be a relatively clear relation between gear outer diameter and maximum output torque.
This maximum torque can easily be referred to the vehicle weight for different applications. For general truck applications, the factor of 1 kNm/tonne may be used, whereas for small vans, this value may be 1.35. This relation can be considered to be valid for vehicles from 1 tonne up to 50 tonne GCW and gear outer diameters from 100 to 500 mm.
Gear outer diameters that are based on these values appear to be based on one and the same maximum allowable bending stress in the tooth root. This stress gives a safety factor of 1.5 to static overload breakage at the considered vehicle weight on a slope of 15%. It is not said that all gears **are** designed according to this criterium, but many bevel and hypoid gears **can** be arranged within this relation.
Other power transmitting elements such as couplings and hydraulic motors have similar relations based on scale effects. For these elements, the maximum output torque is an important parameter that determines the general dimensions.
In Nature, similar relations exist between body weight of mammals and their most important biological functions, such as respiratory and cardiovascular functions. The dimensions of the bones at landgoing mammals appear to be scaled according to one and the same maximum allowable stress. Based on this comparison of generalised scale laws, Nature and Technology both appear to apply the priciple of designing to a constant maximum allowable material stress.

Based on the vehicle weight it is possible to determine the basic gear geometry. With this, a design lay-out may be made by using different dimensionless and general applicable gear geometry values, that have been derived here.
Pinion and gear for automotive applications are normally designed for equal life by adding a tooth thickness correction for both pinion and gear. The factors that determine the required thickness correction are the gear ratio and the slope of the SN-curve. Because of differences in assumed slope, stress sensitivity to tooth thickness corrections and the ratio gear to pinion stress at zero thickness correction, large differences may occur between the required tooth thickness corrections, when calculated according to Gleason or Oerlikon.

7.2 Outlook

Further investigations on the **Non Linear** behaviour between tooth root stress and output torque for bevel and hypoid gears will be required. The influence of the contact pattern on the relation between stress and load needs to be better described as well as the influence of relevant parameters such as contact pattern dimension as well as it's position.
The proposed expressions for the Contact Pattern Factor are to be extended and improved, thereby introducing the influence of deflections, gear geometry and gear curvature.
The effect of the cutter diameter on the sensitivity of the contact pattern should further be defined. Here, the effect of the ratio cutter diameter to the mean cone distance or to the gear outer diameter on the change of tooth root stress should be incorporated. In that way, the effect of the gear curvature, and with this the contact pattern sensitivity, will indirectly be introduced.
The same values for the slope of the SN curve that are used on helical/spur gears should be used for bevel/hypoid gears. In that situation there will be no difference required between the slope of the SN curve for material values of different gear types.

Further investigations on the influence of **Hypoid Offset** of the pinion on tooth root stress need to be preformed. Here, specific tests on tooth breakage are required. It is to be assured that, by selecting the torque and the geometry in terms of module and teethnumber, clearly gear tooth breakage will occur. Strain gauge measurements can also be used .
The only variable should be the hypoid offset at three different spiral angle strategies. The influence of other parameters should be minimised as much as possible. Limitations with regard to manufacturing should also be excluded as much as possible.
Emphasis should be given on the range of 0-10% relative hypoid offset.

A more precise definition of the **Face Load Distribution Factor** is advised. General values for the gear deflections and the crowning, for which the expressions are valid, should also be given.

More attention should be paid on determining the actual torque values that are to be expected in field operations. The representative **Load Spectrum** of different applications should be determined. Not only is this valid for automotive apllications; for general industrial applications as well. Even for the use of different gear calculation standards for spur, helical, herringbone gears, as well as for bevel and hypoid gears and even for worm gears, this is relevant.
Most of the calculation standards are coming to a level of accuracy that is surprisingly good. Still almost all factors of influence are incorporated in the stress calcutations. On the other hand there is the relative large lack of knowledge on the actual loads during operation. If these actual operating loads are not known or hardly known, it will still be hard to dimension gears to their limit. Therefore, future work on gear calculation standards should for a large part be focussed on **Establishing Actual Operating Loads.**
This means that statistical aspects will require more importance in the near future than the deterministic aspects. In view of this, stochastic analysis of operating loads and load spectra will have to be developed with more emphasis than the deterministic description of gear geometry.

In the future, the already ongoing development of Finite Element and Boundary Element Methods for the calculation of tooth root stresses will be driven further. It needs however to be coupled with two very important aspects, concerning rear axle gears for automotive applications.
First there is the need of including the housing and bearing stiffness and the gear deflections that are a result of finite stiffness. Misalignment between both meshing members does have a relatively large influence on the face load distribution and thus on the maximum root stress.
Secondly the possibility to incorporate numerical life calculations, based on known driveline load spectra will further enhance the design method.
When these two aspects can be incorporated in these numerical methods without many numerical difficulties and without operating problems, than the exact stress definition and thus designing of these gears will be even better optimised.

One has to bear in mind that every **Reliable** calculation method on tooth root stress for automotive rear axle gears in specific and for gear drives in general, always will have to be based on or strongly accompanied by **Practical Experience**. In fact, all stress calculations, however complex they may be, are merely simplifications of reality. Only the degree of complexity may determine the difference between the actual and the calculated stress value.
Practical experience is therefore always required in order to correlate calculated stress values or calculated endurance life cycles with actual stress or actual registered life cycles. This practical experience may be based on either testing methods on testrigs or actual vehicle field experience. Only by using the results of practical experience on actual vehicle rear axle gears, it is possible to develop a reliable calculation method.

8 LITERATURE.

Chapter 2

2.1 H. Graf v. Seherr-Thoss.
Die Entwicklung der Zahnradtechnik. Springer Verlag, 1965.

2.2 H. Winter.
Kegelradgetriebe; Entwicklungstendenzen in Berechnung und Fertigung.
Expert Verlag, 1990.

2.3 ANSI/AGMA 2003-A86.
Rating the Pitting Resistance and Bending Strength of Generated Straight Bevel, Zerol Bevel and Spiral Bevel Gear Teeth.
AGMA Standard, approved as national Standard May 1986.

2.4 DIN 3991. Tragfähigkeitsberechnung von Kegelrädern ohne Achsversetzung; Teil 1 und Teil 3. DK621.833.2.001.24; Deutsche Norm September 1988.

2.5 G. Niemann, H. Winter.
Maschinenelemente; Band III. ISBN 3-540-10317-1, Springer Verlag 1983.

2.6 Bending Stresses in Bevel Gear Teeth.
Gleason Works Publication SD3103E/April 1981.

2.7 Gleason metod for estimating the fatigue life of bevel and hypoid gears.
Gleason Works Publication SD4052A, May 1966.

2.8 Design and Manufacture of Spiral Bevel and Hypoid Gears for Heavy Duty Drive Axles. Gleason Works Publication ETI4041A.

2.9 W. Coleman.
Improved method for estimating fatigue life of bevel gears and hypoid gears.
SAE Transactions; vol.6, no.2; pp.314-331; April 1952.

2.10 L. Wilcox, W. Coleman.
Application of Finite Elements to the Analysis of Gear Tooth Stresses.
ASME Publication 72-PTG-30, July 1972.

2.11 W. Coleman
A new perspective on the strength of bevel gear teeth. AGMA 229.13, October 1969.

2.12 L. Wilcox.
An Exact Analytical Method for Calulating Stresses in Bevel and Hypoid Gear Teeth.
Gleason Works Publication SD4171.

2.13 Allowable stress values for bevel and hypoid gears.
Gleason Works Publication SD 5340D, March 1982.

2.14 L. Wilcox.
Analyzing gear Tooth Stress as a Function of Tooth Contact Pattern Shape and Position. Gleason Works Publication ETI 4191.

2.15 Spiral bevel gear system. Gleason Works Publication SD30006H / April 1982.

2.16 Guide to bevel gears. Gleason Works Publication SD4155/7, 1981.

2.17 G. Niemann.
Maschinenelemente, Band II. Springer Verlag, 1960, pp. 78-90.

2.18 R. Werner.
Calculation of the load capacity of spiral bevel and hypoid gears by Prof. Niemann's method with analytical determination of the tooth form factor.
Oerlikon Machines, Zurich, 29-07-1980.

2.19 Neue Erkenntnisse bei der Beanspruchung und Auslegung von hochbeanspruchten Spiralkegelrad- und Hypoidgetrieben. Oerlikon.
2.20 Oerlikon Spiral Bevel Gear Cutting/Gear design N. Oerlikon WA 310214.
2.21 K. Keck.
Kennzeichnende Merkmale der Oerlikon-Spiralkegelradverzahnung.
Konstruktion, 18 Jahrgang, 1966, Nr.2, pp. 58-64.
2.22 Auslegung eines Kegelradgetriebes mit Klingelnberg Zyklo-Palloid Verzahnung.
Klingelnberg-Werknorm KN 3028, Ausgabe Nr. 2.
2.23 Tragfähigkeits-Berechnung fur Spiralkegelrader mit Klingelnberg Zyklo-Palloid-Verzahnung. Klingelnberg Werknorm KN 3030, Ausgabe Nr. 1.1.
2.24 E. Wildhaber.
Relationships of bevel gears. American Machinist Aug, Sept, Oct 1945.
2.25 Z. Fong, C. Tsay.
A Mathematical Model for the Tooth Geometry of Circular-Cut Spiral Bevel Gears.
Transactions of the ASME vol.113, June 1991, pp.174-181.
2.26 R. Huston, Y. Lin, J. Coy.
Tooth Profile Analysis of Circular Cut Spiral-Bevel Gears.
Transactions of the ASME vol.105, March 1983, pp.132-137.
2.27 Empfehlung fur die Festigkeitsberechnung metallischer Bauteile.
VDI-Richtlinie 2226, July 1965.
2.28 G. Niemann, H. Glaubitz.
Zahnfussfestigkeit geradverzahnter Stirnräder aus Stahl
VDI-Zeitschrift Bd.92, nr.33, 21. Nov. 1950, pp.923-932.
2.29 Th. Hosel.
Einfluss der Zahnform auf die Flanken- und Zahnfusstragfähigkeit nach DIN 3990 und AGMA 218.01 - Grenzen fur Optimierungsrechnungen.
Antriebstechnik 27 (1988) nr.9, pp. 65-69.
2.30 W. R. Rollins.
Lewis bending strength equations Centennial. Gear Technology, Nov./Dec. 1992.
2.31 W. Young.
Roark's Formulas for Stress and Strain. Mcgraw-Hill, 6th Edition, 1989, pp. 201-204.
2.32 M. Weck, S. Lachenmaier, H. Stadtfeld
Einfluß der Zahnlängskrummung bei Kegelradverzahnungen.
Industrie-Anzeiger nr.53 v 3.7.1985/107.Jg., pp.18-21.
2.33 M. Schweicher.
Einfluß von Spiralwinkel und Zahnlängskrummung auf die Zahnfussspannung und Zahnflankenpressung bogenverzahnter Kegelräder.
30. Arbeitstagung WZL "Zahnrad- und Getriebeuntersuchnungen", 17/18 May 1989.
2.34 A. Skoc
Einfluß des Zahnschrägungswinkels und des Flankenspiels auf die dynamische Belastung des Kegelradgetriebes. Konstruktion 44 (1992) pp. 377-380
2.35 H. Winter, M. Paul.
Tragfähigkeitsberechnung von Kegelrädern nach DIN 3991 und AGMA 219.
VDI-Berichte 626, pp. 69-95.
2.36 Th. Hosel.
Vergleich genormter Tragfähigkeitsberechnungen fur Stirnräder nach AGMA 218.01, DIN 3990, ISO/DIS 6336 und TGL 10545. Antriebstechnik 27 (1988) nr.1, pp. 37-39.
2.37 Th. Hosel.
Vergleich der Tragfähigkeitsberechnungen fur Stirnräder nach ANSI/AGMA-, ISO/DIN- und RGW-Normen. Antriebstechnik 28 (1989) nr.11, pp. 77-84.

2.38 D. Walton, Y. Shi, S. Taylor
Review of gear standards - part II.
Gear Technology, January/February 1991, pp. 24-29.

2.39 G. Notzel.
Doppelt rechnen gibt Sicherheit; Faktoren bestimmen den Betriebslastwert fur Evolventenverzahnungen nach DIN, Niemann und AGMA.
Maschinenmarkt 93 (1987) nr. 34, pp. 32-37.

2.40 D. Petersen
Lastverteilung und Zahnfusstragfähigkeit bei hoch uberdeckenden Zahnradpaarungen. VDI-Berichte 1056.

2.41 M. Paul
Einfluss von Balligkeit und Lageabweichungen auf die Zahnfussbeanspruchung spiralverzahnter Kegelräder. Dissertation TU Munchen, November 1985.

2.42 M. Paul
Zahnfussspannungen an Kegelrädern.
Teil I: Einfluss der Balligkeit. Antriebstechnik 25 (1986) nr.10, pp. 53-58.
Teil II: Einflusse von Lageabweichungen. Ant.25 (1986) nr.11, pp. 54-56.

2.43 H. Winter, M. Paul
Tooth root stresses of spiral bevel gears.
Gear Technology May/June 1988, pp. 13-19.

2.44 T. Tobe, K. Inoue.
Longitudinal load distribution factor for straddle and overhung mounted spur gears.
Gear Technology July/August 1987, pp. 11-19.

2.45 V. Golovkin
Load concentration in a bevel gear transmission.
Russian Engineering Journal Volume XLVI no.1, pp. 16-27.

2.46 J. Oehme.
Wirksamkeit von Breitenballigkeit und Endrucknahme an Stirnrädern bei Verzahnungsabweichungen. Konstruktion 42 (1990), pp. 120-126.

2.47 D. Wingate, R. Walsh.
Evaluating the load distribution factor for spur gears. SAE Paper 891930.

2.48 M. Hirth.
Einfluß der Zahnfußausrundung auf Spannung und Festigkeit von Geradstirnrädern.
Dissertation TU München, 1974.

2.49 F. Litvin et all.
Computerised generation and simulation of meshing contact of spiral bevel gears with improved geometry.
Comp. methods in Appl. Mech. and Eng. Vol. 158 (issue 1-2), 1998, pp. 35-46.

2.50 A. Kubo, C. Gosselin et all.
A computer based approach for evaluation of operating performance of bevel and hypoid gears. JSME, Intern. Journal, series C, vol. 40, no.4, 1997, pp. 749-758.

2.51 M. Weck, H. Stadtfeld.
Ubergeordnete Analysen bogenverzahnter Kegelradgetriebe mit der "Programmkette Kegelradberechnung".
VDI Berichte nr. 226, 1987, pp. 97-111.

2.52 M. Weck, H. Stadtfeld.
Einfluß des Spiralwinkels auf Flankenpressung und Zahnfußspannung an Spiralkegelradern.
VDI-Zeitschrift, Bd. 128, 1986, nr. 13, pp.525-528.

2.53 H. Stadtfeld.
Taking a new approach to quiet gears.
Machine Design, april 1996, pp. 79-82.
2,54 E. Piepka.
Berechnung der 30°-Tangente und der Lewis Parabel an Stirnrädern.
Antriebstechnik 22, 1983, nr. 7, pp. 33-36.
2.55 J. Pedrero, C. Garcie, A. Fuentes.
On the location of the tooth critical section for the determination of the AGMA J-factor. AGMA Paper 97FTM6, nov. 1997.
2.56 M. Albert.
Berechnung der Zahnfusstragfahigkeit - ein schwieriges Normungsproblem.
Konstruktion 39 (1987), nr. 11, pp. 447-455.
2.57 H. Linke, J. Borner.
Prazisierte Ergebnisse zur Spannungskonzentration am Zahnfuss.
VDI Berichte Nr. 1230, 1996.
2.58 V. Baumann, A. Haase.
Last- und Spannungsverteilung bei bogenverzahnter Kegelradern.
Antriebstechnik 34, 1995, nr. 1, pp. 64-65.

Chapter 3

3.1 B. Griffith.
Hypoid gear design for automotive axles. SAE paper 680076.
3.2 E. Wildhaber.
Basic relationship of hypoid gears, part 1 to 8.
The machinist, June to December 1946.
3.3 Method for designing hypoid gear blanks.
Gleason Works Publication SD 3030D, 1971.
3.4 Passenger car drive axle gear design.
Gleason Works Publication SD 4084B/MLI, April 1972.
3.5 Oerlikon Spiral Bevel Gear Cutting/Gear design HG. Oerlikon WA 310 232-7209-500.
3.6 Auslegung von Hypoid Getrieben mit Klingelnberg Zyklo-Palloid Verzahnung.
Klingelnberg-Werknorm KN3029, Ausgabe Nr. 108.
3.7 F. Litvin, K. Petrov, V. Ganshin.
The Effect of Geometrical Parameters of Hypoid and Spiroid gears on its Quality Characteristics. Mechanism and machine Theory, 1973, vol.8, pp. 187-196.
3.8 G. Fresen.
Untersuchungen uber die Tragfähigkeit von Hypoid- und Kegelradgetrieben.
Dissertation TU Munchen,. June 1981.
3.9 H. Winter, G. Fresen
Tragfähigkeit von Kegelrad- und Hypoidgetrieben.
VDI-Berichte Nr. 488, 1983, pp. 1-10.
3.10 F. Vollhuter.
Grubchen- und Zahnfusstragfähigkeit von Kegelradern mit und ohne Achsversatzung. Dissertation TU Munchen, January 1992.
3.11 H. Winter, K. Michaelis, F. Vollhuter.
Grubchen- und Zahnfusstragfähigkeit von Kegelradern mit und ohne Achsversatzung, Teil I: Versuche zur Festigkeit und Beanspruchung.
Antriebstechnik 32 (1993), nr.6, pp. 64-70.

3.12 H. Winter, K. Michaelis, F. Vollhuter.
Grubchen- und Zahnfusstragfähigkeit von Kegelradern mit und ohne Achsversatzung; Teil II: Tragfähigkeits Berechnungsverfahren und Vergleich mit Praxisergebnissen. Antriebstechnik 32 (1993), nr.7, pp 53-58.

3.13 M. Weck, H. Stadtfeld.
Programmkette Kegelradberechnung: Lauf- und Beanspruchungsverhalten bogenverzahnter Kegelradgetriebe. Antriebstechnik 27 (1988), nr.4, pp 72-77.

3.14 H. Stadtfeld.
Anforderungsgerechte Auslegung bogenverzahnter Kegelradgetriebe. Dissertation RWTH Aachen, December 1987.

3.15 M. Weck, H. Stadtfeld.
Bogenverzahnte Kegelradgetriebe; Einfluss des Achsversatzes und der Spiralwinkelaufteilung auf Zahnkontakt- und Verlagerungsverhalten. VDI-Z band 129 (1987) nr.7, pp 127-132.

3.16 M. Schweicher.
Einfluss des Achsversatzes auf die Beanspruchung von Hypoidgetrieben. 31. Arbeitstagung WZL "Zahnrad- und Getriebeuntersuchnungen". 30/31 May 1990, Aachen.

3.17 M. Weck, M. Schweicher, C. Weyand, B-R. Hohn, H. Winter, K. Michaelis, F. Vollhuter. Berechnung und Messung von Einflussgrossen auf die Beanspruchung von Kegelradern mit und ohne Achsversatz.
VDI-Z Special Antriebstechnik, April 1993, pp 6-15.

3.18 L. Wilcox, T. Chimmer, G. Nowell.
Improved Finite Element Model for Calculating Stresses in bevel and Hypoid Gear Teeth. AGMA Paper 97FTM5, nov. 1997.

Chapter 4

4.1 R. Reynders.
Tooth root stress on hypoid gears (in Dutch).
Internal report DAF Trucks Eindhoven, June 1992.

4.2 H. Rettig, T. Weiss.
Statistisch belegte Wohlerlinien der Zahnfussfestigkeit fur gebrauchliche Zahnradstähle. Stahl und Eisen 101 (1981), pp. 413-416

4.3 T. Weiss.
Zahnfussfestigkeitsuntersuchungen an gebrauchlichen Zahnradstählen.
Antriebstechnik 25 (1986) nr.12, pp. 43-44

4.4 D. Miltenovic.
Lebensdauerverteilung der Zahnfussfestigkeit von Zahnrädern
International Conference on gearing, Paris 1986, pp. 247-257.

4.5 H. Thum.
Bewertung der Lebensdauer von Zahnradpaarungen.
Maschinenbautechnik 39 (1990), nr.8, pp. 344-348.

4.6 H. Fuchs, M. Johns.
The risk of extrapolations of metal fatigue data. ASTM, 1988, pp. 276-279.

4.7 Q. Yang.
Cumulative Damage Hypothesis in Reliability Design of Gears.
VDI-Berichte nr.1230, 1996, pp.615-629.

4.8 W. Ireson, C. Coombs.
Handbook of Reliability Engineering and Management.
McGraw-Hill Book Company 1988.

4.9 S. Rao.
Reliability Based Design. Chapter 15, pp.505-543.

4.10 F. Jarchow, Q. Yang.
Zuverlässigkeit von Zahnradgetrieben unter besonderer Berucksichtigung der Zahnfusstragfähigkeit. Antriebstechnik 29 (1990) nr.1, pp. 44-47.

4.11 G. Schönnenbeck.
Pulsatoruntersuchnungen an CVT-kettenproben - Basis fur Festigkeitsrechnungen und Qualitätssicherung. Antriebstechnik 30 (1991) nr.1, pp. 48-53.

4.12 ISO/TC60/WG6 283.
Calculatios of load capacity of cilindrical gears. Application Standard for Vehicle Gears. January 1983.

4.13 J. Grosch.
Werkstoffauswahl im Maschinenbau. Expert Verlag 1986; Chapter 4, pp 47-76.

4.14 H. Dietrich.
Mechanische Werkstoffprufung. Expert Verlag 1989; Chapter 8, pp. 244-263.

4.15 B. Bertsche, G. Lechner.
Verbesserte Berechnung der Systemlebendsauer von Produkten des Maschinenbaus. Konstruktion 38 (1986) H.8, pp.3 15-321.

4.16 O. Buxbaum.
Betriebsfestigkeit: sichere und wirtschaftliche Bemessung schwingbruchgefährdeter Bauteile. Stahleisen Verlag mbH, Dusseldorf 1986.

4.17 P. Venhuizen.
Deflectieresultaten van diverse astypen.
Internal report DAF Trucks Eindhoven, June 1993.

4.18 J. Van Wijk.
Resultaten van vermoeiingsproeven op tandwielstalen.
Internal report DAF trucks, Department Central Laboratory, March 1991.

4.19 H. Winter, P. Oster, M. Anzinger.
Werkstoff- und Fertigungseinflüsse auf die Zahnfußtragfähigkeit, Teil II.
Antriebstechnik 34, 1995, nr. 6, pp. 59-61.

4.20 J. Lehmann.
Development of Contact Patterns on Tractor Spiral Bevel and Hypoid Gears.
SAE 841091.

4.21 F. Leistner, G. Liebetrau.
Tragbildlack - ein Mittel zur schnellen und genauen Sichtbarmachung des Tragbildes bei Zahnradgetrieben. Maschinenbautechnik 25, 1976, nr.3, pp. 133-136.

4.22 J. Goebbelet.
Tragbildprufung von Zahnradgetrieben; eine Methode zur Qualitätsbeurteilung.
Dissertation RWTH Aachen, June 1980.

4.23 X. Wang, S. Ghosh, X. Wu.
Analysis of the rates of change of contact situations of a gear pair under vertical (V) and horizontal (H) check.
European Journal of Mech. Eng., vol. 38, 1993, vol. 38, nr.2, pp. 73-83.

4.24 R. Cohen, P. Haagensen et all.
Assesment of Bending fatigue limits for Carburised Steel.
SAE paper 910140, 1991.

4.25 S. Preston.
Bending Fatigue Strength of Carburising Steel SS 2506.
Materials Science and technology, February 1991, vol. 7, pp. 105-110.
4.26 Y. Okada, M. Yoshida et all.
Fatigue Strength Analysis of Carburised Transmission Gears.
JSAE Review, July 1990, vol.11, nr. 3, pp. 82-84.
4.27 D. Hoffman.
Understanding failure will help gear designers.
Design Engineering, October 1994, pp. 50-56.
4.28 K. Nagamura, Y. Terauchi et all.
Study on Gear Bending Fatigue Strength Design based on Reliability Engineering.
JSME International Journal, series C, vol. 37, nr. 4, 1994, pp. 795-803.

Chapter 5

5.1 T. Schlenka.
Ein Verfahren zur indirekten Ermittlung von Lastkollektiven in Antriebsstrangen.
Fortschritt-Berichte VDI, Reihe 11, nr. 84, 1986.
5.2 B. Klein.
Nutzungsdauerabschätzung von schwingend beanspruchten Fahrzeugbauteilen.
Automobil-Industrie nr.2, 1988, pp.181-189.
5.3 B. Klein.
Schadensrechnung fur Fahrzeugbauteile. Automobil-Industrie nr.6, pp. 789-799.
5.4 Z. Jaskiewicz, A. Wasiewski.
Equivalent torque determination according to AGMA and ISO for calculation of gears load capacity in automotive gearboxes.
International Conference on Gearing, Paris 1986, pp.
5.5 J. Vanheck.
Mathematical model for equivalent torque, based on two continuous load spectra.
Internal report DAF Trucks Eindhoven, September 1994.
5.6 TGL 10 545/04.
Tragfähigkeitsberechnung von aussenverzahnten Stirnrädern. Zeitlich veränderliche Belastung. November 1988.
5.7 J. Leitner, G. Raab.
Equivalente Belastung linearer Kollektivabschnitte.
Konstruktion 46 (1994), pp. 381-385.
5.8 F. Kucukay.
Rechnerunterstutzte Getriebedimensionierung mit representativen Lastkollektiven.
ATZ 92 (1990), nr.6, pp. 328-333.
5.9 F. Kucukay, W. Pfau.
Extrembelastungen in Personenwagen Antriebsstrangen.
ATZ 91 (1989), nr.7/8, pp. 391-396.
5.10 A. Seifried, P. Muller.
Wechselnde Betriebsbelastungen, ihre rechnerunterstutzte Bestimmung und Berucksichtigung in der Konstruktion von Zahnradgetrieben.
VDI-Berichte nr.434, 1982, pp. 29-44.
5.11 G. Buck.
Probleme bei der Berechnung von Fahrzeuggetrieben mit Lastkollektiven.
VDI-Berichte nr.195, 1973, pp. 37-46.

5.12 K. Renius.
Last- und Fahrgeschwindigkeitskollektive als Dimensionierungsgrundlagen fur die Fahrgetriebe von Ackerschleppern.
Forstchritt-Berichte VDI, reihe 1, nr.49, pp. 13-44.

5.13 K. Renius.
Betriebsfestigkeitsberechnungen von Maschinenelementen in Ackerschleppern mit Hilfe von Lastkollektiven. Konstruktion 29, 1977, nr.3, pp. 85-93.

5.14 F. Rockstroh, K. Dirlam.
Verallgemeinerung von Gangbenutzungsanteilen in LKW.
Kraftfahrzeugtechnik nr.6, 1969, pp. 174-176.

5.15 H. Gross.
Beitrag zur Lebensdauerabschätzung von Stirnrädern bei Zahnkraftkollektiven mit geringem Volligkeitsgrad. Dissertation RWTH Aachen, 1974.

5.16 D. Heinisch.
Ein Verfahren zur lebensdauerorientierten Dimensionierung von Zahnradgetrieben mit Hilfe von Lastkollektiven. Konstruktion 38, 1980, nr.11, pp. 417-422.

5.17 D. Heinisch.
Lebensdauerorientierte Getriebedimensionierung mit Hilfe von Lastkollektiven.
Antriebstechnik 24, 1985, nr.6, pp. 4751.

5.18 W. Ammermann.
Lebensdauerorientierte Bauteildimensionierung unter Berucksichtigung von Betriebsbelastungen. Antriebstechnik 26, 1987, nr.5, pp. 50-55.

5.19 G. Rehlich.
Lebensdauerberechnung von Bauteilen bei Beanspruchungskollektiven mit Normalverteilung. Maschinenbautechnik 21, 1972, nr.9, pp. 402-407.

5.20 G. Friedrich.
Anwendung der Lebensdauerberechnung beim Entwurf und der Auswahl von Zahnradgetrieben. Maschinenbautechnik 32, 1983, nr.10, pp. 457-462.

5.21 D. Herrwig.
Lebensdauerberechnung von Zahnradgetrieben.
Maschinenbautechnik 26, 1977, nr.12, pp. 564-567.

5.22 J. Beelen.
ROSI, systeembeschrijving van het DAF-ROuteSImulatie programma.
Internal Report DAF Trucks, Department Systeembeheer; 1993.

5.23 Anon.
Several Vehicle Testreports of Department Vehicle Testing, DAF Trucks.

5.24 C. MacDougall, T. Topper.
The influence of variable amplitude loading on crack closure and notch fatigue behaviour. Int. Journal of Fatigue, vol. 19, 1997, no.5, pp. 389-400

Chapter 6

6.1 Z. Jaskiewicz, A. Wasiewski.
Preliminary draft selection of geometrical parameters in external and internal spur and helical gears in automotive drive lines.
SAE Technical Paper Series 841193, 1984.

6.2 General rear axle data from information leaflets of Eaton, Rockwell, Dana, Raba, Scania, Volvo and Daf Trucks during the period of 1986-1993.

6.3 Design and Manufacture of Spiral Bevel and Hypoid Gears for Heavy-Duty Drive Axles. Gleason Works Publication ETI4041A.
6.4 The Design of Automotive Spiral Bevel and Hypoid Gears. Gleason Works Publication SD3187A, February 1983.
6.5 Vehicle Axle Drive Gear Design. Gleason Works Publication SD4113A, May 1972.
6.6 Passenger Car Drive Axle Gear Design. Gleason Works Publication SD4084B, April 1972.
6.7 Oerlikon. Oerlikon Spiral Bevel Gear design. Oerlikon WA 310214.
6.8 M. Cuijpers. Schaalwetten in de techniek: enkele voorbeelden. De Constructeur, no. 4, april 1995, pp. 40-43.
6.9 General information brochures of gear drives from ZF, Lohman & Stolterfoht, TGW, Flender, Voith and Eickhoff, during 1990-1995.
6.10 General information brochures of Fichtel & Sachs, Hydraulic motors, mechanical couplings for industrial applications, during 1990-1994.
6.11 A. Horowitz. Schaalwetten en constructies. De Ingenieur, no.48, 1966, pp. W238.
6.12 W. Schlösser, P. Hezemans. Schaalregels voor overbrengingen. Aandrijftechniek, 12 nov. 1976, pp. 962-969.
6.13 G. Ricci. Weight and rated characteristics of machines - a statistical-descriptive analysis. Mechanism and machine theory, vol.17, no.2, 1982, pp. 99-106.
6.14 S. J. Gould. Honderd jaar na Darwin; translation of "Ever since Darwin, reflections in natural history". Het Spectrum, 1979.
6.15 D'Arcy Wentworth Thompson. On growth and form. Cambridge University Press, 1961.
6.16 M. French. Invention and Evolution; Design in Nature and Engineering. Cambridge University Press, 1993.
6.17 M. Hildebrand. Analysis of Vertebrate Structure; Third Edition. John Wiley & Sons, 1988.
6.18 H. Judson. The search for solutions. Holt, Rinehart and Winston, 1980.
6.19 K. Gartner. Wie ahnlich sind sich Mensch und Tier. Umschau, Heft 8, 1984, pp. 254-258.
6.20 B Gunther. Dimensional analysis and theory of biological similarity Physiological Reviews, vol. 55, no. 4, 1975, pp. 659-699.
6.21 Th. McMahon, J. Bonner. De maat van het leven; translation of "On size and live" Natuur en Techniek, Maastricht, 1987.
6.22 J. Haldane. Warum die Natur keine Riesen schuf. Bild der Wissenschaft, no.2, 1981, pp.116-120.
6.23 P. Kerz. Biologie und Technik-Gegensatz oder sinnvolle Erganzung? Konstruktion, no 39, 1987, pp. 321-327.

6.24 W. Nachtigall.
Fantasie van de schepping; translation of "Phantasie der Schöpfung".
Meulenhoff, Baarn, 1974.

6.25 A. Kalashnikov.
Improvement in the Performance of Hypoid and Bevel Gears cut with Reduced Diameter Head. Stanki i Instrument, vol. 51, Issue 11, 1980, pp. 19-29.

6.26 R. Erichello.
A rational procedure for Designing Minimum-Weight Gears.
Gear Technology, nov/dec 1991,pp. 10-14

6.27 K. Wittig.
Zur Auslegung kreisbogenverzahnter Kegelräder mit Achsversatz.
Maschinenbautechnik 20, 1971, nr.9, pp. 431-435.

6.28 R. Drago.
Design Guidelines for High-Capacity Bevel Gear Systems.
Gear Technology jan/febr 1992, pp.16-29.

9 Symbols, Definitions and Units

Here the symbols of the different calculation standards are summarised. As these standards mostly use different symbols for one and the same item, the source of the symbol is indicated.

SYMBOL	DESCRIPTION	UNITS
a	Centre distance for spur / helical gear drive	mm
a_k	Vertical pinion offset on hypoid gears	mm
a	Addendum (AGMA, Gleason)	mm
b	Dedendum (AGMA, Gleason)	mm
b	Facewidth (DIN, Oerlikon)	mm
b_{ef}	Effective facewidth (DIN)	mm
c	General coefficient in allometric expressions for animals	--
$c_{a,b,c,d}$	Coefficients in cardiovascular and respiratory expressions	--
c_{gF}	Geometry coefficient for root failure	--
c_{gH}	Geometry coefficient for surface failure	--
c_{lF}	Load coefficient for root failure	--
c_{lH}	Load coefficient for surface failure	--
c_{mF}	Material coefficient for root failure	--
c_{mH}	Material coefficient for surface failure	--
c	Clearance (AGMA, Gleason)	mm
c_c	Clearance factor (AGMA, Gleason)	--
c_1	Gear addendum factor (AGMA, Gleason)	--
d	Diameter	mm
e	General exponent in allometric expressions for animals	--
h	Bending lever arm of tooth load (general)	mm
h	Whole depth (AGMA, Gleason)	mm
h_w	Working depth (AGMA, Gleason)	mm
h_{fw}	Addendum factor (Oerlikon)	--
i	Gear ratio	--
k	Depth factor (AGMA, Gleason)	--
k	Slope of SN curve for bending fatigue at limited life region	--
k_s	Clearance factor (DIN, Oerlikon)	--
m_{mn}	Module in middle facewidth in normal section	mm
m	Exponent in equation for synthetic load spectrum	--
m_F	Face contact ratio (AGMA, Gleason)	--
m_N	Load sharing factor (AGMA, Gleason)	--
m_O	Modified contact ratio (AGMA, Gleason)	--
m_P	Profile contact ratio (AGMA, Gleason)	--
q_w	Tooth form factor (Oerlikon)	--
r_c	Cutter head radius	mm
r_t	Radius to Point of Load Appliocation (AGMA, Gleason)	mm
s	Tooth thickness at the point of maximum root stress	mm
s_{at}	Allowable Bending Stress Number (AGMA, Gleason)	N/mm^2
s_t	Calculated Bending Stress Number (AGMA, Gleason)	N/mm^2
s_{wt}	Working Bending Stress Number (AGMA, Gleason)	N/mm^2
x_m	Profile shift factor (DIN, Oerlikon)	--
z	Teethnumber	--

SYMBOL	DESCRIPTION	UNITS
F	Facewidth (AGMA, Gleason)	mm
F_e	Effective Facewidth (AGMA, Gleason)	N
F_{mt}	Tangential gear load at middle facewidth	N
GCW	Gross Combination Weight	kg
GVW	Gross Vehicle Weight	kg
H	Working depth (Oerlikon)	mm
H_f	Dedendum heigth (Oerlikon)	mm
H_k	Addendum heigth (Oerlikon)	mm
H_z	Whole depth (Oerlikon)	mm
L_b	Crowning value in direction of facewidth	μm
M	Mass	kg
N	Number of loading cycles	--
P	Power	W
P_d	Diametral Pitch at the Tooth Large End	mm
P_m	Mean Diametral Pitch	mm
Q	Volumetric delivery	m^3/s
R_m	Mean cone distance (DIN, Oerlikon)	mm
R	Mean Transverse Pitch Radius (AGMA, Gleason)	mm
R_t	Mean Transverse Radius to Point of Load Application (AGMA, Gl.)	mm
S_B	Safety factor for root failure (Oerlikon)	--
S_H	Safety Factor for surface failure (DIN)	--
S_{FS}	Safety Factor for root failure (DIN)	--
T	Torque	Nm
Y	General allometric function for animals	--
Y_{CP}	Proposed Contact Pattern Factor	--
$Y_{CP\text{-}size}$	Contact Pattern Factor for Size	--
$Y_{CP\text{-}shift}$	Contact Pattern Factor for Shift	--
α	Pressure angle	°
α_0	Coefficient for shear stress	--
β	Spiral angle	°
δ	Pitch cone angle	°
ϵ_α	Profile contact ratio (DIN, Oerlikon)	--
ϵ_β	Face contact ratio (DIN, Oerlikon)	--
ϵ_γ	Total contact ratio (DIN, Oerlikon)	--
φ	Angle of of tooth load to tooth centreline (general)	°
φ	Ratio of minimum to maximum torque for load spectrum	--
ϕ	Ratio of pinion diameter for hypoid to bevel	--
ξ	Ratio of facewidth to outerdiameter crownwheel	--
σ_b	Bending Stress in generalised tooth loading model	N/mm^2
σ_d	Compressive Stress in generalised tooth loading model	N/mm^2
σ_D	Fatigue Limit (Oerlikon)	N/mm^2
σ_F	Tooth Root Bending stress according to DIN	N/mm^2
σ_H	Contact stress according to DIN	N/mm^2
τ	Shear Stress in generalised tooth loading model	N/mm^2
Δs	Tooth thickness correction factor	--
Φ_N	Cumulative fraction of loading cycles	--

SYMBOL	DESCRIPTION	UNITS
Πk_{load}	Product of Load Factors	--
$\Pi Y_{geometry}$	Product of Geometry Factors for root stress	--
$\Pi Y_{material}$	Product of Material Factors for root stress	--
$\Pi Z_{geometry}$	Product of Geometry Factors for surface stress	--
$\Pi Z_{material}$	Product of Material Factors for surface stress	--
Γ	Fraction of GCM to crownwheel output torque	$Nm/10^3kg$
Calculation Factors according to **DIN**		
K_A	Load Application Factor (DIN)	--
K_v	Dynamic Load Factor (DIN)	--
$K_{F-\beta}$	Face Load Distribution Factor (DIN)	--
$K_{F-\alpha}$	Adjecent Load Distribution Factor (DIN)	--
Y_{fa}	Tooth Form Factor (DIN)	--
Y_{sa}	Stress Concentration Factor (DIN)	--
Y_ϵ	Load Sharing Factor (DIN)	--
Y_β	Helical Factor (DIN)	--
Y_k	Bevel Gear Factor (DIN)	--
Y_x	Size Factor (DIN)	--
$Y_{\delta relT}$	Support Factor (DIN)	--
Y_{RrelT}	Roughness Factor (DIN)	--
Calculation Factors according to **AGMA, Gleason**		
m_N	Load Sharing Ratio	--
J	Geometry Factor for Bending Strength	--
Y_K	Tooth Form Factor for Bending Strength	--
K_o	Overload Factor	--
K_f	Stress Concentration and Stress Correction Factor	--
K_i	Inertia Factor	--
K_m	Load Distribution Factor	--
K_s	Size Factor	--
K_v	(Internal) Dynamic Factor	--
K_L	Life Factor	--
K_R	Reliability (Safety) Factor	--
K_T	Temperature Factor	--
K_x	Cutter Radius Factor	--
W_t	Transmitted Tangential Load	N
Calculation Factors according to **Oerlikon**		
B_e	Nominal Tooth Stress Value	N/mm^2
B_w	Effective Tooth Stress Value	N/mm^2
C_D	Dynamic Factor	--
C_S	Shock Factor	--
C_T	Load Distribution Factor	--
C_β	Overlap Factor	--
q_w	Gear load per mm facewidth	--
d_{p1}	Pinion diameter	--
r_e	Radius of virtual helical gears	mm
z_e	Teeth number of virtual helical gears	mm

Subscripts and general indices:

( )e	at the outer diameter / outer cone distance
( )e	for the virtual helical gears (for Oerlikon)
( )m	at the mean diameter / mean cone distance
( )n	in the normal section
( )t	in the transverse section
( )v	for the virtual gears
( )ef	effective
( )1	at the pinion
( )P	at the pinion
( )2	at the crownwheel
( )G	at the crownwheel
( )H	tooth surface failure related
( )F	tooth root failure related
( )all	allowable
( )a-d	general indices for allometric functions
( )cont	continuous
( )eq	equivalent
( )max	maximum
( )min	minimum
( )∞	knickpoint of endurance fatigue limit

10 ATTACHMENTS

The attachments are given in the order of importance. The number of the individual attachments refers to the chapter of the specific subject.

Attachment 2.3 Tooth Root Stress Expressions for different Standards

Derivation of the generalised expressions for tooth root stress.
The basic lay-out for tooth root stress calculations is expressed here, with the three groups of Load, Geometry and Material Factors given. The different formulations of all calculation standards will be rewritten into this generalised form.
The basic lay-out for the tooth root stress is:

$$\sigma_{1,2} = \Pi F_{load} * \frac{F_{mt}}{b * m_{m_n}} * \Pi F_{geometry} \leq \sigma_{allowable} * \Pi F_{material}$$

ANSI/AGMA and Gleason
The original expressions here are:

$$S_t = \frac{W_t * K_o}{K_v} * \frac{P_d}{F} * \frac{K_s * K_m}{J * K_x} * 0.061 \qquad \text{(Gl.1)}$$

$$J = \frac{Y_K}{m_N * K_i} * \frac{R_t}{R} * \frac{F_e}{F} * \frac{P_d}{P_m} \qquad \text{(Gl.2)}$$

The Tooth Form Factor, inclusive the Stress Concentration, is expressed as:

$$Y_K = \frac{P_d}{\frac{3}{2} * (X_N - \frac{\tan\Phi_N}{3t_n}) * K_f} \qquad \text{(Gl.3)}$$

The tangential tooth load is:

$$W_t = \frac{2 * T_P}{d_{e_P}} \qquad \text{(Gl.4)}$$

First Gl.3 is rewritten and inverted into:

$$\frac{1}{Y_K} = \frac{1}{2t_N} * [6(\frac{h_N}{2t_N}) - \tan\phi_N] * \frac{K_f}{P_d}$$

Then Gl.2 is rewritten and inverted into:

$$\frac{1}{J}=\frac{1}{Y_K}*m_N*K_i*\frac{R}{R_t}*\frac{F}{F_E}*\frac{P_m}{P_d}$$

Now when the original expression Gl.1 is rearranged into Load and Geometry Factors by implementing the last two expressions, we obtain:

$$s_t=K_o*\frac{1}{K_v}*K_m*\frac{2*T_1}{d_{e_1}}*\frac{P_d}{F}*\frac{1}{2t_N}[6(\frac{h_N}{2t_N})-\tan\phi_N]*\frac{K_f}{P_d}*m_N*K_i*\frac{R}{R_t}*\frac{F}{F_e}*\frac{P_m}{P_d}*\frac{1}{K_x}*K_s$$

Now

$$d_{e_1}=d_{m_1}*\frac{A_0}{A} \quad \textit{as well as} \quad \frac{P_m}{P_d}=\frac{A_0}{A}$$

This leads to the following equality:

$$2*\frac{T_1}{d_{e_1}}*\frac{1}{F}*\frac{P_m}{p_d}=2*\frac{T_1}{d_{e_1}}*\frac{1}{F}*\frac{A_0}{A}=2*\frac{T_1}{d_{m_1}}*\frac{1}{F}=\frac{F_{m_t}}{F}$$

Now the Size Factor Ks is moved to the side of the Material Factors. The root stress then is no longer equal to the root stress of the original Gleason equation; reason for an addition in the symbol by adding " to St. If also the last expression is multiplied by m_{mn} / m_{mn}, we obtain:

$$s''_t = K_0 *\frac{1}{K_v} *K_m *\frac{F_{mt}}{F*m_{mn}}* \frac{1}{Y} *K_f *m_N K_i *\frac{1}{K_x} *\frac{R}{R_t} *\frac{F}{F_e}$$

In which the general Tooth Form Factor is:

$$\frac{1}{Y} = \frac{m_{mn}}{Y_K}*\frac{P_d}{K_f} = \frac{m_{mn}}{2t_N}*[6(\frac{h_N}{2t_N})-\tan\phi_N]$$

The complete expression is:

$$s''_t=K_0*\frac{1}{K_v}*K_m*\frac{F_{mt}}{F*m_{mn}}*\frac{m_{mn}}{2t_N}*[6(\frac{h_N}{2t_N})-\tan\phi_N]*K_f*m_N K_i*\frac{1}{K_x}*\frac{R}{R_t}*\frac{F}{F_e}$$

The original expression for the working stress number is:

$$s_w=\frac{s_{at}*K_L}{K_T*K_R}$$

Which now leads to:

$$s''_t \leq s_{at} * \frac{1}{K_R} * K_L * \frac{1}{K_S} * \frac{1}{K_T}$$

The same operations may be performed on the expressions according to ANSI/AGMA, so the above described procedure also is valid for this standard.

DIN 3991

Here the original expressions can directly be rewritten.

$$\sigma_F = \sigma_{Fo} * K_A * K_V * K_{F_\beta} * K_{F_\alpha}$$

$$\sigma_{F_o} = \frac{F_{mt}}{b_{ef} * m_{m_n}} * Y_{fa} * Y_{sa} * Y_\epsilon * Y_\beta * Y_K$$

$$\sigma_{Fp} = \frac{\sigma_{FE}}{S_{F\min}} * Y_{\delta_{relT}} * Y_{R_{relT}} * Y_x = \frac{\sigma_{FG}}{S_{f\min}}$$

$$S_f = \frac{\sigma_{FG}}{\sigma_F} \leq S_{f\min}$$

Rewriting these equations to the basic uniform way yields the following expression:

$$\sigma_F = K_A * K_v * K_{F_\beta} * K_{F_\alpha} * \frac{F_{mt}}{b * m_{m_n}} * Y_{fa} * Y_{sa} * Y_\epsilon * Y_\beta * Y_K * \frac{b}{b_{ef}}$$

$$\sigma_F \leq \frac{\sigma_{FE}}{S_{F\min}} * Y_x * Y_{\delta_{relT}} * Y_{R_{relT}}$$

Oerlikon

The four basic equations are:

$$\sigma_b = B_w * q_w * z_e \qquad \text{(Oe.1)}$$

$$B_w = C_s * C_D * C_T * C_\beta * B_e \qquad \text{(Oe.2)}$$

$$B_e = \frac{10^3 * M_d}{d_{p1} * b * r_e} \qquad \text{(Oe.3)}$$

$$\sigma_b \leq \frac{\sigma_D}{S_b} \qquad \text{(Oe.4)}$$

Equations Oe.2 and Oe.3 can be inserted in Oe.1; when the individual parts are also placed in the same way as has been done with other standards, this leads to:

$$\sigma_b = C_s * C_D * C_T * \frac{10^3 M_d}{d_{p_1} * b} * \frac{z_{e_1}}{r_{e_1}} * q_w * C_\beta$$

Furthermore:

$$z_{e_1} = \frac{z_1}{\cos\delta_1 * \cos\Delta_\alpha}$$

and

$$r_{e_1} = \frac{d_{p_1}}{2 * \cos\delta_1 * \cos\Delta\alpha}$$

Leading to:

$$\frac{z_{e_1}}{r_{e_1}} = \frac{2 * \cos\beta_{p_1}}{m_{p_n}}$$

The difference between the module in the design point P and the mean facewidth is relatively small, therefore the mean normal module may be substituted. If this last xepression is inserted in the expression for the stress and if directly the tangential load in the mean facewidth is determined, we obtain:

$$\sigma_b = C_s * C_D * C_T * \frac{2 * 10^3 M_d}{d_{m_1} * b} * \frac{1}{m_{m_n}} * q_w * C_\beta * \cos\beta_m * \frac{d_m}{d_p}$$

The unified expression of the Oerlikon equations therefore gives:

$$\sigma_b = C_S * C_D * C_T * \frac{F_{mt}}{b * m_{m_n}} * q_w * C_\beta * \cos\beta_m * \frac{d_m}{d_p}$$

Attachment 2.7 Calculation Example

A 2.7.1 General Gear Geometry Data.

Gear Ratio	3.31	6.14	--
Teethnumbers z1 / z2	13 / 43	7 / 43	--
Mean Normal Module m_{mn}	6.78	6.56	mm
Outer Transverse Module m_{et}	9.58	9.86	mm
Gear Outerdiameter d_{e2}	421	424	mm
Gear Facewidth b2	65	65	mm
Mean Spiral Angle $ß_{m2}$	30 / 36 / 42	32 / 38.5 / 45	degr
Pressure Angle α_n	22.5	22.5	degr
Addendum Factor H_a	1.00	1.00	--
Dedendum Factor H_f	1.30	1.30	--
Profile Shift Factor x_{m-1}	0.45	0.40	--
Toothhickness Corr.Factor	0	0	--
k	4.00	4.00	--
c-1	0.275	0.30	--
c			--
Strength Bal. Factor	-0.058	-0.009	--
Cutter Radius - Gleason	6"	6"	inch
Cutter Radius - Oerlikon	190	190	mm
Blade Edge Radius	0.50/2.92	0.5/2.92	--
Gear Quality DIN/AGMA	8/9	8/9	--
Gear Tooth Form - Gleason	Formate	Formate	--
Gear Tooth Form - Oerlikon	Spirac	Spirac	--
Failure Probability fp	10	10	%
Maximum Output Torque (acc 6.13)	32.000	32.000	Nm
Output Speed	100	100	rpm
Vehicle Weight GVW	30	30	tons
Output torque for calculation @ 25% maximum Torque	8.000	8.000	Nm
Material / Heat Treatment	Case Carburised Steel / Hardened 60 HR_C		

A 2.7.2 Calculated Profile, Face Contact and Total Contact Ratio's.

Ratio 13 / 43 = 3.31									
Spiral Agle β_{m2} [°]	30	30	30	36	36	36	42	42	42
Calculation Method	ANSI Gleas	DIN	Oerl.	ANSI Gleas	DIN	Oerl.	ANSI Gleas	DIN	Oerl.
m_p, $\epsilon_{-v-\alpha}$ [--]	1.19	1.19	1.19	1.09	1.09	1.09	0.98	0.98	0.98
m_F, $\epsilon_{-v-\beta}$ [--]	1.44	1.21	1.42	1.79	1.53	1.80	2.21	1.90	1.23
m_0 [--]	1.87	---	---	2.10	---	---	2.42	---	---
ϵ_{-v-v} [--]	---	2.41	2.62	---	2.62	2.89	---	2.88	3.22

Ratio 7 / 43 = 6.41									
Spiral Agle β_{m2} [°]	32	32	32	38.5	38.5	38.5	45	45	45
Calculation Method	ANSI Gleas	DIN	Oerl.	ANSI Gleas	DIN	Oerl.	ANSI Gleas	DIN	Oerl.
m_p, $\epsilon_{-v-\alpha}$ [--]	1.10	1.10	1.08	0.99	1.00	0.99	0.89	0.88	0.88
m_F, $\epsilon_{-v-\beta}$ [--]	1.55	1.32	1.55	1.97	1.68	1.98	2.46	2.11	2.49
m_0 [--]	1.90	---	---	2.21	---	---	2.61	---	---
ϵ_{-v-v} [--]	---	2.41	2.63	---	2.67	2.97	---	2.99	3.37

All values are rounded off to two decimals accurate.
The face contact and the total contact ratio according to DIN are calculated for an effective facewidth of 0.85 x b2. When the full geometric facewidth is taken into account, the difference between the calculated face contact ratio's will be negligible.

A 2.7.3 Results of Stress Calculations.

The individual calculated factors are summarised in both following tables.
The values there are not the same as given in each calculation standard. They are however conform to fig. 2.4 where the stress equations are rewritten.
Whena value is indicated with **, the value has not been calculated explicitely.

Ratio 7/43 @ 25 % T-max with ß-m2 = 38.5^0

Calculation Method	**AGMA**	**DIN**	**Gleason Oerlikon**		
Application Factor	1.00	1.00	1.00	1.00	(---)
Dynamic Load Factor	1.07	1.03	1.05	1.01	(---)
Face Load Distribution Factor	1.20	1.50	1.33	1.10	(---)
Adjecent Load Factor	----	1.05	----	----	(---)
Tooth Form Factor	1.80	2.47	1.80	q_w	(---)
Stress Concentr. Factor	2.15	1.93	2.15	1.0	(---)
Load Sharing Factor	0.87	0.75	0.87	**	(---)
Helical Factor	----	0.75	----	0.78	(---)
Cutter Radius Factor	1.06	----	1.06	----	(---)
Factor for Point of Load Application	~0.9	----	~0.9	----	(---)
Factor for Effective Facewidth	**	1.18	**	----	(---)
Mean Facewidth Factor	----	----	----	**	(---)
Unified stress	105	105	105	105	(N/mm^2)
Product of Geometry Factors	2.35	3.15	2.33	1.74	(---)
Nominal Stress Pinion (excl. Load factors)	247	330	246	365	(N/mm^2)
Product of Loadfactors	1.28	1.62	1.40	1.11	(---)
Actual Local Stress Pinion	317	536	345	405	(N/mm^2)
Allowable Stress (Endurance)	430	640	210	430	(N/mm^2)
Safety Factor	0.83	1.19	0.61	1.00	(---)
Size Factor	0.79	0.99	0.79	----	(---)
Life Factor	1.0	1.0	1.0	----	(---)
Temperature Factor	1.0	----	1.0	----	(---)
Roughness*Support Factor	----	----	1.01	----	(---)

Ratio 13/43 @ 25 % T-max with ß-m2 = 36^0

Calculation Method	**AGMA**	**DIN**	**Gleason**	**Oerlikon**	
Application Factor	1.00	1.00	1.00	1.00	(---)
Dynamic Load Factor	1.06	1.01	1.05	1.01	(---)
Face Load Distribution Factor	1.76	1.50	1.33	1.10	(---)
Adjecent Load Factor	----	1.05	----	----	(---)
Tooth Form Factor	1.80	2.47	1.80	q_w	(---)
Stress Concentr. Factor	2.15	1.93	2.15	1.0	(---)
Load Sharing Factor	0.87	0.75	0.87	**	(---)
Helical Factor	----	0.75	----	0.78	(---)
Cutter Radius Factor	0.95	----	0.95	----	(---)
Factor for Point of Load Application	~0.9	----	~0.9	----	(---)
Effective Facewidth Factor	**	1.18	**	----	(---)
Mean Facewidth Factor	----	----	----	**	(---)
Unified stress	419	419	419	419	(N/mm^2)
Product of Geometry Factors	**	3.15	2.35	1.74	(---)
Nominal Stress Pinion (excl. Load factors)	986	1325	772	730	(N/mm^2)
Product of Loadfactors	1.86	1.56	1.40	1.11	(---)
Actual Local Stress Pinion	1830	2075	1078	810	(N/mm^2)
Allowable Stress (Endurance)	430	690	210	430	(N/mm^2)
Safety Factor	0.23	0.33	0.19	0.53	(---)
Size Factor	0.79	0.99	0.79	----	(---)
Life Factor	1.0	----	1.0	----	(---)
Temperature Factor	1.0	----	1.0	----	(---)
Roughness*Support Factor	----	----	1.01	----	(---)

Attachment 2.8.1 Proposal for the Face Load Distribution Factor

The general expression for the total load over the entire gear facewidth is:

$$F_{tot} = \int f(x)\, dx$$

For a constant and equally distributed faceload, the faceload distribution function is:

$$f(x) = f_m$$

Introducing this in the integral, leads to:

$$F_{tot} = f_m * b$$

When an elliptical distribution of the faceload over the facewidth is assumed, the expression for the load distribution f(x) may be assumed:

$$f(x) = f_{max}\, x\, [1-(\frac{2x}{b})^2]$$

When this function is integrated over the entire facewidth, then the total load is:

$$F_{tot} = f_{max} * \frac{2}{3} b$$

This means that the maximum value of the load distribution function for an elliptical load distribution will be:

$$f_{max} = \frac{3}{2} * f_m = 1.50 * f_m$$

This means that only assuming an elliptical load distribution over the facewidth, the maximum value of the load distribution is 1.50 times the evenly distributed value. The coincidence of this value with the multiplication factor of the DIN standard, referring to the Face Load Distribution factor, may be not that far besides the viewpoint.
The assumption of an elliptical load distribution function may be relatively unfavourable, as several measurements have shown a distibution that is more flattended out around the middle of the facewidth. A better assumption for the load distribution function may be:

$$f(x) = f_{max} * [1-10(\frac{x}{b})^3+(\frac{x}{b})^2]$$

With this distribution, the load over half of the facewidth is more than 90% of the maximum load in the middle of the facewidth.
Now when this function is integrated over the facewidth, the total load is:

$$F_{tot} = f_{max} * 0.7708\ b$$

This means that:

$$f_{max} = \frac{1}{0.7708} * f_m = 1.297 * f_m \approx 1.30 * f_m$$

the maximum value of the face load now is about 30% higher than when a purely elliptical distribution for the faceload is assumed.
Therefore the multiplication factor for the Face Load Distribution factor in DIN is more likely to attain a value of 1.30 than 1.50.

Attachment 5.5 Mathematical Equations for Equivalent Torque.

The general expression for the equivalent torque is:

$$\frac{T_{eq}}{T_{max}} = [\frac{1}{N_\infty} * \int (\frac{T(N)}{T_{max}})^k * dN]^{\frac{1}{k}} \qquad (5.1)$$

When the theory according to Corten-Dolan is applied, all torques are involved in the damage accumulation; this means that the bordervalues for the integration range from 1 to N_∞, which covers the entire load spectrum.The following is part of [5.5] of Jos Van Heck, in which expressions have been derived for the equivalent torque for both spectra.

The mathematical expression for the **"Log-log"-Spectrum** is:

$$\log T(N) = \log T_{max} - \frac{\log\varphi}{\log N_\infty} * \log N \qquad (5.2)$$

This can be rewritten as:

$$T(N) = 10^{[\log T_{max} + \frac{\log\varphi}{\log N_\infty} * \log N]}$$

Then

$$\int T(N)^k * dN$$

becomes:

$$10^{(k.\log T_{max})} * \int 10^{(k * \frac{\log\varphi}{\log N_\infty} * \log N)} dN$$

When

$$b = k * \frac{\log\varphi}{\log N_\infty} \qquad (5.3)$$

is substituted, the expression becomes:

$$\int 10^{(b * \log N)} dN = \int N^a da = \frac{N^{b+1}}{b+1}$$

This leads to the expression for the equivalent torque:

$$\frac{T_{eq}}{T_{max}} = [\frac{N_\infty^{\,a}-1}{N_\infty} * \frac{1}{a}]^{\frac{1}{k}} \qquad (5.4)$$

The mathematical expression for the **"Lin-Log"-Spectrum** is:

$$T(N) = T_{max} * [1 - \frac{(1-\varphi)}{\log N_\infty} * \log N] \qquad (5.5)$$

The expression for the equivalent torque is:

$$\frac{1}{N_\infty} * (\int T(N)^k * dN)$$

When (5.5) is substituted in this last expression, then it becomes:

$$\frac{1}{N_\infty} * \int (1 + D * \ln(N))^k * dN$$

in which

$$D = \frac{C}{\ln(10)}$$

and

$$C = -\frac{(1-\varphi)}{\log N}$$

When this is partial integrated, this leads to the following recurrent expression:

$$I_k = S_k - k * D * I_{k-1}$$

for k = 2, 3, 4, 5, ... and so on, where:

$$I_k = \frac{1}{N} * \int (1 + D * \ln(n))^k \, dn$$

and

$$S_k = (1 + D*\ln(N))^k - \frac{1}{N}$$

The value for I-k when k=1 is:

$$I_1 = 1 + D * \ln(N) - \frac{1}{N} - D + \frac{D}{N}$$

Now this recurrent expression is written out for k = 2, 3, 4, 5, and further. After that it can be rearranged in a general formulation. Then this expression gives the formulation for the ratio of the equivalent torque to the maximum torque for the load spectrum.
The equivalent torque for the "Lin-Log" spectrum now can be described as:

$$\frac{T_{eq}}{T_{max}} = \Sigma[\frac{k!}{(k-1)!}*(-D)^i*\{(1+D*lnN_\infty)^{k-i}-\frac{1}{N_\infty}\}]+k!*(-D)^{k-1}*I_1 \qquad (5.7)$$

where:

$$I_1 = 1+D*\ln N_\infty-\frac{1}{N_\infty}-D+\frac{D}{N_\infty} \quad where \quad D=-\frac{\varphi}{ln10} \qquad (5.8)$$

Attachment 5.7 Results of Variable Amplitude Endurance Tests

Spectrum Type	Output Torque [Nm]	Individual Fraction [--]	Ti/Tmax Spectrum [--]	Cumulative Fraction [--]
LOW	57.195	3.5*10^-4	1.00	3.5*10^-4
	46.740	2.0*10^-3	0.82	2.4*10^-3
	36.285	1.7*10^-2	0.63	1.9*10^-2
	26.445	1.3*10^-1	0.46	1.5*10^-1
	18.450	8.5*10^-1	0.32	1.0*10^0
HIGH	56.630	2.6*10^-4	1.00	2.6*10^-4
	52.000	6.6*10^-4	0.92	9.2*10^-4
	46.200	3.3*10^-3	0.82	4.2*10^-3
	39.950	1.1*10^-2	0.71	1.5*10^-2
	33.950	2.9*10^-1	0.60	4.5*10^-2
	27.925	1.2*10^-1	0.49	1.7*10^-2
	21.640	8.4*10^-1	0.38	1.0*10^-1

Table 5.2. Loadspectra for Variable Amplitude Tests.

Spectrum	Pinion Cycles	Failure Mode
LOW	$5.50*10^6$	Cracks at the toothroot; several teeth pitting.
	$4.05*10^6$	Large cracks on the teeth; severe pitting.
	$2.60*10^6$	Many cracks at midtooth; two teeth spalling.
	$1.50*10^6$ +	Inspection: small cracks.
HIGH	$2.22*10^6$	All teeth cracks; three teeth broken.
	$1.52*10^6$	Inspection: one crack, one tooth spalling.
	$0.74*10^6$	Many teeth cracks.
	$0.64*10^6$ +	Inspection: 6 teeth cracks.

Table 5.2. Results of Variable Amplitude Tests

Attachment 6.2.1 Crownwheel Outer Diameter versus Crownwheel Output Torque

Derivation of crownwheel outerdiameter in function of load, geometry and material.
For this, the basic equations according to DIN 3991 are used, although any other calculation standard may be used.

For **tooth root** stress, the general equations are:

$$\sigma_F=\sigma_{Fo}*K_A*K_V*K_{F_\beta}*K_{F_\alpha}=\sigma_{Fo}*\Pi K_{load}$$

$$\sigma_{F_o}=\frac{F_{mt}}{b_{ef}*m_{m_n}}*Y_{fa}*Y_{sa}*Y_\epsilon*Y_\beta*Y_K=\frac{F_{mt}}{b_{ef}*m_{mn}}*\Pi Y_{geometry}$$

$$\sigma_{Fp}=\frac{\sigma_{FE}}{S_{f\min}}*Y_{\delta_{relT}}*Y_{R_{relT}}*Y_x=\frac{\sigma_{FE}}{S_{f\min}}*\Pi Y_{material}$$

When the basic geometry relations are introduced in the above mentioned equations, the following expression for the crownwheel outerdiameter on basis of the tooth root stress is generated:

$$d_{e2}=(2.10^3)^{1/3}*(\frac{S_f}{\sigma_{FE}})^{1/3}*[\frac{\Pi K_{load}*\Pi Y_{geometry}*z_2}{\Pi Y_{material}*\xi*(1-\xi*\sin\delta_2)^2*\cos\beta_{m2}}]^{1/3}*T_2^{1/3}$$

For **tooth surface** stress, the general equations are:

$$\sigma_H=\sigma_{Ho}*\sqrt{K_A*K_V*K_{F_\beta}*K_{F_\alpha}}=\sigma_{Fo}*\sqrt{\Pi K_{load}}$$

$$\sigma_{H_o}=\sqrt{\frac{F_{mt}}{d_{v1}*b_{ef}}*\sqrt{\frac{i^2+1}{i^2}}}*Z_H*Z_E*Z_\epsilon*Z_\beta*Z_K=\sqrt{\frac{F_{mt}}{d_{v1}*b_{ef}}*\sqrt{\frac{i^2+1}{i^2}}}*\Pi Z_{geometry}$$

$$\sigma_{HP}=\frac{\sigma_{Hlim}}{S_{H\min}}*Z_L*Z_V*Z_R*z_X=\frac{\sigma_{Hlim}}{S_{H\min}}*\Pi Z_{material}$$

When the basic geometry relations are introduced in the above mentioned equations, the following expression for the crownwheel outerdiameter on basis of tooth surface stress is generated:

$$d_{e2}=(2.10^3)^{1/3}*(\frac{S_H}{\sigma_{Hlim}})^{2/3}*[\frac{\Pi K_{load}*(\Pi Z_{geometry})^2*\sqrt{i^2+1}}{(\Pi Z_{material})^2*\xi*(1-\xi*\sin\delta_2)^2*\phi}]^{1/3}*T_2^{1/3}$$

Basic gear geometry relations.

* $d_{m2} = d_{e2} - b_2*\sin(\delta_2)$
* $b_2 = \xi * d_{e2}$
* $d_{m2} = d_{e2} * [1-\xi*\sin(\delta_2)]$
* $m_{mt} = d_{m2} / z_2$
* $m_{mn} = m_{mt} * \cos(\beta_{m2})$
* $m_{mn} = d_{e2} * [1- \xi*\sin(\delta_2)] * \cos(\beta_{m2}) * 1/z_2$
* $d_{m1} = \phi * 1/i * d_{m2}$
* $F_{mt} = 2*10^3*T_2 / d_{m2}$

For automotive applications, several variables may have the following range of minimum and maximum numerical values:

	Minimum Value	Mean Value	Maximum Value	
Product of Load Factors ΠK_{load}	1.30	1.40	1.50	[---]
For Tooth Root Stress:				
Product of Geometry Factors $\Pi Y_{geometry}$	1.85	2.35	3.00	[---]
Product of Material Factors $\Pi Y_{material}$	0.95	1.00	1.05	[---]
For Tooth Surface Stress:				
Product of Geometry Factors $\Pi Z_{geometry}$	195	250	315	[---]
Product of Material factors $\Pi Z_{material}$	0.95	1.00	1.05	[---]
Gear ratio i	2	4	6	[---]
Mean Spiral Angle β_{m2}	30	35	38	[°]
Gear Teethnumber z_2	38	41	45	[---]
Gear Pitch Angle δ_2	65	75	85	[°]
Ratio Facewidth/diameter	0.12	0.135	0.15	[---]
ϕ (for hypoid offset)	1.0	1.10	1.20	[---]
Allowable Tooth Root Stress:				
- Static Limit	2000	2100	2200	[N/mm^2]
- Safety factor	1.8	2.0	2.2	[---]
- Endurance Limit	550	620	690	[N/mm^2]
- Safety factor	1.25	1.35	1.50	[---]
Allowable Tooth Surface Stress:				
- Static Limit	2200	2350	2500	[N/mm^2]
- Safety factor	1.3	1.4	1.5	[---]
- Endurance Limit	1300	1350	1400	[N/mm^2]
- Safety factor	1.00	1.05	1.10	[---]

When these values are introduced in the two basic equations for the crownwheel outerdiameter, the following expressions arise.

* For static tooth root stress:

$$d_{e2}=(11.5\div16.0)*T_{2\,max}^{1/3}$$

* For continuous tooth root stress:

$$d_{e2}=(15.5\div21.0)*T_{2\,cont}^{1/3}$$

* For static tooth surface stress:

$$d_{e2}=(7\div17.5)*T_{2\,max}^{1/3}$$

* For continuous tooth surface stress:

$$d_{e2}=(8.5\div21.5)*T_{2\,cont}^{1/3}$$

By far the largest crownwheel diameters are required for tooth root breakage. This means that tooth root breakage will mostly determine the required gear dimensions.
For truck applications, the maximum ratio between the maximum and the equivalent output torque can be expected at typical National Transport Applications. It may amount to:

$$\frac{T_{eq}}{T_{max}} = 0.27 \div 0.33$$

The highest value still is lower than the ratio of static to endurance strength for tooth root failure of case carburised gears, which is mostly almost higher than 0.35. This means that a continuous load will give a higher safety factor for fatigue than a maximum load gives for static breakage.
If the value for $T_{eq} = 0.33 \times T_{2\,max}$, representing the maximum situation, is inserted now for $T_{2\,cont}$ in both expressions of the crownwheel outer diameter for continuous tooth root and surface stress diameter to continuous torque, the required outer diameter still remains smaller than for the maximum torque. This means that the failure type of static loading due to the maximum torque determines the required crownwheel outer diameter; at least based on this numerical excercise.
For continuous tooth root stress:

$$d_{e2}=(10.0\div15.0)*T_{2\,max}^{1/3}$$

For continuous tooth surface stress:

$$d_{e2}=(6.0\div15.0)*T_{2\,max}^{1/3}$$